Matriptase-2 and the biological behaviours of prostate cancer cells: A possible role for β-catenin

by

Siobhan L. Webb

Metastasis and Angiogenesis Research Group

Cardiff University School of Medicine

Cardiff

PhD. 2011

Thesis submitted to Cardiff University for the degree of Doctor of Philosophy

UMI Number: U584571

UMI U584571

DECLARATION

This work has not previously been accepted in substance for any degree and is not concurrently submitted in candidature for any degree.

Signed........*Swebb*............. (candidate)   Date.....8./02./12......

STATEMENT 1

This thesis is being submitted in partial fulfilment of the requirements for the degree of PhD.

Signed........*Swebb*............. (candidate)   Date.....8./02./12......

STATEMENT 2

This thesis is the result of my own independent work/investigation, except where otherwise stated. Other sources are acknowledged by explicit references.

Signed......*Swebb*............. (candidate)   Date.....8./02./12......

STATEMENT 3

I hereby give consent for my thesis, if accepted, to be available for photocopying and for inter-library loan, and for its title and summary to be made available to outside organisations.

Signed........*Swebb*............. (candidate)   Date......8./02./12......

STATEMENT 4

I hereby give consent for my thesis, if accepted, to be available for photocopying and for inter-library loans **after expiry of a bar on access previously approved by the Graduate Development Committee.**

Signed.................................... (candidate)   Date....................

i

Acknowledgements

Summary

The type II transmembrane serine proteases (TTSP) are cell surface proteolytic enzymes that mediate a diverse range of cellular functions, including tumour invasion and metastasis. Matriptase-2 is a relatively newly identified member of the TTSP family whose role in cancer is currently poorly understood. Sanders *et al* 2008 investigated the effect of matriptase-2 in PC3 and DU145 prostate cancer cells. This study aims to further elucidate the role of matriptase-2 in cancer development and progression. The relationship between matriptase-2 and β-catenin was examined as previous preliminary data (unpublished) showed β-catenin to be a protein of interest from a screen of molecules associated with cell:cell and cell:matrix adhesion performed during previous studies.

To build on the data gained from Sanders *el al* 2008, normal prostate cell lines PZHPV7 and PNT2C2 had matriptase-2 stably knocked down and were used in assays to asses cell functionality. Knock-down of matriptase-2 did not alter the growth or adhesion of PZHPV7 or PNT2C2 cells but did however; cause a significant reduction in their motile and invasive capabilities. HECV cells were also used to examine the effect of matriptase-2 on angiogenesis. The over-expression of matriptase-2 in these cells had no effect on growth and adhesion but significantly reduced the motile and tubule formation abilities of the HECV cells. This is a similar effect to that seen in the PZHPV7 and PNT2C2 cells.

PC3 and DU145 cells over-expressing matriptase-2 were also used to examine possible mechanisms of matriptase-2 action. Examination into the possible relationship between matriptase-2 and β-catenin revealed that a knockdown of matriptase-2 increased the β-catenin levels and conversely, over-expression decreased the β-catenin levels in PC3 cells. In DU145 cells the β-catenin levels increased. This may be due to the differing expression levels of key molecules such as E-cadherin. The HECV cells appeared to show no change in β-catenin levels. Angiogenesis factor MMP-7 was found to be altered in response to β-catenin levels. Additionally matritpase-2 over-expression was found to reduce uPA and the converse with matriptase-2 knockdown in all cell lines examined.

These results indicate that matriptase-2 may have a regulatory function over β-catenin and uPA in prostate cells. This is possibly two mechanisms by which matriptase-2 protects against cancer metastasis and angiogenesis in normal cells and tissues. However, due to the differences seen in the β-catenin experiments, there are obviously other possible mechanisms to be considered. This study provides a valuable insight into how this poorly understood protease functions in prostate cancer.

Contents

List of Figures

Chapter 2:

Chapter 3:

Chapter 4:

Chapter 5:

Chapter 6:

List of Tables:

Publications

The influence of matriptase-2 on prostate cancer in vitro: a possible role for β-catenin

Webb, SL, Sanders, AJ, Mason MD, Jiang WG

Unknown (Upcoming submission)

Matriptase-2 inhibits HECV motility and tubule formation *in vitro* and tumour angiogenesis *in vivo*

Webb SL, Sanders AJ, Mason MD, Jiang WG.

Molecular Cancer Research (In submission)

Type II transmembrane serine protease deregulation in cancer

Webb SL, Sanders AJ, Mason MD, Jiang WG.

Front Biosci. 2011 Jan 1; 16;539-552

The type II transmembrane serine protease, matriptase-2: Possible links to cancer?

Sanders AJ, **Webb SL**, Parr C, Mason MD, Jiang WG.

Anticancer Agents Med Chem. 2010 Jan;10(1):64-9.

Abstracts and conference presentations

The influence of matriptase-2 on prostate cancer in vitro: a possible role for β-catenin, November 2011. **Siobhan L Webb,** Andrew J Sanders, Malcolm D Mason, Wen G Jiang. NCRI Liverpool, UK

The influence of matriptase-2 on angiogenesis and tumour growth *in vivo*. December 2010, **Siobhan L Webb,** Andrew J Sanders, Malcolm D Mason, Wen G Jiang. San Antonio Breast Cancer Symposium (SABCS), San Antonio, Texas

The influence of Matriptase-2 on angiogenesis and tumour growth *in vitro* and *in vivo*. November 2010, **Siobhan L Webb,** Andrew J Sanders, Malcolm D Mason, Wen G Jiang. Postgraduate Research Day 2010, Cardiff University School of Medicine, Cardiff (1st Place poster prize)

Type II transmembrane serine protease, Matriptase-2, reduces motility and tubule formation in human endothelial cells. November 2009, **Siobhan L Webb,** Andrew J Sanders, Malcolm D Mason, Wen G Jiang. Postgraduate Research Day 2009, Cardiff University School of Medicine, Cardiff.

Abbreviations

AR: Androgen receptor

ARE: Androgen responsive elements

ATCC: American Type Culture Collection

BM: Basement membrane

BMP: Bone morphogenetic protein

Bp: Base pair

BPH: Benign prostatic hypertrophy

BSA: Bovine serum albumin

BSS: Balanced salt solution

CAMs: Cellular adhesion molecules

CUB: Cls/clr urchin embryonic growth factor

CO_2: Carbon dioxide

ddH2O: Double-distilled water

DEPC: Diethyl pyrocarbonate

DES: Diethylstilbesterol

DECS1: Differentially expressed in squamous cell carcinoma gene 1

DHT: Dihydrotestosterone

DMEM: Dulbecco's modified eagles medium

DMSO: Dimethyl sulphoxide

DNA: Deoxyribonucleic acid

dNTP: Deoxyribonucleoside triphosphate

DRE: Digital rectal examination

E. coli: Esherichia coli

ECACC: European Collection of Animal Cell Culture

ECD: Extracellular domain

ECE: Extra-capsular extension

ECL: enhanced chemiluminescence

ECM: Extracellular matrix

EDTA: Ethylene diaminetetraacetic acid

EGF: Epidermal growth factor

ELISA: Enzyme-linked immunoabsorbant assay

EMT: Epithelial-mesenchymal transdifferentiation/transformation

ERK: Extracellular regulated MAP kinase

ET-1: Endothelin-1

ETAR: Endothelin receptor type A

ETS: E26 transformation specific

FAK: Focal adhesion kinase

FBS: Foetal bovine serum

FGF: Fibroblast growth factor

FNA: Fine needle aspiration

FITC: Fluorescein isothiocyanate

FZ: Frizzled

G gravity's (unit of relative centrifugal force)

GFP green fluorescent protein

H_2O_2: Hydrogen peroxide

HAI-1: Hepatocyte growth factor activator inhibitor-1

HAT: Human airway trypsin-like

HCl: Hydrogen acid

HGF: Hepatocyte growth factor

Hr: hour

HRP: horseradish peroxidise

HSP: Heat shock protein

IF: Immunofluorescence

Ig: Immunoglobulin

IGF: Insulin-like growth factor

IL: interleukin

IP: Immunoprecipitation

Kb: kilo-base

kDa: kilo-dalton

LB: Luria-Bertani

LDLA: Low density lipoprotein A

LH: Leutenising hormone

LHRH: LH releasing hormone

m: metre

M: Molar

mA: milli-amp

MAM: Receptor protein phosphatase μ domain

MAPK: Mitogen-activated protein kinase

mg: Milligram

m-HJV: membrane bound hemojuvelin

ml: milli litre

mM: milli molar

MMP: Matrix metalloproteinase

mRNA: Messenger ribonucleic acid

MW: Molecular weight

NaCl: Sodium chloride

NaOH: Sodium hydroxide

ng: nano-gram

NPI: Nottingham prognostic index

PAGE: polyacrylamide gel electrophoresis

PAR: Protease activated receptors

PBS: Phosphate buffered saline

PCR: Polymerase chain reaction

PDAC: Pancreatic ductal adenocarcinoma

PDGF: Prostate derived growth factor

PIN: Prostatic intraepithelial neoplasia

PSA: Prostate specific antigen

RANK: Receptor activator of nuclear factor-κB

RANKL: RANK ligand

Rb: Retinoblastoma

RGMc: Repulsive guidance molecule c

RNA: Ribonucleic acid

RNAse: Ribonuclease

rpm: Revolutions per minute

RT: Reverse transcription

SEA: Sperm protein, enterokinase & agrin domain

SD: Standard deviation

SDS: Sodium dodecyl sulphate

Smad: Sma and MAD

SP: Serine protease

SR: group A scavenger receptor domain

TBE: Tris/Borate/EDTA electrophoresis buffer

TBS: Tris-buffered saline

TEMED: N,N,N',N'-tetramethylethylenediamine

TFPI2: Tissue factor pathway inhibitor 2

TGF-β: Transforming growth factor-β

TIMP: tissue specific inhibitor of matrix metalloproteinase

TNF-α: Tumour necrosis factor-alpha

TNM: Tumour, node and metastasis

Tris: Tris-(hydoxymethyl)-aminomethane

TRUS: Trans-rectal ultrasonography

TTSP: Type II transmembrane serine protease

μg: microgram

μl: Microlitre

μM: Micro molar

uPA: Urokinase plasminogen activator

UV: Ultraviolet

V: Volt

VEGF: Vascular endothelial growth factor

Wiskott-Aldrich syndrome protein: WASP

Wnt: Wingless-type

WT: Wild type

Chapter 1

Introduction

1.1   Introduction to prostate cancer

1.1.1   Prostate cancer incidence, risk factors

Prostate cancer is the most commonly diagnosed cancer in men in the UK. Approximately a quarter of new cancer cases diagnosed in men are prostate cancer. In 2007 around 36,000 men were diagnosed with prostate cancer in the UK. In 2008, there were 37,051 new cases of prostate cancer diagnosed in the UK, which is around 101 men every day or one man every 15 minutes. The lifetime risk of being diagnosed with prostate cancer is 1 in 9 for men in the UK. This was calculated in January 2011 using incidence and mortality data for 2008 (CRUK 2010). Although prostate cancer incidence rates appear to be rising, this is thought to be attributed to the advancement in detection methods, such as the advancement in PSA serum testing and ultrasound imaging.

The strongest known risk factor for prostate cancer is age, with very low risk in men under 50 and rising risk with increasing age thereafter. Very few cases are registered in men under 50 and around three-quarters of cases occur in men over 65 years. The largest number of cases is diagnosed in those aged 70+ (**Figure 1.1**). It is estimated from post-mortem data that around half of all men in their fifties have histological evidence of cancer in the prostate, which rises to 80% by age 80, but only 1 in 26 men (3.8%) will die from this disease (Sakr *et al.*, 1996). It is commonly believed that more men die *with* prostate cancer than *from* it. Another risk

2

factor is familial history. A family history of prostate cancer is one of the strongest known risk factors for this disease. It has been estimated that 5-10% of all prostate cancer cases and 30-40% of early-onset cases (men diagnosed <55 years) are caused by inherited susceptibility genes (Bratt, 2002). If a first degree family member is diagnosed with prostate cancer the risk of developing the disease increases two to three times, which further increases as the person ages.

It has been noted that incidence rate vary round the world suggesting that risk is associated with ethnicity. In the UK, black Caribbean and black African men have around two to three times the risk of being diagnosed or dying from prostate cancer than white men, while Asian men generally have a lower risk than the national average (Wild *et al.*, 2006).

Due to the large variations in the incidence of prostate cancer between different cultures and their diet there has been interest in the potential risks involved. It has been suggested that the 'western' diet may increase risk compared to that of the lower incidence 'asian' diet, though there is little evidence supporting this. A recent review of the evidence concluded that foods containing lycopenes and selenium probably have a protective effect while diets high in calcium may increase risk. Other risk factors that are being considered are alcohol, smoking, body weight, endogenous hormones and diabetes mellitus.
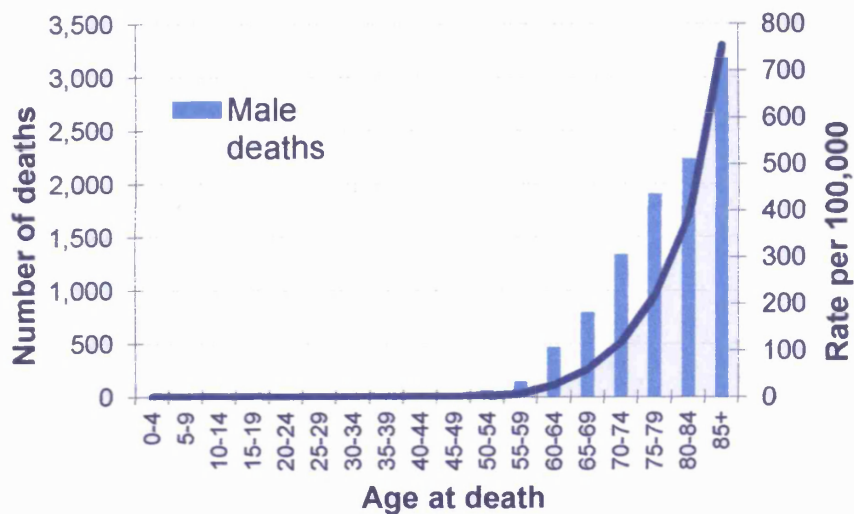
Figure 1.1 Number of deaths and age-specific mortality rates, prostate cancer, UK (taken from CR-UK, 2007).

1.1.2 Anatomy and histology of the prostate

The prostate is a tubuloalveolar walnut sized gland of the male reproductive system, which is situated within the pelvis at the base of the bladder, and surrounds the urethra. The prostate is also surrounded posteriorly by the rectum, through which it can be felt during rectal examination. The prostate is believed to be enclosed by a capsule composed of collagen, elastin, and large amounts of smooth muscle. Although this capsule may be partially transgressed by normal glands making the determination of extracapsular disease problematic. The prostate is mainly composed of glandular epithelium which is deposited in a fibromuscular stroma. This non-glandular fibromuscular stroma makes up around a third of the gland, and stretches from the bladder neck to the striated sphincter. It comprises of fibroblasts, smooth muscle, nerves and lymphatics. The stroma is immediately continuous with the

4

capsule, and progressively lengthens into fibrous tissue that terminates in loose connective, and adipose tissue. Although the prostate lacks discernible lobes, it is characterised as having a zonal architecture as defined by McNeal (McNeal, 1969, 1981, 1981). There are four major zones within the normal prostate: the peripheral zone, the central zone, the transition zone and the anterior fibromuscular stroma (Figure 1.2).

The peripheral zone extends posterolaterally around the prostate from the apex to the base and has the largest volume, accounting for around 70% of the gland. The central zone accounts for around 25% of the prostate gland and surrounds the ejaculatory duct apparatus and constitutes the majority of the prostatic base. Finally the transition zone, which is the smallest zone and accounts for 5% of total prostate volume; comprises two small lobules that adjoin the prostatic urethra. The peripheral zone is the most common site for the development of prostatic carcinomas whereas the transition zone is region where benign prostatic hyperplasia (BPH) more commonly originates. The prostate is believed to be enclosed by a capsule composed of collagen, elastin, and abundant smooth muscle. Although this capsule may be partially transgressed by normal glands making the determination of extracapsular disease problematic.

On the whole, the prostatic glands are simply branched and tubuloalveolar in structure, lined with both cuboidal and columnar secretory epithelial cells androgen-dependant for their growth. These terminally differentiated columnar cells are rich in secretory granules, keratin and enzymes such as prostatic acid phosphatase,

leucine amino peptidase and PSA.   They are tightly packed together via cellular

adhesion molecules (CAMS), and attached to a basement membrane through integrin

receptors which connect them to the stromal cells via an extracellular matrix,

enhancing epithelial cell growth.   The prostate also contains a pseudostratified

epithelium with three differentiated epithelial cell types: luminal, basal, and

neuroendocrine (Foster *et al.*, 2002; Hudson, 2004; Peehl, 2005). The luminal

epithelial cells form a continuous layer of polarised columnar cells that produce

protein secretions and express high levels of the androgen receptor (AR). Basal cells

are located beneath the luminal epithelium and above the basement membrane,

express AR at much lower levels. Neuroendocrine cells are rare cells of unknown

function that express endocrine markers such as chromogranin A, but are AR

negative.
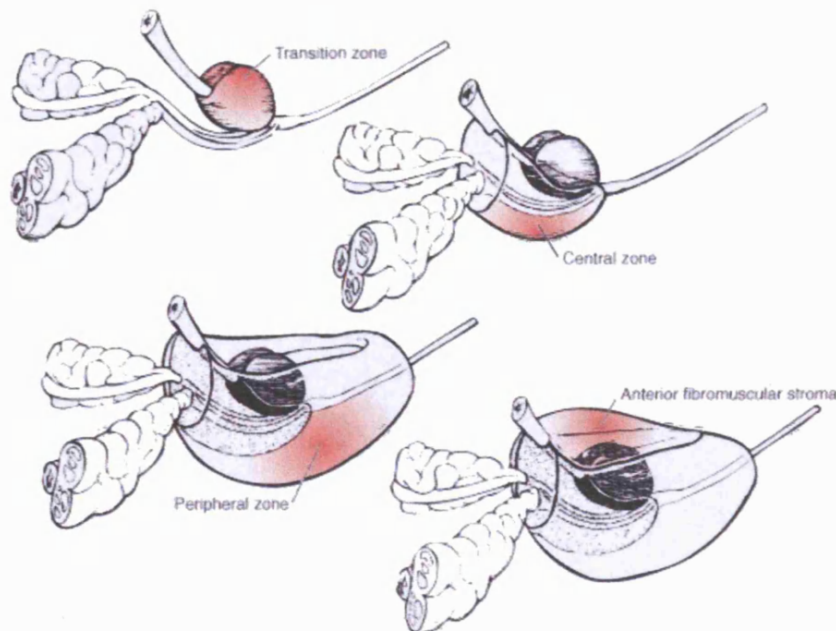
Figure 1.2 Zonal anatomy of the prostate: the three glandular zones of the prostate and the anterior fibromuscular stroma (Cancer medicine 6th edition 2000)

1.1.3   Biology of prostate cancer

The majority of prostate cancers are classified as adenocarcinomas that originate from the prostatic epithelium (~95%). The other 5% is composed of other categories such as ductal adenocarcinoma, mucinous carcinoma, and signet ring carcinoma, and are all extremely rare. The most significant histological variant is the neuroendocrine prostate cancer, which is generally classified as either small cell carcinoma or a carcinoid tumour, and represents <2% of prostate cancer cases (Grignon, 2004). The

development of solid tumours is generally thought to be a multi-step process in which successive genetic events occur in a normal cell to render it increasingly malignant. In prostate cancer the genetic and epigenetic processes that result in cancer are poorly understood. It is believed that the occurrence of pre-malignant lesions may pre-date the development of cancer by many years (Figure 1.3).

The umbrella term 'prostatic intraepithelial neoplasia' or 'PIN' describes the heterogeneous morphologic lesions prostatic dysplasia or atypia. PIN is generally characterised at the histological level by the appearance of luminal epithelial hyperplasia, reduction in basal cells, enlargement of nuclei and nucleoli, cytoplasmic hyperchromasiam and nuclear atypia (Bostwick and Foster, 1999). These abnormalities are generally found within architecturally benign-appearing glands and acini. PIN is graded depending on the degree of basal cell layer disruption (with more disruption being present in high grade PIN): grade 1 is a mild manifestation; grade 2 is moderate, and grade 3 is severe. Grades 2 and 3 are often combined as 'high grade' PIN. PIN is presumed to be a pre-malignant lesion due to its common presence adjacent to prostate adenocarcinomas.
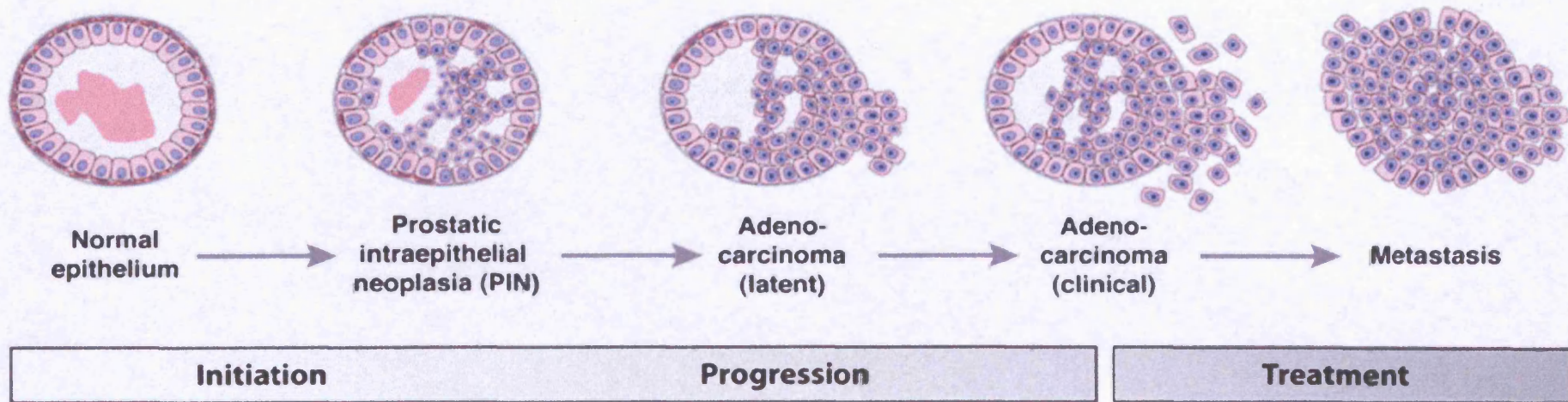
Figure 1.3 Progression pathway for human prostate cancer. PIN is the pre-cursor to the development of malignant disease and ultimately cancer metastasis. Adapted from (Abate-Shen and Shen, 2000)

1.1.4   Prostate cancer detection

The probability of developing prostate cancer rises with age, with an incidence percentage of over 30% in men over the age of 50, and up to 80% by the age of 80. As prostate cancer is typically a slow growing cancer, most never grow to the point of causing symptoms. Because of this the majority of men die with prostate cancer rather than of it. Due to this lack of symptoms, prostate cancer is often diagnosed in an already advanced state. Around 75% of patients exhibit locally extensive or metastatic disease, resulting in a poor prognosis of less than 15% surviving over 5 years (Foster, 1990). The patients that do present with symptomatic prostate cancer experience bladder outlet obstruction resulting in reduced urinary flow, and bladder emptying. However, these symptoms are also present in those with benign prostate hyperplasia which makes the correct diagnosis of a malignant disease more important. This also adds to the difficulties in managing the disease. Other symptoms of prostate cancer include a feeling of pain in the pelvis and bones, fatigue or blood in the urine, are usually associated with advanced or metastatic prostate cancer (Foster and Abel, 1992).

Three main strategies exist in the detection of prostate cancer; serum prostate specific antigen (PSA) analysis, digital rectal examination (DRE), and trans-rectal ultrasound (TRUS) detection. It has been shown that a higher rate of detection can be achieved if a combination of these methods is used in diagnosis. PSA in combination with DRE for example, leads to a doubling in detection rates, in comparison to DRE alone (Littrup and Goodman, 1994).

1.1.4.1 Serum PSA test

PSA is a glycoprotein, serine protease that is produced by the prostatic epithelium and periurethral glands and is present in large amounts in prostatic secretions. Although PSA is not cancer specific, a rising serum PSA level can indicate the potential presence of prostate cancer. PSA was first described in 1966 and has revolutionised the diagnosis and management of prostate cancer. It is now the most common screening test used for the detection of prostatic disease (Elgamal *et al.*, 1994).

A serum PSA level of 4–10 ng/ml indicates the presence of prostate cancer and patients presenting with a serum PSA in this range usually have a needle biopsy to confirm the presence of the disease. Around 2-3% of men screened for prostate cancer using the PSA serum test will have prostate cancer. It is reported that a PSA level of greater than 4ng/ml has a sensitivity of 80% in detecting prostate cancer in asymptomatic men (Catalona *et al.*, 1994).

PSA exists in several forms in the circulation, and although most is complexed to protease inhibitors, a small fraction remains unbound. The percentage of free-PSA (free:total PSA ratio) is lower in men with prostate cancer. A cut off value of less than 25% free-PSA yielded a 95% cancer detection rate in men with total serum PSA levels between 4 and 10ng/ml (Catalona *et al.*, 1998).

Although PSA testing is used worldwide, questions have been asked involving limitations that reduce the accuracy of the test. This is mainly due to data from

several groups which showed that a significant number of men with PSA levels within the 'normal range' actually had prostate cancer, some even of a high grade. In addition, as BPH, prostatis, and ejaculation can also cause an increase in PSA levels, patients who have PSA levels in the range of 4ng/ml-10ng/ml, sometimes have to undergo unnecessary and painful biopsies (Thompson *et al.*, 2005; De Angelis *et al.*, 2007).

Because of these limitations, attempts have been made to improve the specificity of the PSA test. As PSA production from benign epithelium rises with age, age-specific PSA cutoff points were developed (Oesterling *et al.*, 1993). Another modification is PSA density. The serum concentration of PSA appears to be influenced by total prostate volume. The PSA concentration is divided by the total gland volume as measured by TRUS. A PSA density of >0.15ng/ml increased the specificity of detection of prostate cancer compared with total PSA, although the optimal cut-off point is debated (Ohori *et al.*, 1995). Another common modification is the monitoring of PSA velocity. This involves monitoring the rate of change (PSA velocity) of serum PSA levels rather than PSA level. An increase of 0.75ng/ml per year has reported a specificity of over 90% in distinguishing prostate cancer from BPH (Carter *et al.*, 1992)

1.1.4.2 Digital Rectal Examination (DRE)

Digital rectal examination (DRE) is the oldest detection test for prostate cancer and was common before the development of PSA testing. It is still used today

alongside PSA testing and has the benefit of detecting non-PSA secreting tumours. The process involves a physician inserting a gloved, lubricated finger into the rectum in order to inspect the size, shape, and texture of the prostate, and any lumps or nodules that may be present. Areas deemed irregular then go through further evaluation to determine whether they are cancerous or not. The sensitivity of this test is limited as the examining finger can only palpate the posterior and lateral aspects of the prostate gland. Studies suggest that 25-35% of tumours occur in portions of the prostate that are inaccessible to DRE (McNeal *et al.*, 1986). Prostate cancer tumours that are detected via DRE are often at a more pathologically advanced state of disease compared to those found by PSA testing. Before PSA testing was introduced most men diagnosed with prostate cancer ultimately died of their disease (Smith and Catalona, 1995). Due to these limitations DRE is rarely used as the sole diagnostic indicator of prostate cancer, rather in conjunction with other more reliable tests.

1.1.4.3 Trans-rectal Ultrasonography (TRUS)

Trans-rectal ultrasonography was presented over 20 years ago and is the preferred method by which to obtain prostate needle biopsies. The process involves inserting an ultrasound probe into the rectum of the patient, and using the resulting image to direct spring loaded 18-gauge biopsy needles into abnormal areas of the prostate. Although TRUS is not recommended for the detection of early-stage prostate cancer, it can however, image the outline of the prostate, identify cysts, abscesses and calcifications within the prostate, and can be used to determine prostate volume. The most commonly used biopsy technique is the six-core or

sextant biopsy, with 10 to 12 being carried out to sample the prostate as it leads to significantly improved cancer detection rates (Borley and Feneley, 2009).

1.1.5 Tumour grading systems

To tailor the treatment of prostate cancer to a specific person the tumour first needs to be graded and classified using well established cancer grading systems such as the Gleason grading system and the TNM classification system.

1.1.5.1 The Gleason grading system

The Gleason grading system for prostate carcinomas is the dominant method used around the world and was first described by Gleason and Mellinger in 1974. The grading is based on the histological pattern of the distribution and growth of the tumour cells in the prostatic stroma, as well as the degree of glandular differentiation in H&E stained prostatic tissue samples from either a biopsy, or if after radical prostatectomy, a whole prostate (Gleason and Mellinger, 1974).

The various growth patterns (shown in Figure 1.4) are combined to form 5 basic grade patterns ranging from 1 (least aggressive) to 5 (most aggressive). This enables the generation of a histological score ranging from 2-10, by the addition of the primary grade pattern; the prevailing one in that area, to the secondary pattern, which is the subsequently most widespread pattern. However, if only one grade is present, or if the second grade covers less than 3% of the total tumour, its value is doubled in order to give a corresponding Gleason score.

14

The cell arrangement seen in each Gleason pattern is described in Table 1.1 and ranges from the closely packed well-differentiated carcinoma cells seen in pattern 1, to smooth rounded masses of necrotic and very poorly differentiated carcinoma cells in pattern 5 (Humphrey, 2004).
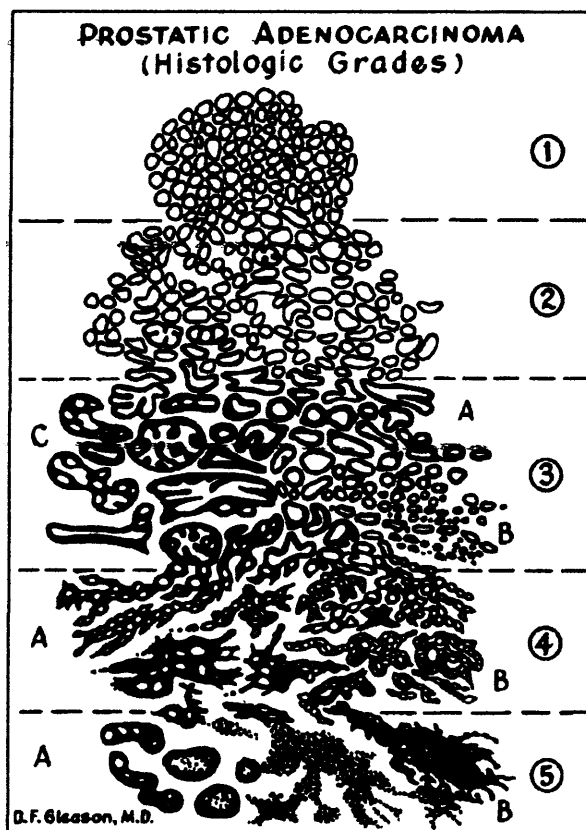
Figure 1.4: Schematic drawing of Gleason histological grading (Taken from (Humphrey, 2004).

Pattern	Tumour shape and borders	Stromal invasion	Tumour cell arrangements	Gland size
1	Nodular, well-defined and smooth edges	Pushing	Single, round to oval, closely packed, but separate glands	Medium
2	Masses less well defined and less well-confined	Some gland separation at tumour edge	Single, separate, round to oval glands, with more variation in gland size and shape	Medium
3A	Ill-defined infiltrating edges	Irregular extension	Single separate glands of variable shape and size, with elongated, angular and twisted forms with wide stromal separation	Medium
3B	Ill-defined infiltrating edges	Irregular extension	Same as 3A but glands are smaller	Small to very small
3C	Masses and cylinders with smooth rounded edges	Expansile	Papillary and cribriform epithelium, without necrosis	Medium to large
4A	Raggedly infiltrative	Diffusely permeative	Fused glands, creating masses, cords or chains	Small, medium or large
4B	Raggedly infiltrative	Diffusely permeative	Similar to 4A but cells have cleared cytoplasm (hypernephromatoid)	Small, medium or large
5A	Smooth, rounded cylinders	Expansile	Papillary, cribriform or solid masses with central necrosis (comedocarcinoma)	Variable
5B	Diffusely infiltrative	Diffusely permeative	Masses and sheets of anaplastic carcinoma, with few tiny glands or signet ring cells	Small

Table 1.1. Gleason grading system adapted from (Humphrey, 2004).

1.1.5.2 Tumour Nodal Metastasis (TNM) classification

The TNM classification of the prostate was first developed in the 1940s by Pierre Denoix, but was updated by the American Joint Committee on Cancer and International Union against Cancer (UICC), in 2002. The system is based on primary tumour (T), lymph node (N), and metastases (M) categories, with each one being built on a series of clinical examinations, radiological imaging, biopsies, and biochemical analyses (Greene and Sobin, 2002). Clinical T staging is the most

important prognostic factor for clinically localised prostate cancer, and is usually carried out using DRE. Regional lymph node metastases meanwhile are strong predictors of progression, and imaging using nomograms is essential for men who have a greater risk of developing metastases. Finally, staging for bone metastases has been widely used as the established norm for distinguishing outlying metastases of the axial skeleton, with MRI being the most reliable means of detection (Borley and Feneley, 2009). The TNM staging is fully described below in Table 1.2, and represented in diagram form in Figure 1.5.

PROSTATE CANCER TNM STAGING

TX - Primary tumour cannot be assessed in prostate
TO - No evidence of primary tumour
TI - Tumour not clinically apparent
TIa-c

T2 - Tumour palpable/confined to prostate
T2a - Tumour involves one prostate lobe

T2b - Tumour involves both prostate lobes

T3 - Tumour palpable and extends beyond prostate capsule
T3a - Tumour extends beyond prostate capsule, either on one side (unilaterally) or both sides (bilaterally)

T3b - Tumour invades seminal vesicles

T4 - Tumour is fixed or invades adjacent anatomy other than seminal vesicles: bladder neck, external sphincter, rectum, levator muscles, and/or pelvic wall

NX - Regional lymph nodes cannot be assessed
NO - No regional lymph node metastasis
NI - Metastasis in regional lymph node or nodes

MX - Presence of distant metastasis cannot be assessed
MO - No distant metastasis
MI - Distant metastasis
MIa - Metastasis to nonregional lymph nodes
MIb - Metastasis to bone
MIc - Metastasis to other distant sites

Figure 1.5: Diagram showing the three categories of TNM classification

(Cancer Update 2005).

18

Stage	Characterisation
Primary tumour (T)	
TX	Primary tumour cannot be assessed
T0	No evidence of primary tumour
T1	Clinically inapparent tumour, neither palpable or visible by inaging
T1a	Tumour (non-palpable) as incidental histological finding at transurethral resection of prostate in 5% of tissue resected
T1b	Tumour (non-palpable) as incidental histological finding at transurethral resection of prostate in >5% of tissue resected
T1c	Tumour (non-palpable) identified by needle biopsy (for elevated serum PSA): includes bilateral non-palpable tumour needle biopsy
T2	Tumour confined within prostate (including prostatic apex, prostate capsule) that is either palpable or visible on imaging or (with p-prefix) demonstrated in radical prostatectomy specimen
T2a	Tumour involving one-half of one lobe or less
T2b	Tumour involving more than one half of one lobe but not both lobes
T2c	Tumour involving both lobes
T3	Tumour extends through prostatic capsule
T3a	Extra-capsular extension (ECE)
T3b	Invasion of seminal vesicle(s)
T4	Tumour fixed or invades adjacent structures: bladder neck, external sphincter, rectum, levator muscles and pelvic wall
Regional lymph nodes (N)	
NX	Regional lymph nodes cannot be assessed
N0	No regional lymph node metastases
N1	Regional lymph node metastases within true pelvis, below common iliac artery bifurication, either unilateral or bilateral
Metastases (M)	
MX	Distant metastases cannot be assessed
M0	No distant metastases
M1a	Non-regional lymph node metastasis
M1b	Metastasis to bone(s)
M1c	Other site(s) of metastasis

Table 1.2: The 2002 TNM classification of adenocarcinoma of the prostate

(adapted from (Borley and Feneley, 2009).

1.1.6 Prostate cancer treatment and management

Treatment for prostate cancer may involve active monitoring, surgery, radiation therapy including brachytherapy and external beam radiation, chemotherapy, hormonal therapy, or a combination of these therapies. Which treatment is chosen depends on the stage of the disease, the Gleason score and serum PSA level. Also to be considered are the age and general health of the patient and his feelings about possible treatments and their side effects.

1.1.6.1 Active monitoring

Active monitoring refers to the process of observing and monitoring without invasive treatment. This is the standard treatment for those with T1a early stage tumours as most men never develop metastases within 10-15 years. It is also used when risks of surgery, radiation therapy, or hormonal therapy outweigh the benefits. Active surveillance entails strict monitoring of a patient's progression by carrying out PSA serum tests, DREs, and tissue biopsies, until further action is carried out, if required (Wu *et al.*, 2004). The age of the patient at the time of diagnosis must also be taken into account when considering active monitoring. As most tumours remain localised for up to 10 years, those with a life expectancy of less than 10 years may view active monitoring as a preferred option to invasive treatment. In younger men a period of three years of active monitoring is more common as the risk of metastasis increases. This treatment delay would allow younger patients to avoid the quality of life impact of invasive treatment until such treatment became necessary.

1.1.6.2 Radical prostatectomy

Radical prostatectomy, which involves the complete removal of the prostate gland, is currently the most common treatment in patients that have organ confined prostate cancer (Bracarda et al., 2005). Previously radical prostatectomy was associated in loss of sexual potency and incontinence. However, developing surgical techniques have reduced the likelihood of patients encountering these complications (Garnick, 1993).

1.1.6.3 Androgen ablation therapy

The male sex hormones, androgens, are essential for the development of the prostate gland and for the growth of early stage hormone-dependent prostate cancer. Locally confined tumours are able to be treated with surgery or radiation but disseminated disease presents a more difficult problem. Early metastatic prostate cancer is usually hormone dependant; this means that it can be treated with androgen ablation treatments that would slow the continued spread of the cancer. Prostate cancer survival depends on the signalling initiated by the androgen receptor in the nucleus of the cells. If androgen receptor activation is prevented then the cell is unable to survive. Unfortunately, androgen ablation therapy rarely cures prostate cancer. This is due to the development of androgen insensitive cancer cells that are able to survive without the presence of androgens. These hormone insensitive cancer cells then continue to disseminate and further treatment measure must be utilised.

Androgen ablation therapy must take into account the complex negative feedback loop that stimulates the production of androgens and their subsequent translocation in to the prostate cell nucleus to initiate transcription of cell survival factors. The majority of androgens are produced by the testes (95%) and the rest is produced by the adrenal glands (5%). Androgens bind to androgen receptors (AR) present in the hypothalamus and stimulate production of luteinising hormone releasing hormone (LHRH). LHRH travels to the pituitary where it interacts with LHRH-receptors. This stimulates the release of luteinising hormone (LH) which is released by the pituitary to bind to LH-receptors in the testes, inducing the production of testosterone, which is synthesised from cholesterol. The testosterone enters the prostate cell and is converted to dihydrotestosterone (DHT) by the enzyme 5α-reductase. DHT has an even higher affinity for the AR than testosterone, and binds tightly to the AR. The binding of DHT causes the AR to be released from the heat shock proteins (HSP) that hold it inactive in the cytoplasm. AR then dimerises and is translocated to the nucleus where is activates the transcription of genes that promote cell survival and growth. Increased testosterone levels can also decrease LHRH and LH production through a negative feedback loop. This maintains the serum testosterone at a physiological level. The testosterone that is produced by the adrenal gland enters the feedback loop alongside the testosterone produced by the testes (Lytton, 2001; Denmeade and Isaacs, 2002).

There are currently two methods to achieve androgen ablation: chemical and physical castration. Physical castration (orchiectomy) involves the removal of one or both (bilateral orchiectomy) of the testes. As the testes produce 95% of testosterone,

orchiectomy results in a massive drop in serum testosterone levels. This in turn results in the atrophy of the tumour. However, due to the psychological effects of orchiectomy, chemical castration is the preferred method (Fan, 2002).

The first method of chemical castration was developed by Huggins and Hodges in 1941. They developed the synthetic oestrogen diethylstilbestrol (DES) for use as a reversible form of chemical castration. DES inhibits the release of luteinising hormone releasing hormone (LHRH) from the hypothalamus. However, this drug induced significant side effects including cardiovascular complications (Blackard *et al.*, 1970) and new drugs were developed. The most commonly used drugs are LHRH agonists, these include goserelin, leupolide and buserelin. Treatment with these agonists causes LHRH receptor desensitisation and inhibition of LH and testosterone production. LHRH agonists initially cause in increase in LH production which in turn causes increased production of testosterone (Tammela, 2004). This testosterone 'flare' can result in severe bone pain, obstructive renal failure, spinal cord compression and fatal cardiovascular problems (Heidenreich *et al.*, 2008) for some patients for the first 1-2 weeks of treatment. However, with continued use, after around 2-3 weeks, the high levels of testosterone act to down-regulate LHRH receptors of the pituitary, resulting in a reduction in LH and testosterone levels (Vilchez-Martinez *et al.*, 1979). Side effects are rather mild and include; hot flashes, fatigue, reduced libido, impotence, and weight gain. This method therefore proves to be a successful form of chemical castration, and results compare to surgical and DES castration with significant reductions in PSA levels in 70-80% of patients, and a decrease in pain in 60-80% (Tolis *et al.*, 1982).

Another form of drug affecting LHRH is the LHRH antagonists such as, abarelix, degarelix and cetrorelix. These antagonists occupy the LHRH receptors on the anterior pituitary and prevent LHRH binding. This causes a major and rapid reduction of LH and serum testosterone levels. LHRH antagonists also have the advantage of not inducing a testosterone flare that is present with LHRH agonists (Kirby *et al.*, 2009).

The final type of androgen ablation drugs are the anti-androgens such as, the non-steroidal Flutamide, Bicalutamide, and Finasteride. These drugs function by competitively inhibiting the binding of testosterone and DHT to the AR and by inhibiting the activity of 5-α reductase. This prevents the activation of the AR and subsequent transcription of growth and survival factors (Vis and Schroder, 2009). However, these drugs have the ability to cross the blood-brain barrier raising the LH secretions and, therefore testosterone secretion in the testes making monotherapy with anti-androgens a less preferable method of androgen ablation (Tammela, 2004).

Also important for the achievement of total androgen blockade is the removal of adrenal androgens. The removal of the adrenal glands, adrenalectomy, is often performed along with chemical or surgical castration to produce total androgen blockade. This offers the complete removal of serum testosterone and offers a survival benefit to those with only a testicular androgen blockade (Samson *et al.*, 2002). See figure 1.6 for a diagrammatical overview of androgen ablation therapy.
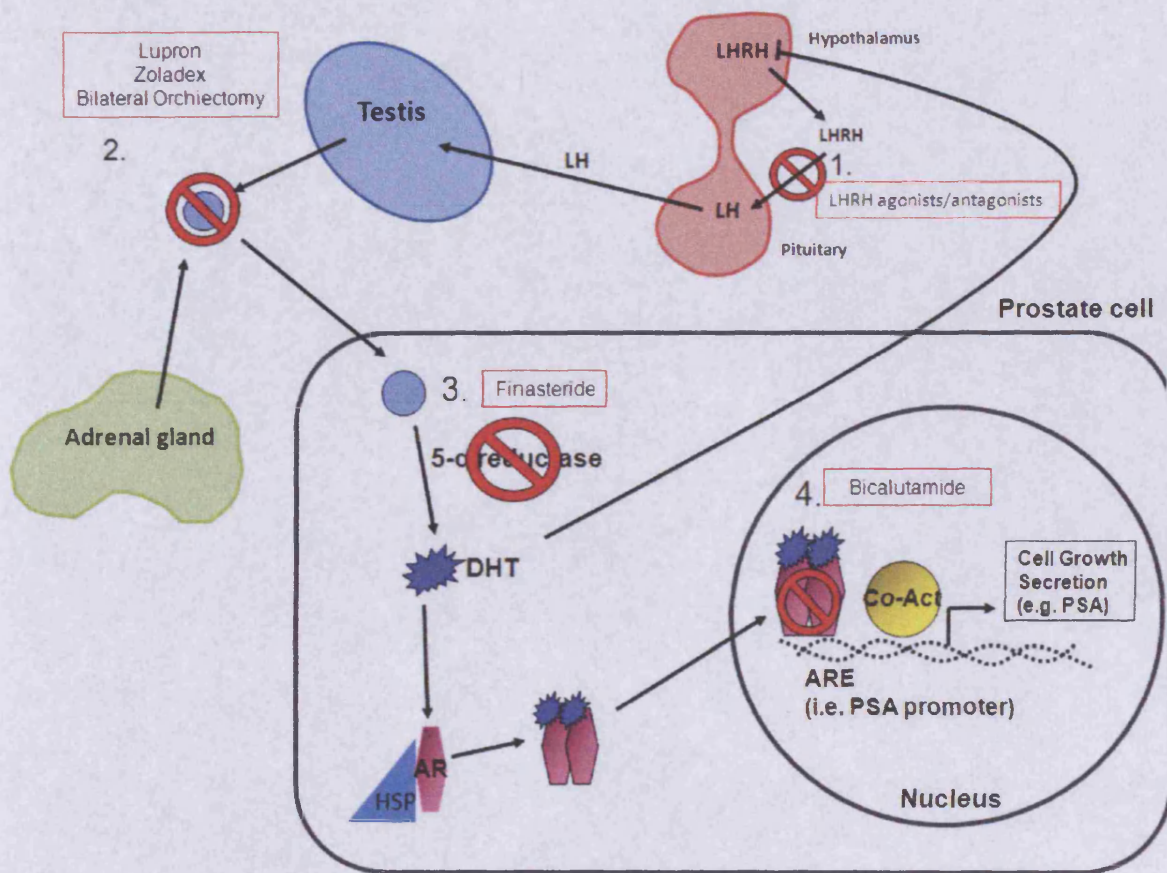
Figure 1.6: Schematic diagram detailing methods of androgen ablation therapy. **1.** LHRH agonists and antagonists prevent release of luteinising hormone (LH) which inhibits the production of testosterone in the testes. **2.** Chemical and surgical castration prevents release of androgens into blood circulation. **3.** Finasteride is a synthetic anti-androgen that acts by inhibiting type II 5-alpha reductase, the enzyme that converts testosterone to dihydrotestosterone (DHT). **4.** Bicalutamide acts as a pure anti-androgen by binding to the androgen receptor (AR) and preventing the activation of the AR and subsequent up-regulation of androgen responsive genes by androgenic hormones. Adapted from (Garnick, 1993).

1.1.6.4 Radiation therapy

Radiation therapy is used to treat all stages of prostate cancer and uses ionising radiation to cause DNA damaging in the cells receiving the radiation. Cancer cells are less able to repair the damage and subsequently have a higher rate of death. There are two main types of radiation therapy: external beam radiotherapy and brachytherapy. External beam radiotherapy involves targeting the prostate and immediately surrounding tissue with a high level radiation beam. This allows a specific area to be treated, although inflammation of the bladder and rectum is inevitable due to the placement of the prostate gland. Treatment occurs over a number of weeks during which time the inflammation to surrounding structures occurs. Brachytherapy involves inserting a number of small radioactive 'seeds' directly into the prostate, guided by TRUS imaging, under either general or spinal anaesthesia. These seeds emit lower-level radiation that only travels a short distance enabling the radiation to be confined to the prostate. This method minimises the damaging effects on the bladder and rectum that are caused by external beam radiation therapy (Garnick, 1993).

1.1.6.5 Chemotherapy

While many patients initially respond well to androgen ablation therapy, in time the patients develop hormone refractory disease. This form of disease does not depend on androgen for survival and therefore is immune to conventional hormone ablation therapy and is often fatal. Chemotherapy is the last resort for those with hormone refractory disease, although treatment with cytotoxic compounds will only extend the life of the patient for a number of months. A combination of compounds

is often used in treatment, such as estramustine, vincristine, etoposide, doxorubicin and the taxanes paclitaxel and docetaxel (Pienta *et al.*, 1994; Sella *et al.*, 1994; Hudes *et al.*, 1997; Savarese *et al.*, 2001).

1.1.6.6 Angiogenesis inhibitors

Angiogenesis is a necessary requirement for the metastasis of cancer. As cancer growth is dependent on the diffusion of nutrients and waste, establishing a blood supply is crucial for the continued enlargement of the tumour. Investigation into the mechanisms that initiate angiogenesis has led to the development of novel therapies that target the angiogenic pathway. There is some possible advantage to using angiogenesis inhibitors over cytotoxic chemotherapy. As most cells are not actively relying on angiogenesis, treatment with angiogenesis inhibitors will be more accurately targeted to cancer cells than a cytotoxic compound and will have a lower level of toxicity to normal non-cancerous cells. Some of the angiogenesis inhibitors that are currently being investigated are Bevacizumab, Sorafenib, Sunitinib, Thalidomide and Imatinib (Hwang and Heath, 2010).

1.2   Cancer metastasis

The metastasis of cancer to secondary sites in the body is responsible for the majority of cancer related deaths. There is however, no curative treatment for cancer metastasis. Due to this fact metastasis is the subject of intense research in the hope of producing treatments to delay or even prevent the process of metastasis. Prostate

cancer metastasis is a complex multi-stage process that involves several crucial steps that facilitates the spread of the cancer cells to secondary sites. The steps involve mutation of cells, epithelial to mesenchymal transition (EMT), degradation of the extracellular matrix (ECM), invasion, angiogenesis, intravasation, extravasation and colonisation of secondary sites.

1.2.1 Metastatic process

Metastasis has long remained poorly understood due to its increasing complexity. In order for cancer cells to metastasis they must undergo several epigenetic changes that facilitate their spread around the body. In order for the primary tumour to arise it must accumulate genetic changes that drive the cell toward a cancerous phenotype from which the cells can progress to metastasis. An overview of this process is given in figure 1.7.

1. Mutation and uncontrolled cell growth

2. Invasion and migration through ECM and degredation of basement membrane

3. Angiogenesis, intravasation and cancer cell dissemination

4. Cancer cell adhesion and extravasation

5. Migration and metastasis to distant sites
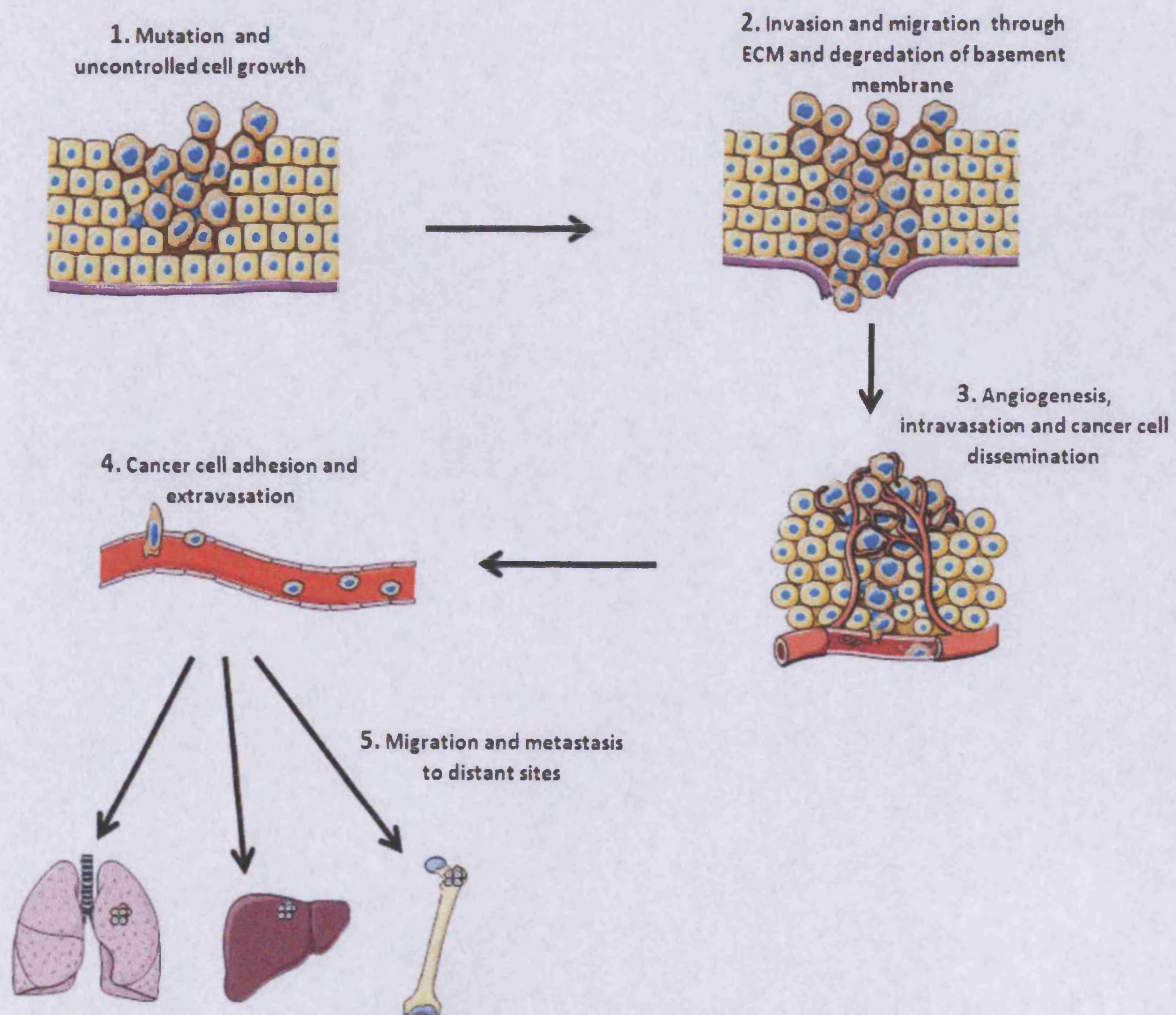
Figure 1.7 The metastatic process. Diagram detailing the process through which cancer arises and metastases.

Local invasion is a crucial step in early metastasis. Without the ability to invade through surrounding tissues, metastasis cannot occur. In order to begin the process of local invasion the cells must acquire an invasive and motile phenotype by down-regulating cell-cell, and cell-matrix adhesion. A major mechanism in the loss of adhesion is the loss of the tumour suppressor gene, E-cadherin. The loss of E-cadherin induces cell detachment and invasive potential (Frixen et al., 1991). The loss of E-cadherin can also potentially indicate outcome for cancer patients (Hong et al., 2011). E-cadherin also plays an important role in epithelial to mesenchymal transition (EMT). Cells are required to undergo this process to become metastasising cells. The transition involves the loss of cell polarity, and cell-cell binding, as the cells take on a mesenchymal phenotype and increase their expression of N-cadherin, granting them with the ability of invading the extracellular matrix (ECM) and breaking through the basement membrane (BM). It does this by using degrading enzymes such as those in the matrix metalloprotease (MMP) family (Overall and Lopez-Otin, 2002). Over-expression of MMP-21 is associated with poor survival of colorectal cancer patients (Huang et al., 2011).

Cell motility is also a key factor in the metastasis of many types of cancer cells. Cell motility and migration depend on GTP-binding proteins such as Ras and Rho, which are involved in processes such as cytoskeletal construction, intracellular signalling, as well as whole cell, and cell membrane movement (Oxford and Theodorescu, 2003). Ras for example, regulates cell proliferation, gene transcription, apoptosis, and invasion. Rho GTPases act downstream of Ras, and regulate actin dynamics to lead cell growth and movement, important during cell migration and

prostate metastasis. Their importance was proven when the use of inhibitors to the Rho-Ras pathway resulted in a reduction of the migratory and motile capacity of prostate cancer cells, suggesting that the pathway is activated during metastasis (Sequeira *et al.*, 2008). RhoC especially has been highly implicated in the development, invasion and metastasis of prostate cancer (Iiizumi *et al.*, 2008; Bu *et al.*, 2011).

As a primary tumour grows, it requires more oxygen and nutrients in order to progress. In order to overcome this problem, it starts to develop new blood vessels through the secretion of angiogenic factors such vascular endothelial growth factor (VEGF), reviewed in (Saharinen *et al.*, 2011), allowing a greater flux of resources to build up, and the tumour to grow. In addition, these blood vessels offer a means of escape for the cancer cells to leave the primary tumour, penetrate into the vessel, and shed into the blood's circulatory system through a process called intravasation. This process involves multiple adhesive interactions, and is facilitated by the loss of CD82, normally responsible for anchoring tumour cells to the endothelium (Bandyopadhyay *et al.*, 2006).

Alternatively, some tumour cells might also enter the circulation through the lymphatic system. Cancer cells can invade the lymphatics in the primary site, where they are drained into the lymph nodes, and enter the blood circulation either via efferent lymphatic vessels that end up in the venous system, or by newly formed blood vessels serving the lymph node metastases (Paget, 1989). Tumour cells are then disseminated throughout the body, where the vast majority are destroyed during cellular clearance from the circulation, mainly due to their large size. The 0.1% that

do survive, probably do so by aggregating with platelets in the blood, concealing them from immune surveillance through the production of chemokines, cytokines, and growth factors (Im *et al.*, 2004). These cells need to survive long enough in order to colonise a distant site of preference.

The idea that metastasising cancer cells can 'home' to a specific organ was first recognised by Paget over a hundred years ago with the proposal of the 'seed and soil' hypothesis. This states that certain cancer cells (seeds) will only capably grow in a specific site (soil) (Paget, 1989). The specificity of certain cancers to metastasise to a specific organ is often seen in the propensity of prostate and breast cancer to spread commonly to the bone. However, more recent research has proposed that this propensity is likely due to the ability of a particular cancer type to grow in the microenvironment of a specific organ, so 'the compatibility of the 'seed' with the 'soil'.

Upon arrival at the distant site, the cancer cells arrest on the endothelial surface of the blood vessel and undergo transendothelial migration, a process involving numerous adhesive interactions initially involving selectins and stabilised by integrin binding (1995). Once within the secondary site, the new micro-environment surrounding the metastatic cells is initially hostile and the survival of the cells depends on their molecular features and the ability to successfully engage in cross-talk with their surrounding environment. In addition, growth-factor receptor ligand interactions between the cancer cells and host cells result in an interactive signalling loop, thereby up-regulating survival pathways and angiogenesis (Derynck

et al., 2001). These processes allow the cells to survive and establish themselves in their new environment, developing a secondary tumour.

1.3   Prostate cancer metastasis

Advanced prostate cancer has a very high tendency to metastasise. This presents a huge clinical challenge in treating the disease. The most common sites of prostate cancer metastasis are the bone, lymph nodes, liver, lungs and dura (Edwards *et al.*, 2003; Taplin *et al.*, 2003). Bone metastases are most common in the red bone marrow of the axial skeleton and occur in approximately 90% of patients with advanced disease and are a leading cause of morbidity (Bubendorf *et al.*, 2000). Once the tumours spread to the bone they are virtually incurable and lead to several complications such as severe pain, pathological fractures, hypercalcaemia and compression syndromes. Due the almost incurable nature of these metastases the treatments currently available are mostly palliative.

1.3.1   Bone metastases

As stated above the bone is the most common site of prostate cancer metastasis. Bone metastasis initiates in the same manner as in section 1.2.1 but undergo several genetic and phenotypic changes that enable the metastasising cells to interact with the bone micro-environment. One theory for the propensity of bone metastasis is the placement of the Batson's Plexus. This is a collection of veins that surround the prostate and connects to the venous drainage of the spine and may provide a short-

cut for metastasising tumour cells (Batson, 1995). Elevated expression of BMPs and TGF-β in prostate cancer cells has been implicated in bone metastases (Paget, 1989; Autzen *et al.*, 1998; Shariat *et al.*, 2001). Vascular endothelial growth factor (VEGF) secreted by the tumour cells may also contribute to bone metastasis because of the promotion of angiogenesis and activation of osteoblasts (Chen *et al.*, 2004; Dai *et al.*, 2004). These features can direct the metastases to the bone. Another theory that was proposed over a century ago is the 'seed and soil' theory by Steven Paget. He compared the distribution of cancer cells to the dispersal of plant seeds. He proposed that osteotropic cancer cells possess certain attributes that enable them to grow in a particular environment and the bone micro-environment provides a fertile soil in which the cancer cells can thrive (Paget, 1889).

1.3.1.1 Bone micro-environment

The bone micro-environment is as important to facilitating bone metastases as the metastasising cancer cells themselves. Bone is a highly mineralised tissue that provides mechanical support and metabolic functions to the skeleton. It can be formed by either intramembranous ossification or endochondral ossification. Intramembranous ossification occurs when mesenchymal precursor cells differentiate directly into bone-forming osteoblasts, a process utilised in adding new bone to the outer surfaces of long bones as well as in generating the flat bones of the skull. In comparison, endochondral bone formation involves the conversion of an initial cartilage template into bone. This process is responsible for generating the majority of the bones of the skeleton (Erlebacher *et al.*, 1995).

The bone itself is an organic matrix that is strengthened by deposits of calcium salts. Type-1 collagen constitutes approximately 90-95% of the organic bone matrix and non-collagenous proteins comprise the remaining 5-10%. Crystalline salts deposited in the matrix are primarily calcium and phosphate in the form of hydroxyapatite (Erlebacher *et al.*, 1995). The non-collagenous proteins can be sub-divided into 1) cell attachement proteins, 2) proteoglycans, 3) γ-carboxylated (gla) proteins, and 4) growth factors (Robey *et al.*, 1993). Adult bone is being constantly remodelled in a process that ensures that the rate of bone formation is in equilibrium with bone resorption. Most bones have a centre that consists of spongy bone or a bone cavity, which are lined by endosteal cells. These spaces are occupied by red or yellow bone marrow. The bones containing red bone marrow are the flat bones, such as the iliac crest and sternum, and at the proximal ends of the long bones femur and humerous. These bones are the most often affected by cancer metastases indicating the red bone marrow may have a role in cancer metastasis (Galasko, 1986).

1.3.2 Osteoblastic metastases

Prostate cancer predominantly produces osteoblastic metastases. Osteoblasts are derived from mesenchymal cells and their growth and differentiation are regulated by complex signalling pathways mediated by growth factors such as bone morphogenetic proteins (BMPs), insulin-like growth factor (IGF)-I and IGF-II, transforming growth factor-β1 (TGFβ1) and TGFβ2, fibroblast growth factor (FGF), platelet-derived growth factor (PDGF), and Wnt (Canalis, 1980; Hauschka *et al.*, 1986; Globus *et al.*, 1988; Wang *et al.*, 1990). The cells secrete a collagen-

proteoglycan bone matrix known as osteoid, capable of binding calcium salts which induces its mineralisation, converting it to bone. This bone matrix deposition occurs in both intramembraneous and endochondral bone formation, and is regulated with spatiotemporal coordination by a variety of endocrine, paracrine, and autocrine factors (Ducy et al., 1999).

Analysis of prostate cancer bone metastases has typically shown that a large number of osteoblasts adjacent to the prostate cancer cells. This is in contrast to other cancer metastases, which usually contain a large number of osteoclasts (Logothetis and Lin, 2005). tases from other cancers (such as breast, lung, and kidney), which largely contain osteoclasts. The increase in prostate cancer bone-forming activity gives rise to a woven bone, characterized by an osteosclerotic appearance distinct from the typical lamellar structure seen in normal bone. These lesions are associated with an increase in bone mass at the lesion site, and often have an elevated osteoid surface area, osteoid volume, and mineral apposition rate. An increase in serum levels of osteoblast proliferation markers, such as bone-specific alkaline phosphatise and type-1 protocollagen C-propeptide, has been observed in patients with metastatic prostate cancer (Jung et al., 2004). Several studies have confirmed the involvement of osteoblast cells in prostate cancer metastasis. One study showed that factors secreted by bone fibroblasts, but not other cells, accelerated prostate cancer growth (Gleave et al., 1991)and the stimulation of prostate cancer cells grown in osteoblast-like cell culture medium (Fizazi et al., 2003).
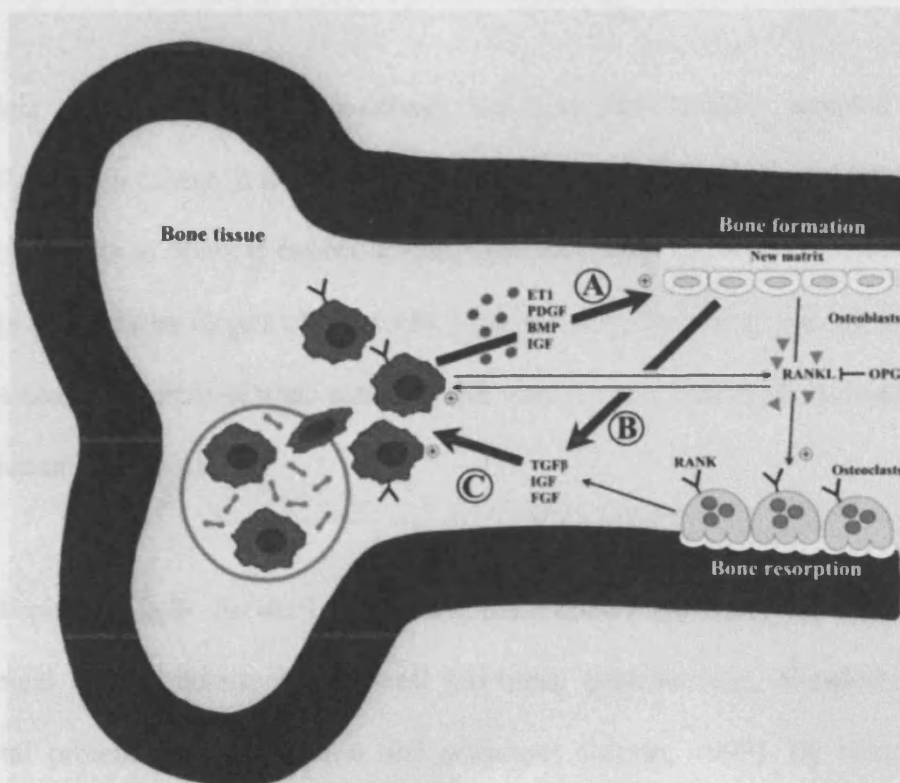
Figure 1.8 The vicious cycle of osteoblastic bone metastasis is shown. **(A)** Prostate cancer cells secrete osteogenic growth factors, activating osteoblasts to deposit new bone matrix. **(B)** Osteoblasts secrete a range of additional factors such as insulin-like growth factor (IGF), fibroblast growth factor (FGF), and transforming growth factor-β (TGFβ). **(C)** These factors attract prostate cancer cells, further enhancing their proliferation and growth. ET1 indicates endothelin 1; PDGF, platelet-derived growth factor; BMP, bone morphogenetic protein; RANK, receptor activator of the nuclear factor-jB; RANKL, RANK ligand; OPG, osteoprotegerin. Taken from (Ibrahim *et al.*, 2010)

1.3.3 The role of β-catenin in prostate cancer

The nuclear signalling molecule β-catenin has long been widely accepted as an oncogene in human cancer. It acts a co-factor for the AR which further substantiates the ability of β-catenin to promote cancer development and progression (Mulholland et al., 2002). The downstream targets of β-catenin, such as cyclin-D1 and c-myc, play a large role in the development of prostate cancer which adds to the evidence of the importance of β-catenin in human cancer.

In normal epithelial cells, β-catenin is found at the plasma membrane where it provides a mechanical linkage between cell-to-cell junctional proteins (e.g., E-cadherin) and cytoskeletal proteins (e.g., α catenin and actinin-4) (Morin, 1999). By contrast, in tumour cells, β-catenin is often found in the cytoplasm and nucleus where it associates with TCF family members to form a complex, which activates transcription of pro-mitotic proteins including c-Myc and cyclinD1 (Figure 1.9). Nuclear transduction of β-catenin also occurs as part of the epithelial-mesenchymal transition (EMT) process, which is essential to organ development in the embryo. The importance of EMT in the progression of prostate cancer is widely known. As β-catenin plays a central role in EMT this reiterates the importance of β-catenin in prostate cancer progression.

A great deal of current biomedical research is directed towards determining the signal transduction pathways that modulate β-catenin localisation, degradation, and function. It has been recently established that phosphorylation of β-catenin by Src is necessary for its dissociation from E-cadherin (Coluccia et al., 2006). β-catenin is additionally phosphorylated by the glycogen synthase kinase 3-β: adenomatous polyposis coli

(GSK:APC) complex leading to its ubiquination and proteosome-mediated degradation. Significantly, GSK3 activity is decreased by the canonical Wnt signaling pathway, which involves the growth factor Wnt, the Wnt receptor Frizzled, and associated regulatory proteins such as Disheveled and Frat (Krishnan *et al.*, 2006). Thus, increased Wnt signaling results in diminished phosphorylation and reduced degradation of β-catenin, and accumulation of β-catenin in the cytoplasm and nucleus.

Downstream components of the β-catenin signalling pathway have been implicated in several human cancers, not just in prostate. Abberant up-regulation of β-catenin nuclear activity is possibly due to APC deficiency or β-catenin mutations that prevent its degredation and leads to accumulation of β-catenin in the cytoplasm. This accumulation subsequently results in increased nuclear transduction and therefore to increased β-catenin target gene transcription. Because of this there has been huge interest in developing therapeutics to block the signalling of β-catenin for treatment of cancer. To date many therapeutics aim to disrupt TCF/ β-catenin interaction and to stabilise axin as this promotes the degredation of β-catenin.

There is very little information regarding the involvement of β-catenin with serine proteases. The TTSP family members are in an ideal location to affect the signals that are passed across the plasma membrane. As the regulation of β-catenin is dependent on signalling cascades initiated from the cell membrane, TTSP family members are ideally located to affect signals that originate on the extracellular surface. β-catenin was selected to be examined in this study based on unpublished data from a previously conducted study. As matriptase-2 was found to affect the migratory and adhesive

capabilities of PC3 and DU145 cells a screen of molecules involved in cell:cell and cell:matrix adhesion was performed in an attempt to determine if any of these molecules had been altered by the presence of matriptase-2. β-catenin was identified as a molecule of interest from this panel of molecules. Due to the fact that β-catenin is already a well known oncogene and has already been shown to be highly deregulated in prostate cancer it was felt that the involvement of matriptase-2 with the regulation of β-catenin warranted further investigation.
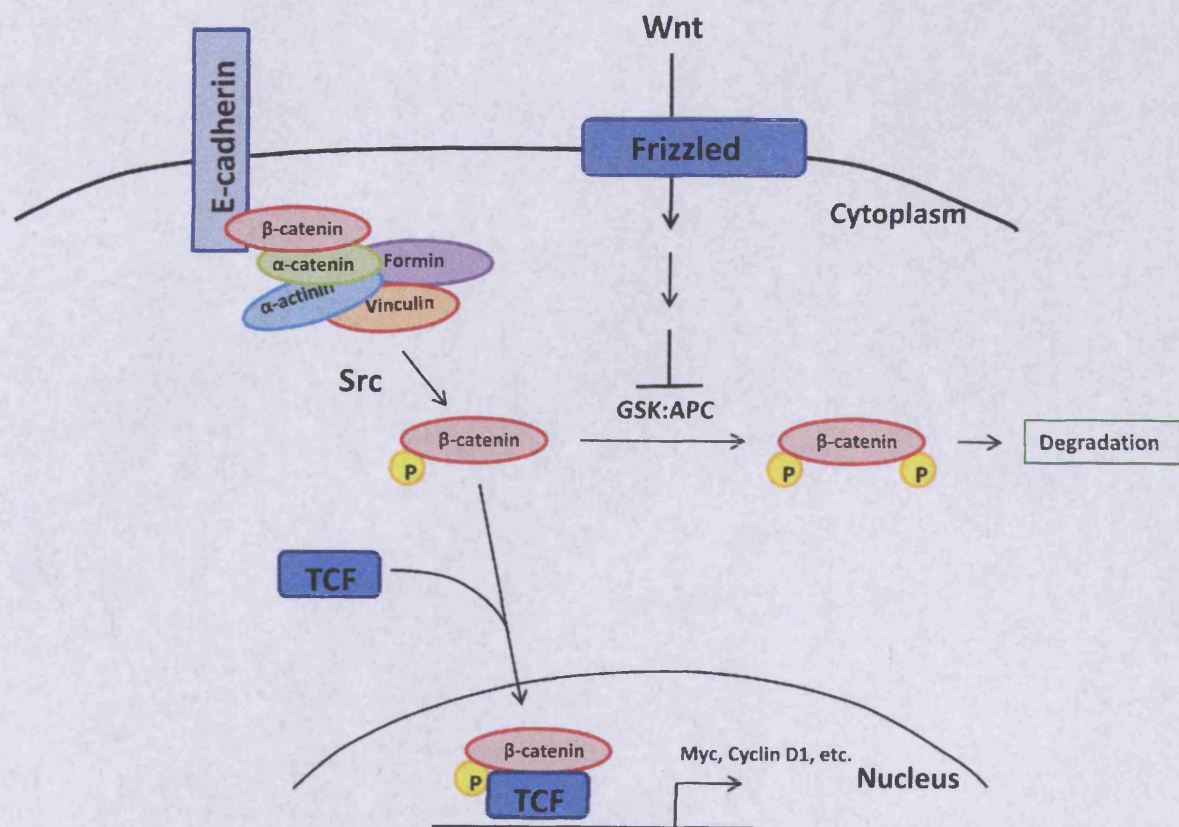
Figure 1.9 Signal transduction pathways modulating β-catenin localization and degradation (Adapted from ValaSciences).

1.4 Type II Transmembrane Serine Proteases (TTSP)

Cell surface proteolysis has become known as an important mechanism for the activation of proteins involved in managing a wide range of cellular functions. The chymotrypsin (S1) fold group, of which trypsin and chymotrypsin are prototypic members, are one of the largest subfamilies of the serine proteases, one of the largest and most conserved (Rawlings and Barrett, 1994) family of proteases. Recently, a group of S1 serine proteases has been recognized that possess domains which anchor them directly to cell membranes. These are the type I and type II serine proteases. Type I serine proteases are anchored to the cell membrane with a carboxy-terminal transmembrane domain (Wong et al., 1999) . The type II transmembrane serine proteases (TTSPs) are anchored to the membrane via an amino-terminal transmembrane domain with a cytoplasmic extension (Netzel-Arnett et al., 2003). Members of the TTSP family include enteropeptidase (Maestracci et al., 1975) matriptase/MT-SP1 (Lin et al., 1999), matriptase-2/TMPRSS6 (Velasco et al., 2002), matriptase-3/TMPRSS7 (Szabo et al., 2005), TransMembrane PRoteaSe Serine 1 (TMPRSS1) /Hepsin (Leytus et al., 1988), TransMembrane PRoteaSe Serine 2 (TMPRSS2) (Paoloni-Giacobino et al., 1997), TransMembrane PRoteaSe Serine 3 (TMPRSS3) (Scott et al., 2001), TransMembrane PRoteaSe Serine 4 (TMPRSS4) (Wallrapp et al., 2000), TransMembrane PRoteaSe Serine 5 (TMPRSS5)/spinesin (Yamaguchi et al., 2002), TransMembrane PRoteaSe Serine 9 (TMPRSS9)/polyserase-1 (Hayama et al., 2007), Corin/TMPRSS10 (Yan et al., 1999), Differentially expressed in squamous cell carcinoma gene 1 (DESC1) (Lang and Schuller, 2001) and Human airway trypsin-like (HAT) (Yamaoka et al., 1998) (See Table 1.3 for summary) (Figure 1.10).

Based on the phylogenetic analysis of the serine protease domains and the domain structure of the extracellular stem region, the TTSPs have been divided into four subfamilies (Szabo *et al.*, 2003). The largest of these is the HAT/DESC subfamily which consists of HAT, DESC1-4 and HATL3, 4 and 5. The second subfamily is the Hepsin/TMPRSS family which is comprised of TMPRSS2-5, hepsin and enteropeptidase. The next family is the matriptase subfamily which includes matriptase, matriptase-2, matriptase-3 and polyserase-1. The final subfamily is the corin subfamily of which the only member is corin.

Protease	Alternate name	Chromosomal localisation	Molecular weight (kDa)
Matriptase-1	MT-SP1/TADG-15	11q25	95
Matriptase-2	TMPRSS6	22q12-13	89
Matriptase-3	TMPRSS7	3q13.11	101
TMPRSS9	Polyserase-1	19p13.3	114
Hepsin	TMPRSS1	19q13.1	51
TMPRSS2	Epitheliasin	21q22.3	53.8
TMPRSS3	TADG-12	21q22.3	49
TMPRSS4	TMPRSS3	11q23.3	68
TMPRSS5	Spinesin	11q23.3	52
Enteropeptidase	Enterokinase	21q21	156
Corin	TMPRSS10	4p12-13	116
HAT	-	4q13.2	48
DESC1	-	4q13.3	47
DESC2	-	4q13.3	46.2
DESC3	-	4q13.3	44

Table 1.3. Summary of human membrane anchored serine proteases
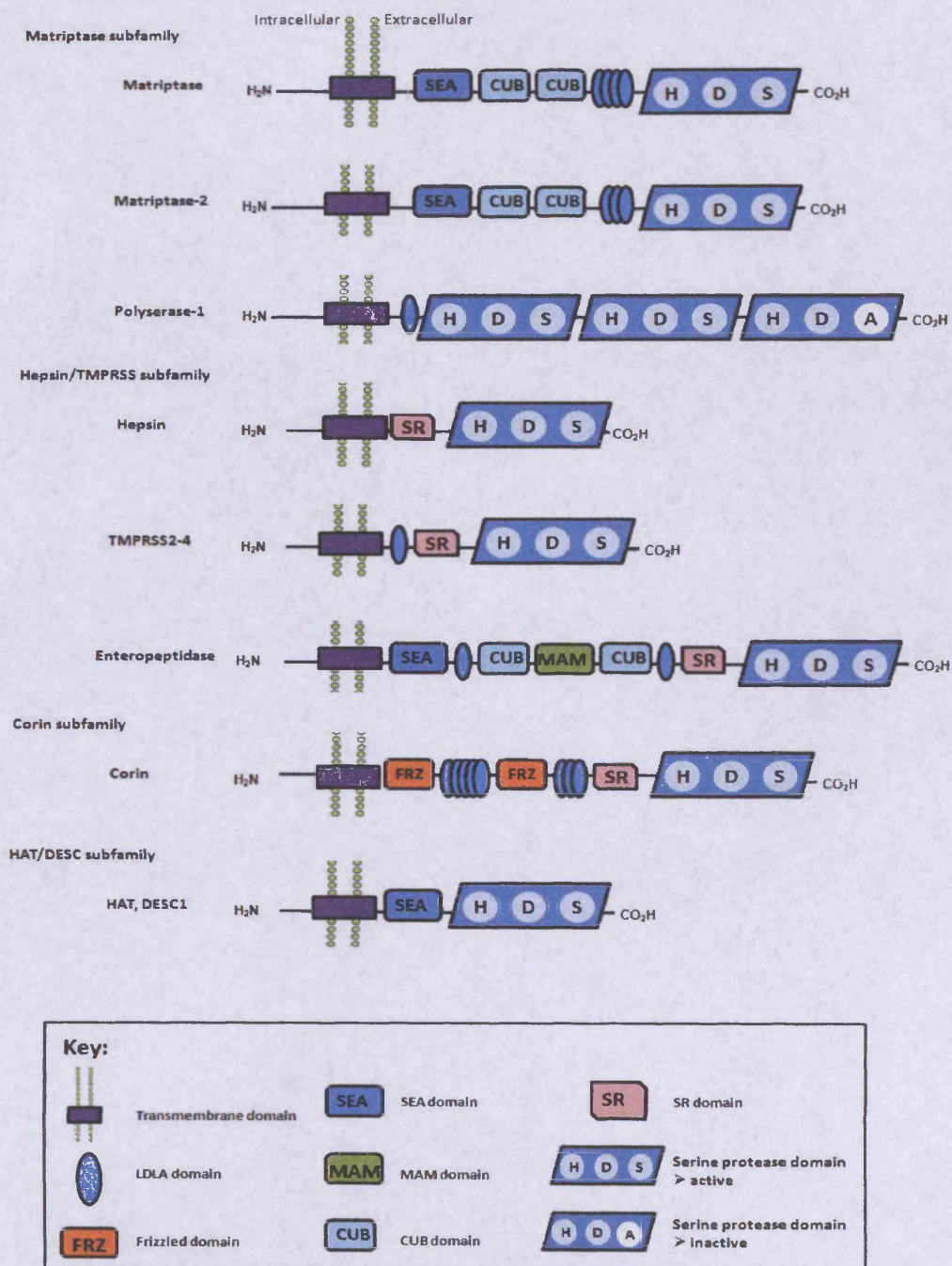
Figure 1.10 Multi-domain structures of human type II transmembrane serine proteases.

Structures are grouped according to phylogenetic analysis. Adapted from (Netzel-Arnett *et al.*, 2003)

1.4.1 General structure and function

The TTSPs are characterized by a single pass transmembrane domain which separates the short intracellular region from the larger, more variable, extracellular section of the protease. The extracellular section is composed of a stem region of variable length and a C-terminal serine protease domain containing histidine (H), aspartate (D), and serine (S) residues essential for catalytic function (Hooper *et al.*, 2001; Szabo *et al.*, 2003; Choi *et al.*, 2009). The N-terminal cytoplasmic domain of TTSPs may allow signal transduction across the plasma membrane and effect changes within the cell (Fig. 1.11).
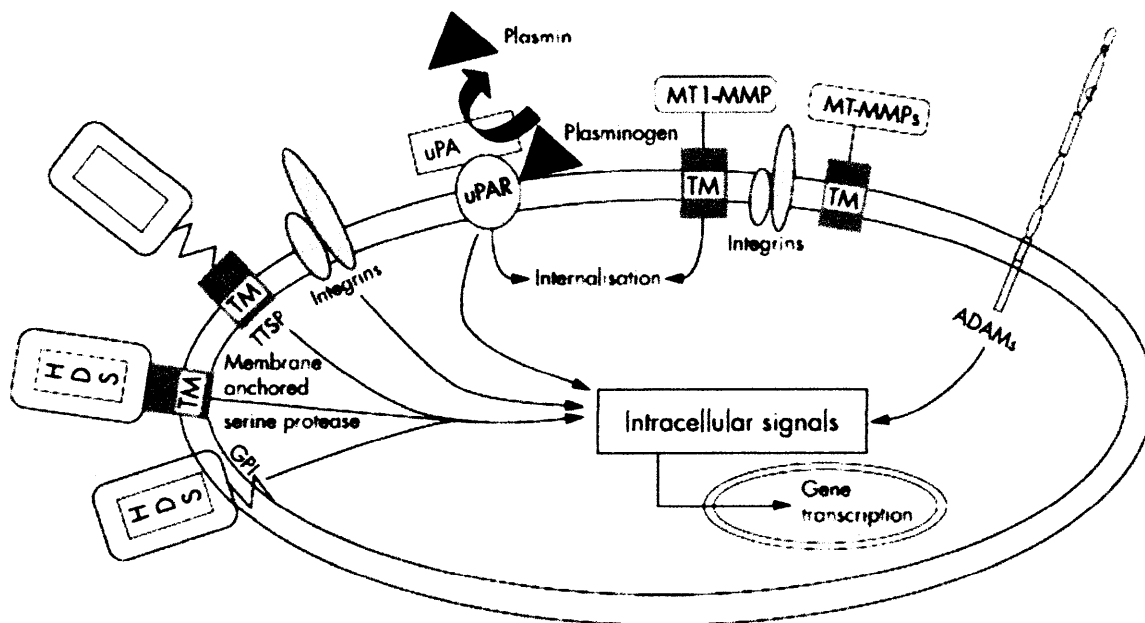
Figure 1.11 Potential for intracellular signalling through membrane bound proteases.

Metalloproteases (MTMMPs, ADAMs), membrane anchored serine proteases (SPs), TTSPs, and the plasminogen/plasmin system are adequately positioned at the plasma membrane to participate in a cascade of protease activation, to activate receptors, growth factors, and cytokine/chemokines, to shed cell surface molecules, and to participate in extracellular matrix (ECM) remodelling. Taken from Noel *et al* (Noel *et al.*, 2004).

The stem region of TTSPs is believed to regulate diverse processes and contain as many as 11 structural domains that may serve as regulatory and/or binding domains (Hooper *et al.*, 2001; Choi *et al.*, 2009)(Figure 1.11). These include a low density lipoprotein (LDL) receptor domain class A, which binds Ca2+ and is involved in the binding of lipoproteins (van Driel *et al.*, 1987; Esser *et al.*, 1988), Cls/Clr urchin embryonic growth factor (CUB) domain, a (SEA) domain named after the first three proteins it was identified in (sperm protein, enterokinase and agrin), a group A scavenger receptor domain (SR), frizzled (FRZ) and meprin, A5 antigen and receptor protein phosphatise µ domain (MAM) in various combinations in each of the TTSPs (Hooper *et al.*, 2001; Netzel-Arnett *et al.*, 2003; Szabo and Bugge, 2008). The catalytic activity of the serine protease domain is dependent on the presence of the previously mentioned residues histidine, aspartate and serine (Szabo and Bugge, 2008). This domain activates or degrades protease activated receptors (PARs) (Choi *et al.*, 2009), cytokines, growth factors and components of the extracellular matrix (Del Rosso *et al.*, 2002; Lopez-Otin and Matrisian, 2007). Soluble forms of several TTSPs have been detected. This suggests that the extracellular domains of these proteases may be shed from the cell surface (Louvard *et al.*, 1973; Yamaoka *et al.*, 1998; Lin *et al.*, 1999; Afar *et al.*, 2001). The mechanisms involved in the regulated release of these extracellular domains and whether release may occur in response to specific cellular signals or environments have yet to be fully characterized.

Although the functional purpose of these proteases is largely unknown, the TTSPs have gained intense attention from the field of cancer research. This interest in TTSPs stems from the observation that many of them are aberrantly expressed in tumours compared to normal tissue. Increasing evidence demonstrates that this aberrant expression of TTSPs is a hallmark of several cancers and recent studies have attempted to define the molecular mechanisms underlying TTSP-promoted carcinogenesis. Loss of the basement membrane is a mandatory step that occurs during local invasion early in the metastatic process (Abate-Shen and Shen, 2000; Robinson *et al.*, 2004). To accomplish local invasion, tumour cells use extracellular and cell surface proteolytic enzymes to degrade the basement membrane proteins (Chang and Werb, 2001; Del Rosso *et al.*, 2002). The TTSP family is ideally located to perform this crucial task. Many recent studies have focused on the expression of specific TTSPs during tumourigenesis and their potential to influence tumour cell proliferation, motility and invasion (Szabo and Bugge, 2008).

1.4.2 Matriptase subfamily

1.4.2.1 Matriptase/MT-SP1

Matriptase, also known as MT-SP1, has been identified in the epithelial components of the prostate, stomach, small intestine, colon, lung, kidney, placenta and peripheral blood leukocytes (Takeuchi *et al.*, 2000; Oberst *et al.*, 2003). Matriptase protein is 95kDa in length and is composed of a short cytoplasmic extension with unknown function, a transmembrane domain, a SEA domain, two CUB domains, four tandem repeats of a LDLA domain and a C-terminal active serine protease (Netzel-Arnett *et al.*,

2003; Szabo *et al.*, 2003; Uhland, 2006) (Figure 1.10). Matriptase is expressed as a zymogen that has to be activated by proteolytic cleavage to gain its biological function. The activation site is located directly N-terminal to the catalytic domain. Once processed, the active catalytic domain stays attached to the membrane by a disulfide bond linking the pro-domain to the catalytic domain (Lin *et al.*, 1999; Takeuchi *et al.*, 2000) unless it is shed at either of the shedding sites at residues 190 or 205 (Oberst *et al.*, 2003; Oberst *et al.*, 2003). Shed matriptase has been found in a complex with hepatocyte growth factor activator inhibitor (HAI-1) in human milk, indicating that HAI-1 might be a cognate inhibitor of the protease. Paradoxically, HAI-1 has not only inhibitory function, but is also required for matriptase activation (Oberst *et al.*, 2003). This is thought to ensure that matriptase can be quickly inactivated once it is set free from the membrane to protect the cells from uncontrolled matriptase activity (Uhland, 2006). However, a recent study by Miyake *et al* using stably transfected canine kidney cells, proposes that matriptase activation does not require HAI-1 (Miyake *et al.*, 2010).

Due to its notably consistent expression in tumours of epithelial origin, matriptase has received significant attention in the field of cancer biology. This protease was first described as a matrix degrading enzyme with major gelatinolytic activity in breast carcinoma (Shi *et al.*, 1993; Lin *et al.*, 1997), and was later found to be expressed in a wide variety of other benign and malignant tumours of epithelial, but not mesenchymal, origin. In most carcinomas, tumour progression is associated with a significant increase in matriptase mRNA and protein expression. Matriptase has been found to be up-regulated in many epithelial tumours, including breast, colon, kidney, liver, lung, mesothelioma, ovarian and prostate cancers, and is a potential diagnostic and prognostic

biomarker (Jin *et al.*, 2006; Uhland, 2006; Kobel *et al.*, 2008; Szabo and Bugge, 2008; Tsai *et al.*, 2008; Darragh *et al.*, 2010).

It is suggested that matriptase is able to promote cancer development and progression by processing the pro-forms of urokinase-type plasminogen activator (pro-uPA) and hepatocyte growth factor (pro-HGF), both of which are known to promote invasive tumour growth (Lee *et al.*, 2000; Takeuchi *et al.*, 2000; Uhland, 2006). In addition, matriptase might promote tissue invasion by modulating cell–cell adhesion via degradation of components of the extracellular matrix (Jin *et al.*, 2006) or by activating PAR-2 (Takeuchi *et al.*, 2000; Bocheva *et al.*, 2009), a regulator of inflammation and cell–cell adhesion. However, involvement of any of these targets in matriptase-dependent tumourigenesis has yet to be tested and further investigation will be needed to validate matriptase as a novel biomarker, a predictor of patient outcome, and as a possible therapeutic target for at least some types of carcinoma.

A direct role for matriptase in tumourigenesis has been demonstrated with transgenic mice that over-express the protease in skin. This study found that increased protease expression in the epidermis induced strong proliferation of keratinocytes and squamous cell carcinoma formation (List *et al.*, 2005). By contrast, double transgenic mice, which expressed both matriptase and a cognate inhibitor, HAI-1, did not develop carcinomas. Importantly, both the epidermal hyper-proliferation and the formation of matriptase-induced skin tumours was completely abolished by co-expression of the cognate inhibitor of matriptase, HAI-1, providing further evidence of matriptase proteolytic activity being the underlying causative agent in the formation of these lesions.

Interestingly stable knockdown of HAI-1 was shown to mimic the epithelial to mesenchymal transition (EMT) in both pancreatic and lung cancer cell lines. Over-expression of HAI-1 in these cell lines re-established epithelial morphology (Cheng *et al.*, 2009). There is also increasing evidence that an altered ratio of matriptase and HAI-1 might have a role in cancer development. Indeed, increased matriptase expression relative to HAI-1 expression has been demonstrated in several studies (Oberst *et al.*, 2002; Vogel *et al.*, 2006). It appears that matriptase is involved in both the development and progression of diverse cancers and may be a viable biomarker and therapeutic target. However, further characterization of this protease will be necessary to fully elucidate its potential in the field of cancer therapy.

1.4.2.2 Matriptase-2

See section 1.5 below for full description of matriptase-2.

1.4.3 Hepsin/TMPRSS subfamily

1.4.3.1 Hepsin/TMPRSS1

Hepsin is a transmembrane serine protease that was originally identified from a human hepatoma HepG2 cell library using a homology-based cloning strategy (Leytus *et al.*, 1988). Expression and characterization of recombinant hepsin show that the protein is synthesized as a single-chain zymogen with an apparent molecular mass of 51kDa (Netzel-Arnett *et al.*, 2003). Hepsin expression is highest in the liver but has also been indentified in several tissues including thymus, thyroid, lung, pancreas, pituitary

gland, prostate and kidney (Szabo and Bugge, 2008). Hepsin consists of a short cytoplasmic amino terminal extension, a transmembrane domain, a SR domain and an active serine protease at the carboxy terminal (Netzel-Arnett *et al.*, 2003; Szabo and Bugge, 2008; Choi *et al.*, 2009) (Figure 1.10).

Hepsin has become a high interest topic because of its marked over-expression in prostate and ovarian cancer (Tanimoto *et al.*, 1997; Dhanasekaran *et al.*, 2001; Luo *et al.*, 2001; Magee *et al.*, 2001; Stamey *et al.*, 2001; Welsh *et al.*, 2001; Rhodes *et al.*, 2002; Chen *et al.*, 2003; Adib *et al.*, 2004; Huppi and Chandramouli, 2004; Lai *et al.*, 2004; Herter *et al.*, 2005; Wu and Parry, 2007), renal cell carcinoma (Zacharski *et al.*, 1998; Betsunoh *et al.*, 2007) and endometrial cancer (Matsuo *et al.*, 2008). Hepsin has also been shown to be a potential biomarker for the presence of prostate cancer (Parekh *et al.*, 2007; Sardana *et al.*, 2008; Leman *et al.*, 2009; Talesa *et al.*, 2009; Huang *et al.*, 2010) and to be associated with poor patient outcome (Betsunoh *et al.*, 2007; Matsuo *et al.*, 2008). The physiological function of hepsin remains unknown, but within the carcinogenesis pathway it appears to play a role in cancer cell migration/invasion rather than cell proliferation (Holt *et al.*, 2010). The effect of deregulated hepsin has been shown to promote cancer progression and metastasis in mouse models by causing disorganization of the basement membrane (Klezovitch *et al.*, 2004).

Although it is clear that hepsin plays a role in cancer progression, the possible mechanisms that may be responsible for this remain largely undetermined. However, studies have begun to elucidate routes through which hepsin could exert its pro-tumourigenic effect. It has been suggested that hepatocyte growth factor (HGF) is a

possible substrate for hepsin with high degree of specificity (Herter *et al.*, 2005; Qiu *et al.*, 2007; Owen *et al.*, 2010). Herter *et al* 2005 showed that hepsin can cleave sc-HGF and that hepsin cleaved sc-HGF is biologically active in ovarian cancer cells, and may influence tumourigenesis through inappropriate activation and/or regulation of the HGF receptor c-met (Herter *et al.*, 2005). Laminin-332 (Ln-332) is an ECM macromolecule associated with prostate cancer cell motility, and its expression is lost in cancer progression. Hepsin has been shown to cleave Ln-332, possibly aiding cancer progression by increasing the motility of cancer cells. Cleavage is specific, since it is both inhibited in a dose-dependent manner by a hepsin inhibitor (Kunitz domain-1) and does not occur when catalytically inactive hepsin is used (Tripathi *et al.*, 2008; Li *et al.*, 2009). Hepsin has also been shown to efficiently activate pro-uPA, suggesting it may initiate plasmin-mediated proteolytic pathways at the tumour/stroma interface that could lead to basement membrane disruption and tumour progression (Moran *et al.*, 2006). In light of the evidence gained, hepsin appears to be a promising therapeutic target for slowing or even preventing the development and progression of cancer.

1.4.3.2 TMPRSS2

TMPRSS2 is expressed widely in the epithelia of the gastrointestinal, urogenital and respiratory tracts, with the highest levels detected in prostate luminal epithelial cells (Szabo and Bugge, 2008). TMPRSS2 was originally cloned in 1997 and consists of a short cytoplasmic amino terminal extension, a transmembrane domain, a LDLA domain, a SR domain and an active serine protease at the carboxy terminal and forms a protein of 53.6kDa in length (Paoloni-Giacobino *et al.*, 1997) (Figure 1.10). Activation of the serine protease requires its cleavage, which is autocatalytic. The active serine

protease with trypsin-like specificity is then shed into the extracellular space, where it is predicted to interact with other proteins on the cell surface, as well as soluble proteins, matrix components and proteins on adjacent cells (Afar *et al.*, 2001).

TMPRSS2 is a TTSP that has gained significant interest owing to its highly localized expression in the prostate and its over-expression in neoplastic prostate epithelium (Wilson *et al.*, 2005). The detection of chromosomal abnormalities in tumours is not a recent discovery but their significance has only recently become clear. A central aim in cancer research is to identify recurrent chromosomal rearrangements that play a vital role in cancer development. These rearrangements are of two general types. In the first, the promoter and/or enhancer elements of one gene are aberrantly juxtaposed to a proto-oncogene, thus causing altered expression of an oncogenic protein (Rabbitts, 1994). In the second, the rearrangement fuses two genes, resulting in the production of a fusion protein that may have a new or altered activity (Rowley, 1973; de Klein *et al.*, 1982). Fusion proteins formed after chromosomal translocations are common in a range of tumour types; these are unique tumour antigens and are therefore potentially valuable targets for therapy design.

Recently a small number of fusion transcripts, specific to prostate cancer have been discovered (Scheble *et al.*, 2010), that were the result of a chromosomal rearrangement involving two genes. The first gene, TMPRSS2, is secreted by prostate epithelial cells in response to androgen exposure (Afar *et al.*, 2001). TMPRSS2 was fused to either ERG or ETV1, two members of the ETS family of oncogenes. It had earlier been reported that the ERG gene was the most commonly over-expressed proto-oncogene in

prostate cancer (present in about 72% of cases of prostate cancer) (Petrovics *et al.*, 2005). It was discovered that both intra-chromosomal and inter-chromosomal genetic rearrangements led to the creation of a fusion transcript called TMPRSS2–ETS (Tomlins *et al.*, 2005), it results in the translocation of an ETS (E26 transformation specific) transcription factor (ERG or ETV1) to the TMPRSS2 promoter region, which contains androgen responsive elements. ETS is a family of transcriptional activators and inhibitors and their activity is regulated by phosphorylation and protein–protein interactions (Seth and Watson, 2005). The TMPRSS2:ERG genetic rearrangement has been reported to occur in approximately 40% of primary prostate tumours (ETV1 genetic rearrangements occur at a much lower frequency), and it results in the aberrant androgen-regulated expression of ERG and could be a mechanism whereby the ETV1 or ERG oncogenes are over-expressed, leading to prostate cancer.

TMPRSS2:EGR fusion gene transcripts were found to promote proliferation, motility and invasion of PNT1A cells (Wang *et al.*, 2008) and Tomlins *et al.* concluded that ETS genetic rearrangements are sufficient to initiate prostate neoplasia. However, Carver *et al.* have shown that ETS genetic rearrangements may in fact represent progression events rather than initiation events in prostate tumourigenesis (Carver *et al.*, 2009). The role of TMPRSS2:ERG fusion protein in clinical outcome also remains unclear, with 10 studies receiving contradictory results (Huang and Waknitz, 2009). Another study, involving mice lacking TMPRSS2, showed no effect on the development, fertility, overall survival or function of the prostate (Kim *et al.*, 2006). Despite the disparity in these findings there is promising evidence that TMPRSS2:ERG fusion proteins may be a useful biomarker, present in urine, for early detection of

prostate cancer (Laxman *et al.*, 2006; Hessels *et al.*, 2007; Han *et al.*, 2008; Tomlins *et al.*, 2009; Cao and Yao, 2010; Huang *et al.*, 2010; Rice *et al.*, 2010). There is also evidence to suggest that TMPRSS2 is capable of cleaving and thereby activating the PAR-2 receptor and this may be another method through which TMPRSS2 contributes to cancer progression (Wilson *et al.*, 2005). Thus, TMPRSS2 and the TMPRSS2:ERG gene fusion presents an exciting opportunity for use as a therapeutic target and drug development for the treatment of patients with TMPRSS2:ERG expressing prostate cancers.

1.4.3.3 TMPRSS3

The expression of TMPRSS3 was detected in several human tissues, including heart, lung, kidney, liver, placenta, pancreas, small intestine, colon, spleen, ovary, prostate, testis and thymus (Scott *et al.*, 2001). TMPRSS3 is expressed as a 49kDa polypeptide and consists of a short cytoplasmic extension, a amino terminal transmembrane domain, a LDLA domain, a SR domain and an carboxy terminal active serine protease (Netzel-Arnett *et al.*, 2003) (Figure 1.10).

There is little information to date regarding the role of TMPRSS3 in the progression of cancer. A splice variant, TADG-12 has been shown to be over-expressed in ovarian cancer (Underwood *et al.*, 2000; Wallrapp *et al.*, 2000). TADG-12 was also found to be more highly expressed in advanced clinical stage ovarian cancer and this variant may be useful both as a molecular target for therapy and/or a diagnostic marker (Sawasaki *et al.*, 2004). A study by Bellone *et al.* identified potential immunogenic peptides derived from TADG-12 for immunotherapy of ovarian carcinoma. The TADG-12

YLPKSWTIQV peptide is an immunogenic epitope in ovarian tumours and may represent an attractive target for immunotherapy of ovarian cancer (Bellone et al., 2009). This discovery may allow the development of a TADG-12 peptide-derived cell-based therapy for the vaccination of ovarian cancer patients possessing chemotherapy-resistant or residual disease.

1.4.3.4 TMPRSS4

TMPRSS4 expression has been detected on the cell surface in oesophagus, stomach, small intestine, colon, kidney and bladder (Szabo and Bugge, 2008). It is also markedly up-regulated in gastric, liver, lung, ovarian, pancreatic, primary basal cell carcinomas, squamous cell carcinomas, thin melanomas and thyroid cancers (Jung et al., 2008; Riker et al., 2008) although its oncogenic potential and mechanism of action remain unclear. TMPRSS4 is expressed as a 68kDa protein which consists of a short cytoplasmic extension, a amino terminal transmembrane domain, a LDLA domain, a SR domain and an carboxy terminal active serine protease (Netzel-Arnett et al., 2003) (Figure 1.10).

In pancreas cancer cells, TMPRSS4 is involved in the process of metastasis formation and tumour invasion, and its expression is correlated with the metastatic potential (Wallrapp et al., 2000). TMPRSS4 has also been identified as a possible diagnostic marker in thyroid cancer and to improve the accuracy of fine needle aspiration (FNA) biopsy (Jarzab et al., 2005; Kebebew et al., 2005; Kebebew et al., 2006). Although the mechanisms of action of TMPRSS4 remain unclear several studies have proposed potential pathways by which TMPRSS4 exerts its function. Dawelbait et

al. 2007 proposed that the interaction between the up-regulated TMPRSS4 and the down-regulated tissue factor pathway inhibitor 2 (TFPI2) in pancreas cancer cells could explain the mechanism of metastasis that makes pancreatic ductal adenocarcinoma (PDAC) a very aggressive type of cancer. TFPI2 is an extracellular protein that belongs to the small Kunitz inhibitor family. TFPI2 plays a major role in extracellular matrix degradation during tumour cell invasion and metastasis, wound healing and angiogenesis and is known to be down-regulated in PDAC (Dawelbait *et al.*, 2007). Dawelbait *et al.* hypothesized that TFPI2 acts as a natural inhibitor of TMPRSS4. Since TFPI2 is down-regulated, the up-regulated TMPRSS4 is no longer inhibited and might facilitate tissue invasion and metastasis.

Jung *et al.* 2008 proposed that TMPRSS4 mediates the invasive and metastatic potential of human cancer cells by facilitating an epithelial–mesenchymal transition (Jung *et al.*, 2008). Kim et al. 2010 further explored the mechanisms by which TMPRSS4 mediates EMT and invasiveness in tumour cells. TMPRSS4 mediated FAK signalling pathway activation and extracellular signal-regulated kinase (ERK) activation via integrin a5 up-regulation, resulting in epithelial-mesenchymal transition (EMT) and invasiveness. Furthermore, TMPRSS4 over-expression in human colorectal cancer tissues correlated with enhanced expression of integrin a5. These observations implicate integrin a5 up-regulation as a molecular mechanism by which TMPRSS4 induces invasion and contributes to cancer progression (Kim *et al.*, 2010). To further implicate TMPRSS4 in EMT, Cheng *et al.* 2008 suggests that interactions between HAI-1/SPINT1 and TMPRSS4 contribute to transcriptional and functional changes involved in EMT in certain carcinoma cells (Cheng *et al.*, 2009). Although a specific substrate

molecule of TMPRSS4 that initiates the EMT stimulatory pathway is still not defined, recent studies have contributed to discovering the pathways through which TMPRSS4 may exert its function. Regulation of EMT by proteases such as TMPRSS4 may provide novel therapeutic targets for the treatment of cancer metastasis.

1.4.4 HAT/DESC Subfamily

1.4.4.1 HAT

Human airway trypsin-like (HAT) protease was originally identified in the human trachea and bronchi (Yasuoka *et al.*, 1997; Yamaoka *et al.*, 1998) and subsequently found in diverse tissues including brain, spinal cord, skin, tongue, testis, prostate, urinary bladder and the organs of the gastrointestinal tract (Hansen *et al.*, 2004; Iwakiri *et al.*, 2004; Hahner *et al.*, 2005; Szabo and Bugge, 2008). HAT protein is 48kDa in length and consists of a short cytoplasmic extension, a amino terminal transmembrane domain, a SEA domain and a carboxy terminal active serine protease (Yamaoka *et al.*, 1998) (Figure 1.10). Proposed physiological roles of HAT include mucus production (Chokki *et al.*, 2004), deposition of fibrin in the airway lumen (Yoshinaga *et al.*, 1998), proteolytic activation of hemagglutinin antigen of influenza virus (Bottcher *et al.*, 2006), activation of protease-activated receptor 2 (PAR2) (Miki *et al.*, 2003; Chokki *et al.*, 2004; Iwakiri *et al.*, 2004; Matsushima *et al.*, 2006) and proteolytic inactivation of the urokinase receptor (Beaufort *et al.*, 2007). HAT also appears to be released as a soluble protein from the surface of tracheal serous glands of patients with chronic airway disease (Yamaoka *et al.*, 1998). There are currently no studies investigating the possible involvement of HAT in tumourigenesis. A previous study even presented

evidence against a role in adrenal tumourigenesis (Hahner *et al.*, 2005). Further investigation is required to determine the role, if any, of HAT in cancer.

1.4.4.2 DESC1

Differentially expressed in squamous cell carcinoma gene 1 (DESC1) is expressed in a number of tissues derived from the head and neck, and in skin, prostate and testes. Cell line studies demonstrate that DESC1 expression is epithelial-specific (Lang and Schuller, 2001). The 47kDa DESC1 protein consists of a short cytoplasmic extension, a amino terminal transmembrane domain, a SEA domain and a carboxy terminal active serine protease (Szabo and Bugge, 2008) (Figure 1.10). DESC1 was first investigated in squamous cell carcinoma of the head and neck. A study by Lang *et al* 2001 (Lang and Schuller, 2001), compared DESC1 expression between primary squamous cell carcinoma and matched normal tissue and demonstrated that DESC1 expression was reduced or absent in 11/12 SCC tissue specimens when compared to specimens of matched normal tissue. A further study by Sedhgizadeh *et al* 2006 showed that down-regulation of DESC1 occurs during squamous cell carcinoma progression and up-regulation occurs during normal epithelial differentiation (Sedghizadeh *et al.*, 2006). It has also been reported that DESC1 hydrolyses extracellular components such as fibronectin, gelatine and fibrinogen (Viloria *et al.*, 2007). Madin-Darby canine kidney (MDCK) cells expressing exogenous human DESC1 acquire properties associated with tumour growth such as enhanced motility and an increase of tubular forms in a 3D collagen lattice following HGF treatment (Viloria *et al.*, 2007). A study investigating the substrate specificities of a number of TTSPs demonstrated that DESC1 had a preference for small non-polar amino acids and that antithrombin III has robust

inhibitory properties toward DESC1, whereas plasminogen activator inhibitor-1 and alpha(2)-antiplasmin inhibited DESC1 (Beliveau *et al.*, 2009). In light of these findings it appears that DESC1 could be considered as a potential therapeutic target in some types of tumours.

1.4.5 CORIN Subfamily

1.4.5.1 Corin/TMPRSS10

Human corin was first cloned in the search for novel serine protease genes in the cardiovascular system. The full-length human corin cDNA is approxiametly 5 kb in length and encodes a mosaic serine protease, which is named corin for its abundant expression in the heart (Yan *et al.*, 1999). Independently, Hooper *et al.* (Hooper *et al.*, 2000) also cloned human corin cDNA from a cancer cell line while studying novel serine protease genes in cancer. The human corin polypeptide is 116 kDa in length and consists of a short cytoplasmic extension at the N-terminus followed by an integral transmembrane domain, two frizzled-like cysteine-rich motifs, eight LDLA repeats, a SR domain, and a serine protease domain at the C-terminus (Wu *et al.*, 2005) (Figure 1.10).

Currently there are very few mentions of corin in the field of cancer research. Corin mRNA has been found in cancer cells derived from osteosarcoma, leiomyosarcoma, endometrial carcinoma, and small cell lung cancer (Hooper *et al.*, 2000; Wu and Wu, 2003). It has been proposed that the ectopic expression of corin may contribute to the

pathogenesis of the syndrome of inappropriate secretion of anti-diuretic hormone (SIADH) associated with certain cancers (Wu and Wu, 2003).

1.5 Matriptase-2

1.5.1 Discovery

Matriptase-2 was identified in 2002 when screening for sequences common to the TTSP family (Velasco *et al.*, 2002). The matriptase-2 gene is found on chromosome 22 and encodes an 88,901 kDa protein. In humans matriptase-2 expression is limited to the liver (Velasco *et al.*, 2002), although expression in the kidney, uterus and nasal cavity was seen in mice (Hooper *et al.*, 2003). Matriptase-2 consists of a short cytoplasmic extension with unknown function, a transmembrane domain, a SEA domain, two CUB domains, three LDLA domains and a C-terminal active serine protease (Hooper *et al.*, 2003; Szabo and Bugge, 2008) (Figure 1.10). Matriptase-2 shares a high homology with matriptase, which is also over-expressed in different human cancers (Shi *et al.*, 1993). However, where the over-expression of matriptase leads to cancer progression (Uhland, 2006; Tsai *et al.*, 2008) , matriptase-2 over-expression significantly reduces breast and prostate cancer growth and reduced levels correlate with poor patient outcome (Parr *et al.*, 2007; Sanders *et al.*, 2008). The molecular mechanisms involved in the activation of matriptase-2 remain largely unknown. Active matriptase-2 has been found in both membrane and soluble forms (Silvestri *et al.*, 2008; Ramsay *et al.*, 2009). A recent study by Stirnberg *et al* 2010 demonstrated shed matriptase-2 in a two-chain form that is highly active with a cleavage site located between ARG^{437} and Val^{438} within the second CUB domain of the non-catalytic stem region (Stirnberg *et al.*, 2010).

1.5.2 Substrate specificity

Velasco *et al.* examined the enzymatic function of matriptase-2 by producing a GST-matriptase-2 fusion protein. This fusion protein was found to degrade fibronectin, fibrinogen and type 1 collagen and to have limited action against pro-uPA but was unable to process MMP-2, MMP-9 and plasminogen. It was also found to be inhibited by serine protease inhibitors such as PMSF, leupeptin, aprotinin and plasminogen activator inhibitor-1 but not by inhibitors of cysteine or metallo protease inhibitors (Velasco *et al.*, 2002; Beliveau *et al.*, 2009). Recently, membrane bound hemojuvelin (m-HJV) has also been identified as a substrate of matriptase-2 (Silvestri *et al.*, 2008), giving matriptase-2 a previously unrecognized, but important, role in iron metabolism.

In a recent study Maurer *et al* 2011 used site-directed mutagenesis, kinetic and molecular modelling studies to obtain insights into substrate/inhibitor–enzyme interactions. Based on the active site structure of the related enzyme matriptase, amino acids that enhanced (Phe 665) or reduced (Asp 785, Tyr 712) the affinity of peptide ligands for matriptase-2 were identified (Maurer *et al.*, 2011).

1.5.3 Expression of matriptase-2 in normal and cancerous cells

Altered expression of matriptase-2 in cancer has been reported in several studies. Matriptase-2 transcript was detected in mouse Leydig tumour cells (Odet *et al.*, 2006) and elevated levels of matriptase-2 have been reported in invasive ductal cell carcinoma (Overall *et al.*, 2004). Studies from within our laboratories showed that there were reduced levels of matriptase-2 immunostaining in cancerous breast tissue sections

compared to normal tissue sections with the majority of matriptase-2 staining being confined to the epithelial sections (Parr *et al.*, 2007). In contrast to this quantitative PCR showed that matriptase-2 levels were up-regulated in tumour compared to normal tissues, however matriptase-2 levels were significantly higher in lower NPI and TNM stages and correlated with positive patient outcome and the over-expression of matriptase-2 reduced aggressive *in vitro* and *in vivo* traits of MDA-MB-231 breast cancer cells (Parr *et al.*, 2007). A study by Sanders *et al* 2008 described the effect of matriptase-2 over-expression in PC3 and DU145 cells. It showed that an increase in matriptase-2 caused PC3 growth to decrease but not that of DU145. Also the adhesion of both cell lines was unaffected. The study also showed that matriptase-2 over-expression also significantly reduced the migration and invasion of both cell lines. To further the investigation the PC3 cells over-expressing matriptase-2 were inplanted into nude mice. This caused a significant retardation of the normally highly tumourigenic PC3 cell ability to grow and develop into tumours. Also in the study enhanced matriptase-2 levels were seen to correlate with increased fluorescent staining of paxillin and FAK adhesion molecules, where a greater extent of these molecules were localised to the focal adhesion complexes (Sanders *et al.*, 2008).

1.5.4   Role in iron homeostasis

Recently matriptase-2 has been found to have a role in iron homeostasis. The discovery was made by Du *et al* when examining mouse mutations caused by N-ethyl-N-nitrosurea. One phenotype exhibited low iron plasma levels and iron stores (termed *Mask* mutants) and was found to harbour splice variants of matriptase-2 lacking the protease domain. Du *et al* also noted that the low iron levels in *Mask* mice were paired

with high levels of *Hamp* transcript, the gene from which hepcidin is produced. This suggested that matriptase-2 may play a role in iron homeostasis through the negative regulation of *Hamp* activation (Du *et al.*, 2008). Another study has found that an increase in matriptase-2 protein in the liver from iron deficient rats was detected; suggesting that suppression of hepcidin expression in response to acute iron deprivation is mediated by an increase in matriptase-2 protein levels (Zhang *et al.*, 2011). It is believed that matriptase-2 proteolytically processes membrane hemojuvelin (also known as RGMc) which significantly reduces hepcidin transcription as hemojuvelin induces *Hamp* transcription (Silvestri *et al.*, 2008)(Figure 1.12). Hemojuvelin is produced as a membrane GPI linked protein that acts as a co-receptor for bone morphogenetic protein (BMP) -2, -4 and -6 (Babitt *et al.*, 2006; Xia *et al.*, 2008). It is likely that matriptase-2 exerts its effect directly by proteolytic processing of hemojuvelin and indirectly by creating an imbalance in levels of BMP co-receptor and antagonist (Ramsay *et al.*, 2009). This is further corroborated by a study by Lenoir *et al* that showed that *Tmprss6*^{-/-} mice crossed with *Bmp6*^{-/-} resulted in a correction of the haematological abnormalities brought about by a non-functioning matriptase-2 protein. This indicates that the elevated hepcidin levels in patients with familial iron-refractory iron anaemia are due to excess signalling through the BMP6/HJV pathway (Lenoir et al., 2010). A very recent study has proposed that matriptase-2 expression is regulated by BMP6 and iron levels. Maynard et al 2011 demonstrated that *in vitro*, treatment with BMP6 stimulates TMPRSS6 expression at the mRNA and protein levels and leads to an increase in matriptase-2 activity. And also that ID1, a negative regulator of basic-helix-loop-helix transcription factors, is the key element of the BMP-SMAD pathway to regulate TMPRSS6 expression in response to BMP6 treatment. Finally, they showed

that in mice, TMPRSS6 mRNA expression is stimulated by chronic iron treatment or BMP6 injection, and is blocked by injection of neutralizing antibody against BMP6 (Meynard et al., 2011). Although further elucidation of this pathway is required it is possible that due to the complex role of BMPs and their co-receptors in cancer that this novel pathway could partly be involved in the action of matriptase-2 in cancer progression.
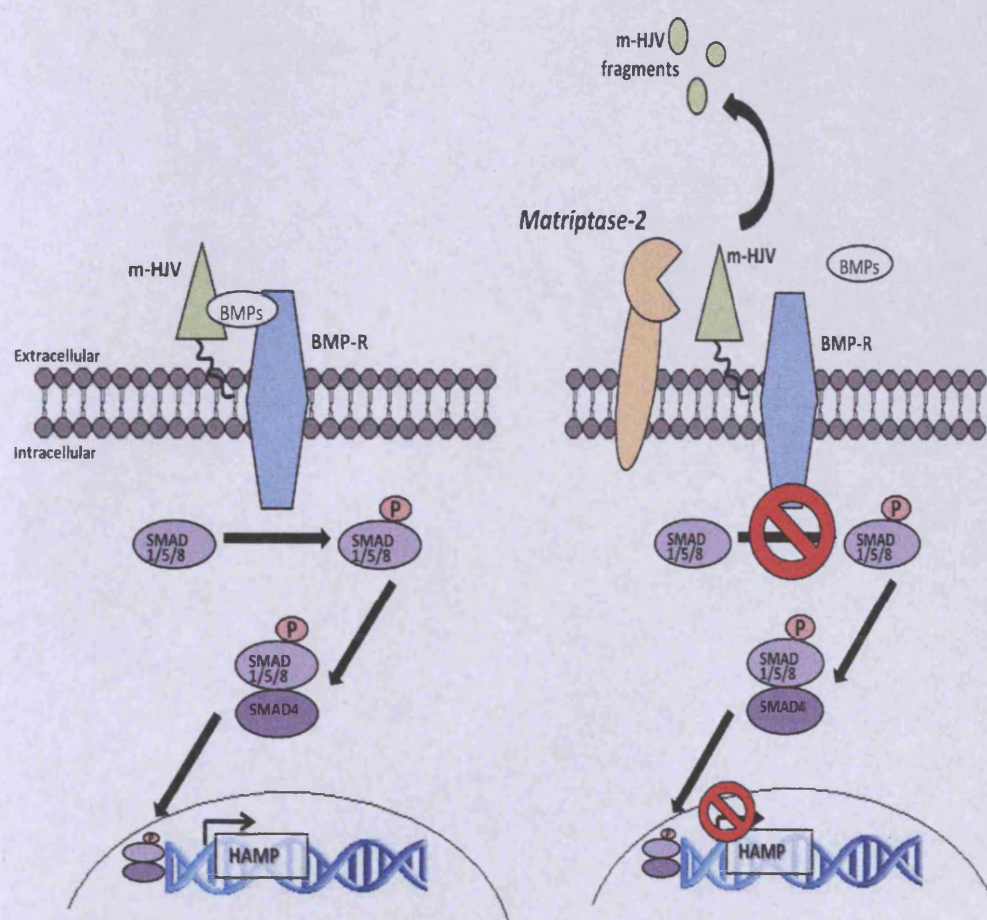
Figure 1.12 Matriptase-2 proteolytically processes mHJV (RGMc) negatively regulating HAMP expression. Matriptase-2 helps to maintain correct iron homeostasis by cleaving mHJV without which the transcription of HAMP cannot proceed.

1.6 Aims and objectives

Cancer metastasis is an increasingly complex problem. Despite the increasing number of studies involving cancer metastasis and the knowledge already gained, there is still much that is unknown. Metastasis is a complex multi-stage process involving cell invasion, secretion of certain angiogenic factors, cell migration and changes in cell adhesive properties. To accomplish local invasion, tumour cells use extracellular and cell surface proteolytic enzymes to degrade the basement membrane proteins. This allows the cancer cells to invade into surrounding tissues. The TTSP family of cell-surface proteases is ideally located to perform this crucial task. Matriptase-1, which is highly homologous to matriptase-2, is known to increase the motile and invasive ability and to decrease the adhesive properties of prostate cancer cells. There is also the question as to whether some TTSPs may prevent the degradation of the basement membrane and therefore protect the surrounding tissues from invasion by the cancer cells. Many recent studies have focused on the expression of specific TTSPs during tumourigenesis and their potential to influence tumour cell proliferation, motility and invasion. Previous studies within this laboratory have already indicated that matriptase-2 is a possible tumour suppressor in breast and prostate cancer. Recent studies have also indicated that matriptase-2 cleaves RGMc, also known as Hemojuvelin, which is a BMP co-receptor. This presents the opportunity for a regulatory involvement of matriptase-2 in the BMP signalling pathway. This study will aim to further elucidate the involvement of matriptase-2 in the process of cancer progression.

The specific aims of this thesis were:

- To produce and/or re-amplify plasmid constructs of matriptase-2, to force-express and knock-down its expression in prostate cancer cell lines, respectively. This would then allow for the effect that matriptase-2 has on biological properties of cancer cells including adhesion, invasion, proliferation, motility, and migration, to be studied.

- To examine the expression of β–catenin in the force-express and knockdown cells and determine if matriptase-2 affects the expression levels and patterns of β-catenin

- To investigate the potential involvement of matriptase-2 in angiogenesis using *in vitro* methods

Chapter 2

Materials and Methods

2.1. General materials

2.1.1 Solutions for regular use

0.05M EDTA

1g KCl (Fisons Scientific Equipment, Loughborough, UK), 5.72g Na2HPO4, 1g
KH2PO4, 40g NaCl and 1.4g EDTA (Duchefa Biochemie, Haarlem, The Netherlands)
was dissolved in distilled water to make a final volume of 5L. The solution was
adjusted to pH 7.4 before autoclaving and storing for use.

Trypsin (25mg/ml)

500mg trypsin was dissolved in 20ml 0.05M EDTA. The solution was mixed
and filtered through a 0.2μm minisart filter (Sartorius, Epsom, UK), aliquoted in 250μl
samples and stored at -20°C until required. For use in cell culture one 250μl aliquot was
diluted in a further 10ml of 0.05M EDTA solution and used for cell detachment

100x Antibiotic cocktail mix

5g streptomycin, 3.3g penicillin and 12.5mg amphotericin B in DMSO, were dissolved
in BSS and filtered. 5ml was then added to a 500ml bottle of DMEM media.

Balanced Saline Solution (BSS)

79.5g NaCl, 2.2g KCl, 2.1g KH_2PO_4, and 1.1g Na_2HPO_4 was dissolved in
distilled water to make a final volume of 10L. pH was adjusted to 7.2 before use.

LB agar

10g of tryptone, 5g yeast extract 10g NaCl and 15g agar was dissolved in distilled water to a final volume of 1L, the pH adjusted to 7.0 and the solution autoclaved. When necessary, the solution was heated to a liquid and cooled slightly before adding selective antibiotic (if required). The solution was then poured into 10cm^2 petri dish plates (Bibby Sterilin Ltd., Staffs, UK), allowed to cool and solidify, before being inverted and stored at 4°C.

LB broth

10g of tryptone (Duchefa Biochemie, Haarlem, The Netherlands), 5g yeast extract (Duchefa Biochemie, Haarlem, The Netherlands) and 10g NaCl was dissolved in distilled water to a final volume of 1L and the pH adjusted to 7.0. It was autoclaved and allowed to cool before adding selective antibiotic (if required) and storing at room temperature.

DEPC water

250μl diethyl pyroncarbonate (DEPC) was added to 4750μl distilled water. Solution was then autoclaved before use.

5X Tris, Boric acid, EDTA (TBE)

540g of tris-Cl (Melford Laboratories Ltd., Suffolk, UK), 275g Boric acid (Duchefa Biochemie, Haarlem, The Netherlands) and 46.5g of disodium EDTA was dissolved in distilled water and made up to a final volume of 10L. Solution was stored

at room temperature and diluted to 1X concentrate prior to use in agarose gel electrophoresis.

Loading buffer (for DNA electrophoresis)

A stock solution was made by dissolving 25mg bromophenol blue and 4g sucrose in distilled water to a final volume of 10ml. Store at 4°C to avoid mould growing in the sucrose until use.

Ethidium bromide

100mg of ethidium bromide powder was dissolved in 10ml of distilled water. Container was wrapped in aluminium foil to protect solution from sunlight and stored safely before use.

Tris-Boric acid-EDTA (TBE)

For a 5×TBE buffer (1.1M Tris; 900mM Borate; 25mM EDTA; pH 8.3), dissolve 540g Tris-Cl (Melford Laboratories Ltd., Suffolk, UK), 275g Boric acid (Duchefa Biochemie, Haarlem, Netherlands) and 46.5g EDTA (Duchefa Biochemie, Haarlem, Netherlands) in 9.5 litres of distilled water. Adjust pH to about 8.3 using NaOH, and then make up to a final volume of 10 litres with distilled water.

Lysis Buffer

2mM $CaCl_2$, 0.5% Triton X-100, 1 mg/ml leupeptin, 1 mg/ml aprotinin and 10 mM sodium orthovanadate was dissolved in distilled water and stored at 4°C until required.

10% Ammonium Persulfate (APS)

1g of ammonium persulfate was dissolved in 10ml of distilled water, separated

into 2.5ml aliquots and stored at 4°C until required.

10X Running buffer

303g tris, 1.44Kg Glycine and 100g SDS was dissolved in distilled water to a

final volume of 10L. Solution was further diluted to 1X concentrate before use.

Transfer buffer

72g of glycine, 15.15g Tris and 1L Methanol (Fisher Scientific, Leicestershire,

UK) were dissolved in distilled water to a 5L final volume.

10X TBS

121g of tris and 400.3g NaCl were dissolved in distilled water, made up to a

final volume of 5L and adjusted to pH 7.4.

Sample buffer (for SDS-PAGE)

Supplied directly by Sigma.

Amido black stain

2.5g of amido black (Edward Gurr Ltd., London, UK) was dissolved in 50ml

acetic acid (Fisher Scientific, Leicestershire, UK) and 125ml ethanol (Fisher Scientific,

Leicestershire, UK). 325ml of distilled water was added and solution mixed well.

Amido black destain

100ml of acetic acid and 250ml ethanol were added to 650ml distilled water.

Coomasie blue stain

1g coomassie blue, 400ml of methanol and 100ml of acetic acid were mixed and made up to a final volume of 1L in distilled water.

Coomasie blue destain

500 millilitres of methanol was mixed with 100ml of acetic acid and made up to a final volume of 1L in distilled water.

2.1.2 Cell lines/animals

The PC3 cell line is derived from a bone metastasis of a grade 6 prostatic adenocarcinoma from a 62 year old male in 1979. PC-3 cells are adherent and epithelial in morphology. The cell line is androgen insensitive and is highly tumourigenic.

The DU145 cell line was derived from a brain lesion of a 69 year old male patient in 1978 with metastatic prostate carcinoma and a history of lymphocytic leukaemia. DU145 is an adherent cell line with an epithelial morphology. The cell line is tumourigenic in nude mice where it forms tumours consistent with the primary prostate cancer originally described. The DU145 cell line is androgen insensitive.

CAHPV10 is a non-tumourigenic cell line originating from a prostatic adenocarcinoma. The cell line originated from the transfection of these prostate cells with HPV18 DNA. The cell line is adherent and epithelial in morphology.

PZHPV-7 is a non-tumourigenic prostate cell line derived from the human prostate epithelium of the peripheral zone in a 70 year old male patient. The cell line was immortalised through transformation with Human Papilloma Virus 18 (HPV18).

PNT1A is a normal prostate epithelial cell line obtained from a 35 year old male patient. This cell line was established by immortalisation of normal adult prostatic epithelial cells by transfection with a plasmid containing SV40 genome with a defective replication origin.

PNT2C2 is a normal prostate epithelial cell line obtained from a 33 year old male patient. The normal prostate cells have been immortalised with SV40.

HECV is a human endothelial cell line obtained from the umbilical cord of a female patient.

The PC3, DU145, LNCaP, CAHPV10 and PZHPV7 cell lines were obtained from the American Type Culture Collection (ATCC, Rockville, Maryland, USA). The PNT1A and PNT2C2 cell lines were generous gifts from Professor Norman Maitland (University of York, England, UK).

The 4-6 week old CD-1 athymic nude mice used in the *in vivo* tumour development model were obtained from Charles Rivers Laboratories (Kent, England, UK) and maintained in filter-hood cages under ethical conditions.

2.1.3 Antibodies

2.1.3.1 Primary antibodies

Antibody name	Species	Molecular Weight (kDa)	Supplier	Product code
Anti-Matriptase-2 (Stem region)	Rabbit polyclonal	89	Abcam plc	Ab28287
Anti-Matriptase-2 (Cytoplasmic region)	Rabbit polyclonal	89	Abcam plc	Ab56180
Anti-GAPDH	Goat polyclonal	40	Santa Cruz Biotechnology Inc	SC-20358
Anti-β-catenin	Rabbit polyclonal	94	Sigma-Aldrich Co. LLC	C2206
Anti-E-cadherin	Goat polyclonal	120/135	Santa Cruz Biotechnology Inc	SC-1500
Anti-N-cadherin	Goat polyclonal	130	Santa Cruz Biotachnology Inc	SC-1502
Anti-MMP-7	Mouse monoclonal	28/19	Calbiochem	IM71
Anti-uPA	Rabbit polyclonal	55	Santa Cruz Biotachnology Inc	Sc-14019

Table 2.5: Primary antibodies used during course of study

2.1.3.2 Secondary antibodies

The secondary antibodies used for Western blotting were horseradish peroxidise (HRP) conjugated anti-goat IgG, goat anti-rabbit IgG, and rabbit anti-mouse IgG antibodies, all supplied by Sigma (Poole, Dorset, UK). Those used for immunofluorescent studies are either goat anti-rabbit IgG TRITC conjugated secondary

antibodies (Sigma, Poole, Dorset, UK), or FITC conjugated sheep anti-mouse, and rabbit anti-goat IgG, supplied by Santa-Cruz Biotechnology (Santa-Cruz, California, USA).

2.1.4 Primers

Molecule	Primer name	Primer sequence (5'-3')	Product size (bp)
Matriptase-2	Matrip2F2	GAAAGACATAGCTGCATTG	454
	Matrip2R2	GTAGTAGCTGGGGAAGTACG	
GAPDH	GAPDHF10	AGCTTGTCATCAATGGAAAT	36
	GAPDHR10	CTTCACCACCTTCTTGATGT	
Matriptase-2 (QPCR)	Matrip2ZF	ACTGAACCTGACCGTACAGCCGAGTACGAAGTGGAC	101
	Matrip2R2	GTAGTAGCTGGGGAAGTACG	
GAPDH (QPCR)	GAPDHZF	ATGATATCGCCGCGCTCA	200
	GAPDHR8	CGCTCGGTGAGGATCTTCA	
pEF6 plasmid specific	T7F	TAATACGACTCACTATAGGG	Depends on insert
	BGHR	CCTCGACTGTGCCTTCTAG	
Matriptase-2 (Cloning)	T7F	TAATACGACTCACTATAGGGA	700
	Matrip2R1	TAGCTGTAGCGGTAACAACC	
Ribozyme orientation	T7F	TAATACGACTCACTATAGGGA	Depends on insert
	RbToP	CTGATGAGTCCGTGAGGACGAA	
	RbBMR	TTCGTCCTCACGGACTCATCAG	
β-catenin	BcateninF22	AAAGGCTACTGTTGGATTGA	500
	BcateninR22	TCCACCAGAGTGAAAAGAAC	
uPA	uPAF1	GGTTGTGTGTGGGTTAGACT	500
	uPAR1	GTGGCTACCAGACATTGATT	
E-cadherin	EcadF22	CAGGAGCCAGACACATTTAT	500
	EcadR22	TCTAAGGTGGTCACTTGGTC	
N-cadherin	NcadF22	CAACGACGGGTTAGTCAC	500
	NcadR22	ATTGGGGTCTGGAGTTC	
MMP-7	MMP-7F2	GCTATGCGACTCACCGTGCTGTG	500
	MMP-7R2	AGCGTGTTTCCTGGCCCATCAAATG	

Table 2.2: Primers for conventional RT-PCR and Q-PCR (Primers were designed by Beacon Design programme (Palo Alto, California, USA) and were synthesised by Invitrogen (Paisley, UK)). These primers were subjected to BLAST search and were found to be unique to the molecule they were created to bind to.

Expression molecule	Primer name	Primer sequence (5'-3')
Matriptase-2	Matrip2ExF4	ATGCCCGTGGCCGAGG
	Matrip2ExR3	GGTCACCACTTGCTGGATCCA

Table 2.3: Primers for amplifying Matriptase-2 coding sequence.

Target	Name	Ribozyme sequence (5'-3')
Matriptase-2	Matrip2RZ1F	CTGCAGCACTAGAGATTCCCGGCGGGTAAC TGATGAGTCCGTCAGGA
	Matrip2RZ1r	ACTAGTTGTACTCAATCGGCACTTCTCCCAG GATTTCGTCCTCACGGA
Matriptase-2	Matrip2RZf2	CTGCAGTTCGTACTCGGCCCTGTAGGGCTG ATGAGTCCTGAGGA
	Matrip2RZr2	ACTAGTAACAGCTCGGCTGCCGTTTCGTCCT CACGGA

Table 2.4: Primers used for ribozyme synthesis.

2.2 Methods of cell culture

2.2.1 Preparation of cell medium

Cells were routinely cultured in DMEM / Ham's F12 with L-Glutamine medium (PAA Laboratories, Somerset, UK), supplemented with antibiotic cocktail and 10% foetal calf serum (PAA Laboratories, Somerset, UK). Transfected cell lines, containing the pEF6 plasmid, were cultured initially in selection medium containing 5µg/ml blasticidin S and then later were routinely cultured in a maintenance medium containing 0.5µg/ml blasticidin S. All handling of was cells performed using class II hoods to maintain sterile conditions.

1.6.1   2.2.2 Revival from liquid nitrogen

When required, cells were removed from liquid nitrogen and revived. Cells were allowed to thaw rapidly following their removal from liquid nitrogen. Once thawed, the cells were placed in a universal container containing 5ml of pre-warmed medium. The universal containers were centrifuged at 1800rpm for 6 minutes to form a cell pellet. The medium was then aspirated to remove all DMSO and the cell pellet was resuspended in 5ml of pre-warmed medium and placed into a sterile $25cm^3$ tissue culture flask placed in the incubator overnight at $37.0^{\circ}C$, 5% CO_2 and 95% humidity. Following the overnight incubation, the flask was examined under the microscope to visually confirm sufficient healthy adherent cells had survived. The medium was changed to remove any dead cells. The flask was returned to the incubator and further standard sub-culture techniques carried out when necessary.

2.2.3 Maintenance of cells

Cells were maintained in supplemented DMEM medium prepared as described in section 2.2.1, and routinely sub cultured upon reaching 80 – 90% approximate confluency. Confluence was assessed by visually assessing the approximate coverage of cells over the surface of the tissue culture flask using a light microscope. Cells were maintained and grown in either $25cm^3$ or $75cm^3$ tissue culture flasks (Greiner Bio-One Ltd, Gloucestershire, UK), in an incubator at $37.0^{\circ}C$, 5% CO_2 and 95% humidity. All tissue culture techniques were carried out following aseptic techniques inside of a class II laminar flow cabinet.

2.2.4 Trypsinisation and determination of cell count

Upon reaching approximately 80 – 90% confluency the cells were prepared for Trypsinisation. Medium was aspirated and the cells rinsed briefly with EDTA to remove any traces of serum which inhibits the enzymatic action of trypsin. Following this, cells were detached from the tissue culture flask by incubating with trypsin/EDTA for several minutes. Once detached the cell suspension was placed in 20ml universal container (Greiner Bio-One Ltd, Gloucestershire, UK) and centrifuged at 1800rpm for 6 minutes to pellet the cells. The cell pellet was resuspended, in an appropriate volume of fresh medium, before either determining cell number per millilitre (for use in cellular assays), or transferring a small volume of cell suspension into new tissue culture flasks. A Neubuaer haemocytometer was used to determine the cell density. Cells were counted on the haemocytometer counting chamber using an inverted microscope (Reichet, Austria) under 10 x 10 magnification. This allowed the number of cells per millilitre to be determined and accurate numbers of cells to be seeded in the *in vitro* and *in vivo* cellular functional assays. The dimensions of each 16 square area, containing cells to be counted, is 1mm x 1mm x 0.2mm which allowed the number of cells per millilitre to be determined using the following equation:

Cell number / ml = (number of cells counted in 16 squares $\div$ 2) x (1 x 10^4)

Two 16 squared areas were counted to confirm consistent approximate cell density per millilitre between the two counts.

2.2.5 Storage of cells in liquid nitrogen

Stocks of low passage cells were stored in liquid nitrogen. Cells were detached from a large 75cm^3 flask using EDTA/Trypsin as described in section 2.2.5 and placed in a centrifuge to form a cell pellet. These cells were resuspended in the required volume (dependent on the number of samples to be frozen) of a protective medium consisting of 10% dimethyl sulphoxide (DMSO) in normal growth medium. Following resuspension, 1 ml of cells was aliquoted into cryotubes (Nunc, Fisher Scientific, Leicestershire, UK), wrapped loosely in tissue paper and stored overnight in a -80°C freezer. Cells were then transferred to liquid nitrogen tanks for long term storage.

2.3 Methods for detecting mRNA

2.3.1 RNA isolation

Ribonucleic acid (RNA) is present within the nucleus, cytoplasm and mitochondria of all living eukaryotic cells and it is of particular importance as it carries the genetic information for protein formation. The presence of specific mRNA sequences indicates which protein is being produced by a cell at any given time. RNA isolation was completed using the ABgene Total RNA Isolation Reagent (TRIR) Kit and protocol (ABgene, Surrey, UK). Cells were grown until 85-90% confluent, the medium was removed and 1ml of TRIReagent (Sigma-Aldrich, Dorset, UK) was added to the cell monolayer. The cell lysate was then scraped from the flask and passed

through a pipette several times before being transferred into a 1.8ml eppendorf. The homogenate was kept at 4°C for 5 minutes before adding 0.2ml chloroform and vigorously shaking the samples for 15 seconds, samples were centrifuged in a refrigerated centrifuge (Boeco, Wolf laboratories, York, UK) at 4°C and 12,000g for 15 minutes. The homogenate will form two phases: the lower phase is the organic phase and the upper phase is the aqueous phase. DNA and protein are in the organic phase and in the interface while RNA is in the aqueous phase. The volume of the aqueous phase should be about 40–50% of the total volume of the homogenate plus chloroform. Following centrifugation, the upper aqueous phase containing RNA was carefully removed and added to a pre-labelled eppendorf containing an equal volume of isopropanol, the samples were then stored at 4°C for 10 minutes before centrifuging at 12,000g and 4°C for 10 minutes. This causes any RNA present to precipitate which forms a white pellet at the bottom of the tube after the centrifugation. The supernatum was discarded and the RNA pellet washed twice in 75% ethanol (prepared in a 3:1 ratio of absolute ethanol:DEPC water). Each wash consisted of the addition of 1ml of 75% ethanol, vortexing and subsequent centrifugation at 4°C and 7,500g for 5 minutes. Following the final wash, as much ethanol as possible was removed from the eppendorf before briefly drying the pellet in a Techne, Hybridiser HB-1D drying oven (Wolf laboratories, York, UK) at 50°C to remove any remaining ethanol. Finally the pellet was dissolved in 50 – 100µl (depending on pellet size) of DEPC water before proceeding to quantify the RNA present in the sample. DEPC water was used in RNA isolation to reduce the effects of any RNases that may be present. DEPC is a histidine specific alkylating agent and inhibits the action of RNases which rely on histidine active sites for their activity.

2.3.2 RNA quantification

Following isolation, RNA was quantified using a UV1101 Biotech Photometer(WPA, Cambridge, UK), that had been configured to detect ssRNA ($\mu g/\mu l$) in a 1 in 10 dilution based on the difference in absorbance at 260nm wavelength to a DEPC blank. All samples were measured in a Starna glass cuvette (Optiglass limited, Essex, UK). The RNA samples were either stored at -80°C for later use or used immediately for reverse transcription (RT).

2.3.3 Reverse transcription polymerase chain reaction (RT-PCR) of RNA

RT-PCR is a simple, rapid and versatile method for the detection and analysis of mRNA. It provides a more sensitive approach than that of northern and southern blotting and requires smaller amount of RNA. Following RNA isolation and quantification, the RNA samples were normalised to 250ng. The volume of RNA required to make each sample 250ng depended on the concentration ($\mu g/\mu l$) of RNA in each sample. 250ng of RNA was converted into complementary DNA (cDNA) using an Enhanced Avian Reverse Transcriptase-PCR-100 kit (Sigma-Aldrich, Dorset, UK). RT-PCR was undertaken following the DuraScript Reverse Transcription for Two-Step RT-PCR protocol which is outlined below:

- X μl of RNA (volume depends on concentration)
- 1 μl of deoxynucleotide mix

- 1 μl of anchored oligo (dT)23

- 8 μl (-volume of RNA) PCR H₂O

The tube was then mixed gently and centrifuged before placing the mix in a T-Cy Thermocycler (Creacon Technologies Ltd, The Netherlands) and heating at 70°C for 10 minutes. This initial step may denature the RNA secondary structure and allow more effective reverse transcription. Once this initial incubation step had finished, the tubes were removed from the thermal cycler and placed on ice before centrifuging and adding the following to each tube:

- 6μl – PCR water

- 2μl – 10X buffer for DuraScript RT

- 1μl – RNase inhibitor

- 1μl – Enhanced Avian Reverse Transcriptase (eAMVRT)

The tubes were mixed, centrifuged and placed back in the thermal cycler to be heated at 42°C for 50 minutes. The cDNA generated was diluted 1:3 with PCR water and conventional PCR probing for GAPDH expression to confirm successful reverse transcription. Samples were stored at -20°C until further required.

2.3.4 Conventional Polymerase Chain Reaction (PCR)

PCR was carried out using a REDTaq ReadyMix PCR Reaction mix (Sigma, Dorset, UK). Sixteen microlitre reactions were set up for each sample to be tested as follows:

- 8μl - 2X REDTaq ReadyMix PCR Reaction mix

- 1μl – Specific forward primer

- 1μl – Specific reverse primer

- 5μl – PCR water

- 1μl - cDNA

Primers were designed using the Beacon Designer programme (Palo Alto, California, USA) and were synthesised by Invitrogen (Paisley, UK). Primers were diluted to a concentration of 10pM before being used in the PCR reaction. The PCR reaction was set up in a 200μl PCR tube (ABgene, Surrey, UK), mixed briefly and centrifuged before being placed in a T-Cy Thermocycler and subjected to the following temperature shifts:

- Step 1: Initial denaturing period – 94oC for 5 minutes

- Step 2: Denaturing step – 94oC for 1 minute

- Step 3: Annealing step – reaction specific temperature for 1 minutes

- Step 4: Extension step – 72oC for 1 minute

- Step 5: Final extension period – 72oC for 10 minutes

Steps 2 – 4 were repeated over 36 cycles. Specific reaction annealing temperatures together with primer sequence data is detailed in table 2.2. Primer binding sites and predicted product sizes were verified using the Primer3 (v.0.4.0) software available online (http://frodo.wi.mit.edu/). RT-PCR products which corresponded with this predicted size following electrophoresis and staining were taken as being accurate. Positive and negative controls were also tested to verify RT-PCR primers. A collection of mixed RNA extracted from a large number of prostate cancer tissue sections and subsequently converted to cDNA was used as the positive control for most of the primer pairs. The exception to this was the matriptase-2 primer pairs as matriptase-2 mRNA levels were found to be very low in prostate cancer samples. In these cases the PLC/PRF/5 liver cancer cell line was used as a positive control for matriptase-2. In all cases a negative control where PCR water replaced cDNA in the reaction was included.

2.3.5 Agarose gel electrophoresis

Agarose gel electrophoresis is the easiest and most common method to separate DNA fragments. Nucleic acid molecules are separated by applying an electric field to move the negatively charged molecules through an agarose matrix. Shorter molecules move faster and migrate farther than longer ones because shorter molecules migrate more easily through the pores of the gel. Once the samples had completed the sufficient number of cycles in the thermocycler, the amplified DNA was separated according to size using agarose gel electrophoresis. Dependent on the predicted size of the DNA produced, the samples were loaded into either 0.8% (samples greater than approximately 500bp), or 2% (samples less than 500bp), agarose gels. Agarose gels

were made by adding the required amount of agarose (Melford Chemicals, Suffolk, UK) to TBE solution. This was then heated to fully dissolve the agarose, poured into the electrophoresis cassette and allowed to set around a plastic comb to create loading wells for approximately 30-40 minutes. Once set, the gel was submerged in TBE running buffer, 4µl of a 1Kb ladder (Invitrogen, Paisley, Scotland), or 10µl of sample was then added to the wells. The samples were then electrophoretically separated at a constant voltage of 100V until the samples had run three quarters of the gel depending on the size of the PCR product. Once the electrophoresis was completed the gel was placed into ethidium bromide diluted in TBE with continuous agitation to ensure even staining of the agarose gel for 15 minutes. Once stained the gel was visualised under ultra violet light using a UV transilluminator (UVitech, Cambridge, UK).

2.3.6 Quantitative Polymerase Chain Reaction (Q-PCR)

Q-PCR, or real-time PCR, is a very sensitive technique which is used to amplify and simultaneously quantify a targeted DNA molecule. It enables both detection and quantification (as absolute number of copies or relative amount when normalized to DNA input or additional normalizing genes) of one or more specific sequences in a DNA sample. Due to its sensitivity this method allows the detection and quantification of very small quantities of cDNA in a sample. The cDNA for use in Q- PCR was generated as described above; this cDNA was then used to make up a master reaction mixture containing the following amounts of each component per reaction:

- Forward Z primer – 0.3μl (1pmol/μl)

- Reverse primer – 0.3μl (10pmol/μl)

- Q-PCR Master Mix – 5μl

- Probe Ampiflour – 0.3μl (10pmol/μl)

- PCR H2O – 2.1μl

- cDNA – 2μl

In each reaction, one of the primer pairs (see table 2.2), will contain a Zsequence (ACTGAACCTGACCGTACA) at a 1/10 concentration of the other primer and the probe. The Amplifluor system was used to detect and quantify transcript copy number. The ampliflour probe consists of a region specific to the Z-sequence together with a hairpin structure labelled with a fluorescent tag (FAM). Whilst in the hairpin structure this fluorescent tag is effectively quenched and produces no signal. However, the specificity of the 3' region of the ampilflour probe to the Z-sequence causes the incorporation of this uniprimer. Subsequent DNA polymerisation, following incorporation, results in the disruption of the hairpin structure and effective signalling of the fluorescent tag within this structure. The degree of fluorescence within each sample compared to a range of standards of known transcript copy number allows the calculation of transcript copy number within each sample. Detection of GAPDH copy number within these samples was subsequently used to allow further standardisation and normalisation of the samples. Figure 2.2 (A) and 2.2 (B) show the detection of a range of standard samples (108 to 102 copy number) and the subsequent generation of a standard curve from these samples. Sample cDNA was amplified and quantified over a large number of shorter

cycles using an iCyclerIQ thermal cycler and detection software (BioRad laboratories, Hammelhempstead, UK) and experimental conditions are outlined below:

- Step 1: Initial denaturing period – 94°C for 5 minutes

- Step 2: Denaturing step – 94°C for 10 seconds

- Step 3: Annealing step – 55°C for 15 seconds

- Step 4: Extension step – 72°C for 20 seconds

Step 2 – 4 was repeated over 60 cycles. The camera used in this system is set to detect signal during the annealing stage. The experimental procedure was repeated twice and data representative of the expressional trends is presented. It should be noted that the high number of cycles was not necessarily needed to detect the product, as calculation of the transcript number arises based on when fluorescent detection reaches a certain threshold point. Furthermore, in this established method, approximately 20 cycles are required for the generation of Z-tagged products (Nazarenko *et al.*, 1997).

This is illustrated in figure 2.2 where the 108 sample was similarly run at a high number of cycles but reaches threshold relatively early on (approx 18 cycles). Subsequently, calculation of sample copy number will depend on point at which the sample reaches threshold cycle (TC) in comparison to the standards, automatically generated by the instrument software. Specific Q-PCR primers were verified using a positive control known to express the molecule of interest and a negative control, where PCR water replaced cDNA, was also included to rule out contamination of the reaction.

(A)
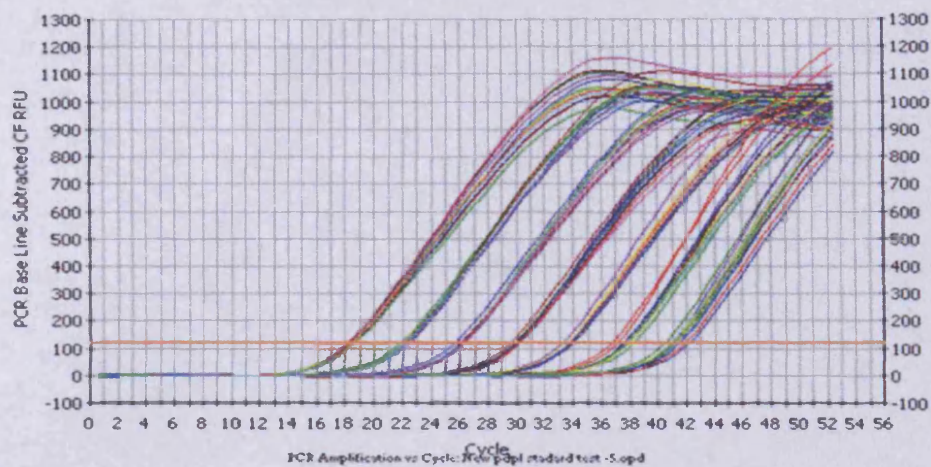
(B)

Correlation Coefficient: 0.999   Slope: -3.737   Intercept: 48.409   Y = -3.737 X + 48.409
PCR Efficiency: 85.2 %

□   Unknowns
♦   Standards
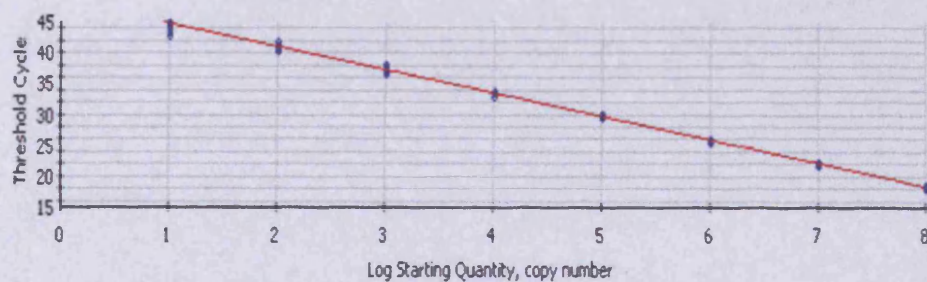
Figure 2.1: Generation of Q-PCR standard curve (A) Detection of transcript levels from a range of standard samples (108 to 102 copy number) using the iCycler^{IQ} thermal cycler. (B) Subsequent generation of a standard curve from these samples.

2.4 SDS-PAGE and Western Blotting

2.4.1 Cell Lysis and Protein Isolation

Upon reaching 85% confluency, the cell monolayer was removed from the flask using a disposable cell scraper; the detached cells were then transferred to a universal container. The cell suspension was centrifuged for 5 minutes at 1800 rpm to pellet cells and protein at the bottom of the universal container. Following centrifugation, the medium was aspirated and the cells were lysed in 200 – 250μl (depending on pellet size) of lysis buffer, before being transferred to a 1.8ml eppendorf (A Laboratories, Hampshire, UK) and placed on a Labinco rotating wheel (Wolf laboratories, York, UK) for 1 hour. The lysis solution was then spun at 13,000 rpm in a microcentrifuge for 15 minutes to remove any insolubles and the pellet removed from the eppendorf tube. The protein samples were quantified and used in SDS-PAGE or stored at 20°C until needed.

2.4.2 Protein Quantification

Prior to use in Western blotting the protein samples were standardised to a specific concentration. Protein concentration was determined using a Bio-Rad DC Protein Assay kit (Bio-Rad laboratories, Hemmelhempsted, UK) and the supplied microplate protocol. A range of standard samples of known concentrations were produced using a serial dilution of 10mg/ml bovine serum albumin (BSA) standard (Sigma, Dorset, UK). The standard was serially diluted from 10mg/ml to 0.005mg/ml in the lysis buffer used in the previous protein extraction. Prior to quantification 'working

reagent A' was prepared by adding 20μl reagent S to every millilitre of reagent A needed for the quantification. Five microlitres of either sample or standard was pipette into a well before adding 25μl 'working reagent A' followed by 200μl of reagent B. After the addition of reagent B the samples were mixed and incubated in the dark for 45 minutes. Absorbance of samples and standards at 620nm was then read using an ELx800 plate reading spectrophotometer (Bio-Tek, Wolf laboratories, York, UK). Using the absorbances from the BSA standards a standard curve was produced and used to determine sample concentration. All samples were normalised to the chosen concentration by dilution in the appropriated amount of lysis buffer. The samples were then further diluted 1:1 with 2x Lamelli sample buffer concentrate. Samples were then boiled and used in SDS-PAGE or stored at 20°C for future use.

2.4.3 Sodium dodecyl sulphate polyacrilamide gel electrophoresis (SDS-PAGE)

SDS-PAGE was used to detect the presence, or absence, of specific proteins. SDS-PAGE was undertaken using an OmniPAGE VS10 vertical electrophoresis system (OminPAGE, Wolf Laboratories, York, UK). Resolving gels of a required percentage (depending on the predicted size of the protein of interest) were made up in a universal container. The amount of each ingredient required to make up 15ml (enough for two gels) for both 8% and 10% resolving gels is indicated below:

Component	8% Resolving gel	10% Resolving gel
Distilled water	6.9ml	5.9ml
30% acrylamide mix (Sigma-Aldritch, St Louis, USA)	4.0ml	5.0ml
1.5M Tris (pH8.8)	3.8ml	3.8ml
10% SDS	0.15ml	0.15ml
10% Ammonia persulphate	0.15ml	0.15ml
TEMED (Sigma-Aldritch, St Louis, USA)	0.009ml	0.006ml

Table 2.6 Components for resolving gel.

The resulting mixture was then poured in between two glass plates held in place by a loading cassette, until a level 1cm below the top of the plate, and in order to prevent gel oxidation, the top of the resolving gel was covered with a 0.1% SDS solution. The gels were then left to polymerise at room temperature for approximately 30 minutes, or until fully set. The excess SDS solution was then poured off before adding a sufficient amount of stacking gel in its place, prepared as shown below:

Component	Stacking gel
Distilled water	3.4ml
30%acrylamide mix (Sigma-Aldritch, St Louis, USA)	0.83ml
1.0M Tris (pH 6.8)	0.63ml
10% SDS	0.05ml
10% Ammonium persulphate	0.05ml
TEMED (Sigma-Aldritch, St Louis, USA)	0.005ml

Table 2.7 Components for stacking gel

Immediately after the addition of the stacking gel, a well forming Teflon comb is inserted before allowing the gel to polymerise at room temperature for around 20 minutes. Once set, the loading cassette was transferred into an electrophoresis tank and covered with 1X running buffer before removing the well comb, and by use of a 50µl syringe (Hamilton), loading 6-8µl of ColorPlus Prestained Protein Marker (New England BioLabs Ltd., Herts, UK), followed by 10-15µl of the required protein samples. The gels were then run at 125V, 40mA, and 50W for a length of time appropriate for the size of the protein of interest, in order to separate the proteins according to charge and molecular weight.

2.4.4 Western Blotting

Once SDS-PAGE was completed, the protein samples were transferred to a nitrocellulose membrane using Western blotting. Gels were removed from the glass plates and the stacking gel cut away and discarded. The resolving gel was then placed on the bottom graphite base electrode in a SD20 SemiDry Maxi System blotting unit (SemiDRY, Wolf Laboratories, York, UK) on top of 3 pieces of 1x transfer buffer pre-soaked filter paper (Whatman International Ltd., Maidstone, UK), and 1 sheet of Hybond nitrocellulose membrane (Amersham Biosciences UK Ltd., Bucks, UK). An additional 3 sheets of pre-soaked filter paper were placed on top of the gel to form a sandwich arrangement of paper: membrane: gel: paper: as shown in Figure 2.2. Electroblotting was then carried out at 15v, 500mA, and 8W for around 1 hour. Once complete, membranes were removed and stored at 4°C in 10% skimmed milk, 0.1% polyoxyethylene (20) sorbitan monolaurate (Tween 20) (Sigma-Aldrich, St Louis, USA) in TBS until required for specific antibody probing.

SD20 Semi-dry blotting unit

- electrode

———————————————]— **Filter paper**
———————————————
———————————————

| Polyacrylamide gel |

———————————————

———————————————]— **Filter paper**
———————————————
———————————————

+ electrode
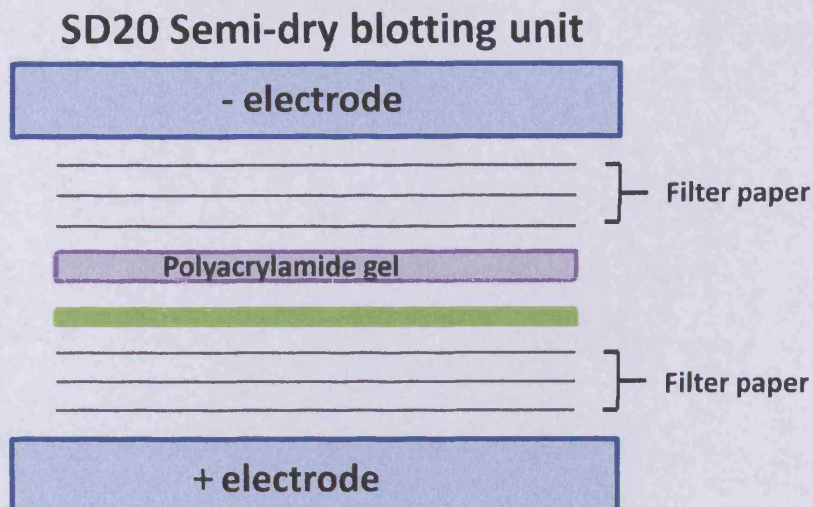
Figure 2.2 Diagram showing structure of Western blotting.

2.4.5 Staining of proteins

2.4.5.1 Staining membranes in Ponceau S

Ponceau S is a reversible and re-usable protein stain that does not interfere with any subsequent immune-probing. It is used to confirm transfer of proteins from the polyacrylamide gel to the nitrocellulose membrane. After the transfer was completed and before probing began, the membrane was immersed in Ponceau S solution for a few minutes at room temperature. The solution was then washed off with distilled water until the bands become visible. If required, the membrane was then cut into several sections using a sharp and clean scalpel. Once the Ponceau S was completely washed off it was placed in 10% milk solution.

2.4.6 Detection of proteins using specific antibody probing

Membranes were transferred to 50ml falcon tubes (Nunc, Fisher-Scientific, Leicestershire, UK) ensuring that the membrane surface that was in contact with the gel was facing upwards. The membranes were then placed in 10% milk blocking solution and left to rotate on a roller mixer (Stuart, Wolf Laboratories, York, UK) for 1 hour. After this blocking period was removed and a specific primary antibody at 1:200 in 3% milk solution (3% milk powder, 0.1% Tween 20 in TBS) was added to the falcon tube and the tube was placed on the roller mixer for 1 hour (See table 2.5 for full primer information). After 1 hour the primary antibody was removed and any remaining unbound antibody was washed off with three 15 minute washes with 3% milk solution. Once washing was completed, the membranes were incubated with 5ml of 1:1000 HRP conjugated secondary antibody (of the same species) diluted in 3% milk. The tubes were again placed on the roller mixer for a further hour. After this incubation two 15 minute washes in 10ml of t-TBS were conducted to remove any unbound secondary antibody. A final two 15 minute washes with TBS alone were carried out to remove any residual detergent, before placing the membrane in weighing boats containing TBS solution, ready for chemiluminescent detection.

2.4.7 Chemiluminescent protein detection

Chemiluminescent protein detection was carried out using the Supersignal™ West Dura system (Pierce Biotechnology, Inc., Rockford, IL, USA), which contains a highly

sensitive chemiluminescent substrate that detects the horseradish peroxidise (HRP) used during the western blot procedure. The two reagents provided were added in a 1:1 ratio into the weighing boat containing the membrane. After 5 minutes incubation the membrane was removed from the solution using forceps. Any excess solution was drained over a piece of tissue paper before being transferred to a new weighing boat. The chemiluminescent signal was detected using a UVITech Imager (UVITech Inc, Cambridge, UK) which was linked to a computer to directly capture and store the resulting image. Each membrane was subjected to varying exposure times until the protein bands were sufficiently visible. These images were then captured and further analysed with the UVIband software package (UVITEC, Cambridge, UK), which allows for protein band quantification. In this study, GAPDH was used as a housekeeping gene and run alongside any other proteins to be detected, so as to allow for additional normalisation of the samples, and to compensate for any other negligible inaccuracies which may have occurred during the process. Because the GAPDH gene is often stably and constitutively expressed at high levels in most tissues and cells, it is considered a housekeeping gene. For this reason, GAPDH is commonly used as a loading control. In order to confirm reliability of the results, each Western blot was carried out three times and the protein bands quantified and standardised separately, followed by calculation of mean values and graphical presentation of the results.

2.4.8 Immunocytochemical staining

This study uses a previously reported method of Immunocytochemical staining (Jiang *et al.* 2005) and was carried out as follows:

97

20,000 cells in 200μl DMEM media were seeded into chamber slides (Nalge, NUNC International, LAB-TEK®, USA) and left to incubate overnight at 37°C, with 5% CO_2. The cells were then fixed in formalin for 30 minutes at 4°C, before being rehydrated with BSS for an hour at room temperature. This was followed by cell permeabilisation in 0.1% TritonX100 in TBS for 5-10 minutes at room temperature. This causes the cell membranes to rupture, releasing intracellular proteins. Permeabilisation was followed by blocking of the cells with horse serum (Vector Laboratories Inc., Burlingame, USA) in OptiMax Wash Buffer (BioGenex, San Ramon, USA) for 30 minutes at room temperature. 1-2 drops of horse serum per 5ml of wash buffer was diluted 1:20 in distilled water and used as the blocking solution. After blocking, the cells were washed four times with wash buffer before being incubated for an hour at room temperature with primary antibody diluted 1:100 (depends on antibody used) in blocking solution. Any unbound antibody was subsequently washed off with wash buffer. This was repeated 4 times before incubating the cells for a further 30 minutes at room temperature, with the corresponding secondary antibody diluted 1:1000 in blocking solution. After 4 washes with wash buffer, the cells were incubated with 200μl of working VECTASTAIN® Universal ABC complex (Vector Laboratories Inc., Burlingame, USA). The ABC complex was made up 30 minutes before use by mixing 4 drops of the supplied reagent A, with 4 drops of reagent B. The ABC solution was subsequently removed by washing four times with wash buffer before a few drops of DAB chromogen (Vector Laboratories Inc., Burlingame, USA) were added to the cells and left to incubate for 5 minutes in darkness. DAB was made up as follows; 2 drops of the provided buffer (pH 7.5), 4 drops of DAB, and 2 drops of hydrogen peroxide diluted in 5ml of distilled water. Following DAB addition, the solution should turn brown and

once this had occurred, the DAB was washed off using distilled water before the cells were counterstained with Mayer's haemotoxylin for approximately 1 minute.

2.4.9 Immunoflourescent staining

The method used in this study for fluorescent staining was carried out as previously reported (Jiang et al., 1999). 20,000 cells in 200μl DMEM media were seeded into chamber slides (Nalge, NUNC International, LAB-TEK®, USA) and left to incubate overnight at 37°C, with 5% CO_2.

After incubation the media was aspirated and the cells fixed with 200μl ice-cold pure ethanol for 20 minutes at 4°C. Following fixation, the cells were rehydrated with 200μl BSS for a minimum of 30 minutes at room temperature. The cells were permeabilised with 0.1% Tritonx100 in TBS for 5-10 minutes at room temperature before being blocked with horse serum in OptiMax Wash Buffer (BioGenex, San Ramon, USA) for 30 minutes at room temperature as explained in section 2.4.7. Blocking was followed by four washes with wash buffer before the cells were incubated for an hour at room temperature with primary antibody diluted 1:100 (depending on antibody used) in blocking solution. After a further four washes with wash buffer, the cells were incubated with the corresponding secondary antibody labelled with either FITC or TRITC diluted 1:100 in blocking serum. The secondary antibodies were subsequently washed off twice using wash buffer before the slides were mounted with Flouro-Save (CalBiochem, Nottingham, England) and viewed under a fluorescent microscope (Olympus). Photos were taken and analysis carried out using the Cell Analyser software (Olympus).

2.5 Alteration of Matriptase-2 gene expression

2.5.1 Knocking down gene expression using Ribozyme Transgenes

In order to knockdown the expression of Matriptase-2, it was targeted at the mRNA level using hammerhead ribozyme transgenes that specifically target and cleave the Matriptase-2 mRNA transcript. This method of knockdown is used within the laboratory instead of siRNA because the ribozyme method proved to be consistently more reliable and stable than the siRNA method. The hammerhead ribozyme was first described by Forster and Symons in 1987 as a self-cleaving region in the RNA genome of various plant viroids and virusoids. The hammerhead motif was subsequently integrated into short synthetic oligonucleotides, transforming it into a turnover catalyst capable of cleaving various RNA targets (Uhlenbeck, 1987; Haseloff and Gerlach, 1988).

Hammerhead motifs contain a conserved secondary structure that consists of three helical stems (I, II, and III) enclosing a junction known as the catalytic core, typified by various invariant nucleotides. The best codons demonstrated to be suitable for cleavage are AUC, GUC and UUC (Figure 2.3a). In order to generate a ribozyme transgene specific to Matriptase-2, primers were designed using Zuker's RNA mFold programme (Zuker, 2003) according to the secondary structure of the gene. Subsequently, an appropriate GUC ribozyme target site was chosen from within matriptase-2's secondary structure (Figure 2.3b) and the ribozyme created to specifically bind the sequence adjacent to this GUC codon. This made it possible for the hammerhead catalytic region

of the ribozyme to bind to and specifically cleave the GUC sequence within the target mRNA transcript.

Following ribozyme design, the sequences were ordered from invitrogen as sense/antisense strands (as shown in Table 2.4) and joined to the transgene by carrying out touchdown PCR under the following conditions:

-

- Step 1: Initial denaturing period – 94°C for 5 minutes

- Step 2: Denaturing step – 94°C for 10 seconds

- Step 3: Various annealing steps – 70°C for 15 seconds, 65°C for 15 seconds,

- 60°C for 15 seconds, 57°C for 15 seconds, 54°C for 15 seconds and 50°C for 15seconds.

- Step 4: Extension step – 72°C for 20 seconds

- Step 5: Final extension period – 72oC for 7 minutes

- Step 2 – 4 was repeated over 48 cycles, each different annealing temperature comprising 8 cycles.

Once combined, the transgenes were run electrophoretically on a 2% agarose gel to confirm presence and correct size before being inserted into the pEF6 plasmid in the TOPO cloning reaction, as described in a later section.

```
        3'    5'
         :     :
         U ---- A
         G ---- C        Substrate
Helix III  C ---- G
         C  —  G        Cleavage site
         A  —  T            ↙
      A  A  —  C
   A  A  GGCC G A        GGTCGCC ------- 3'
   A        | | | |       | | | | | | |
      G  CCGG  A         CCAGCGG ------- 5'
              G              C
   Helix II      U  A  G  U     Helix I
```

Hammerhead ribozyme
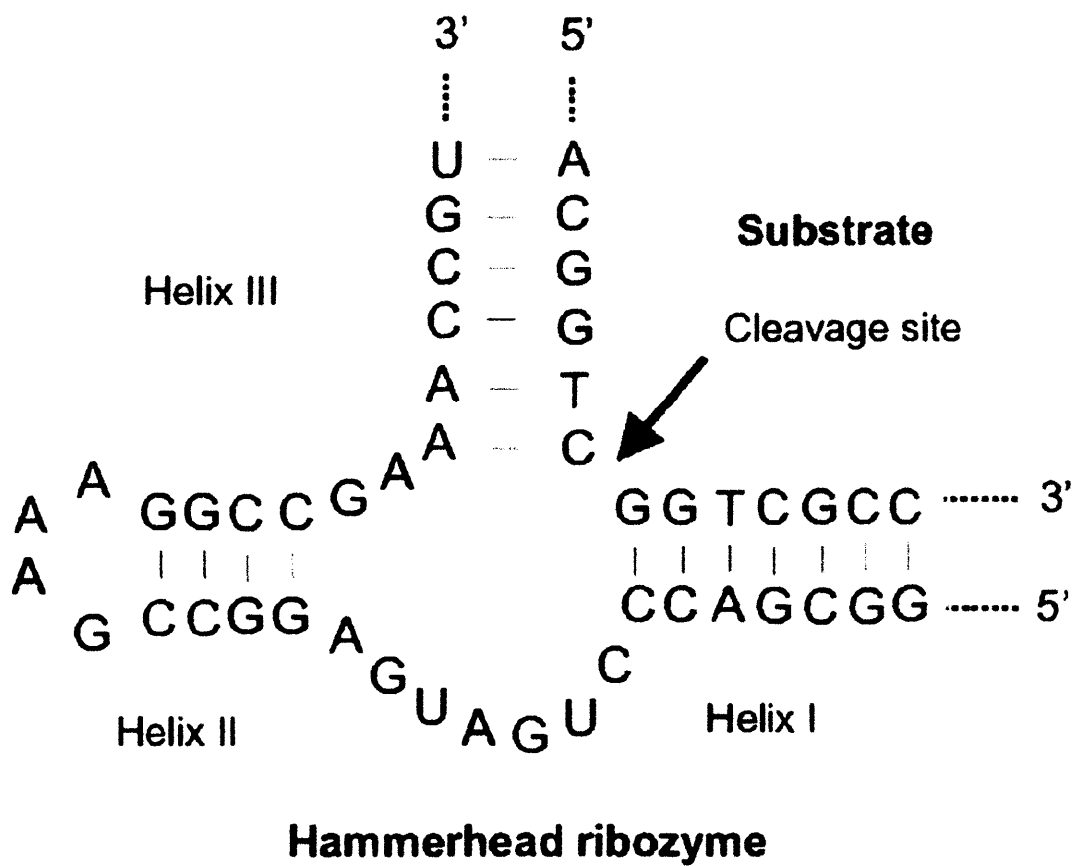
Figure 2.3a: Secondary structure of hammerhead ribozyme with bound substrate.
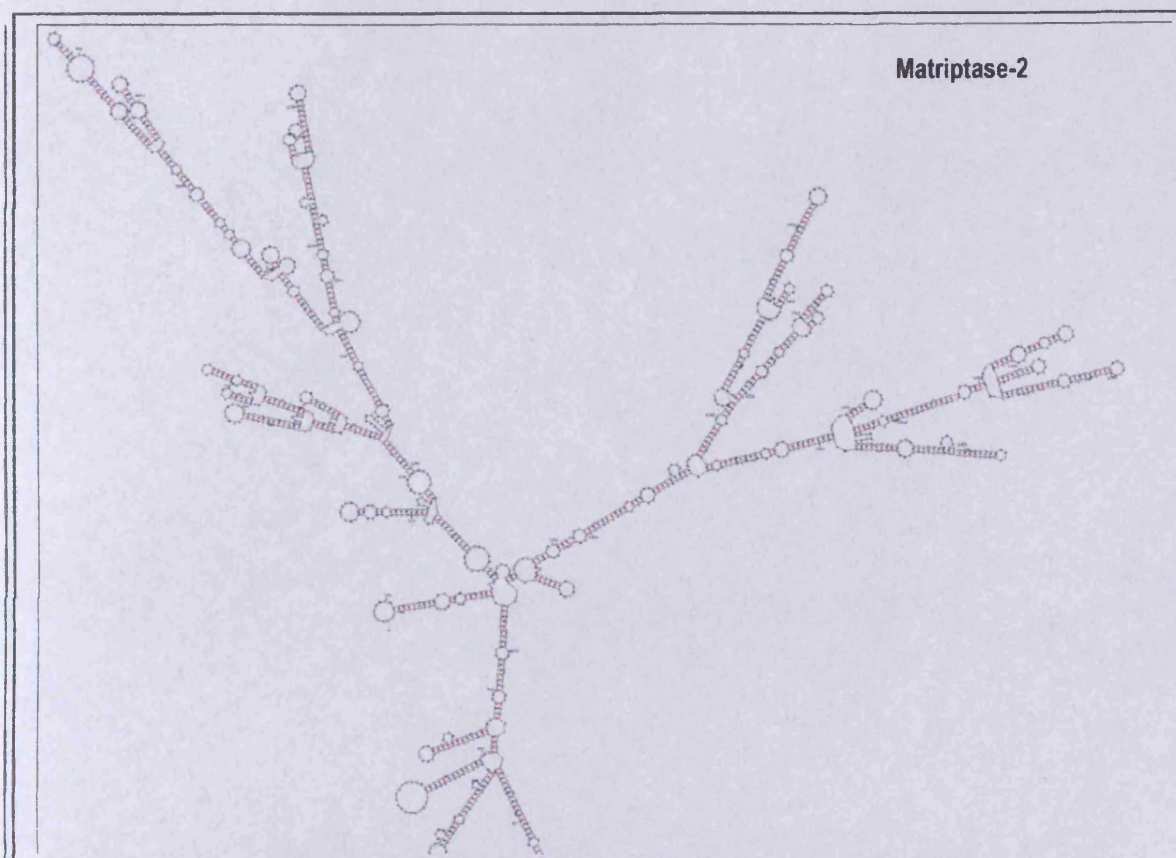
Figure 2.3b The predicted secondary structure of human matriptase-2 mRNA

2.5.2 Matriptase-2 gene over-expression

In addition to generating ribozyme transgenes against matriptase-2, the full sequence of matriptase-2 was also cloned into the pEF6 plasmid and used to transform mammalian cancer and human endothelial cells. Prior to the initiation of this PhD study, a pEF6 plasmid, containing the full sequence of matriptase-2, had been generated by Dr C. Parr. This cloning work has been recently fully described in Parr *et al* 2007 (Parr *et al.*, 2007). It is unkown if the original creator of the expression plasmid intended to utilise the V5/His tagged pEF6 vector for purification or immunolabelling procedures. It does not appear that these tags affect matriptase-2 function although in depth examination should be conducted in the future. Briefly, matriptase-2 was found to

be modestly expressed in the PLC/PRF/5 hepatocellular carcinoma cell line; cDNA from this cell line was subsequently used to generate the full matriptase-2 cDNA sequence for further use in cloning. In order to isolate the full matriptase-2 sequence expression primers (see table 2.1) were designed based on the *Homo sapiens* matriptase-2 mRNA sequence (PubMed accession number AJ319876). These primers, together with PLC/PRF/5 cDNA, were used in a PCR reaction (using an annealing temperature of 58°C over 35 cycles). Following electrophoretic separation on a 0.8% gel and staining, a band of approximately 2.5Kbp was revealed. This band corresponds with matriptase-2 sequence size listed in PubMed. This product was later inserted into the pEF6 plasmid using the TOPO cloning reaction described later. Prior to this current study, a study by Sanders *et al* 2008 used this matriptase-2 expression plasmid to extensively investigate the effect of matriptase-2 over-expression on the cancerous cell lines PC3 and DU145 (Sanders *et al.*, 2008). Any further mention of the functional aspects of these two cell lines relating to matriptase-2 expression status was derived from the Sanders *et al* study.

2.5.3 TOPO cloning reaction

Cloning of both the ribozyme and expression sequence was carried out using the pEF6/V5-His TOPO TA Expression Kit (Invitrogen, Paisley, UK), following the provided protocol. This protocol allows rapid five minute one step cloning of *Taq* polymerase amplified products for expression in mammalian cells. Once cloned, analysed, and transfected into a mammalian host cell line, the PCR product can be constitutively expressed (Figure 2.2). The reaction was performed in accordance with the manufacturers' protocol which is outlined in the following sections.
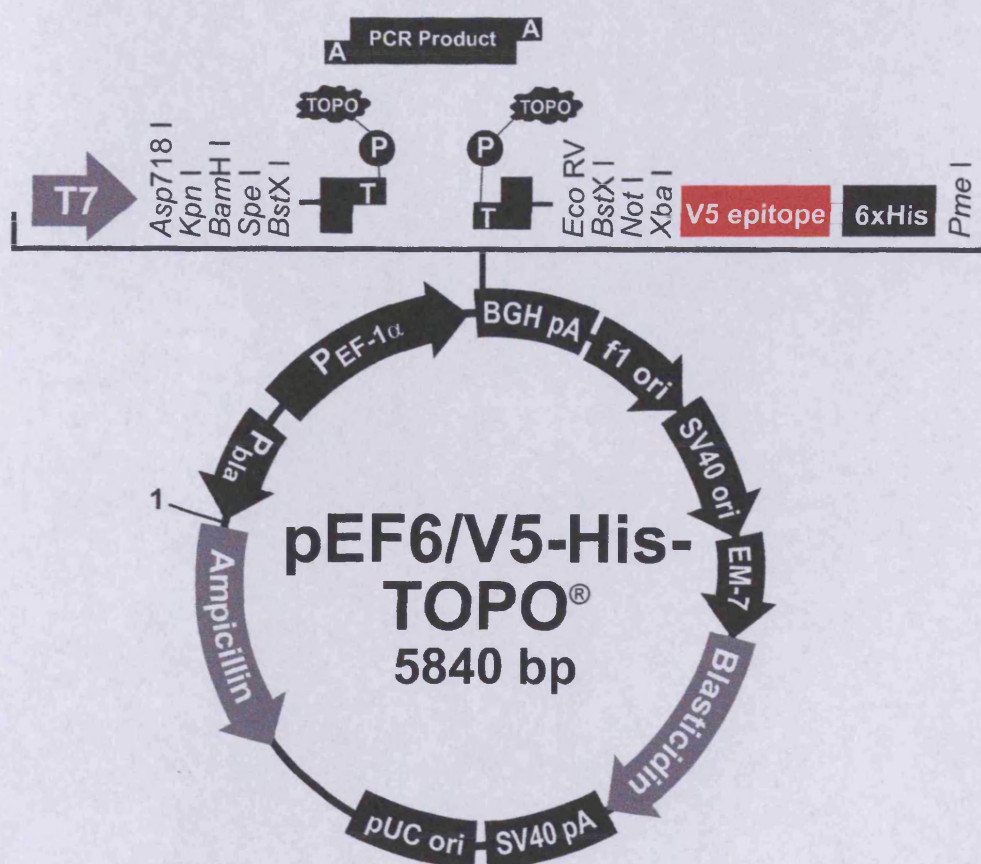
Figure 2.4: Schematic of the pEF6 plasmid (taken from pEF6/V5-His TOPO TA Expression Kit protocol).

The following TOPO cloning reaction was set up for each ribozyme transgene or expression sequence used in a labelled PCR tube:

- PCR product (ribozyme or expression sequence) – 4μl
- Salt solution – 1μl
- TOPO vector – 1μl

This reaction was gently mixed and incubated at room temperature for 30 minutes and stored in ice until proceeding to One Shot Chemical Transformation.

2.5.4 One Shot Chemical Transformation of chemically competent *Escheria coli*

Five microlitres of the TOPO cloning reaction from previously completed in 2.3.2 was added to a vial of One Shot Chemically Competent E. coli and mixed by stirring gently with the pipette tip as pipetting up and down may damage the bacteria. The vial was then incubated on ice for 30 minutes. After this incubation, the cells were heat-shocked for 30 seconds at 42°C without shaking and immediately placed back on ice. Two hundred and fifty microlitres of room temperature SOC medium was added to each tube, which were then capped tightly and shaken horizontally at 200 rpm on a horizontal orbital shaker (Bibby Stuart Scientific, UK), at 37°C for 1 hour. Following this incubation period, the contents of each tube were spread onto two pre-warmed selective agar plates (containing 100μg/ml ampicillin). One plate was seeded at a high concentration and the other at a low concentration. The plates then were incubated

overnight at 37°C to allow the *E. coli* to grow and form colonies. The pEF6 plasmid contains two antibiotic resistance genes that allow cells containing the plasmid to grow under ampicillin and blasticidin S selection, a schematic of the plasmid is shown in figure 2.1.
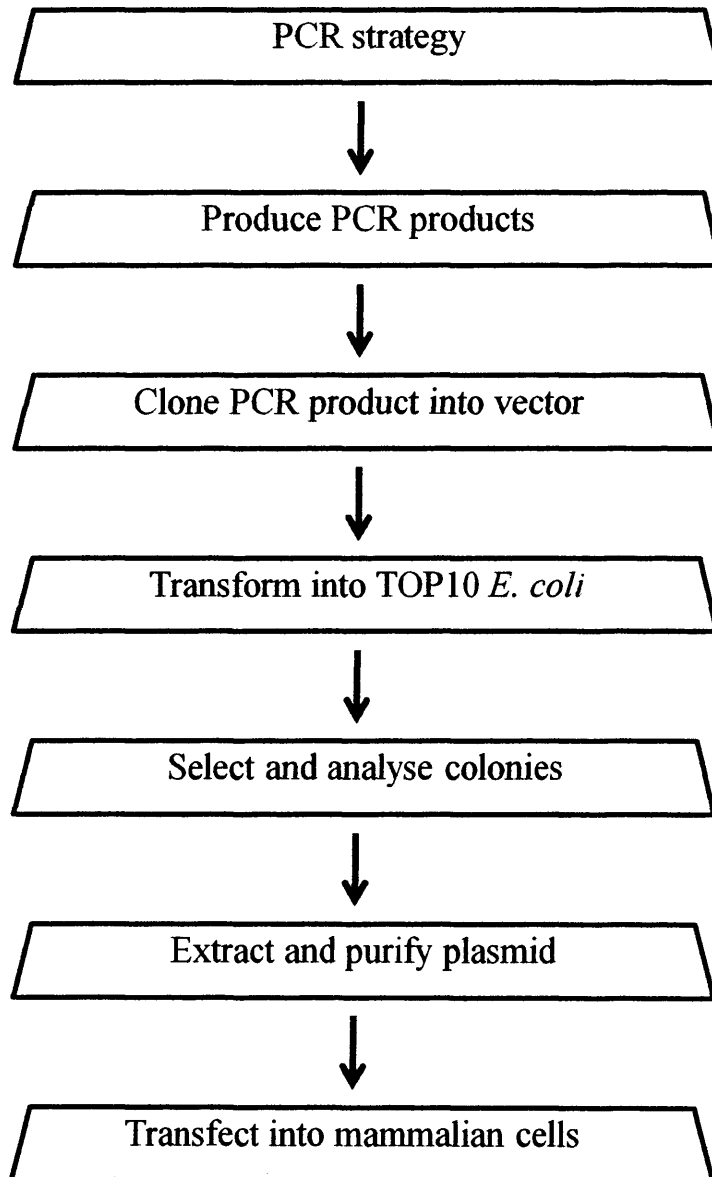
Figure 2.5 Flow chart detailing the process of TOPO TA cloning reaction

2.5.5 Selection and orientation analysis of positive colonies

Correct insertion and orientation of the ribozyme/expression sequence in the plasmid was analysed to ensure that the resulting product would be viable. The colonies were tested using PCR with primers specific to either the ribozyme/expression sequence, or the pEF6 plasmid. The size of the product obtained using the plasmid specific primers (T7F and BGHR) will give an indication of the inserted sequence size and can then be used to check that the full sequence had been inserted without degradation. Although T7F vs. BGHR indicate if the complete sequence has inserted it does not give an indication of the orientation of the insert. Therefore, in order to check correct size and orientation of the sequence, a mixture of plasmid specific and sequence specific primers were used. To check the ribozyme sequences a combination of T7F vs. RbToP and T7F vs. RbBMR were used. RbToP and RbBMR recognise and bind to sequences within the ribozyme transgene that are common to all of the ribozymes used. There are approximately 90bp between the T7F promoter and the beginning of the insert. Thus, correct orientation and ribozyme size (based on approximate ribozyme size of 50bp), would be confirmed by a band of approximately 140bp in the T7F vs. RbBMR reaction. Likewise, a band of approximately 140bp in the T7F vs. RbToP would indicate incorrect orientation of the sequence.

Following overnight incubation, the plates were examined for colony growth. Ten colonies were randomly selected for orientation analysis and marked and labelled on the plates. For each colony, two PCR reactions were carried out as follows (full primer sequences are given in table 2.2):

Ribozyme orientation reaction 1

- 8μl - 2X REDTaq ReadyMix PCR Reaction mix

- 1μl – T7F plasmid specific forward primer

- 1μl – Ribozyme specific forward primer (RbToP)

- 6μl – PCR water

Ribozyme orientation reaction 2

- 8μl - 2X REDTaq ReadyMix PCR Reaction mix

- 1μl – T7F plasmid specific primer

- 1μl – Ribozyme specific reverse primer (RbBMR)

- 6μl – PCR water

In order to test the DNA present in the colonies, a sample was picked from the plate using a sterile pipette tip and inoculated into both mixes before the addition of the specific primers. Each reaction mix was then placed in a thermal cycler and subjected to the following conditions:

- Step 1: Initial denaturing period – 95°C for 10 minutes

- Step 2: Denaturing step – 94°C for 1 minute

- Step 3: Annealing step – 55°C for 1 minute

- Step 4: Extension step – 72°C for 1 minute

- Step 5: Final extension period – 72°C for 10 minutes

The mixture was run on a 2% agarose gel and visualized under ultra violet light. Colonies showing correct orientation of the insert were picked off the plate and used to inoculate 10ml of ampicillin selective LB broth and incubated overnight whilst being horizontally shaken at 225 rpm.

Orientation checking for the larger matriptase-2 expression sequence products follows the same basic theory and principle. As mentioned earlier, the generation of a pEF6 plasmid containing the matriptase-2 expression sequence had been previously completed by Dr C. Parr prior to the initiation of this PhD study and is outlined in Parr et al, 2007 (Parr et al., 2007). Thus correct orientation of this molecule had already been confirmed by Dr Parr using the following PCR reactions T7F vs. BGHR (indicating full sequence) and T7F vs. matrip2R1 (indicating correct orientation). A sample of the matriptase-2 expression plasmid was generously donated by Dr Parr for use in the prostate study conducted in this thesis. This plasmid was then used to inoculate fresh One Shot TOP10 Chemically Competent E. coli and subsequently subjected to further orientation and size checks before being used to transfect the prostate cancer cell lines. Additional information, together with results of orientation checking, is outlined in chapter 3.

2.5.6 Plasmid extraction, purification and quantification

Plasmid extraction was performed using the Sigma GenElute Plasmid MiniPrep Kit according to the provided protocol. Five millilitres of the LB broth previously inoculated with the chosen colony and cultured overnight was centrifuged at 3,000 RCF to obtain a pellet of bacteria. The supernatum was removed and the bacterial pellet was resuspended in 200μl of resuspension solution (containing RNase A) and mixed by pipetting. Two hundred microlitres of lysis solution was then added and the container and inverted 5 - 6 times. This stage was completed within 5 minutes before adding 350μl of the neutralisation solution, inverting 4 – 6 times and centrifuging at 12,000 x g

in a micro centrifuge. Plasmid DNA was bound to the column by transferring the cleared lysate to a Mini Spin Column placed inside a collection tube, spinning at 12,000 x g for 30 seconds to 1 minute and discarding the flow through. Seven hundred and fifty microlitres of wash solution (containing ethanol) was added to the column before spinning at 12,000 x g for 30 seconds to 1 minute and again discarding flow through. The column was spun at 12,000 x g for 30 seconds to 1 minute to remove any remaining flow through before transferring the Mini Spin Column to a fresh collection tube. Plasmid DNA was eluted through the addition of 100μl of elution solution and spinning the column at 12,000 x g for 1 minute. The eluted plasmid solution was then electrophoretically run on a 0.8% agarose gel to confirm presence and correct size of the plasmid.

2.5.7 Transfection of plasmid using electroporation

In order to introduce the plasmid DNA to the mammalian cells the method of electroporation was used. This involves using electricity to induce pores in the cell membrane to allow plasmid DNA to enter the cell. Following plasmid purification and quantification, 1-3μg of the extracted plasmid was used to transfect the mammalian cancer cell lines. Near confluent wild type cells were detached from tissue culture flasks using trypsin/EDTA, pelleted and counted following resuspension as previously described. One million cells in 1000μl were added to an electroporation curvette (Eurgenetech, Southampton, UK) together with the purified plasmid. This was briefly mixed before being subjected to an electrical pulse of 310V and 1500 capacitance from an electroporator (Easyjet, Flowgene, Surrey, UK). Following this pulse, the cell and

plasmid suspension was quickly transferred into 5ml of pre warmed medium and placed in an incubator to allow any surviving cells to recover from the electroporation process.

2.5.8 Selection and maintenance of transfected cell lines

The pEF6/V5-His-TOPO plasmid used to transform the cells, encodes two antibiotic resistance genes. As previously described, the ampicillin resistance gene allows initial selection of prokaryotic bacterial cells containing the plasmid. The plasmid also contains a blasticidin S resistance gene. Blasticidin S is a potent microbial antibiotic that inhibits protein synthesis in both prokaryotes and eukaryotes and is used to specifically select for mammalian cells containing the pEF6 plasmid. The use of two antibiotic resistance genes allows more accurate selection of the plasmid throughout the cloning process. Following electroporation the cells were incubated overnight. The cells were then subjected to an intense 5 day period of blasticidin S selection. During this period the cells were cultured in medium supplemented with 5ug/ml of the blasticidin S antibiotic to kill any cells that did not harbour the pEF6 plasmid. After this initial 5 day period the cells were placed in to medium containing $0.5\mu g/ml$ of blasticidin S to place the cells under a selection pressure to maintain long term transformation of the cells. All cells were tested initially and following long periods of use, to estimate the efficacy and stability of both the transformation and the ribozyme transgene or expression sequence using RT-PCR and Western blot analysis.

2.6 *In vitro* cell function assays

2.6.1 *In vitro* cell growth assay

Cells were detached from the culture flask and cell density (per millilitre) was determined. Cells were then seeded into a 96 well plate (Nunc, Fisher Scientific, Leistershire, UK) at a seeding density of 3,000 cells in 200µl of normal medium per well. Four plates were set up to obtain a cell density reading following, 1, 3 and 5 day incubation periods at 37°C, 5% CO_2 and 95% humidity. After the appropriate incubation period, the medium was aspirated and cells fixed in 4% formaldehyde in BSS for at least 10 minutes. The cells were then stained in 0.5% crystal violet solution in distilled water. The stain was then extracted from the cells using 10% acetic acid and cell density determined by measuring the absorbance at 540nm on a plate reading spectrophotometer (ELx800, Bio-Tek, Wolf Laboratories, York, UK) (Figure 2.4). Cell growth was presented as percentage increase and calculated by comparing the absorbance obtained for each incubation period. The following equation was used to perform this task:

Percentage increase = (day 1, 3 or 5 absorbance – (day 1 absorbance/ day 1 absorbance)) x100

Within each experiment at least twelve duplicate wells were set up and the entire protocol was repeated independently a minimum of three times (Smith *et al.*, 2003).
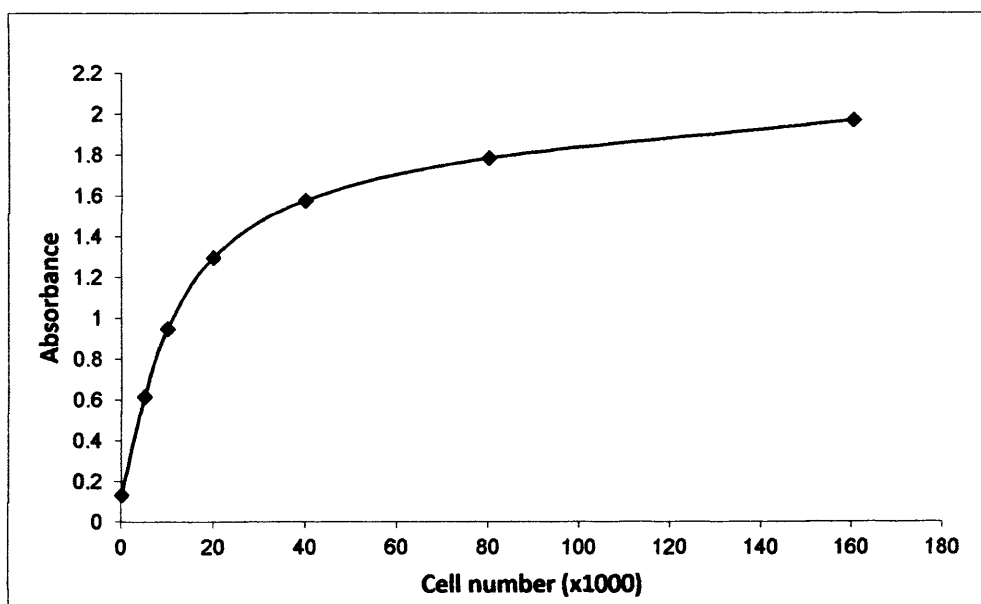
Figure 2.6 Sensitivity of crystal violet assay

Graph shows level of absorbance of crystal violet for a set number of cells.

2.6.2 *In vitro* cell Matrigel adhesion assay

Cells were detached from the culture flask and cell density (per millilitre) was determined. Five micrograms of Matrigel in 100μl of serum free medium was added to wells of a 96 well plate and dried in an oven to form an artificial basement membrane. The membrane was then rehydrated in 100μl of serum free medium for 40 minutes before cell seeding. Forty five thousand cells were seeded onto the Matrigel basement membrane in 200μl of normal medium and incubated for 40 minutes at 37°C, 5% CO_2 and 95% humidity. After incubation, the medium was aspirated and the membrane washed four times with 150μl of BSS solution to remove loosely attached cells. Adherent cells were then fixed in 4% formaldehyde in BSS for 10 minutes before being stained in 0.5% crystal violet solution in distilled water. Adherent cells were then

visualised under the microscope under x40 objective magnification and random fields counted. At least 3 random fields per well were counted and a minimum of 3 duplicate wells were set up per sample. The entire experimental procedure was repeated independently a minimum of three times.

2.6.3 *In vitro* cell matrigel tubule formation assay

This assay was used to measure the ability of endothelial cells to form tubule structures in an artificial Matrigel basement membrane. These tubules are indicative of the cell's ability to form new blood vessels. Cells were detached from the culture flask and cell density (per millilitre) was determined. Wells in a 96 well cell culture plate were coated in 250µg Matrigel in 100µl serum free medium and allowed to set. Once the matrigel had set, 32,000 cells in 200µl normal medium were seeded into the wells and incubated for 6 hours at 37°C, 5% CO_2 and 95% humidity. Following incubation, wells were visualised under x40 objective magnification and random fields counted. At least 5 random fields were counted per well and the whole experimental procedure was repeated 3 independent times. The total internal perimeter of all tubules per field was measured using Image J software. The arbitrary values obtained were converted into µm by multiplying the value by 2 as previously calibrated using a haemocytometer.

2.6.4 *In vitro* cell Matrigel invasion assay

The invasive capacity of the cells used in this study was determined using an *in vitro* Matrigel invasion assay. This assay measures the cells ability to degrade and

invade through an artificial basement membrane and migrate through 8μm pores. Cells were detached from the culture flask and cell density (per millilitre) was determined. Twenty four well cell culture plate inserts (BD Biosciences. Oxford, UK) containing 8μm pores were coated in 50μg of Matrigel (BD Biosciences, Oxford, UK) in 100ul serum-free medium and dried in an oven. Once dried, these inserts were placed into sterile 24 well plates and the artificial membrane was rehydrated with 100μl of serum free media. The serum-free medium was then removed and 1ml of normal medium was added to the wells containing the insert in order to sustain any cells that may have invaded through the insert. 40,000 cells in 200μl of normal medium were then added to the insert over the top of the artificial basement membrane. The plate was then incubated for 72 hours at 37°C, 5% CO_2 and 95% humidity.

After 72 hours, the inserts were removed from the plate and the inside of the insert (which was initially seeded with cells) was cleaned thoroughly with tissue paper. Any cells which had invaded through the membrane and passed to the underside of the insert were fixed in 4% formaldehyde in BSS for 10 minutes before being stained with 0.5% crystal violet solution in distilled water. These cells could then be visualised under the microscope at x40 objective magnification and random fields counted. At least 3 random fields per insert were counted and duplicate inserts were set up for each test sample. The experimental procedure was repeated a minimum of three times (Engelhard et al., 1998).

2.6.5 *In vitro* cell motility assay

This assays allowed the measurement of the motile capacity of the cells. Cells were detached from the culture flask and cell density (per millilitre) was determined. 500,000 cells for each cell type were incubated in 10ml of growth medium containing 100μl of cytodex-2 beads (GE Healthcare, Cardiff, UK) for 3.5 hours to allow the cells to adhere to the beads. The beads were then washed twice in 5ml of normal medium to remove non-adherent or dead cells. After the second wash the beads were resuspended in 5 ml of growth medium. Three hundred microlitres of this solution was then added to a 96 well plate and incubated overnight at 37°C, 5% CO_2 and 95% humidity. Following incubation, any cells that had migrated from the cytodex-2 beads and adhered to the base of the well were fixed in 4% formaldehyde for 10 minutes, stained with 0.5% crystal violet. The cytodex-2 beads were removed through several extensive washes with BSS. Cells were then counted under x20 objective magnification, Three random fields were counted per well and 10 duplicate wells were set up per sample. The entire experimental procedure was repeated three independent times (Rosen *et al.*, 1990).

Chapter 3

Altering the expression of matriptase-2 in prostate cancer, prostate epithelial and endothelial cell lines

3.1 Introduction

Recently the type II transmembrane serine proteases (TTSP) have attracted significant interest due to their various roles in cancer progression and development. Various studies involving the TTSPs have found them to be aberrantly expressed during cancer development and progression (Wallrapp *et al.*, 2000; Magee *et al.*, 2001; Oberst *et al.*, 2001; Huang and Waknitz, 2009). These TTSPs are becoming one of the most intensively studied super families in the cancer field.

Matriptase-2 is a poorly studied protease in the field of cancer progression compared to other members of the TTSP super family. Matriptase-2 consists of a short cytoplasmic extension with unknown function, a transmembrane domain, a SEA domain, two CUB domains, three LDLA domains and a C-terminal active serine protease (Szabo and Bugge, 2008). It was originally presumed that matriptase-2 would drive cancer progression due to its high homology with matriptase-1. Due to previous work within the department it is now known that matriptase-2 acts in to opposite manner to matriptase-1.

Matriptase-2 over-expression significantly reduces breast and prostate cancer growth and reduced levels correlate with poor patient outcome (Parr *et al.*, 2007; Sanders *et al.*, 2008). The molecular mechanisms involved in the activation of matriptase-2 remain largely unknown. Also, little is known about the substrates of matriptase-2, although it has been shown to degrade fibronectin, fibrinogen and type 1

collagen and to have limited action against pro-uPA and to cleave mHJV (Velasco *et al.*, 2002; Silvestri *et al.*, 2008).

No previous studies have investigated a possible role for matriptase-2 in prostate epithelial cells. Therefore, based on the established implications of previous studies within the laboratory investigating matriptase-2, this study aims to establish a role for matriptase-2, by altering its expression levels in two prostate epithelial cell lines. Therefore, by altering the endogenous expression levels of matriptase-2 in prostate epithelial cell lines, it was hypothesised that a loss of matriptase-2 in these epithelial cell lines would result in a push towards a more aggressive phenotype more commonly seen in prostate cancer cell lines such as PC3 and DU145. The HECV endothelial cell line would also be used in another pioneering study to investigate the potential involvement of matriptase-2 in angiogenesis.

In this study, matriptase-2 expression plasmid and ribozyme transgene were used to over-express and silence matriptase-2 expression in several cell lines, respectively. Matriptase-2 expression was knocked-down in PZHPV7 and PNT2C2 cells and over-expressed in PC3, DU145, and HECV cell lines. Following transfection with the plasmids, matriptase-2 expression was verified using both mRNA and protein based methods. The remaining chapters in this study then aim to investigate the effect of altering matriptase-2 expression on the biological properties of prostate cells in order to elucidate the function of matriptase-2 in this cancer. The transfection of HECV cells will also allow the investigation of the effect of matriptase-2 in angiogenesis.

3.2 Materials and methods

1.6.2   3.2.1 Cell lines

PZHPV7, PNT2C2, PC3, DU145, and HECV cell lines were used, cultured and maintained as described in sections 2.2.3.

3.2.2 Creation of over-expression and knock-down cell lines

Matriptase-2 expression plasmids were re-amplified, cloned and transfected into the PC3, DU145 and HECV cell lines. Ribozyme transgenes targeting matriptase-2 mRNA were generated, cloned and transfected into PZHPV7 and PNT2C2 cell lines. Full details of the procedure used to generate the expression plasmid and ribozyme, insert it into the pEF6 plasmid, amplify the plasmid in *E. coli*, extract and electroporate the plasmid into mammalian cells are given in section 2.5. Full expression and ribozyme sequence data are shown in tables 2.2 and 2.3 in the general methods section (chapter 2).

3.2.3 RNA isolation, cDNA synthesis, and RT-PCR

RNA was isolated from the cells using the ABgene Total RNA Isolation Reagent (TRIR) kit (ABgene, Surrey, UK), and converted into cDNA by reverse transcription using the iScript™ cDNA Synthesis Kit (Bio-Rad Laboratories, California, USA), as described in section 2.4. This was then used as a template for RT-PCR, which was carried out at the following conditions; 94°C for 5 minutes, followed

by 30 to 42 cycles of 94°C for 30 seconds, 56°C for 30 seconds, and 72°C for 1 minute, and a final extension of 7 minutes at 72°C. The products were run on an agarose gel and visualised using ethidium bromide.

3.2.8 Protein extraction, SDS-PAGE, and Western blot analysis

Protein was extracted following cell lysis, and was then quantified using the DC Protein Assay kit (BIO-RAD, USA). Following SDS-PAGE, the proteins were transferred onto nitrocellulose membranes which were blocked, and probed with the specific primary (anti-matriptase-2) and the corresponding peroxidise-conjugated secondary antibodies (1:1000). All of the antibodies used in this study are listed in Table 2.5. The protein bands were eventually visualised using the SupersignalTM West Dura system (Pierce Biotechnology, USA).

3.2.9 Immunocytochemistry (ICC)

Twenty thousand cells in 200μl DMEM media were seeded into chamber slides (Nalge, NUNC International, LAB-TEK®, USA) and left to incubate overnight at 37°C, with 5% CO_2. After incubation the media was aspirated and the cells fixed with 200μl formalin for 20 minutes at 4°C. Following fixation, the cells were rehydrated with 200μl BSS for a minimum of 30 minutes at room temperature. Cells were permeabilsed and incubated with β-catenin primary antibody for 1 hour. After 4 washes with wash buffer, the cells were incubated with 200μl of working VECTASTAIN® Universal ABC complex (Vector Laboratories Inc., Burlingame, USA). The ABC solution was

subsequently removed by washing four times with wash buffer before a few drops of DAB chromogen (Vector Laboratories Inc., Burlingame, USA) were added to the cells and left to incubate for 5 minutes in darkness. The DAB solution was washed off using distilled water before the cells were counterstained with Mayer's haemotoxylin for approximately 1 minute. The slides were then viewed under a light microscope.

3.3 Results

3.3.1 Cell line screen for mariptase-2 expression

In order to determine which cell lines should be transfected with either the expression or ribozyme plasmid the expression levels of matriptase-2 in PC3, DU145, CAHPV10, PNT1A, PZHPV7, PNT2C2 and HECV cell lines were examined using PCR. Figure 3.1 shows that PC3, CAHPV10, PNT1A and HECV have minimal or no expression of matriptase-2. DU145 appears to display a small amount of matriptase-2 mRNA. In contrast PZHPV7 and PNT2C2 display a high expression of matriptase-2 mRNA.

3.3.2 Generation of a pEF6 plasmid containing the matriptase-2 ribozyme transgene

Figure 3.2 outlines the process in the generation of a pEF6 plasmid containing the matriptase-2 ribozyme transgene. The ribozyme was examined using touchdown PCR before being cloned into *E.coli* (figure 3.2 A). The plasmids were then checked to ensure that the ribozyme was in the correct orientation. Correct orientation of the ribozyme was indicated by a 140bp band in the T7F vs RbBMR lane and incorrect

orientation was indicated by a band in the T7F vs RbToP lane (figure 3.2 **B**). From this

orientation check, colony 2 was chosen as it contained minimal to no incorrect

orientation. Following an overnight incubation of the *E.coli*, the plasmid from the

chosen colony was extracted and purified. Figure 3.2 **C** shows the purified plasmid

containing the transgene ready for transfection into the PZHPV7 and PNT2C2 cell

lines.

3.3.3 Confirmation of knock-down of matriptase-2 mRNA in PZHPV7 and PNT2C2

Once the PZHPV7 and PNT2C2 cells were transfected with the ribozyme plasmid,

mRNA was isolated and quantitative PCR (q-PCR) was performed. Figure 3.3 **A.** q-

PCR demonstrates that matriptase-2 mRNA has been successfully knocked-down in

PZHPV7 $^{mat2\ rib1}$ cells compared to its pEF6 control. Figure 3.3 **B.** q-PCR also confirms

knock-down of matriptase-2 mRNA in PNT2C2 $^{mat2\ rib1}$ cells compared to the pEF6

control.

3.3.4 Confirmation of knock-down of matriptase-2 protein in PZHPV7 cells

To ensure that the targeting of matriptase-2 mRNA has also resulted in a reduction in

matriptase-2 protein, Western blots were performed to examine protein expression in

the PZHPV7 transfected cells. Figure 3.4 **A.** Western blot showing knock-down of

matriptase-2 protein in PZHPV7 $^{mat2\ rib1}$ cells when compared to control cells PZHPV7

^{pEF6}. Figure 3.4 **B.** Western blot performed 1 month after the blot in A showing that the

matriptase-2 knockdown is stable over a long period of time. Figure 3.4 **C.** Western band quantification normalising matriptase-2 expression to the expression of the housekeeping gene GAPDH. Figure 3.4 **D.** ICC displaying increased brown staining in PZHPV7 $^{mat2\ rib1}$ cells when incubated with anti-matriptase-2 antibody. Staining also appears to be located at the cell membrane.

3.3.5 Confirmation of knock-down of matriptase-2 protein in PNT2C2 cells

To ensure that the malformation of matriptase-2 mRNA has also resulted in a reduction in matriptase-2 protein, Western blots were performed to examine protein expression in the PNT2C2 transfected cells. Figure 3.5 **A.** Western blot showing knock-down of matriptase-2 protein in PNT2C2 $^{mat2\ rib1}$ cells when compared to control cells PNT2C2 ^{pEF6}. Figure 3.5 **B.** Western blot performed 1 month after the blot in A showing that the matriptase-2 knockdown is stable over a long period of time. Figure 3.5 **C.** Western band quantification normalising matriptase-2 expression to the expression of the housekeeping gene GAPDH. Figure 3.5 **D.** ICC displaying increased brown staining in PNT2C2 $^{mat2\ rib1}$ cells when incubated with anti-matriptase-2 antibody. Staining also seems to be predominantly located at the cell membrane of the cells.
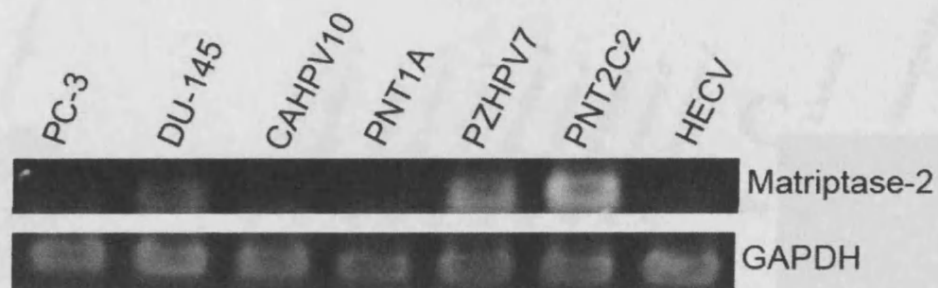
Figure 3.1 Cell line screen for matriptase-2. Seven cell lines were screened for the mRNA expression of matriptase-2 using conventional PCR techniques.
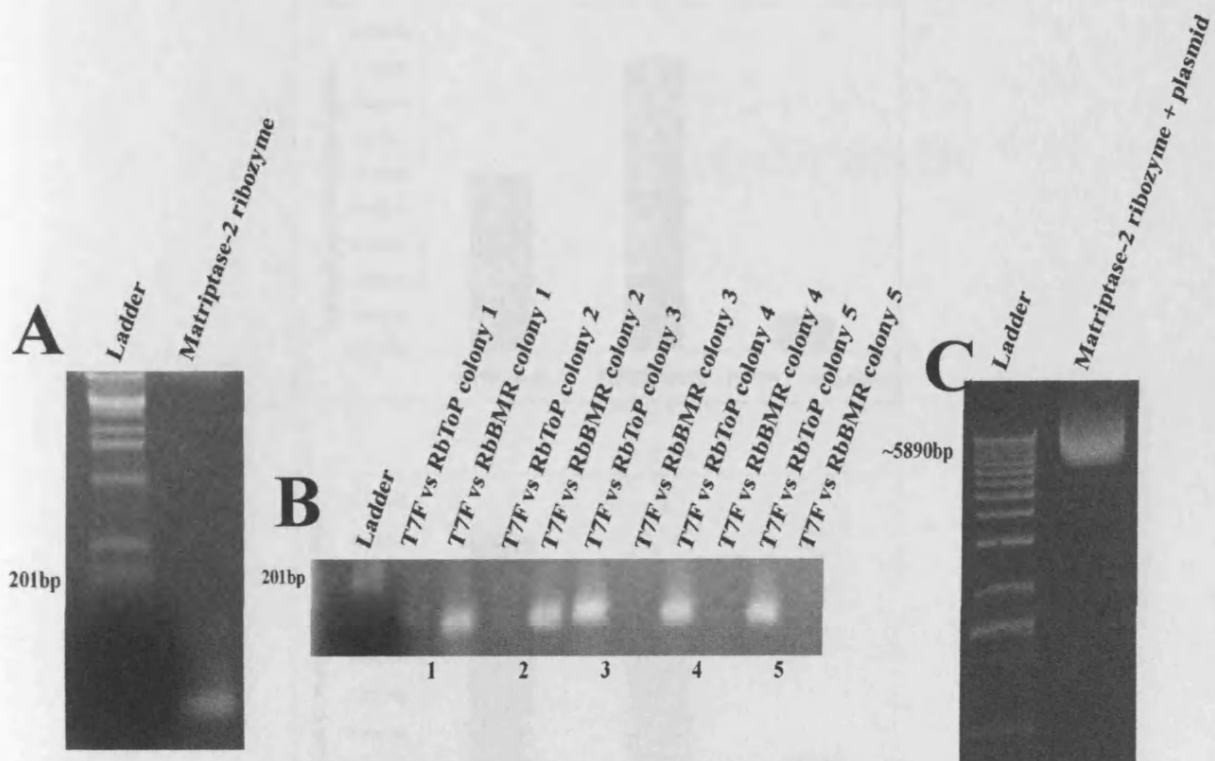
Figure 3.2: Ribozyme transgene synthesis. **A.** The ribozymes were generated using touchdown PCR and run on an agarose gel (Expected band size 50bp). **B.** After transformation into *E.coli* cells, the colonies were analysed using PCR in order to verify correct orientation of the transgene (Expected band size 140bp). **C.** PCR confirming presence and correct size of plasmid after extraction from *E.coli (Approx 5890bp)*.
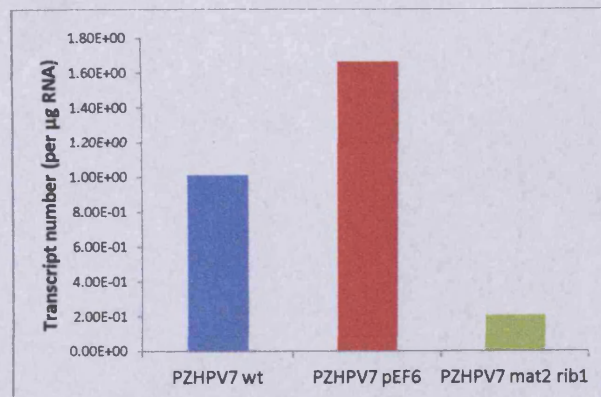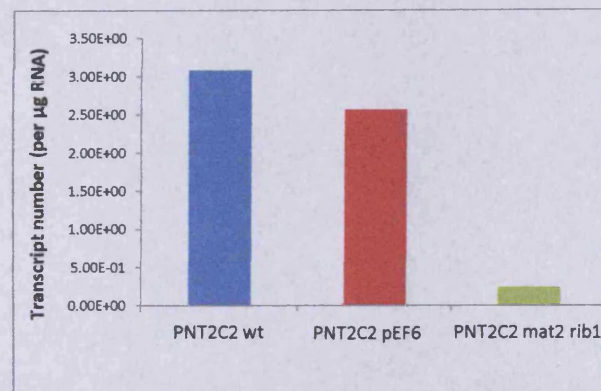
Figure 3.3. Confirmation of matriptase-2 knock-down at the mRNA level. Quantitative PCR was carried out to determine the levels of matriptase-2 mRNA in the control and altered cell lines. **A.** Confirmation of mRNA knockdown of matriptase-2 mRNA in the PZHPV7 [mat2 rib1]. **B.** Successful knock-down of matriptase-2 in PNT2C2 [mat2 rib1] cell line compared to their pEF6 controls.
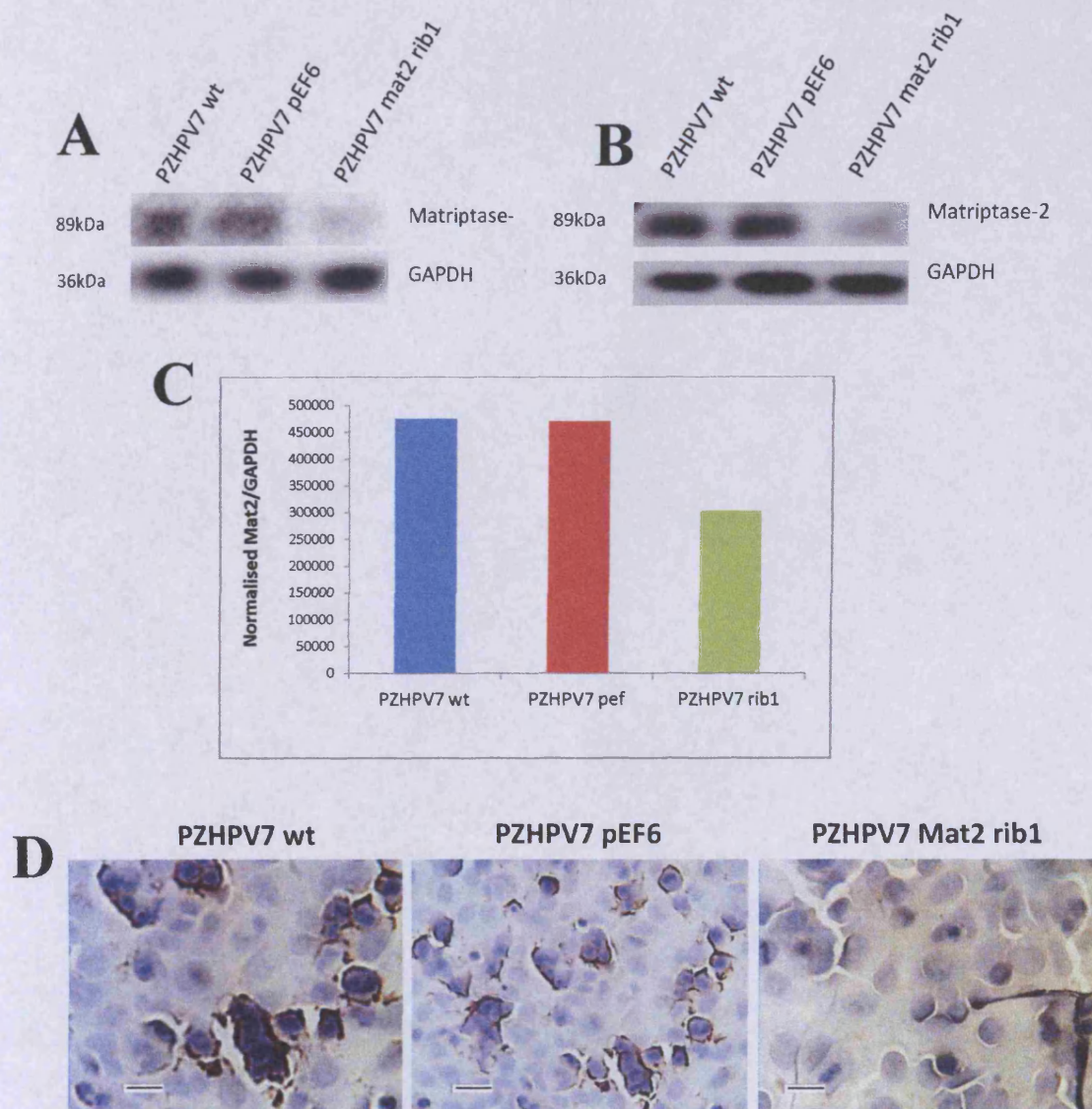
Figure 3.4 Confirmation of knock-down of matriptase-2 protein levels in PZHPV7 cells. **A.** Western blot showing reduced levels of matriptase-2 protein in the PZHPV7 ^{mat2} ^{rib1} cell line compared to the control PZHPV7 ^{pEF6}. **B.** Second Western blot 1 month after blot in A to demonstrate stable knockdown. **C.** GAPDH levels were not equal so band quantification was performed and matriptase-2 levels normalized to GAPDH and represented as a bar chart. **D.** ICC staining for matriptase-2 shows that matriptase-2 staining appears to be predominantly seen at the cell membrane. It also appears reduced in the PZHPV7 $^{mat2\ rib1}$ cells. ($—$ = 50μm).

Figure 3.5 Confirmation of knock-down of matriptase-2 protein levels in PNT2C2 cells. A. Western blot showing reduced levels of matriptase-2 protein in the PNT2C2 [mat2 rib1] cell line compared to the control PNT2C2 [pEF6]. **B.** Second Western blot 1 month after blot in A to show stable knockdown. **C.** GAPDH levels were not equal so band quantification was performed and matriptase-2 levels normalized to GAPDH and represented as a bar chart. **D.** ICC staining for matriptase-2 shows that matriptase-2 staining appears to be predominantly seen at the cell membrane. It also appears reduced in the PNT2C2 [mat2 rib1] cells. (⎯ = 50μm).

3.3.6 Generation of a pEF6 plasmid containing the matriptase-2 expression sequence

The matriptase-2 expression plasmid was kindly donated by Dr. C Parr. The expression plasmid was re-cloned into *E.coli* to amplify the amount of plasmid. Figure 3.6 shows the orientation checking of the colonies chosen for examination. Correct orientation of the expression sequence was indicated by a band in the T7F vs BGHR lane and a 500bp band in the T7F vs Matript2R1 lane (figure 3.6 **A**). From this orientation check colony 4 was chosen as it contained the the strongest expression of the correct bands. Following an overnight incubation of the *E.coli* in liquid broth, the plasmid from the chosen colony was extracted and purified. Figure 3.2 **B** shows the purified plasmid containing the expression sequence ready for transfection into the PC3, DU145 and HECV cell lines.

3.3.7 Confirmation of over-expression of matriptase-2 mRNA

Once the PC3, DU145 and HECV cells were transfected with the expression plasmid, mRNA was isolated and quantitative PCR (q-PCR) was performed. Figure 3.7 **A**. q-PCR demonstrates that matriptase-2 mRNA has been successfully over-expressed in PC3 $^{mat2\ exp}$ cells compared to its pEF6 control. Figure 3.7 **B**. q-PCR also confirms over-expression of matriptase-2 mRNA in DU145 $^{mat2\ exp}$ cells compared to the pEF6 control. DU145 also appears to have a higher basal level of matriptase-2 mRNA compared to PC3. This correlates with the small amount of signal seen in figure 3.1. Figure 3.7 **C**. Confirmation of mRNA over-expression in HECV $^{mat2\ exp}$ cells using q-PCR.

3.3.8 Confirmation of over-expression of matriptase-2 protein in PC3 cells

Western blots were performed to examine protein expression in the transfected cells. Figure 3.8 **A**. Western blot showing over-expression of matriptase-2 protein in PC3 ^{mat2} ^{exp} cells. Figure 3.8 **B**. Western blot performed 1 month after the blot in A showing that the matriptase-2 over-expression is stable over a long period of time. Figure 3.8 **C**. Western band quantification normalising matriptase-2 protein levels to the expression of the housekeeping gene GAPDH. Figure 3.8 **D**. ICC showing the increase in brown staining which is mainly seen at the cell membrane of the cells.

3.3.9 Confirmation of over-expression of matriptase-2 protein in DU145 cells

Western blots were performed to examine protein expression in the transfected cells. Figure 3.9 **A**. Western blot showing over-expression of matriptase-2 protein in DU145 - ^{mat2} ^{exp} cells when compared to control cells DU145 ^{pEF6}. Figure 3.9 **B**. Western blot performed 1 month after the blot in A showing that the matriptase-2 knockdown in stable over a long period of time. Figure 3.9 **C**. Western band quantification normalising matriptase-2 expression to the expression of the housekeeping gene GAPDH. Figure 3.9 **D**. ICC displaying increased levels of brown staining in DU145 - ^{mat2} ^{exp} cells compared to control cells DU145 ^{pEF6} when incubated with anti-matriptase-2 antibody. Staining also appears to be mainly located at the cell membrane.

3.3.10 Confirmation of over-expression of matriptase-2 protein in HECV cells

Western blots were performed to examine protein expression in the transfected cells. Figure 3.10 **A**. Western blot showing over-expression of matriptase-2 protein in HECV $^{mat2\ exp}$ cells. Figure 3.10 **B**. Western band quantification normalising matriptase-2 expression to the expression of the housekeeping gene GAPDH. Figure 3.10 **C**. ICC demonstrating enhanced level of matriptase-2 in cell containing the matriptase-2 over-expression plasmid compared to control cells HECV ^{pEF6}. Staining also confirms location of matriptase-2 protein at the cell membrane.
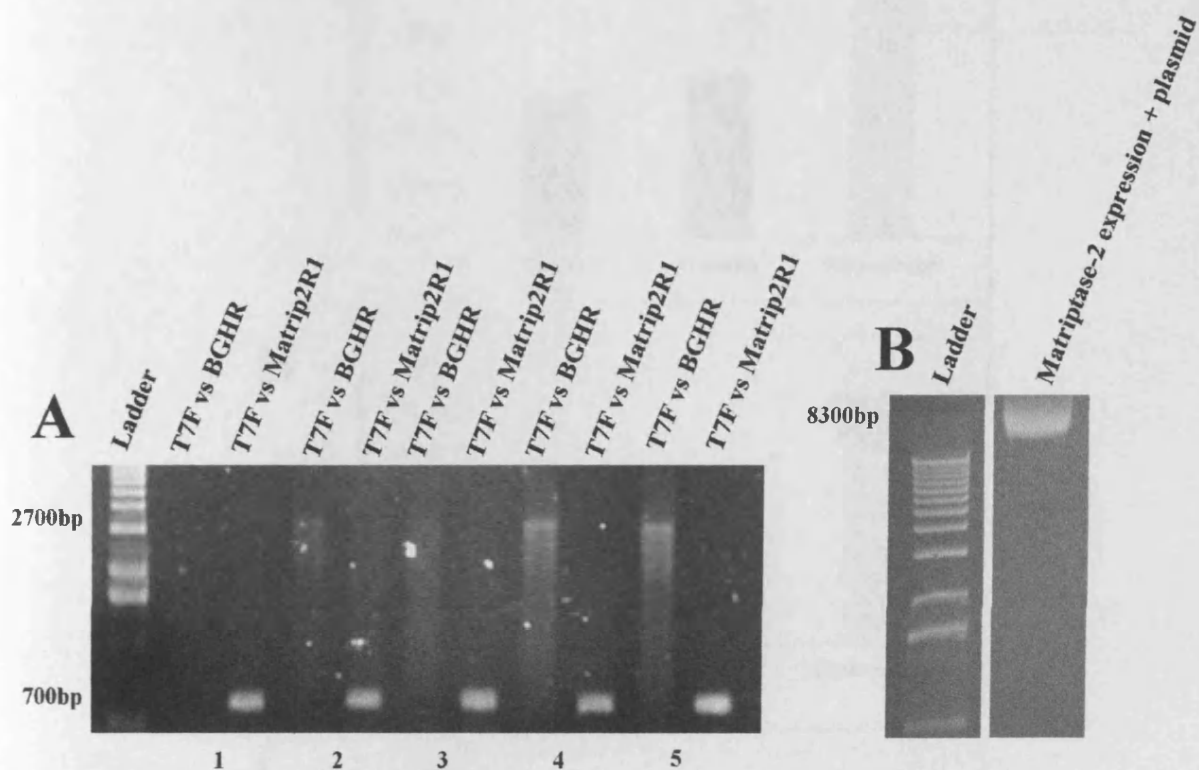
Figure 3.6: Expression plasmid cloning. **A.** After transformation into *E.coli* cells, the colonies were analysed using PCR in order to verify correct orientation of the transgene. **B.** PCR confirming presence and correct size of plasmid and expression sequence after extraction from *E.coli*.
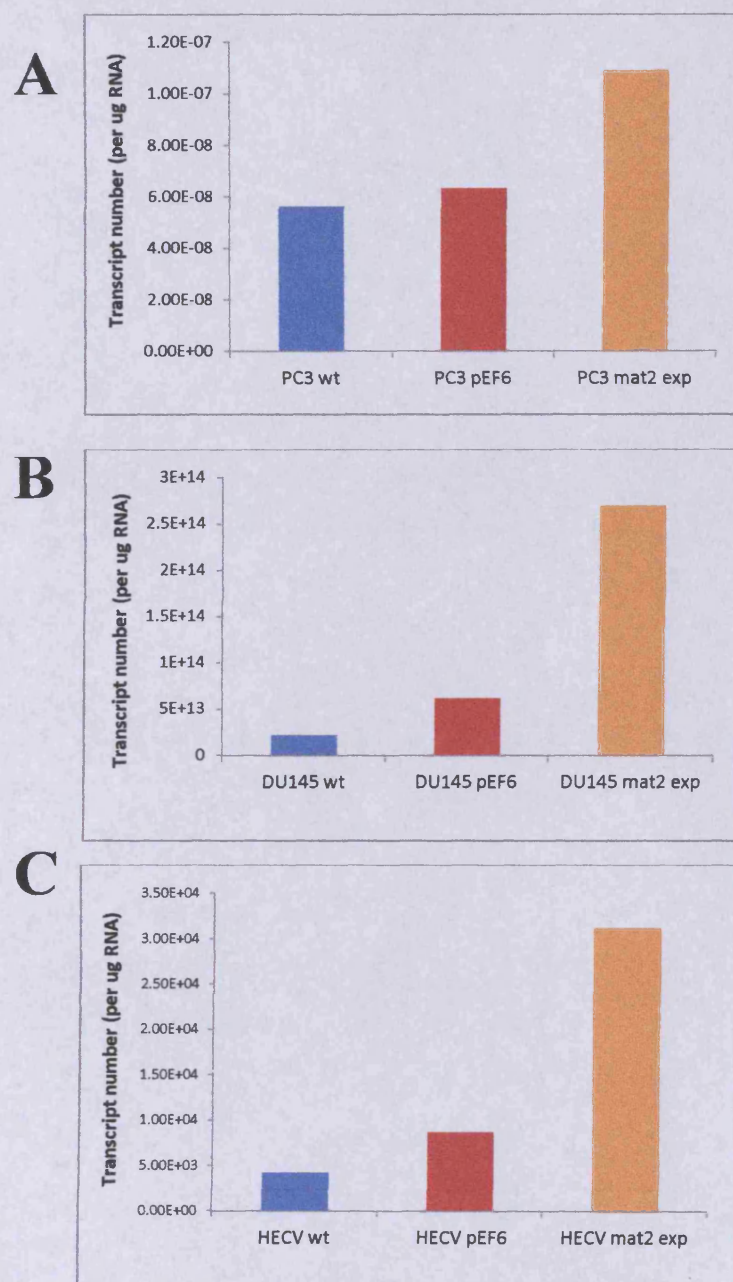
Figure 3.7 Confirmation of matriptase-2 over-expression at the mRNA level. Quantitative PCR was carried out to determine the levels of matriptase-2 mRNA in the control and altered cell lines. These graphs show the over-expression of matriptase-2 mRNA in the HECV $^{mat2\ exp}$, PC3 $^{mat2\ exp}$ and DU145 $^{mat2\ exp}$ cell lines compared to their pEF6 controls. DU145 also shows a higher basal level of matriptase-2 compared to the other cell lines.

A PC3 wt PC3 pEF6 PC3 mat2 exp

89kDa — Matriptase-2

36kDa — GAPDH

B PC3 wt PC3 pEF6 PC3 mat2 exp

89kDa — Matriptase-2

36kDa — GAPDH

C

Mat2/GAPDH protein expression

PC3 wt   PC3 pEF6   PC3 mat2 exp

D

PC3 wt   PC3 pEF6   PC3 Mat2 exp
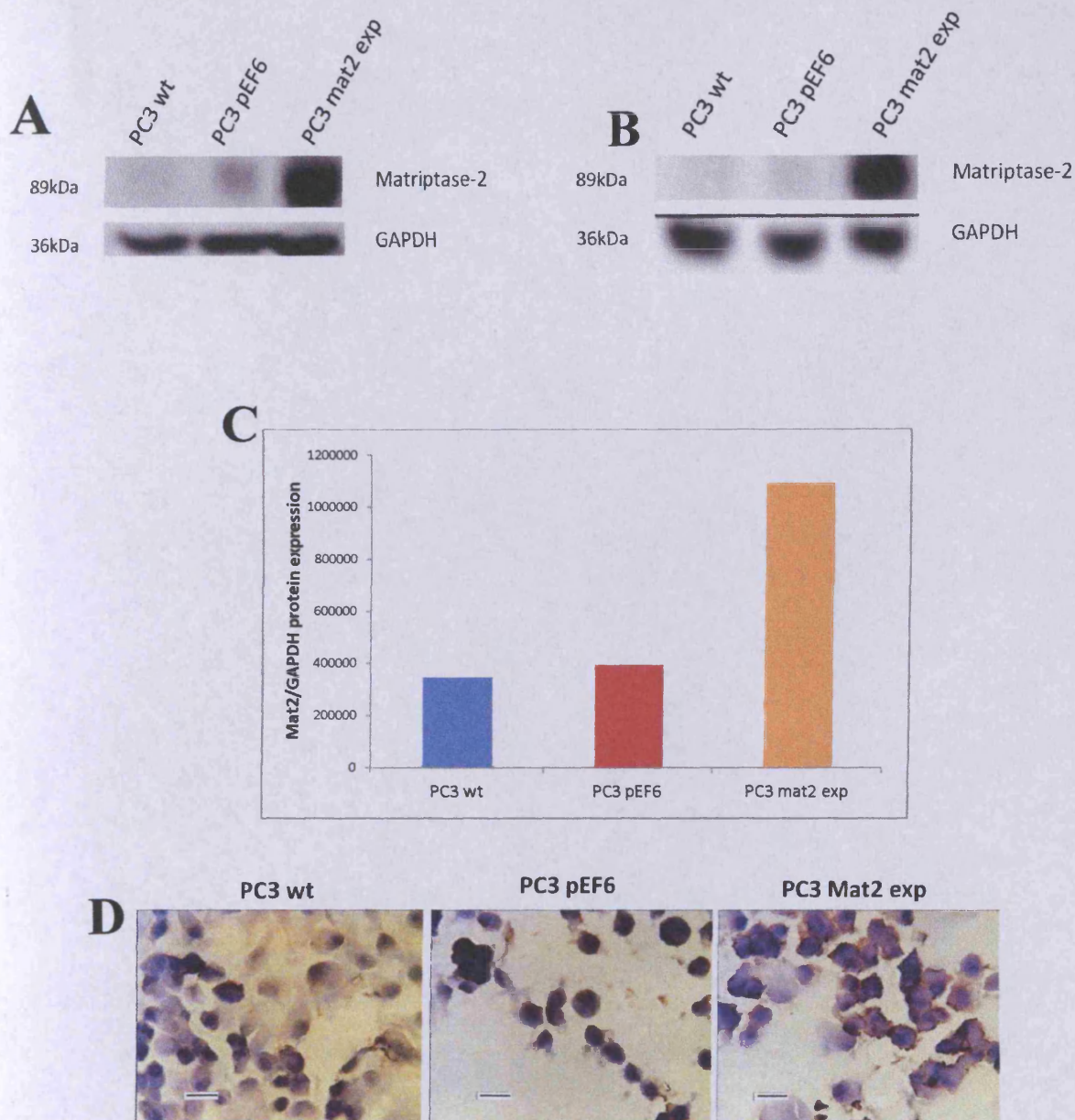
Figure 3.8 Confirmation of over-expression of matriptase-2 protein levels in PC-3 cells.

A. Western blot showing higher levels of matriptase-2 protein in the PC3 [mat2 exp] cell line compared to the control PC3 [pEF6]. **B.** Western blot performed 1 month after the blot in A **C.** GAPDH levels were not equal so band quantification was performed and matriptase-2 levels normalized to GAPDH and represented as a bar chart. **D.** ICC staining for matriptase-2 also shows over-expression and reveals the majority of the staining is seen at the cell membrane. . (⸻ = 50µm).
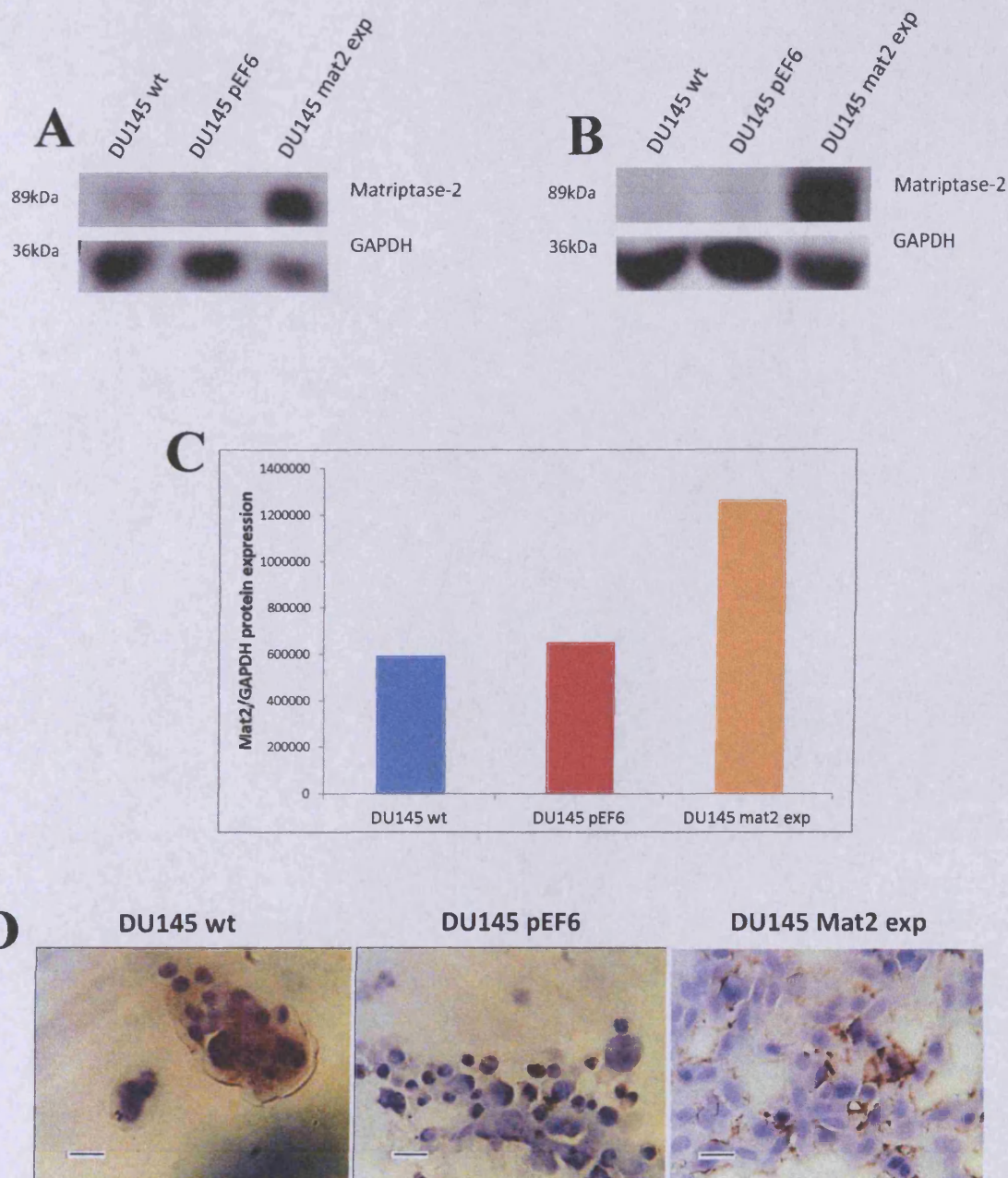
Figure 3.9 Confirmation of over-expression of matriptase-2 protein levels in DU145 cells.

A. Western blot showing higher levels of matriptase-2 protein in the DU145 [mat2 exp] cell line compared to the control DU145 [pEF6]. **B.** Western blot performed 1 month after the blot in **C.** Bar chart representing the Western blot with matriptase-2 expression normalized to the control GAPDH. **C.** ICC staining for matriptase-2 also shows over-expression and shows the majority if the staining is seen at the cell membrane. . (⎯⎯ = 50µm).
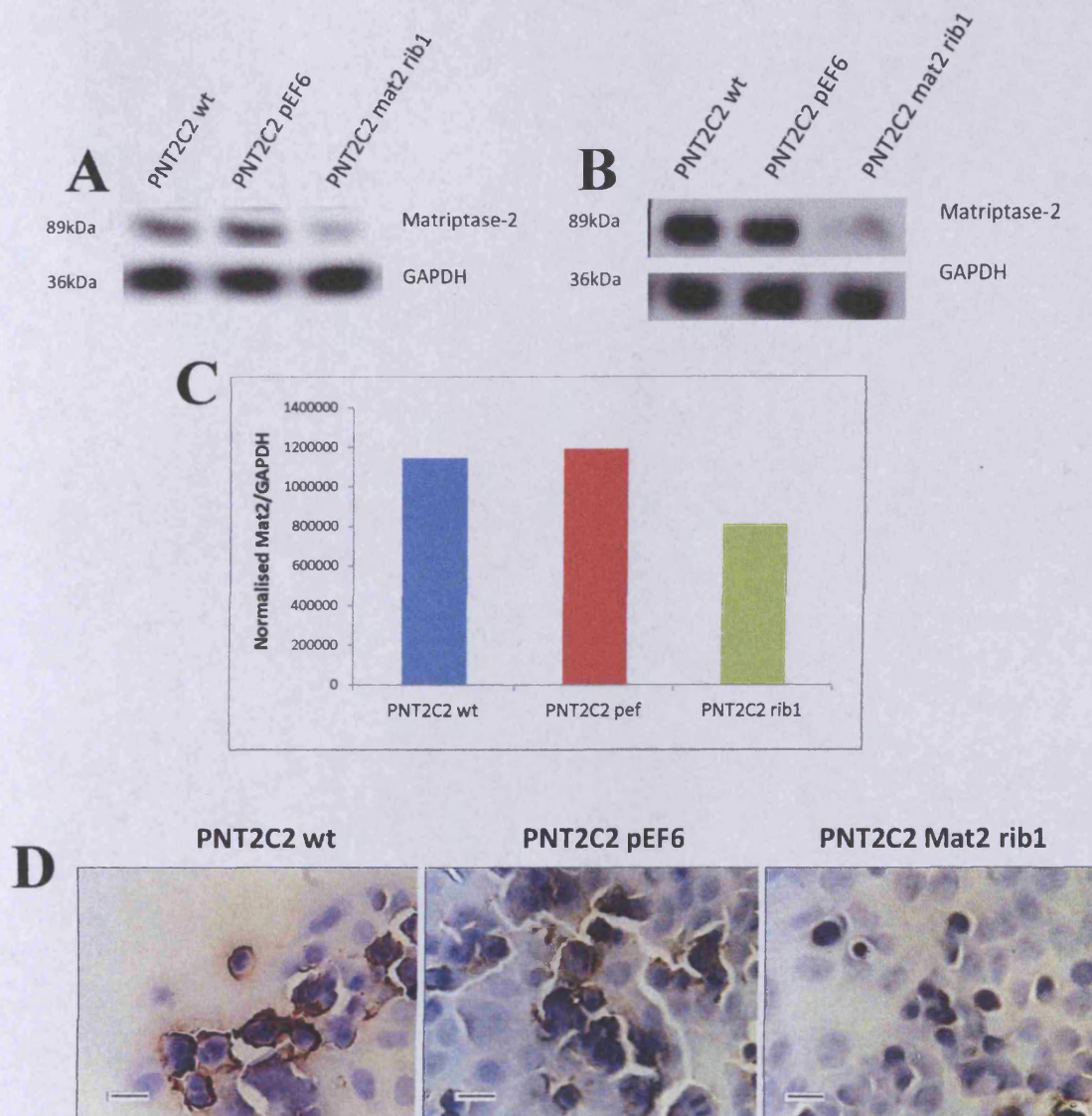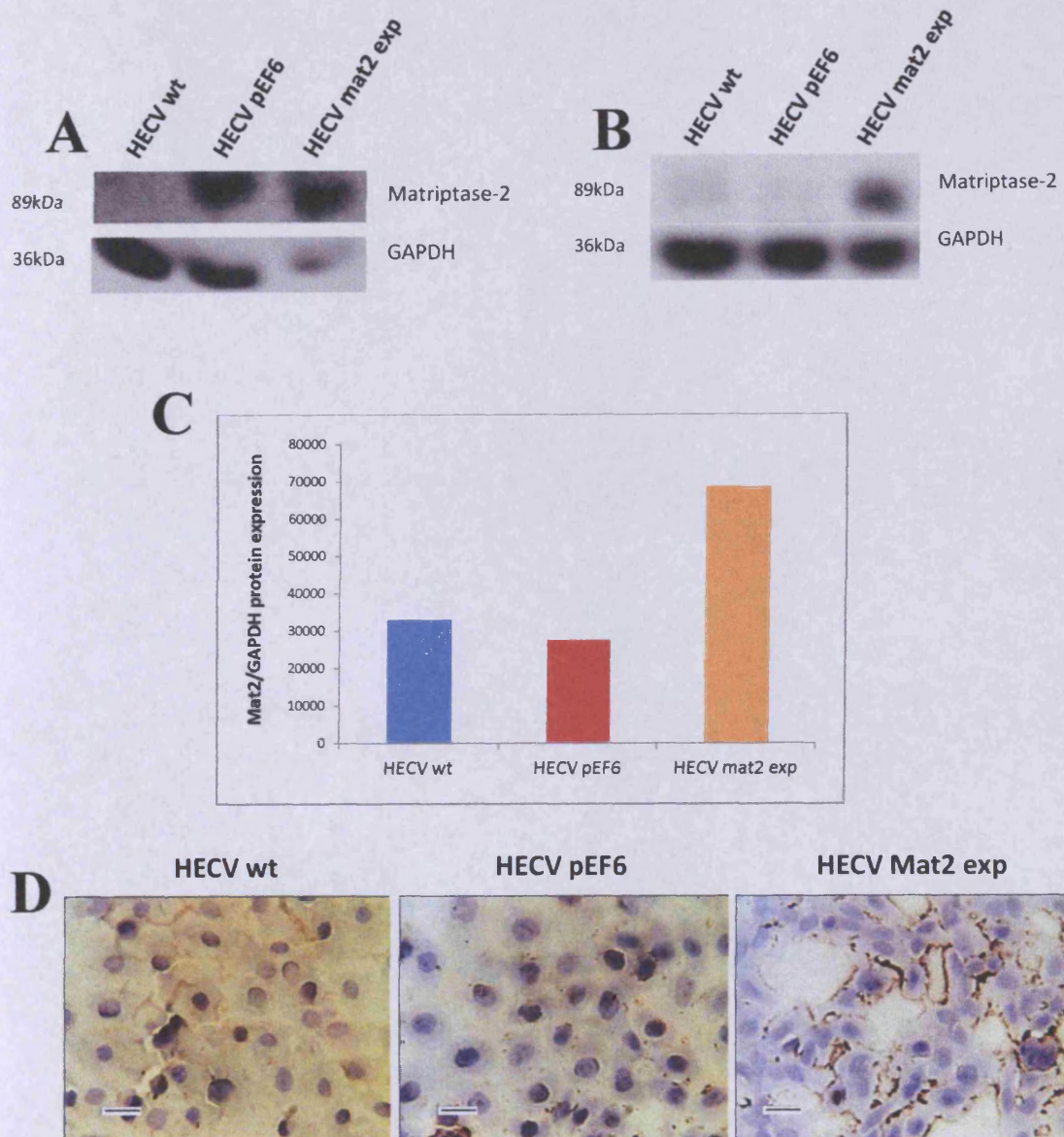
Figure 3.10 Confirmation of over-expression of matriptase-2 protein levels in HECV cells.

A. Western blot showing enhanced levels of matriptase-2 protein in the HECV $^{mat2\ exp}$ cell line compared to the control HECV ^{pEF6}. **B.** Western blot performed 1 month after the blot in A. **C.** GAPDH levels were not equal so band quantification was performed and matriptase-2 levels normalized to GAPDH and represented as a bar chart. **C.** ICC staining for matriptase-2 also shows over-expression and confirms the location of matriptase-2 at the cell membrane. . (—— = 50μm).

3.4 Discussion

Matriptase-2 is a poorly studied protease in the field of cancer progression. What is known demonstrates that matriptase-2 behaves in an opposite manner to that of its closest homologue: matriptase-1. Matriptase-1 has been shown to drive cancer progression (Uhland, 2006; Tsai *et al.*, 2008), whereas, matriptase-2 appears to exert a protective function on breast and prostate cancer cells and is correlated with poor patient outcome (Parr *et al.*, 2007; Sanders *et al.*, 2008). Its expression in tissues shows that matriptase-2 is more highly expressed in non-cancerous epithelial tissues compared to cancerous tissue samples (Parr *et al.*, 2007). No other studies have attempted to define the function of matriptase-2 in prostate epithelial cell and its potential involvement in angiogenesis.

In the current study, we firstly demonstrated the presence of matriptase-2 expression in six prostatic cell lines and one human endothelial cell line. The cell lines used here have extensively been used as models for *in vitro* studies on prostate cancer. PC3, DU145, are aggressive prostatic carcinomas derived from metastatic sites of the bone, and brain, respectively. CAHPV-10 meanwhile represents a less aggressive prostatic adenocarcinoma cell line immortalised with HPV-18. PZHPV7, PNT1A, and PNT2C2 meanwhile, are immortalised prostatic epithelial cell lines.

According to the mRNA levels of matriptase-2, its expression appears to be higher in the cell lines of non-cancerous origin, the prostatic epithelial cell lines PZHPV7 and PNT2C2. The only exception was PNT1A which appeared to have no matriptase-2 expression. The cancerous cell lines PC3, and CAHPV10 displayed little or no matriptase-2 expression. DU145 cells appear to show a slight mRNA signal in the

PCR screen and the Q-PCR confirmation of over-expression. When the protein levels were examined there appeared to be a minimal signal in the Western blot. This could mean that only a small amount of protein is produced from the mRNA in the DU145 cells. These results correlate with the literature in that the highest expression of matriptase-2 is seen in non-cancerous cells lines. The HECV human endothelial cell line displayed no detectable expression of matriptase-2 protein.

This screening process also aided in the determination of which cell lines to use for the remainder of the study. As previously mentioned, matriptase-2 is a cell surface serine protease with a possible role in intracellular signal transduction, as well as being in place to cleave other cell surface proteins. Therefore, in order to investigate the effect of on the biological functions of prostate cells, we altered matriptase-2 expression in PZHPV7, PNT2C2, PC3, DU145, and HECV cells. Due to previous studies within the laboratory, a ribozyme transgene targeting matriptase-2 mRNA and a mammalian expression vector containing the matriptase-2 coding sequence were already constructed. These constructs were re-cloned into *E.coli*, orientation checked and then extracted and purified before transfection into the selected cell lines.

As PZHPV7 and PNT2C2 expressed a high level of matriptase-2, these cell lines were selected as the cell lines to transfect with the ribozyme transgene in order to determine the consequences of knocking-down matriptase-2 on cellular functions. PC3 and DU145 were transfected with the matriptase-2 expression plasmid. As the HECV human endothelial cell line displayed minimal expression, it was also transfected with the expression plasmid to determine the effect, if any, of matriptase-2 on angiogenesis.

The staining location of matriptase-2 was seen in all pictures to be located mainly at the cell membrane. As matriptase-2 is believed to be a cell membrane bound protease, the location of the staining appears to confirm this belief. Some of the images appeared to have a reduced confluency level. There appears to be no definitive reason for this apart from the well that the pictures result from may have received a fewer number of cells due to human error during seeding of the experiment.

In the PC3 and HECV Western blots above there seems to be the possibility that the transfection of the cells with the pEF6 plasmid appears to induce the expression of matriptase-2. This may be an artefact of the Western blots as the blots performed 1 month after the initial Western do not seem to display this increase in the pEF6 transfected cells.

The functional assays that have been used in this study were previously conducted on the PC3 and DU145 cells in Sanders *et al* 2008. Although the PC3 and DU145 cells were re-transfected in this current study the functional assays were not repeated with the fresh cells. The assumption that the more recent transfections would behave in the same manner as the previous transfection was made. It was on this assumption that the functional assays were not repeated.

The ribozyme transgene proved effective at knocking-down the expression of matriptase-2 at both the mRNA and protein level. The expression plasmid was also successful at producing an over-expression of matriptase-2 at both the mRNA and

protein level. These tools of genetic manipulation aid in the generation of useful *in vitro* models allowing for the investigation of the impact a single molecule has in a cell line. Subsequent functional assays carried out in the rest of this study, are based on both the matriptase-2 knock-out and over-expressing cells.

Chapter 4

The role of Matriptase-2 in prostate

epithelial cells

4.1 Introduction

Cancer cells arise from normal cells via mutation. These mutations will allow the previously non-cancerous cells to gain characteristics that will allow the progression to an aggressive cancerous phenotype. A cancer cell relies on varying vital biological processes with which to establish itself in its environment, and to subsequently metastasise. The most important of these include changes in cell growth, adhesive and invasive capacity, motility, and migration. Cancer cells can influence these processes in several ways, most significantly by altering the expression of molecules that play key roles in controlling these cellular traits. Matriptase-2 has previously shown the ability to reduce the migration of PC3 and DU145 cells and the adhesion of PC3 cells. This chapter attempts to determine if a knockdown of matriptase-2 would drive a normal prostate cell lines toward a more cancerous phenotype.

In order to examine the possibility that matriptase-2 could prevent the progression to a cancerous phenotype in the normal prostatic epithelial cell lines PZHPV7 and PNT2C2. They possess a well differentiated morphology with the expression of cytokeratin 8, 18, and 19 with the latter being a feature of differentiated luminal cells of the glandular prostate and are non-tumourigenic in nude mice.

Chapter 3 describes how the expression of matriptase-2 in prostate cancer cells was altered by using a ribozyme transgene to knock-down matriptase-2 expression in the normal epithelial cell lines PZHPV7 and PNT2C2. This following chapter now

goes on to investigate the effect, if any, that these changes in matriptase-2 expression have on these cells. The stable transfected cells were used in various *in vitro* cell function assays including; growth, adhesion, invasion, and motility. These assays are a well established and simple method of investigating the biological properties of cells *in vitro*. As an over-expression of matriptase-2 in PC3 and DU145 cancer cell lines was seen to reduce their aggressiveness it is hypothesised that a knock-down should therefore increase the aggressiveness of the PZHPV7 and PNT2C2 cells lines. This would confirm the fact that matriptase-2 likely prevents the progression of prostate cancer.

4.2 Methods

4.2.1 Cell lines

PZHPV7 and PNT2C2 prostate epithelial cell lines were used in this current chapter, including the wild-type control, empty plasmid control and transfected cell lines. Cells were continuously maintained in DMEM media with 10% FBS and antibiotics. The stable transfected cells were maintained in the same media but with 0.5µg/ml blasticidin following an initial 'selection' period with 5 µg/ml blasticidin.

4.2.2 *In vitro* cell growth assay

The cells were seeded into three 96 well plates, and incubated for 1, 3, and 5 days respectively, as described in section 2.7.1. Following incubation, the cells were fixed and stained with crystal violet before the absorbance was measured in order to

determine cell number. Day 1 was used as an over night reference plate to which day 3 and 5 were compared to in order to determine % increase in growth.

4.2.3 *In vitro* cell Matrigel adhesion assay

The cells were seeded into a 96 well plate coated with matrigel as described in section 2.7.2. The cells were left to adhere for a period of 40 minutes, before being fixed and stained with crystal violet, and the cells counted.

4.2.4 *In vitro* cell motility assay

The protocol followed is described by Rosen and Jiang (Rosen *et al.*, 1990; Jiang *et al.*, 1995b). The cells were incubated with cytodex-2 beads and left over night, by which time the cells will have adhered to the surface of the beads. The beads carrying the cells were then transferred into a 96 well plate, where the cells move from the beads onto the surface of the culture plate. These cells were then fixed and stained with crystal violet, and counted.

4.2.5 *In vitro* cell Matrigel invasion assay

The cells were seeded into transwell inserts with 8µm pores coated with 50 µg matrigel, in a 24 well plate and were incubated for a period of 3 days. Following incubation, the cells which had migrated through the matrigel to the other side of the insert were fixed in formalin, stained with crystal violet and counted.

4.4 Results

4.4.1 Effect of matriptase-2 knock-down on PZHPV7 prostate epithelial cell growth

The cell lines displaying knock-down of matriptase-2 were used in an *in vitro* cell growth assay along with the wild type and empty plasmid controls. There was no significant difference in the growth of the PZHPV7 $^{mat2\ rib1}$ cells (Figure 4.1). The cell growth at 5 days was not significantly different in the PZHPV7 $^{mat2\ rib1}$ (478.20±72.27) compared to the control PZHPV7 ^{pEF6} (495.88±132.99) p=0.716.

4.4.2 Effect of matriptase-2 knock-down on PNT2C2 prostate epithelial cell growth

The PNT2C2 cells displaying knock-down of matriptase-2 were used in an *in vitro* cell growth assay along with the wild type and empty plasmid controls. Similarly there was also no significant difference in cell growth seen in the PNT2C2 cell line. There is no significant difference in the growth of the PNT2C2 $^{mat2\ rib1}$ cells. The cell growth at 5 days was not significantly different in the PNT2C2 $^{mat2\ rib1}$ (367.65±71.54) compared to PNT2C2 ^{pEF6} (347.14±115.04) p=0.711.

4.4.3 Effect of matriptase-2 knock-down on *in vitro* PZHPV7 cell adhesion

The PZHPV7 cells were further analysed for their adhesive capacity in an *in vitro* matrigel adhesion assay. The cells with a knock-down of matriptase-2 displayed no difference in adhesion compared to its controls. Figure 4.3 **A.** Representative images of adhered PZHPV7 cells. Figure 4.3 **B.** There was no significant difference in cell adhesion with PZHPV7 $^{mat2\ rib1}$ cells (29.36±4.90) compared to the control PZHPV7 ^{pEF6} (31.20±7.03) p=0.465.

4.4.4 Effect of matriptase-2 knock-down on *in vitro* PNT2C2 cell adhesion

As with the growth assay the PNT2C2 cells also showed no difference in cell adhesion with a knock-down of matriptase-2. Figure 4.4 **A.** Representative images of adhered PNT2C2 cells. Figure 4.4 **B.** There was no significant difference in cell adhesion with PNT2C2 $^{mat2\ rib1}$ cells (101.53±24.64) compared to the control PNT2C2 ^{pEF6} (100.33±27.25) p=0.900.

4.4.5 Effect of knock-down of matriptase-2 on PZHPV7 cell motility

The cells were further analysed for their motility using a cytodex-2 bead assay. The cells with knock-down of matriptase-2 displayed a significant difference in motility compared to control cells. Figure 4.5 **A.** Representative images of motile PZHPV7 cells. **Figure 4.5 B.** There was a significant increase in cell motility with PZHPV7 $^{mat2\ rib1}$ cells (188.33±12.02) compared to the control PZHPV7 ^{pEF6} (61.20±9.05) p=<0.001.

4.4.6 Effect of knock-down of matriptase-2 on PNT2C2 cell motility

The PNT2C2 cells were further also analysed for their motility using a cytodex-2 bead assay. Figure 4.6 **A.** Representative images of motile PNT2C2 cells. Figure 4.6 **B.** PNT2C2 cells also showed a significant increase in cell motility with a knock-down of matriptase-2. There was a significant increase in cell motility with PNT2C2 $^{mat2\ rib1}$ cells (103.40±8.83) compared to the control PNT2C2 ^{pEF6} (59.93±9.67) p=<0.001.

4.4.7 Effect of knock-down of matriptase-2 on *in vitro* PZHPV7 cell invasion

The cells were further analysed for their invasive capability. The cells with a knock-down of matriptase-2 displayed a significant difference in invasion compared to its controls. Figure 4.7 **A.** Representative images of invaded PZHPV7 cells. Figure 4.7 **B.** There was a significant increase in invasion with PZHPV7 $^{mat2\ rib1}$ cells (21.50±0.70) compared to the control PZHPV7 ^{pEF6} (7.00±0.00) p=0.001.

4.4.8 Effect of knock-down of matriptase-2 on *in vitro* PNt2C2 cell invasion

The matrigel invasion assay was used to assess the invasive capacity of the PNT2C2 cells. PNT2C2 cells also showed a significant increase in invasion with a knock-down of matriptase-2. . Figure 4.8 **A.** Representative images of invaded PNT2C2 cells. Figure 4.8 **B.** There was a significant increase in invasiveness with PNT2C2 $^{mat2\ rib1}$ cells (55.00±10.71) compared to the control PNT2C2 ^{pEF6} (33.25±6.18) p=0.007.
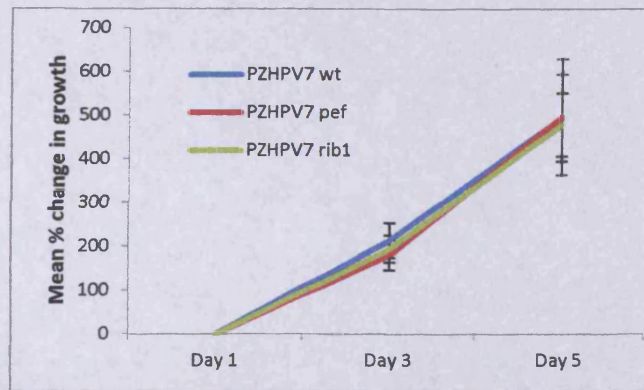
	PZHPV7 wt (Mean±SD)	PZHPV7 pEF6 (Mean±SD)	PZHPV7 mat2 rib1 (Mean±SD)
Day 3	213.14±39.48	179.73±33.72	193.5±30.58
Day 5	493.66±99.75	495.88±132.99	478.20±72.27

Figure 4.1 Knock-down of matriptase-2 has no effect on the growth of PZHPV7 prostate epithelial cells. After 5 days incubation there was no significant effect on the growth of PZHPV7 [mat2 rib1] compared to the control PZHPV7 [pEF6] (p= 0.716). Data shown is representative of at least 3 independent repeats. Error bars represent standard deviation. The 1 day time point was used as a baseline to normalise the data.
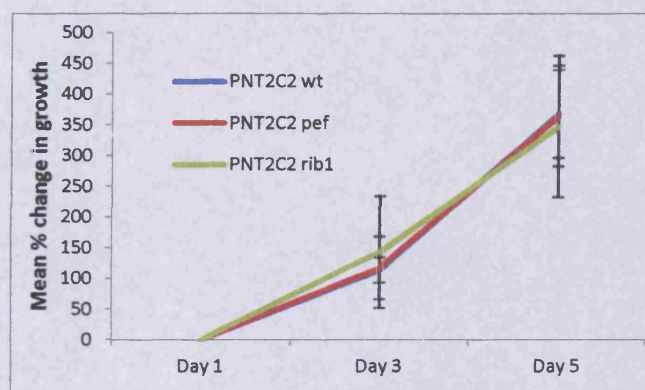
	PNT2C2 wt (Mean±SD)	PNT2C2 pEF6 (Mean±SD)	PNT2C2 mat2 rib1 (Mean±SD)
Day 3	113.73±20.86	119.108±51.02	142.75±90.94
Day 5	367.65±71.54	364.26±81.85	347.14±115.04

Figure 4.2 Knock-down of matriptase-2 has no effect on the growth of PNT2C2 prostate epithelial cells. After 5 days incubation there was no significant effect on the growth of PNT2C2 $^{mat2\ rib1}$ compared to the control PNT2C2 ^{pEF6} (p= 0.711). Data shown is representative of at least 3 independent repeats. Error bars represent standard deviation. The 1 day time point was used as a baseline to normalise the data.

A PZHPV7 wt   PZHPV7 pEF6   PZHPV7 mat2rib1

B

	PZHPV7 wt	PZHPV7 pEF6	PZHPV7 mat2 rib1
Mean	36	31.20	29.36
SD	3.35	7.03	4.90
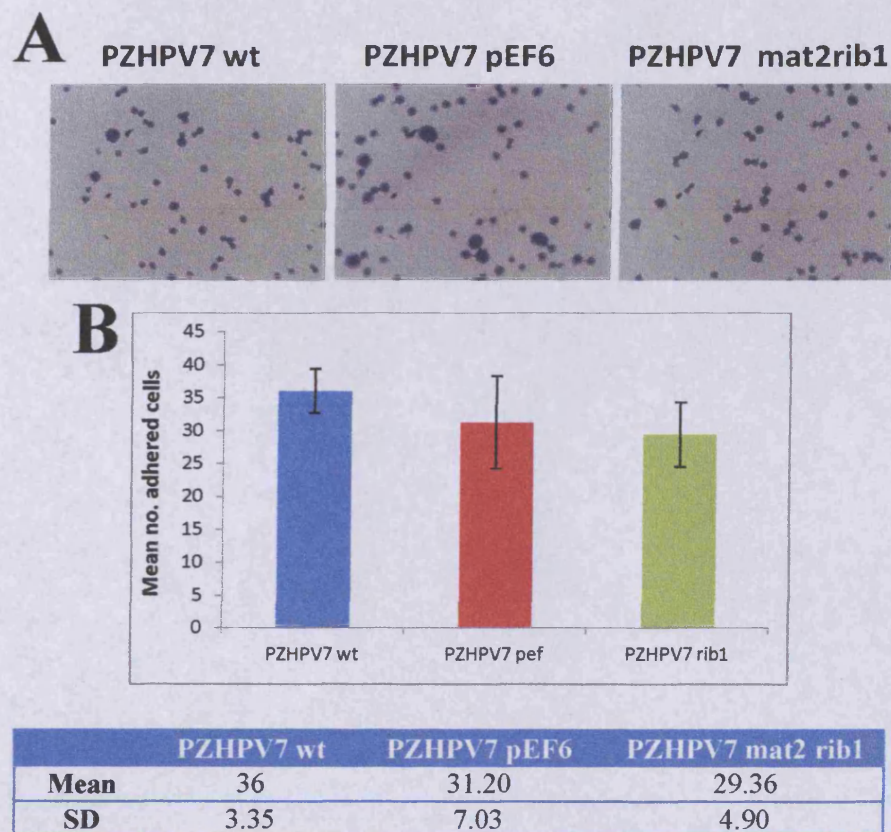
Figure 4.3 Knock-down of matriptase-2 has no effect on the adhesion of PZHPV7 prostate epithelial cells. **A.** Representative images of cells following staining. **B.** After 40 minutes incubation of the cells on an artificial matrigel basement membrane no significant difference in adhesion was seen between the PZHPV7 ^{mat2} ^{rib1} cells compared to the control PZHPV7 ^{pEF6} (p= 0.465). Data shown is representative of at least 3 independent repeats. Error bars represent standard deviation.

A PNT2C2 wt | PNT2C2 pEF6 | PNT2C2 mat2rib1

B
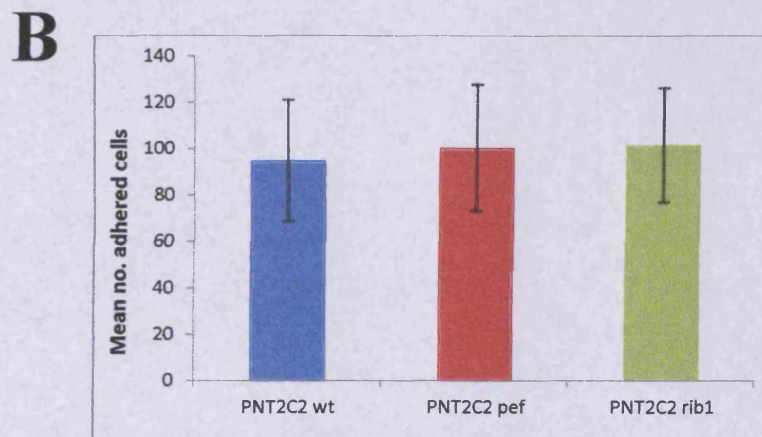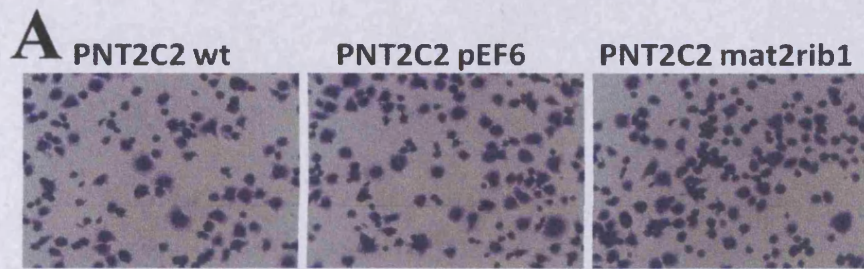
	PNT2C2 wt	PNT2C2 pEF6	PNT2C2 mat2 rib1
Mean	94.87	100.33	101.53
SD	26.19	27.25	24.64

Figure 4.4 Knock-down of matriptase-2 had no effect on the adhesion of PNT2C2 prostate epithelial cells. **A.** Representative images of cells after staining. **B.** After 40 minutes incubation of the cells on an artificial matrigel basement membrane there was no significant difference in adhesion seen between the PNT2C2 [mat2 rib1] cells compared to control PNT2C2 [pEF6] (p= 0.988). Data shown is representative of at least 3 independent repeats. Error bars represent standard deviation.

A PZHPV7 wt   PZHPV7 pEF6   PZHPV7 mat2rib1

B
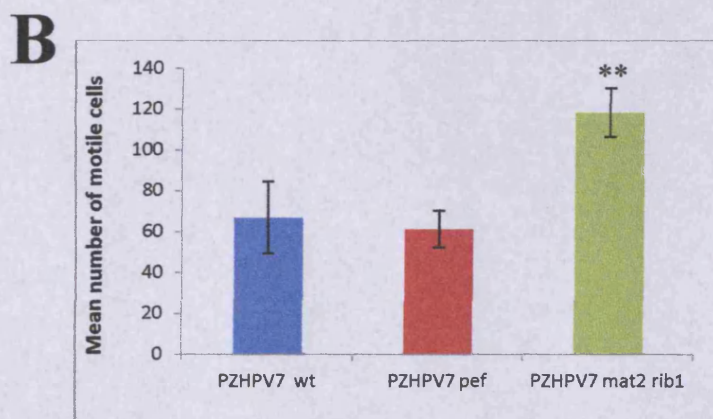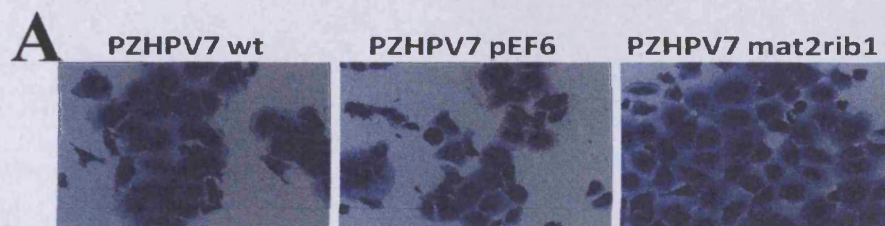
	PZHPV7 wt	PZHPV7 pEF6	PZHPV7 mat2 rib1
Mean	66.96	61.20	188.33
SD	17.57	9.05	12.02

Figure 4.5 Knock-down of matriptase-2 increased the motility of PZHPV7 prostate epithelial cells. Following an overnight incubation the cells that had migrated from the cytodex-2 beads to the base of the well were counted. **A.** Representative images of motile cells after staining.   **B.** The knock-down of matriptase-2 caused a significant increase in the motility of the PZHPV7 [mat2 rib1] when compared to control PZHPV7 [pEF6] cells (**p= <0.001). Data shown is representative of at least 3 independent repeats. Error bars represent standard deviation.

A PNT2C2 wt   PNT2C2 pEF6   PNT2C2 mat2rib1

B

	PNT2C2 wt	PNT2C2 pEF6	PNT2C2 mat2 rib1
Mean	61.20	59.93	103.40
SD	9.56	9.67	8.83
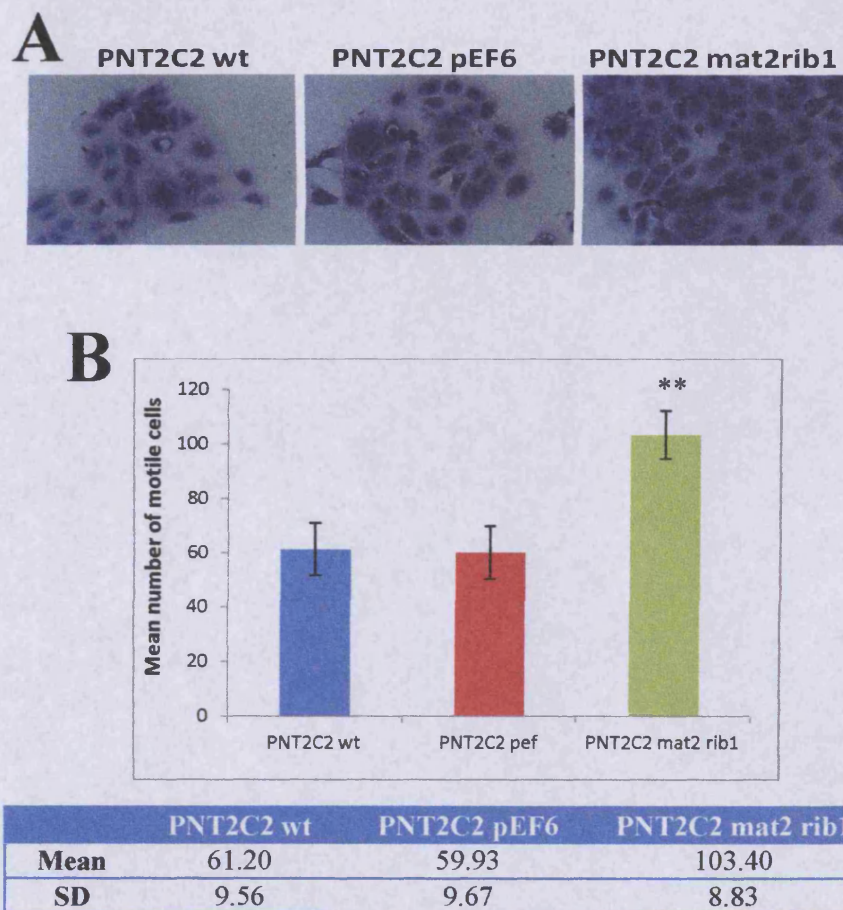
Figure 4.6 Knock-down of matriptase-2 increases the motility of PNT2C2 prostate epithelial cells. Following an overnight incubation the cells that had migrated from the cytodex-2 beads to the base of the well were counted. **A.** Representative images of stained motile cells. **B.** The knock-down of matriptase-2 caused a significant increase in the motility of the PNT2C2 $^{mat2\ rib1}$ when compared to the control cells PNT2C2 ^{pEF6} (**p= <0.001). Data shown is representative of at least 3 independent repeats. Error bars represent standard deviation.

A

PZHPV7 wt   PZHPV7 pEF6   PZHPV7 mat2rib1

B
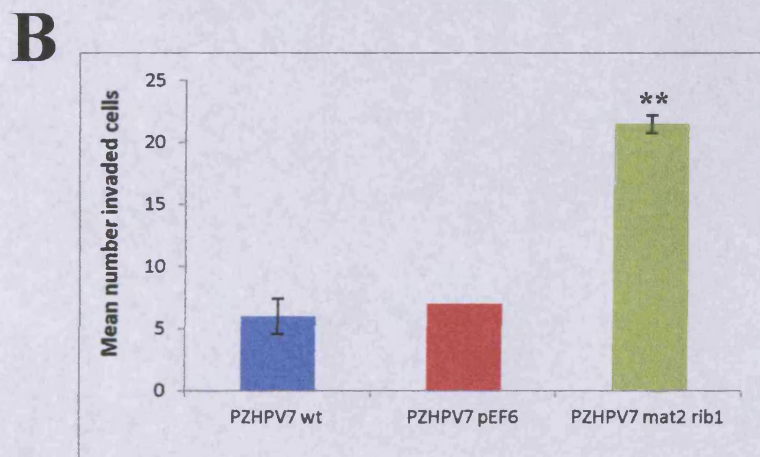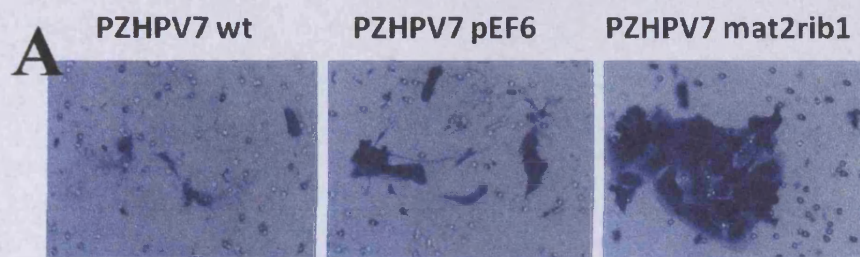
	PZHPV7 wt	PZHPV7 pEF6	PZHPV7 mat2 rib1
Mean	6.00	7.00	21.50
SD	1.41	0.00	0.70

Figure 4.7 Knock-down of matriptase-2 increases the invasive ability of PZHPV7 prostate epithelial cells. Following a 3 day incubation of the cells on an artificial matrigel basement membrane there was a significant increase in the invasion of the PZHPV7 $^{mat2\ rib1}$ cells compared to control PZHPV7 ^{pEF6} cells (**p=0.006). Data shown is representative of at least 3 independent repeats. Error bars represent standard deviation.
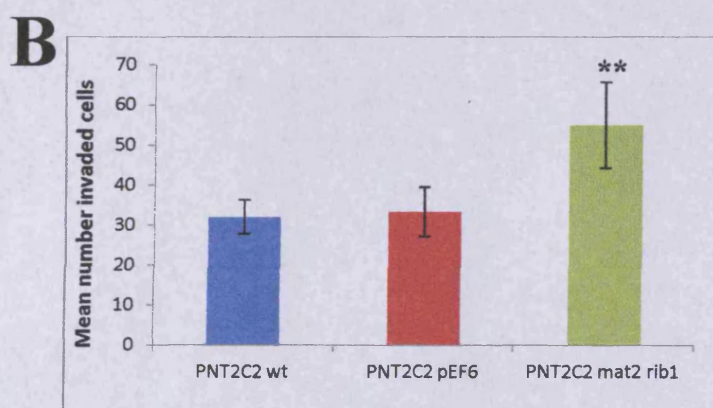
Figure 4.8 Knock-down of matriptase-2 increases the invasive ability of PNT2C2 prostate epithelial cells. **A.** Representative images of invaded cells stained with crystal violet. **B.** Following a 3 day incubation of the cells on an artificial matrigel basement membrane there was a significant increase in the invasion of the PNT2C2 mat2 rib1 cells compared to control PNT2C2 pEF6 cells (**p=0.007). Data shown is representative of at least 3 independent repeats. Error bars represent standard deviation.

4.5 Discussion

Several members of the TTSPs have been linked to cancer progression. Currently a lot of scientific attention is focusing on matriptase-1, which has been reported to play roles in cancer cell invasion and migration and display potential as a therapeutic target (Forbs *et al.*, 2005; Sanders *et al.*, 2006). Matriptase-2 shows a 35% homology to matriptase-1 and early studies implicated this molecule as a matrix degrading molecule potentially involved, as matriptase-1, in cancer progression (Velasco *et al.*, 2002). Due to this homology it was initially believed that matriptase-2 would act in the same manner as matripase-1 and drive cancer progression. As previously mentioned, the expression pattern of these two proteases are seen to be opposite in nature. This suggested that matriptase-2 would function quite differently from matriptase-1 and act as a possible tumour suppressing molecule. This hypothesis has now been shown to be true. Matriptase-2 has been shown to reduce the aggressive nature of breast and prostate cancer cells and to reduce the growth of tumours *in vivo*. It has also been reported to have a prognostic potential for breast cancer patients (Parr *et al.*, 2007; Sanders *et al.*, 2008). This chapter will attempt to further elucidate the role of matriptase-2 in prostate cancer.

The role of matriptase-2 in cancer is a very elusive subject. There is still very little research into the role of matriptase-2 in cancer. This laboratory has previously shown that an over-expression of matriptase-2 in PC3 and DU145 cells showed a reduction of the cells aggressive traits (Sanders *et al.*, 2008). Matriptase-2 has also been shown to be more highly expressed in normal breast tissue compared to cancerous

159

breast tissue and to provide a possible prognostic advantage. Matriptase-2 also reduced the aggressiveness of breast cancer cells (Parr *et al.*, 2007). The current study now shows that by altering the expression of endogenous matriptase-2 in prostate epithelial cells, that matriptase functions to prevent increased cell motility and invasion, suggesting an anti-tumourigenic role for matriptase-2 in cancer.

When matriptase-2 was knocked-down in the PZHPV7 and PNT2C2 cells lines they demonstrated no difference in cell growth compared to their controls. It appears that matriptase-2 knock-down has no effect on the cell growth of these non-cancerous cell lines. A similar effect was seen when examining the cellular adhesion of both cell lines. No significant difference was also seen in between cells with matriptase-2 knock-down and the control cells. In a previous study within the laboratory a similar effect was seen. In Sanders *et al* 2008, an over-expression of matriptase-2 was seen to reduce the growth of PC3 cells but not DU145 cells. It was also shown that the over-expression had no effect on the cellular adhesion of either of these cells. The exact reason for the differential effect of matriptase-2 on the cell growth is currently unknown but is likely to be due to differences in the expression patterns of other proteins between PC3 and DU145. The study also states that the difference in growth in PC3 cells is not through increased rates of apoptosis (Sanders *et al.*, 2008). It is likely that matriptase-2 plays no significant role in the growth or adhesion of prostate cells.

Interestingly the reduction in matriptase-2 expression resulted in a significant increase in the motility of both PZHPV7 and PNT2C2 cell lines. This correlates with the significant reduction in motility in PC3 and DU145 cells over-expressing

matriptase-2 in the Sanders *et al* 2008 study. Similarly matriptase-2 knock-down also resulted in a significant increase in the ability of the previously low-invasive PZHPV7 and PNT2C2 cells to invade through an artificial basement membrane. In contrast, the over-expression of matriptase-2 caused the highly invasive cell lines PC3 and DU145 to become less invasive. A similar effect was seen in the MDA-MB-231 breast cancer cell line, in which an over-expression of matriptase-2 also significantly reduced the invasiveness of these highly aggressive breast cancer cells (Parr *et al.*, 2007).

In the adhesion assays conducted with the PZHPV7 and PNT2C2 cells it was seen that the basal rate of adhesion is higher in the PNT2C2 cells compared to that of the PZHPV7. This effect is likely to be a characteristic of PNT2C2 cells. There is a possibility that this differential ability of PNT2C2 cells to adhere more quickly, or successfully, to matrigel could have an impact on the invasion assay which also uses matrigel as a part of the assay. This effect however, seems unlikely to affect the overall outcome of both the adhesion assay and the invasion assay. Within the adhesion assays of both cell lines the knockdown of matriptase-2 did not alter the adhesion of either cell line when compared to the control cell lines. Although PNT2C2 cells displayed a higher number of adherent cells the trend was conserved. Within the invasion assay the basal rate of invasion is seen to be higher in the PNT2C2 cells compared to the PZHPV7 cells. This may in fact be a reflection of the adherent ability of the cell lines as the cells must first adhere to matrigel before invading through it. But again, within the invasion assay the knockdown of matriptase-2 increased the invasion of both cell lines compared to their respective controls. Therefore the the trend is conserved irrespective of the basal

rate of invasion. In light of this, it is believed that differential rate of adhesion between to two cells lines does not affect the conclusions drawn from these assays.

Due to the scarcity of research involving the possible cellular functions matriptase-2 it is very difficult to hypothesize how the protease may be regulating the motility and invasiveness of prostate and breast cells. Further research may eventually uncover the pathways through which matriptase-2 exerts its effects on motility and invasion. It is however, likely that matriptase-2 exerts its effects on key regulators of motility and invasion to prevent the cells from progressing to a more cancerous phenotype. Although any possible future therapeutic must take into account the major role of matriptase-2 in iron homeostasis and the potential involvement of the BMP pathway.

Due to the potential tumour suppressive role that these results suggest for matriptase-2 there is some discrepancy with the findings of Velasco *et al* 2002 who demonstrated the capacity of the matriptase-2 catalytic domain to degrade ECM components such as fibronectin, fibrinogen and type I collagen (Velasco *et al.*, 2002). This would suggest that matriptase-2 should promote the degradation of the artificial matrigel basement membrane as it contains a large portion of collagen, laminin, and fibronectin. A possible explanation for the opposite trends demonstrated in this chapter may be that Velasco *et al* only examined the catalytic domain of matriptase-2. This domain shows a large degree of homology to the catalytic domain of matriptase-1 (approximately 50%) and contains motifs and sequences which are characteristic of all members of the serine protease family. This would indicate that the catalytic domain of matriptase-2 would

demonstrate the potential to degrade similar substrates to matriptase-1. However, the full length protein must be taken into account, not just the catalytic domain, as the large number of non-catalytic domains will undoubtedly contribute to protein folding and also interaction of the protease with substrates. Indeed the modular domains of the stem region of the TTSPs have been proposed to be involved in protease-substrate interaction (Netzel-Arnett *et al.*, 2003).

To further implicate matriptase-2 in protecting against cancer development several other studies have reported findings that support this theory. Hartikainen *et al* found a SNP in the matriptase-2 gene on 22q12-13 that has been implicated with breast cancer risk (Hartikainen *et al.*, 2006). Studies have also shown that regions of chromosome 22q12-13, where the matriptase-2 gene is located, are frequently altered in breast and colorectal cancers (Allione *et al.*, 1998; Hirano *et al.*, 2001), oral squamous cell (SCC) carcinomas (Miyakawa *et al.*, 1998), pancreatic endocrine cancer (Chung *et al.*, 1998).

This study suggests that matriptase-2 is an important regulator of the biological properties of prostate cells, which possibly has the effect of preventing the progression from a normal to a cancerous phenotype. In order to further determine the role of matriptase-2 in cancer progression the following chapter attempts to examine the potential role of matriptase-2 in cancer angiogenesis.

Chapter 5

The role of Matriptase-2 in angiogenesis

5.1 Introduction

Angiogenesis is a crucial step that most cancers must take in order to progress down the metastasis path. Although angiogenesis is required for normal physiological development, such as wound healing, growth and fertility (Campbell, 1997; Los and Voest, 2001; Tuxhorn *et al.*, 2001), many cancers have the ability to force the growth of new blood vessels to bring enough nutrients to enable the progressive growth of cancer. The process of cancer acquiring the ability to promote blood vessel growth is termed the 'angiogenic switch'. The observation of Dr. Folkman that tumours are unable to grow more than 2-3 mm in the absence of new blood vessel growth (Folkman, 1971) paved the way for the search for successful anti-angiogenic therapies.

Angiogenesis is a complex multi-step process involving close regulation of endothelial cells, extracellular matrix and soluble factors. This process can be divided into four stages: proteolytic degradation of the basement membrane and surrounding extracellular matrix, endothelial cell proliferation, endothelial cell migration and finally tube formation and structural reorganisation (Hanahan and Folkman, 1996). Every stage of the angiogenic process is tightly regulated using inhibitors and inducers of the molecules, such as MMPs, VEGF, FGF2, TGF-β and cyclooxygenase-2, involved in bringing about the stages of angiogenesis. Angiogenesis plays a major role in the progression of prostate cancer. It has been demonstrated that prostate cancer cells express VEGF, and that the expression of VEGF by neoplastic cells is greater that that found in normal prostate stromal tissue (Harper *et al.*, 1996; Ferrer *et al.*, 1997). Also blood and urine VEGF levels hve been correlated with prostate cancer outcomes

(Duque *et al.*, 1999; George *et al.*, 2001), with poorer patient outcomes associated with higher levels of VEGF. As a result of this VEGF inhibitors have been the subject of intense research for many years.

It recently been shown that matriptase-2 proteolytically processes membrane hemojuvelin (also known as RGMc) which significantly reduces hepcidin transcription as hemojuvelin induces *Hamp* transcription (Silvestri *et al.*, 2008). Due to the fact that RGMc is a BMP co-receptor, there could be further implications involving matriptase-2 in angiogenesis. BMPs are essential in the regulation of angiogenesis as they are required for all mesodermally derived tissues, including blood vessels. BMPs also regulate the function of VEGF, a critical inducer of angiogenesis. The ability of matriptase-2 to cleave RGMc could affect the function of the BMP pathway, and therefore the regulation of critical angiogenic factors such as VEGF. This current study intends to elucidate any possible involvement of matriptase-2 in prostate cancer angiogenesis.

As angiogenesis is so important in the progression of cancer it was decided to investigate if matriptase-2 had any role to play in this crucial area of metastasis. As stated above there is a potential link between matritptse-2 and the BMP pathway. As BMPs are integral to the process of angiogenesis this could infer that matriptase-2 does indeed have a potential role in angiogenesis. In order to investigate the effect of matriptase-2 in angiogenesis, the well known angiogenesis cell model, HECV, was used in *in vitro* assays to determine cell functionality. The expression of matriptase-2 was forced in the HECV endothelial cell line, which has been found to display minimal

matriptase-2 expression. A mammalian expression plasmid containing the matriptase-2 gene was used to produce the over-expressed cell line. Following confirmation of over-expression the cells were used in a number of *in vitro* experimental assays designed to investigate the angiogenic process in order to gain insight into the role of matriptase-2 in angiogenesis.

5.2 Methods

5.2.1 Cell lines

The HECV cell line was used in the current chapter, including the wild-type control, empty plasmid control and transfected cell lines. Cells were continuously maintained in DMEM media with 10% FBS and antibiotics. The stable transfected cells were maintained in the same media but with $0.5\mu g/ml$ blasticidin.

5.2.2 *In vitro* cell growth assay

The cells were seeded into three 96 well plates, and incubated for 1, 3, and 5 days respectively, as described in section 2.7.1. Following incubation, the cells were fixed in formalin and stained with crystal violet before the absorbance was measured in order to determine cell number.

5.2.3 *In vitro* cell Matrigel adhesion assay

The cells were seeded into a 96 well plate coated with matrigel as described in section 2.7.2. The cells were left to adhere for a period of 40 minutes, before being fixed in formalin and stained with crystal violet, and the cells in random fields counted.

5.2.4 *In vitro* cell motility assay

The protocol followed is described by Rosen and Jiang (Rosen *et al.*, 1990; Jiang *et al.*, 1995b). The cells were incubated with cytodex-2 beads and left over night, by which time the cells will have adhered to the surface of the beads. The beads carrying the cells were then transferred into a 96 well plate, where the cells move from the beads onto the surface of the culture plate. These cells were then fixed in formalin and stained with crystal violet, and counted in random fields.

5.2.5 *In vitro* cell matrigel tubule formation assay

Cells were seeded into a 96 well plate coated with 250 µg matrigel and incubated for 6 hours. Following incubation, wells were visualised under x40 objective magnification and random fields counted. Using ImageJ the internal perimeter of each tubule was measured, combined, and the units converted into µm.

5.3 Results

5.3.1 Matriptase-2 has no effect on *in vitro* HECV cell growth

The effect of over-expression of Matriptase-2 on the growth of HECV cells was examined using an *in vitro* cell growth assay (Figure 5.1). This showed that at day 5

there was no significant difference seen between $HECV^{mat2\ exp}$ (788.79±91.50) compared to the control $HECV^{pEF6}$ (820.12±79.20) p=0.423.

5.3.2 Matriptase-2 expression did not alter HECV cell adhesion to an artificial Matrigel basement membrane

The capacity of HECV endothelial cells to adhere to an artificial Matrigel basement membrane over a 45 min period was examined using an *in vitro* Matrigel adhesion assay (Figure 5.2). Over-expression of matriptase-2 in the HECV cells did not result in any noteworthy change in the adhesive properties of the HECV cell lines. There was no significant change in adhesive capacity seen between $HECV^{mat2\ exp}$ (66.67±26.98) and the control $HECV^{pEF6}$ (66.80±14.37) p=0.990.

5.3.3 Matriptase-2 greatly reduced the motile capacity of the HECV cells

The effect of matriptase-2 over-expression on cell motility was assessed using an *in vitro* cytodex-2 bead assay (Figure 5.3). Transfection with the matriptase-2 expression plasmid reduced HECV cells ability to move from the beads to the well surface. The $HECV^{mat2\ exp}$ cells (10.93±2.80) were significantly less able to move from the beads to the 96 well plate compared to the control $HECV^{pEF6}$ (46.47±16.18) p= <0.001.

5.3.4 Over-expression of matriptase-2 diminished tubule formation capacity in HECV cells

The effect of matriptase-2 on the tubule forming ability of HECV endothelial cells *in vitro* was examined using a tubule formation assay (Figure 5.4). Over-expression of

matriptase-2 caused a significant decrease in tubule formation in HECV $^{mat2\ exp}$ cells

(9817.83±933.85) compared to the control HECV ^{pEF6} (23841.60±744.75) p= 0.026.
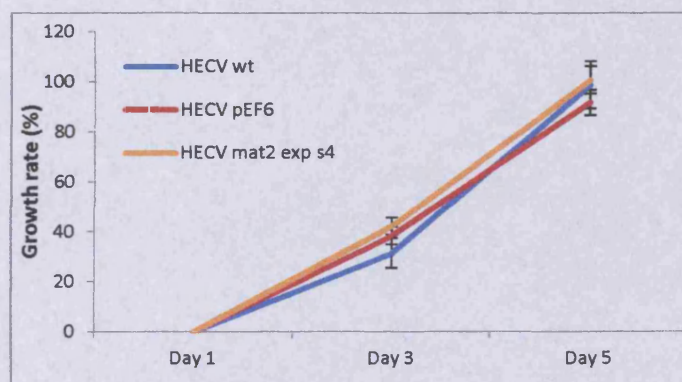
	HECV wt (Mean±SD)	HECV pEF6 (Mean±SD)	HECV mat2 exp (Mean±SD)
Day 3	309.19±99.70	358.81±49.94	372.59±41.32
Day 5	757.37±136.69	820.12±79.20	788.79±91.50

Figure 5.1 Over-expression of matriptase-2 has no effect on the growth of human endothelial cells. After incubation for 5 days there was found to be no significant effect on the growth of HECV [mat2 exp] cells compared to its control HECV [pEF6] (p= 0.364). Data shown is representative of at least 3 independent repeats. Error bars represent standard deviation. The 1 day time point absorbance was used as a baseline in order to normalise the data.

A

HECV wt   HECV pEF6   HECV mat2 exp

B

	HECV wt	HECV pEF6	HECV mat2 exp
Mean	51.52	66.80	66.67
SD	3.61	14.37	26.93
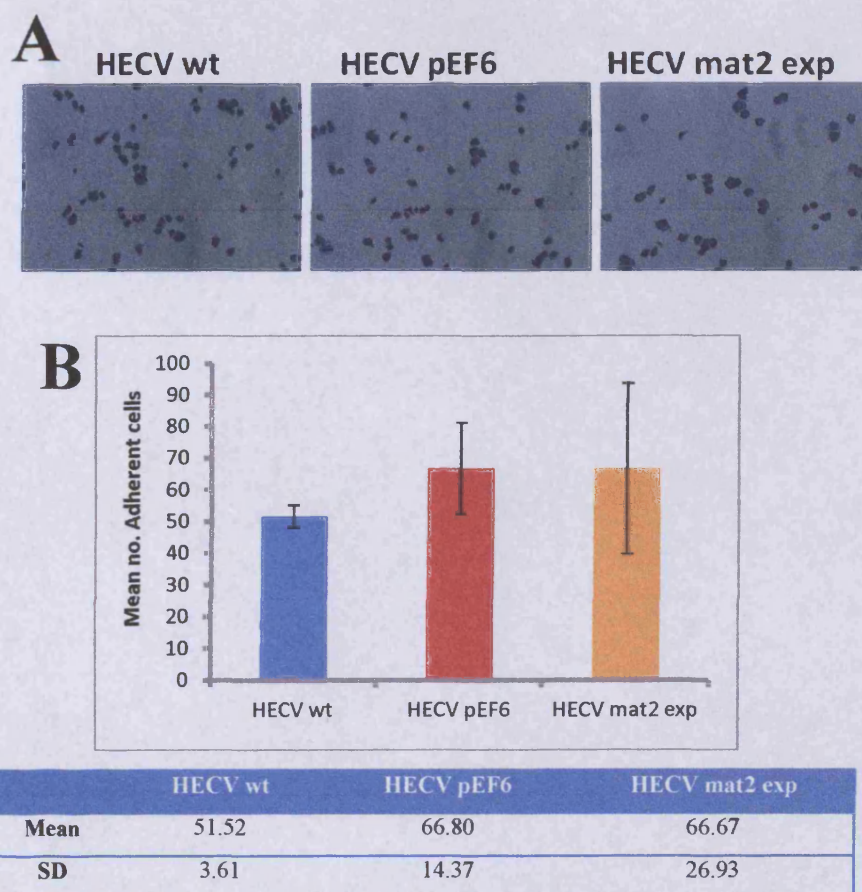
Figure 5.2 Over-expression of matriptase-2 has no effect on the adhesion of human endothelial cells. **A.** Representative images of stained adherent cells. **B.** Following incubation of the cells on an artificial matrigel basement membrane it was seen that over-expression of matriptase-2 has no significant effect on the adhesion of HECV ^{mat2} ^{exp} cells compared to its control HECV ^{pEF6} p= 0.990. Data shown is representative of at least 3 independent repeats. Error bars represent standard deviation.

A

| HECV wt | HECV pEF6 | HECV mat2 exp |

B
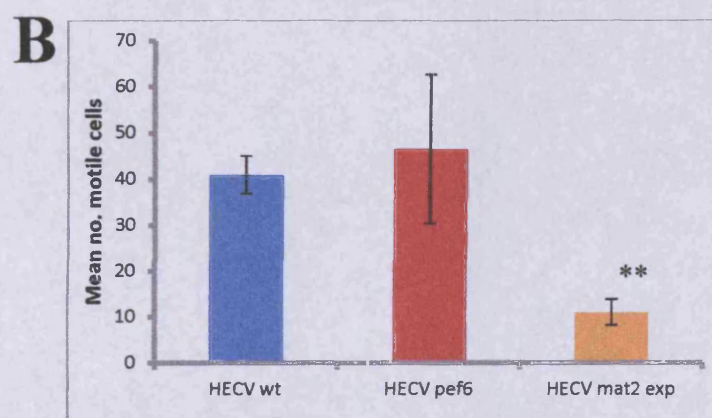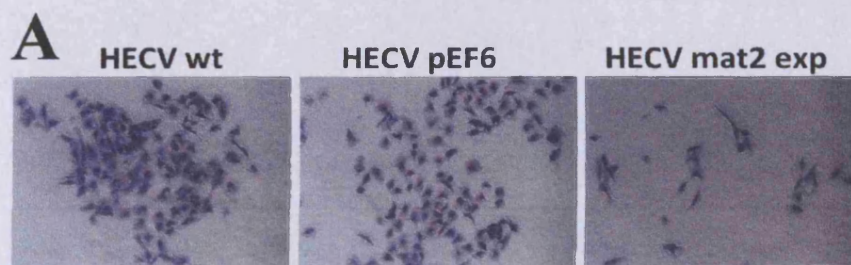
	HECV wt	HECV pEF6	HECV mat2 exp
Mean	40.87	46.47	10.93
SD	4.09	16.18	2.80

Figure 5.3 Over-expression of matriptase-2 decreases the motility of human endothelial cells. **A.** Representative images of motile cells stained with crystal violet. **B.** Following an overnight incubation of the cytodex-2 beads it was seen that over-expression of matriptase-2 significantly decreased the motility of HECV $^{mat2\ exp}$ cells compared to its control HECV ^{pEF6} (**p= <0.001). Data shown is representative of at least 3 independent repeats. Error bars represent standard deviation.

A

HECV wt   HECV pEF6   HECV mat2 exp

B
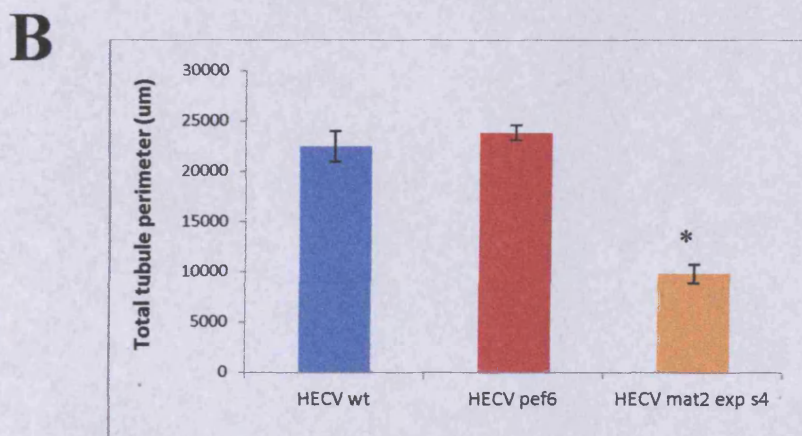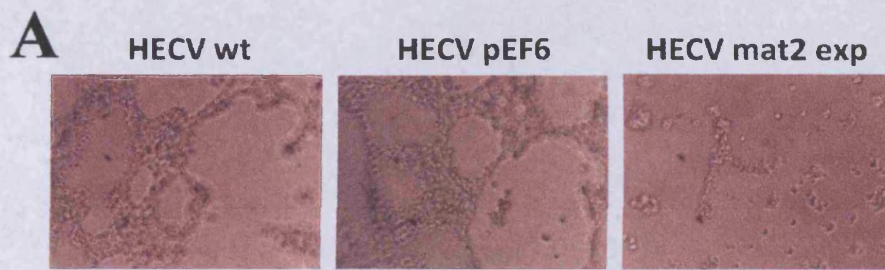
	HECV wt	HECV pEF6	HECV mat2 exp
Perimeter	22488.53	23841.60	9817.83
SD	1517.29	744.75	933.85

Figure 5.4 Over-expression of matriptase-2 decreases the ability of human endothelial cells to form tubules. **A.** Representative images displaying HECV tubules formed in matrigel. **B.** After a six hour incubation of the cells on an artificial matrigel basement membrane it appeared that over-expression of matriptase-2 significantly decreases the tubule forming ability of HECV [mat2 exp] cells compared to its control HECV [pEF6] (*p= 0.026). Data shown is representative of at least 3 independent repeats. Error bars represent standard deviation.

5.4 Discussion

Angiogenesis, the formation of new blood vessels from pre-existing ones, is essential for sustained tumour growth beyond a critical size of 2–3 mm. Moreover, increased angiogenesis promotes tumour cell penetration into the circulation and thereby metastatic dissemination. Tumour vessels can develop through different mechanisms, including sprouting or intussusception from pre-existing vessels, the mobilisation of circulating endothelial precursors from the bone marrow, and the recruitment of lymphatic vessels (lymphangiogenesis) (Carmeliet and Jain, 2000). Different proteolytic enzymes, including serine proteases (SPs) and matrix metalloproteinases (MMPs), have been implicated in angiogenesis (Pepper, 2001). The theory for the involvement of SPs and MMPs during cancer progression was that the degradation of extracellular matrix components should contribute to different events, such as provisional matrix remodelling, basement membrane breakdown, and cell migration and invasion. In addition to degrading extracellular matrix components, proteinases have also been implicated in the activation of cytokines, and in the release of growth factors within the extracellular matrix (Rifkin *et al.*, 1999; Egeblad and Werb, 2002; McQuibban *et al.*, 2002). Several TTSPs, such as hepsin, TMPRSS2 and matriptase, have been reported to be expressed during microvascular endothelial cell morphogenesis (Aimes *et al.*, 2003), suggesting that they have a function in angiogenesis. Membrane anchored SPs probably have complex functions because the upregulation and downregulation of their expression has been associated with cancer progression.

Endothelial cells line the inner surface of all blood vessels in the body. They are essential in the formation of new blood vessels. HECV cells are a human endothelial cell line that has retained the ability of forming tubules in an artificial basement membrane. These tubules can indicate the level of angiogenic potential of the cells. The more tubules that are formed indicate that those particular cells are more angiogenic and therefore more capable of influencing metastasis. By manipulating the expression of matriptase-2 in these HECV cells the influence of matriptase-2 on tumour angiogenesis can be investigated. As seen in chapter 3 a mammalian plasmid construct containing the matriptase-2 sequence was successfully transfected into the HECV cells and over-expression was confirmed using several methods. Functional assays were used to determine the effect of matriptase-2 on the biological functions of the HECV cells.

The over-expression of matriptase-2 had no significant effect on the growth and adhesion of the HECV cells. This is the same effect seen with the PZHPV7 and PNT2C2 matriptase-2 knock-down cells in the previous chapter. It also correlates with DU145 cells over-expressing matriptase-2. The only exception appears to be PC3 cells over-expressing matriptase-2 which had a reduction in growth although the adhesion had no difference (Sanders *et al.*, 2008). This reduction in growth could be due to aberrant expression of cell cycle proteins arising from the cancerous nature of the PC3 cells. The HECV $^{mat2\ exp}$ cells were also used in a motility assay in which resulted in a significant decrease in cellular motility. Again this correlates with the increase in motility seen in the knock-down cells in chapter 4. It also mimics the reduction in motility seen in PC3 and DU145 cells over-expressing matriptase-2 in Sanders *et al.* MDA-MB-231 cells over-expressing matriptase-2 were also seen to have a reduction in

motility (Parr *et al.*, 2007). So far the effects of matriptase-2 on the biological functions of PC3, DU145, PZHPV7, PNT2C2, MDA-MB-231, and HECV cells appear to be largely consistent throughout the three studies investigating the involvement of matriptase-2 in prostate and breast cancer.

The tubule formation assay can only be conducted with the HECV cells. It showed that an over-expression of matriptase-2 significantly reduced the number and size of tubules formed in an artificial matrigel basement membrane. Although the growth and adhesion didn't change the reduced motility and tubule formation suggested that matriptase-2 may have a previously unrecognised role in tumour angiogenesis.

These results show that matriptase-2 possibly has a role in tumour angiogenesis. The results from this study clearly show a reduction in angiogenic potential in the presence of matriptase-2 over-expression. How matriptase-2 exerts its effect on the angiogenic process remains unknown. Several studies have suggested that fibrinogen and components of the uPA system can facillitate tumour angiogenesis and are possibly up-regulated in cancer (Bajou *et al.*, 2001; Noel *et al.*, 2004; Morrissey *et al.*, 2008). As matriptase-2 has been shown to proteolytically process these proteins this may have some impact of the angiogenic ability of these cells. Also to be taken into account is the fact that matriptase-2 can cleave RGMc (m-HJV), a BMP co-receptor. This could alter the BMP signalling pathway and influence not only iron homeostasis but could have implications for preventing cancer development and/or metastasis. As BMPs are widely known for having a role in angiogenesis (Scharpfenecker *et al.*, 2007; David *et al.*, 2009) further investigation into the effect of matriptase-2 on BMP signalling will

determine if the anti-angiogenic nature of matriptase-2 is mediated through the BMP signalling pathway. Further investigation into the role of matriptase-2 in tumour angiogenesis will be needed to elucidate its possibly important anti-angiogenic effects on prostate and to a lesser extent, breast cancer.

Chapter 6

Matriptase-2 affects the protein expression of β-catenin which possibly facilitates the anti-metastatic properties of matriptase-2.

6.1 Introduction

The β-catenin nuclear signalling molecule, a key component of the Wnt signalling pathway, has been widely implicated as an oncogene in human cancer and current research is greatly interested in deepening the understanding of the role of β-catenin in the development of cancer in the hope of providing possible therapeutic strategies for the treatment of cancer.

β-Catenin was first described as a structural component in adherens junction formation, a mechanism of cell–cell adhesion. β-Catenin is normally maintained at low levels in the absence of wnt stimulation due to its constitutive proteasomal degradation (Hart *et al.*, 1999). The regulators that confer this turnover, APC and Axin, position β-catenin for phosphorylation at its N-terminus (encoded by human exon 3) by glycogen synthase kinase-3β (GSK-3β). The targeted serine and threonine residues reside in an IκB consensus destruction motif and upon their phosphorylation by GSK-3β prime β-catenin for ubiquitination and subsequent proteasomal degradation. De-repression of this post-translational regulation of β-catenin through inhibition of GSK-3β kinase activity is induced by the downstream formation of an appropriate wnt/fzd/LRP complex (Liu *et al.*, 2001).

The reduction of β-catenin degredation upon wnt stimulation leads to greater β-catenin participation in two major cellular processes, nuclear signaling and cell–cell adhesion. β-catenin accumulation results in its translocation into the nucleus and interaction with DNA-binding transcription factors, the most prominent of which are those of the TCF/lymphoid enhancer factor (LEF) family. Once localized to the nucleus, β-catenin

complexed with its DNA-binding transcription factors, initiates the transcription of its

target genes. These target genes are highly involved in the regulation of many proteins

of importance in maintaining the proper cell functions. These target genes include c-

MYC (He *et al.*, 1998), MMP-7 (Brabletz *et al.*, 1999; Crawford *et al.*, 1999), VEGF

(Zhang *et al.*, 2001) and MET (Boon *et al.*, 2002). Due to the importance of these target

genes in maintaining the correct function of the cell the balance between the

degradation and activation of β-catenin must remain tightly controlled. Deregulation of

this pathway plays a huge role in the progression and possibly the development of

cancer.

An increase in cellular levels of β-catenin resulting from mutations of β-catenin itself,

or of components of the destruction complex, is frequently observed in many cancer

cells, including prostate cancer. Detection of β-catenin mutations in prostate cancer

samples has been reported previously, with approximately 5% of samples revealing

mutations at the serine ot threonine residues in the NH2-terminal of the β-catenin

protein (Voeller *et al.*, 1998; Chesire *et al.*, 2000; Gerstein *et al.*, 2002). Examination of

the β-catenin protein by immunohistochemical assays revealed aberrant localization of

the protein in prostate cancer specimens (Chesire *et al.*, 2002; de la Taille *et al.*, 2003).

Alterations of APC and b-TrCP1, which directly affect the degradation of β -catenin,

have also been observed in prostate cancer samples (Gerstein *et al.*, 2002). The direct

role of β-catenin in promoting prostate cancer cell growth has been examined recently.

As previously mentioned, β-catenin was selected to be examined in this study

based on unpublished data from a previously conducted study. As matriptase-2 was

found to affect the migratory and adhesive capabilities of PC3 and DU145 cells a screen

181

of molecules involved in cell:cell and cell:matrix adhesion was performed in an attempt to determine if any of these molecules had been altered by the presence of matriptase-2. β-catenin was identified as a molecule of interest from this panel of molecules. This presented the opportunity to investigate any link between matriptase-2 and β-catenin. As the expression and regulation of degradation of β-catenin and transcription of β-catenin target genes have already been shown to be highly deregulated in prostate cancer this seemed a good opportunity to investigate if matriptase-2 did have the ability to influence β-catenin in respect to preventing cancer progression.

Using the five cell lines with altered matriptase-2 from the previous chapters, this chapter will investigate the relationship between matriptase-2 and the expression of β-catenin as a possible mechanism of action for matriptase-2.

6.2 Methods

6.2.1 Cell lines

PZHPV7, PNT2C2, PC-3, DU-145, and HECV cell lines were used, cultured and maintained as described in sections 2.2.3.

6.2.2 RNA isolation, cDNA synthesis, and RT-PCR

RNA was isolated from the cells using the ABgene Total RNA Isolation Reagent (TRIR) kit (ABgene, Surrey, UK), and converted into cDNA by reverse transcription using the iScript™ cDNA Synthesis Kit (Bio-Rad Laboratories,

California, USA), as described in section 2.4. This was then used as a template for RT-PCR, which was carried out at the following conditions; 94°C for 5 minutes, followed by 30 to 42 cycles of 94°C for 30 seconds, 56°C for 30 seconds, and 72°C for 1 minute, and a final extension of 7 minutes at 72°C. The products were run on an agarose gel and visualised using ethidium bromide.

6.2.3 Western blot analysis of β-catenin expression

Cells stably transfected with either the matriptase-2 expression or ribozyme plasmid were lysed and the protein was extracted. This protein was used in SDS-PAGE Western blotting along with a β-catenin antibody to detect the expression of β-catenin in the altered cell lines and their controls.

6.2.4 Immuno-flourescent chemistry (IFC)

Cells were permeabilsed and incubated with β-catenin primary antibody for 1 hour. The primary antibody was then washed off and replaced with the corresponding FITC labelled secondary antibody, before the cells were viewed using a fluorescent microscope.

6.3 Results

6.3.1 Over-expression of matriptase-2 decreased levels of β-catenin in PC3 cells.

Forced expression of matriptase-2 cells resulted in a dramatic reduction in β-catenin protein levels in the PC3 $^{mat2\ exp}$ cells compared to the control cells PC3 ^{wt} and PC3 ^{pEF6}. Figure 6.1 **A** shows that alteration of matriptase-2 causes no change in β-catenin mRNA levels in PC3 cells. Figure 6.1 **B** depicts a Western blot showing a decrease in β-catenin protein levels in the PC3 $^{mat2\ exp}$ compared to PC3 ^{wt} and PC3 ^{pEF6}. Figure 6.1 **C** further demonstrates the reduction in β-catenin protein using band quantification and normalisation against GAPDH expression. Figure 6.1 **D** revealed that through IFC staining, the reduction in β-catenin protein is form the cell membrane rather than globally throughout the cell.

6.3.2 Over-expression of matriptase-2 in DU145 cells increased levels of β-catenin

Forced expression of matriptase-2 resulted in an increase in β-catenin protein levels in DU145 $^{mat2\ exp}$ cells. Figure 6.2 **A** PCR reveals no change in β-catenin mRNA levels in DU145 cells. Figure 6.2 **B** shows a Western blot with increased levels of β-catenin in the DU145 $^{mat2\ exp}$ cells compared to DU145 ^{WT} and DU145 ^{pEF6} control cells. Figure 6.2 **C** further demonsrated the trend following band quantification and normalisation against GAPDH expression. Figure 6.2 **D** confirmed the increased the levels of β-

catenin protein using IFC staining. The increase in β-catenin protein can clearly be seen in the DU145 $^{mat\ exp}$ cells.

6.3.3 Over-expression of matriptase-2 results in no change of β-catenin levels in HECV endothelial cells.

Forced expression of matriptase-2 caused no change in the protein levels of HECV ^{mat2} ^{exp} cells.PCR analysis showed no change in β-catenin mRNA levels in all HECV cells Figure 6.3 A. Western blot detection of β-catenin protein in transfected and control cell demonstrated little difference in β-catenin protein levels between HECV $^{mat2\ exp}$ and HECV ^{wt} or HECV ^{pEF6} control cells (Figure 6.3 B). Figure 6.3 C further demonsrates the trend following band quantification and normalisation against GAPDH expression. Figure 6.3 C confirms there is no change in β-catenin protein levels, although there may be a shift in β-catenin localisation, using IFC staining of β-catenin in the cells.

6.3.4 Knock-down of matriptase-2 results in an increase of β-catenin in PZHPV7 cells.

Knock-down of matriptase-2 caused a marked increase of β-catenin protein in PZHPV7 $^{mat2\ rib1}$ cells when compared to the controls PZHPV7 ^{wt} and PZHPV7 ^{pEF6}. PCR analysis showed that there is no change in β-catenin mRNA levels regardless of matriptase-2 expression status (Figure 6.4 A). Western blot analysis demonstrated a marked increase of β-catenin protein levels in the PZHPV7 $^{mat2\ rib1}$ cells compared to the PZHPV7 ^{pEF6} control cells (Figure 6.4 B). Figure 6.4C corroborates the trend following a band quantification of the Western blot and normalising against GAPDH expression. Figure

6.4 **D** confirms there is a large increase in β-catenin protein levels at the cell membrane using IFC staining in the cells.

6.3.5 Knock-down of matriptase-2 results in an increase of β-catenin in PNT2C2 cells.

Knock-down of matriptase-2 caused a large increase of β-catenin protein in PNT2C2 $^{mat2\ rib1}$ cells when compared to the controls PNT2C2 ^{wt} and PNT2C2 ^{pEF6}. PCR analysis revealed no change in β-catenin mRNA levels regardless of matritptase-2 expression status (Figure 6.5 **A**). Western blot analysis showed that there was a large increase in β-catenin protein in the PNT2C2 $^{mat2\ rib1}$ cells compared to the control cells PNT2C2 ^{pEF6} (Figure 6.5 **B**). Figure 6.5 **C** further demonstrates the trend using band quantification of the Western blot and normalising β-catenin protein expression against GAPDH. Following IFC staining, the increase in β-catenin protein was revealed to be at the cell membrane rather than throughout the whole cell (Figure 6.5 **D**).

Figure 6.3.6 Alteration of matriptase-2 expression affects the expression of E-cadherin and N-cadherin

EMT indicators E-cadherin and N-cadherin were investigated in all cells lines. Western blot analysis showed decreased levels of N-cadherin protein in PC3 $^{mat2\ exp}$ and DU145 $^{mat2\ exp}$ cells. However, there was no change in HECV $^{mat2\ exp}$ cells. The Western blot also showed an increase in N-cadherin protein in the matriptase-2 knockdown cells PZHPV7 $^{mat2\ rib1}$ and in PNT2C2 $^{mat2\ rib1}$ (Fig 6.6 **A**). On investigation of E-cadherin the Western blots displayed increased E-cadherin protein expression in PC3 $^{mat2\ exp}$ and DU145 ^{mat2}

186

^{exp} cells. The Western blot also showed a decrease of E-cadherin protein in matriptase-2 knockdown cells PZHPV7 $^{mat2\ rib1}$ and in PNT2C2 $^{mat2\ rib1}$ (Fig 6.6 **B**).

Figure 6.3.7 Alteration of matriptase-2 expression influences β-catenin target gene MMP-7

Expression levels of the β-catenin target gene MMP-7 were investigated in the matriptase-2 altered cells. PCR analysis showed clearly decreased MMP-7 mRNA in PC3 $^{mat2\ exp}$ and HECV $^{mat2\ exp}$ cells. There was however, an increase in MMP-7 mRNA in DU145 $^{mat2\ exp}$ cells. The PCR also showed an increase in MMP-7 mRNA in matriptase-2 knockdown cells PZHPV7 $^{mat2\ rib1}$ and in PNT2C2 $^{mat2\ rib1}$ (Fig. 6.7 **A**). This trend was also investigated at the protein level. Western blots were conducted and revealed decreased MMP-7 protein expression in PC3 $^{mat2\ exp}$ and HECV $^{mat2\ exp}$ cells. There was again an increase in MMP-7 protein in DU145 $^{mat2\ exp}$ cells. The Western also shows an increase of MMP-7 protein in PZHPV7 $^{mat2\ rib1}$ and in PNT2C2 ^{mat2} ^{rib1}matriptase-2 knockdown cells (Fig 6.7 **B**).

Figure 6.3.8 Matriptase-2 appears to regulate the levels of ECM modulator uPA.

The levels of the potent angiogenic factor uPA were examined in all cell lines. PCR analysis displayed no change in uPA mRNA expression in any cell line regardless of matriptase-2 status (Fig 6.8 **A**). Western blots were then conducted to determine if uPA protein was affected. These revealed a reduction in uPA protein in the PC3 $^{mat2\ exp}$,

DU145 $^{mat2\ exp}$ and HECV $^{mat2\ exp}$ cells compared to the control pEF6 cells for each cell line. It also showed an increase in uPA protein in PZHPV7 $^{mat2\ rib1}$ and PNT2C2 $^{mat2\ rib1}$ cells compared to the control pEF6 cells for each cell line (Fig 6.9 **B**).
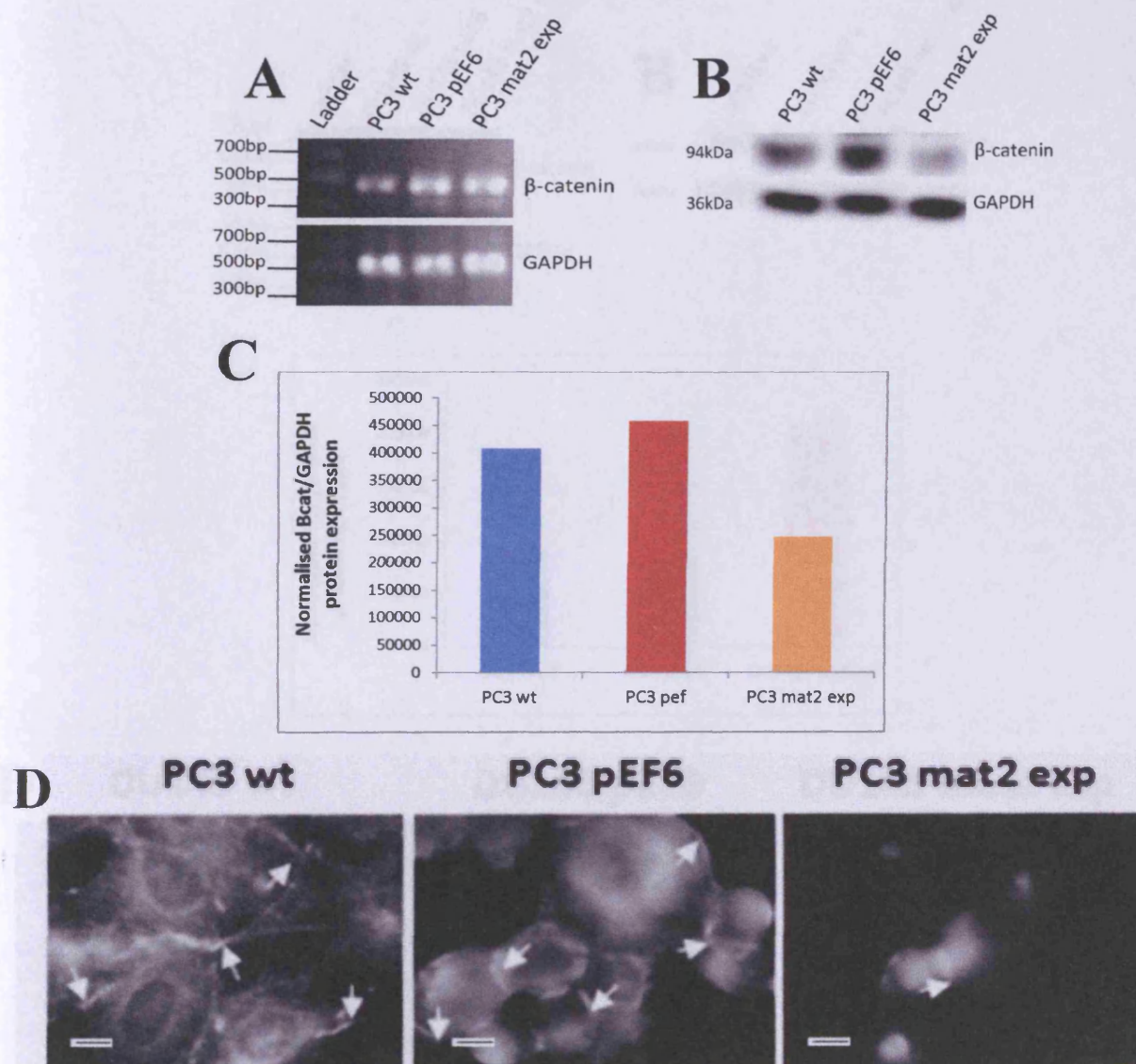
Figure 6.1 Over-expression of matriptase-2 results in reduced β-catenin expression in PC3 cells

A. PCR showing no change in β-catenin mRNA levels. **B.** Western blot displaying reduced β-catenin protein levels in the PC3 [mat2 exp] cell line compared to the control PC3 [pEF6]. **C.** Western blot band quantification showing β-catenin levels normalised to the levels of the control protein GAPDH. **D.** IFC staining shows reduced membrane staining for β-catenin in the PC3 [mat2 exp] cell line compared to the control PC3 [pEF6]. (⎯ = 10μm).

189
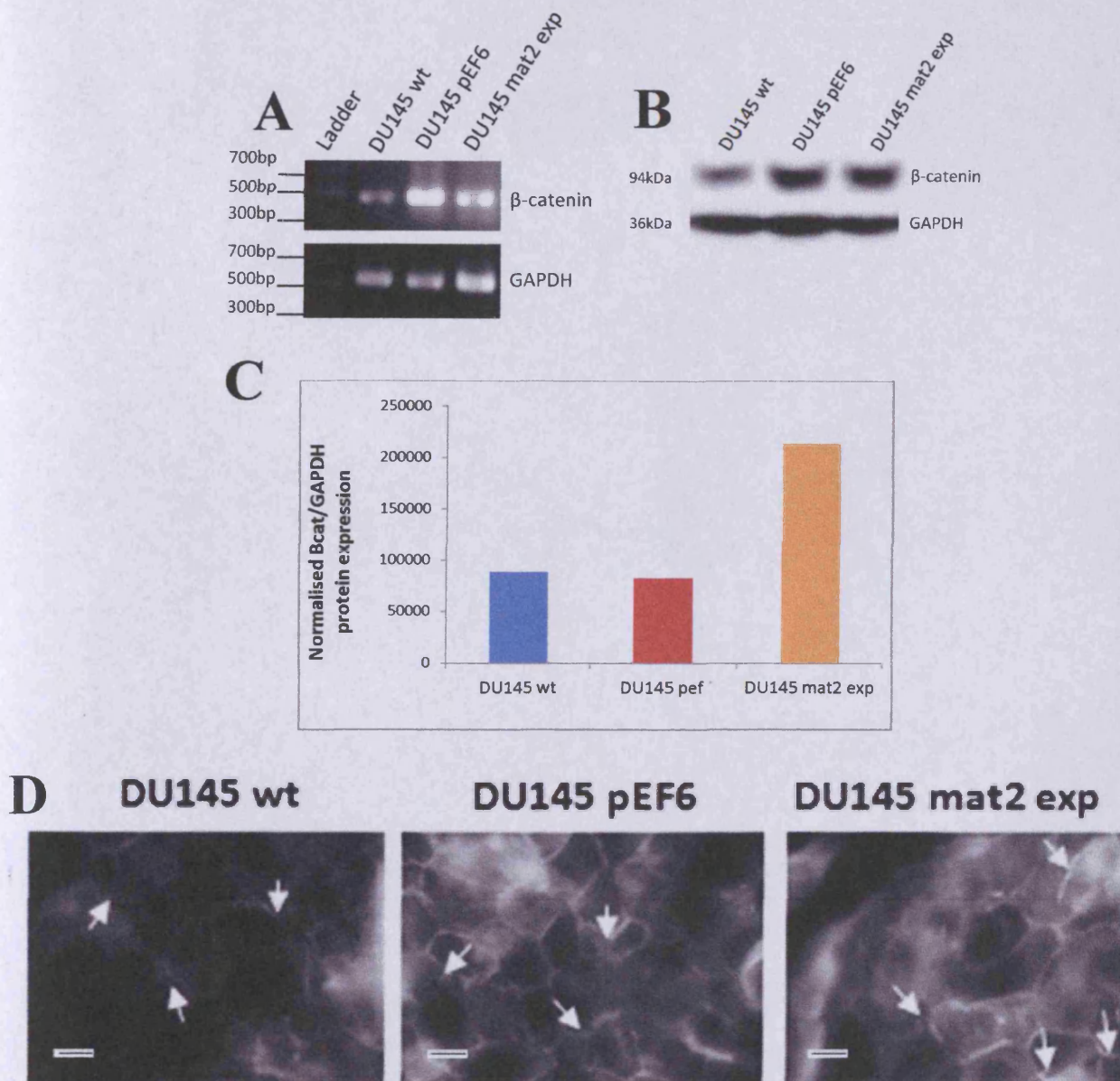
Figure 6.2 Over-expression of matriptase-2 results in increased β-catenin expression in DU145 cells

A. PCR showing a slight increase in β-catenin mRNA levels. **B.** Western blot displaying increased β-catenin protein levels in the DU145 [mat2 exp] cell line compared to the control DU145 [pEF6]. **C.** Western blot band quantification showing β-catenin levels normalised to the levels of the control protein GAPDH. **D.** IFC staining also shows an increase in membrane staining for β-catenin in the DU145 [mat2 exp] cell line compared to the control DU145 [pEF6]. (── = 10μm).
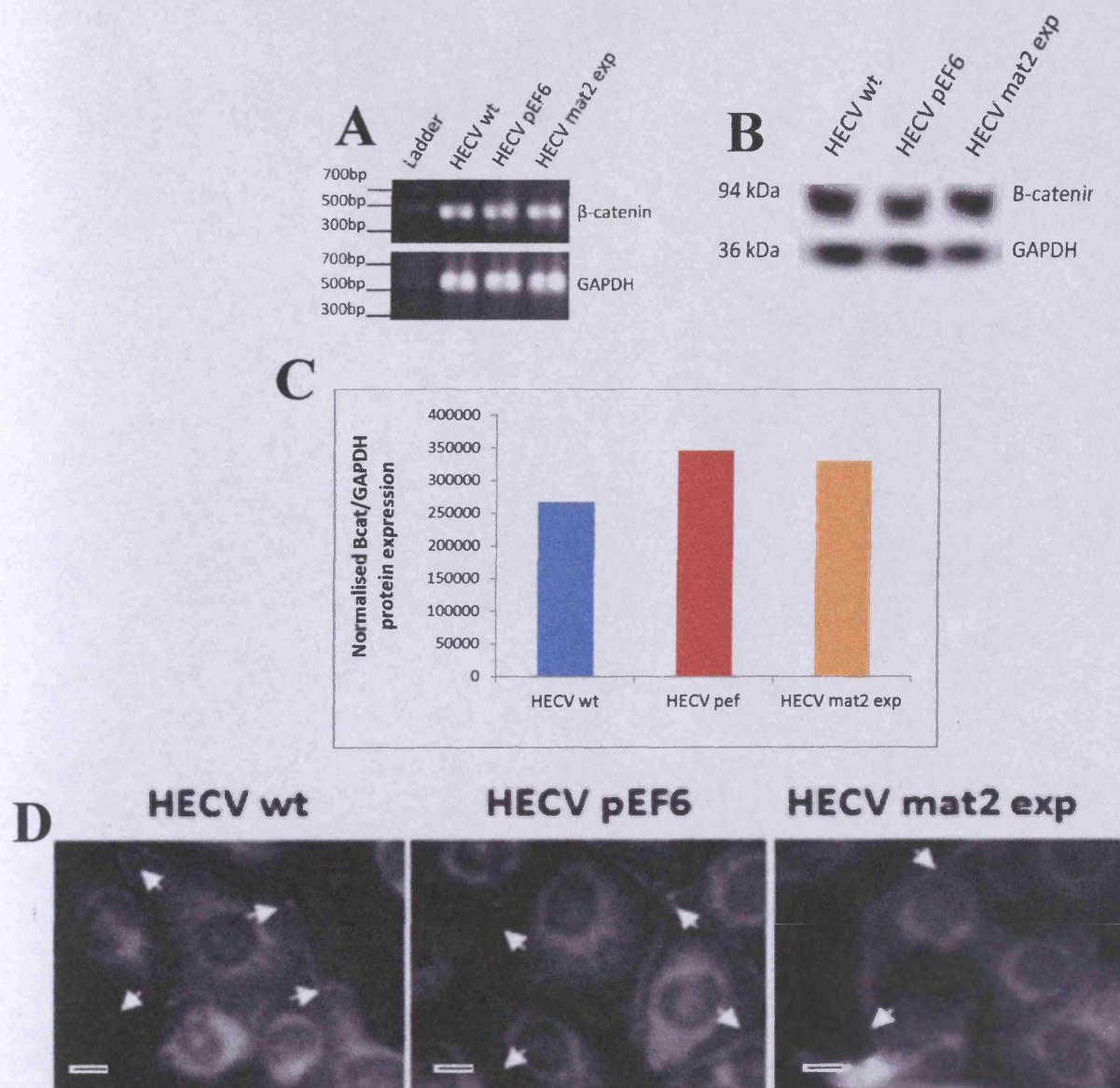
Figure 6.3 Over-expression of matriptase-2 results in no change in β-catenin expression in HECV cells

A. PCR showing no change in β-catenin mRNA levels. **B.** Western blot displaying no change in over-all β-catenin protein levels in the HECV $^{mat2\ exp}$ cell line compared to the control HECV ^{pEF6}. **C.** Western blot band quantification showing β-catenin levels normalised to the levels of the control protein GAPDH. **D.** IFC staining also shows no change in membrane staining for β-catenin in the HECV $^{mat2\ exp}$ cell line compared to the control HECV ^{pEF6}. (— = 10μm).
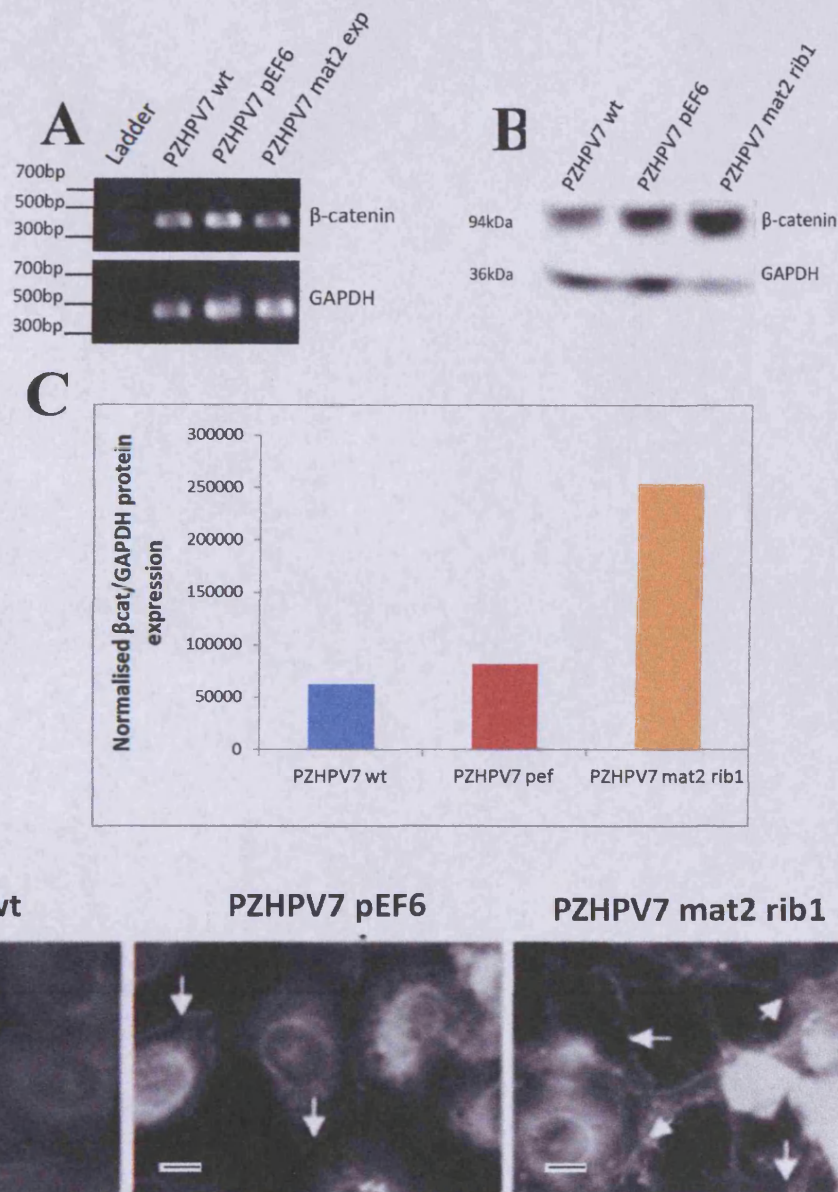
Figure 6.4 Knockdown of matriptase-2 results in an increase in β-catenin expression in PZHPV7 cells

A. PCR showing no change in β-catenin mRNA with a knockdown of matriptase-2. **B.** Western blot displaying an increase in β-catenin protein levels in the PZHPV7 [mat2 rib1] cell line compared to the control PZHPV7 [pEF6]. **C.** Western blot band quantification showing β-catenin levels normalised to the levels of the control protein GAPDH. **D.** IFC staining also shows an increase in membrane staining for β-catenin in the PZHPV7 [mat2 rib1] cell line compared to the control PZHPV7 [pEF6] cells. (——— = 10μm).
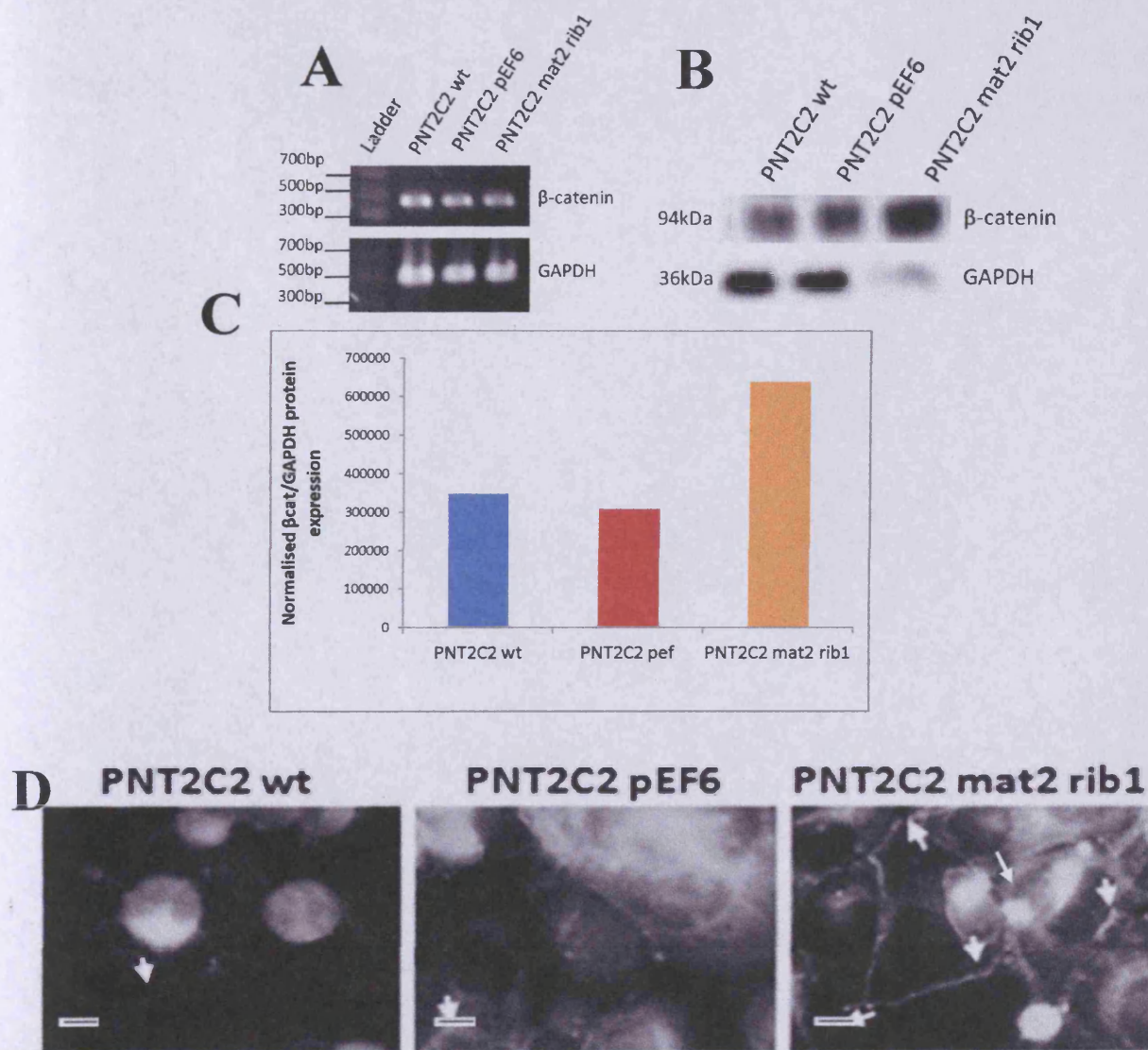
Figure 6.5 Knockdown of matriptase-2 results in an increase in β-catenin expression in PNT2C2 cells

A. PCR showing no change in β-catenin mRNA levels in response to matriptase-2 knockdown. **B.** Western blot displaying an increase in β-catenin protein levels in the PNT2C2 [mat2 rib1] cell line compared to the control PNT2C2 [pEF6]. **C.** Western blot band quantification showing β-catenin levels normalised to the levels of the control protein GAPDH. **D.** IFC staining also shows an increase in membrane staining for β-catenin in the PNT2C2 [mat2 rib1] cell line compared to the control PNT2C2 [pEF6]. (⎯ = 10μm).
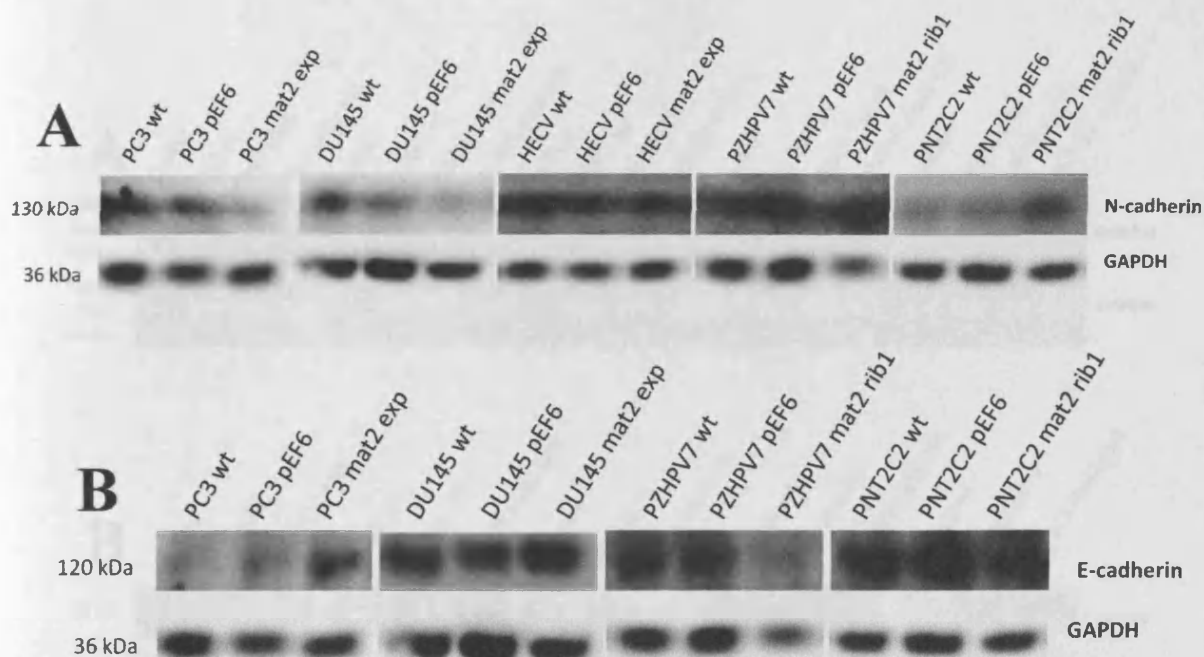
Figure 6.6 Alteration of matriptase-2 expression affects the expression of E-cadherin and N-cadherin

A. Western blot showing decreased levels of N-cadherin protein in PC3 $^{mat2\ exp}$ and DU145 $^{mat2\ exp}$ cells. However, there is no change in HECV $^{mat2\ exp}$ cells. The Western blot also shows an increase in N-cadherin protein in the matriptase-2 knockdown cells PZHPV7 $^{mat2\ rib1}$ and in PNT2C2 $^{mat2\ rib1}$. **B.** Western blots displaying increased E-cadherin protein expression in PC3 $^{mat2\ exp}$ and DU145 $^{mat2\ exp}$ cells. The Western blot also shows a decrease of E-cadherin protein inmatriptase-2 knockdown cells PZHPV7 $^{mat2\ rib1}$ and in PNT2C2 $^{mat2\ rib1}$.
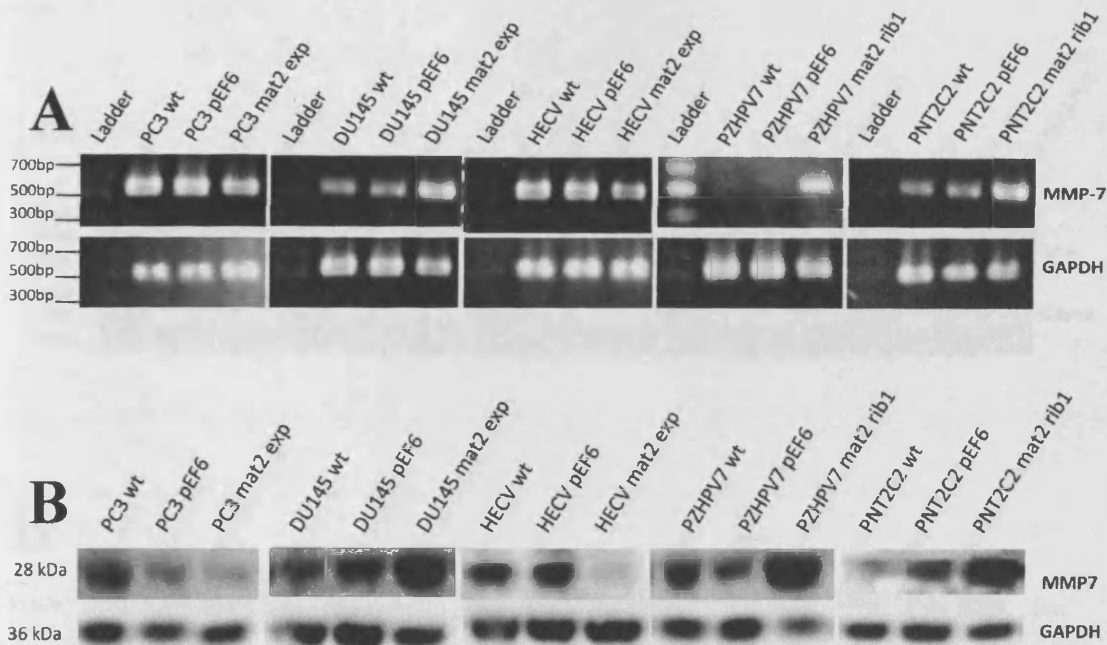
Figure 6.7 Alteration of matriptase-2 expression influences β-catenin target gene and angiogenesis factor MMP-7

A. PCR showing decreased MMP-7 mRNA in PC3 $^{mat2\ exp}$ and HECV $^{mat2\ exp}$ cells. There was however an increase in MMP-7 mRNA in DU145 $^{mat2\ exp}$ cells. The PCR also shows an increase in MMP-7 mRNA in PZHPV7 $^{mat2\ rib1}$ and in PNT2C2 $^{mat2\ rib1}$. **B.** Western blots displaying decreased MMP-7 protein expression in PC3 $^{mat2\ exp}$ and HECV $^{mat2\ exp}$ cells. As with the PCR the Western blot showed increased MMP-7 protein in the DU145 $^{mat2\ exp}$ cell line. The Western also shows an increase of MMP-7 protein in PZHPV7 $^{mat2\ rib1}$ and in PNT2C2 $^{mat2\ rib1}$.
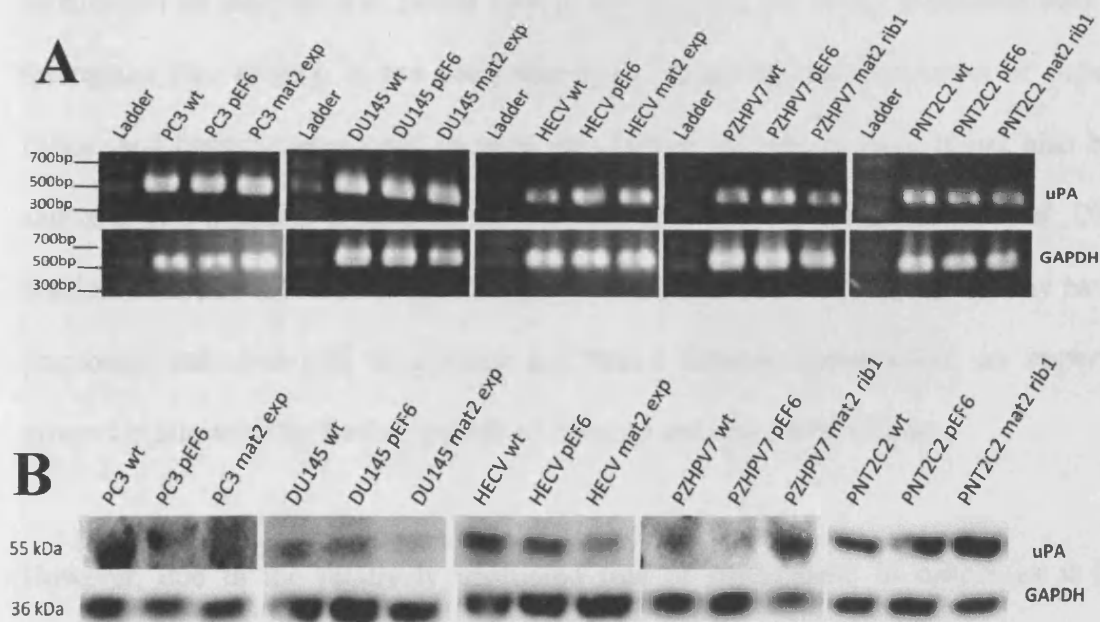
Figure 6.8 Matriptase-2 appears to regulate the levels of ECM modulator uPA.
A. PCR displaying no change in uPA mRNA expression in any cell line regardless of
matriptase-2 status. **B.** Western blot analysis showed a reduction in uPA protein in the
presence of matriptase-2 over-expression. It also showed an increase in uPA protein in
cells with matriptase-2 knockdown.

6.4 Discussion

Matriptase-2 has been shown to potentially be a key player in preventing the progression of prostate and breast cancer not only in previously published data but throughout this project. It has been shown to reduce the aggressiveness of prostate cancer and breast cancer cells *in vitro* and tumour growth *in vivo*. It has also been shown to be a potential prognostic indicator for breast cancer patients (Parr *et al.*, 2007; Sanders *et al.*, 2008). This project has also demonstrated that matriptase-2 may have a previously unknown role in prostate and breast tumour angiogenesis, an important process in allowing the further growth of primary and secondary tumours.

However, due to the relatively unstudied role of matripase-2 in cancer as it is a relatively newly discovered member of the TTSP family, there is little known about the mechanistic action of matriptase-2. In the last few years a crucial role for matriptase-2 in iron homeostasis has been uncovered. It has been shown that matriptase-2 can proteolytically process m-HJV, more commonly known in cancer as RGMc (Folgueras *et al.*, 2008; Silvestri *et al.*, 2008). As RGMc is a BMP co-receptor there is some scope for the involvement of matritpase-2 in the BMP pathway, a highly deregulated pathway in cancer. Investigating the effects of matritpase-2 cleavage of RGMc on the BMP pathway in cancer would be a worthwhile endeavour to give some insight into the proteases mechanism in cancer.

Unpublished work produced previously in the laboratory presented the possibility that there may be some link between the expression status of matriptase-2 and β-catenin. Given that Wnt/β-catenin signalling is another pathway that is highly aberrant in cancer

development the fact that a regulatory link between matriptase-2 and β-catenin may exist was an exciting one. This project attempted to determine the definite existence of this link and consider the effects the link may have on the aggressiveness of prostate cancer.

To fully investigate the effect of matriptase-2 on β-catenin, two aggressive prostate cancer cell lines PC3 and DU145 were utilised in the experiments along with the previously seen cell line HECV, PZHPV7 and PNT2C2. As both of these cell lines displayed low expression of matriptase-2 they were transfected with the matriptase-2 expression plasmid that was also introduced to the HECV cells. Once matriptase-2 over-expression was confirmed, experiments to investigate β-catenin were conducted.

The investigation started with examination of the mRNA levels of β-catenin in each of the five cell lines. The PCR results revealed that matriptase-2 expression status had no effect at all on the mRNA levels of β-catenin in any of the cell lines. In light of this the protein levels of β-catenin were then examined using Western blotting. The Western blots revealed that an over-expression of matriptase-2 greatly decreased the protein levels of β-catenin in the PC3 $^{mat2\ exp}$ cell line. Conversely in the matriptase-2 knockdown cells PZHPV7 $^{mat2\ rib1}$ and PNT2C2 $^{mat2\ rib1}$ there was a large increase in β-catenin protein. The only exception was HECV $^{mat2\ exp}$ cells which showed no change in β-catenin protein levels. These results could indicate that in the normal prostate and prostate cancer cells matriptase-2 is potentially cleaving β-catenin. In the case of DU145 $^{mat2\ exp}$ there was an increase in β-catenin levels. This could be due to the differing expression of E-cadherin in the DU145 cell lines. The odd result with HECV

mat2 exp cells may indicate that β-catenin is not involved in the mechanism of action in endothelial cells.

To further examine the protein expression of β-catenin immunofluorescent staining was conducted on all cell lines. This also revealed a decrease in β-catenin expression in the PC3 mat2 exp cells where the lack of fluorescence is clearly visible. The images from DU145 mat2 exp also reveal the increase in protein seen with the Western blots. The HECV mat2 exp cells also showed no increase in β-catenin but may indicate a shift in location which would need to be further investigated. As with the Westerns the PZHPV7 mat2 rib1 and PNT2C2 mat2 rib1 also showed an increase in β-catenin protein staining. This change in β-catenin levels in the cells may account for the changes in motility and invasion seen in the cells as the β-catenin target genes are often involved in regulating such cellular processes.

There is evidence suggesting that during the process of prostate cancer progression, loss of E-cadherin expression or activation of the Wnt pathway can lead to an increase in the cytoplasmic levels of β-catenin. The excess free β-catenin proteins translocate to the nucleus and activate transcription of its target genes. As an AR co-activator, β-catenin may also play a critical growth-promoting role by compensating for decreased androgen levels in response to androgen ablation therapy (Verras and Sun, 2006). These two proteins obviously have a close relationship in the area of cancer progression; if matriptase-2 can indeed cleave β-catenin then this may in turn lead to a breakdown of the E-cadherin complex at the cell membrane. This would then lead to then cell becoming more aggressive in nature. Figure 6.6b showed that an over-expression of

matriptase-2 increased the levels of E-cadherin in the PC3 $^{mat2\ exp}$ and DU145 $^{mat2\ exp}$ cell. It also showed a decrease in E-cadherin in the matriptase-2 knockdown cells PZHPV7 $^{mat2\ rib1}$ and PNT2C2 $^{mat2\ rib1}$ cells. This change in E-cadherin levels is also associated with a change in N-cadherin levels. Figure 6.6a showed that an increase in E-cadherin levels was twinned with a decrease in N-cadherin levels and the converse with a decrease of E-cadherin levels. This indicates that matriptase-2 not only cleaves β-catenin but has an effect on the EMT of the cells. In addition loss of E-cadherin would reduce cell to cell adhesion and promote motility of the cells. This could be a potential reason for the changes in motility seen in the cells with altered matriptase-2 levels. As EMT promotes a more cancerous phenotype this is another possible effect matriptase-2 has in reducing the aggressiveness of prostate cancer cells.

In an attempt to investigate the anti-angiogenic nature of matriptase-2 the metalloproteinase MMP-7, which has previously been shown to be a β-catenin target gene in colorectal cancer (Brabletz *et al.*, 1999; Crawford *et al.*, 1999), was investigated in the cells. MMPs have widely reported as being one of several angiogenic factors secreted by prostate cancer (van Moorselaar and Voest, 2002), if the accumulation of β-catenin also causes an increase in MMP-7 this could be one explanation to the anti-angiogenic nature of matriptase-2. Figure 6.7a reveals an increase in MMP-7 mRNA in response to matriptase-2 knockdown in the PZHPV7 $^{mat2\ rib1}$ and PNT2C2 $^{mat2\ rib1}$ cells. The PC3 $^{mat2\ exp}$ cells showed a decrease in MMP-7 mRNA. The same trend is true for the MMP-7 protein in figure 6.7b. The only exceptions are DU145 $^{mat2\ exp}$ in which MMP-7 increased in response to the increase in β-catenin levels. HECV $^{mat2\ exp}$ showed no change in MMP-7 levels corresponding to the unchanging β-catenin levels. This data

indicates that MMP-7 may play some role in the anti-angiogenic role of matriptase-2 but obviously cannot be the only player due to the results from DU145 $^{mat2\ exp}$ and HECV $^{mat2\ exp}$.

To further investigate the anti-angiogenic role of matriptase-2 a molecule unrelated to β-catenin was investigated. uPA is an extracellular matrix modulator that has been implicated in angiogenesis (Bajou et al., 2001; Noel et al., 2004; Morrissey et al., 2008). Figure 6.8a showed that there was no change in uPA mRNA irrelevant of matriptase-2 status. Figure 6.8b however, shows a decrease in uPA protein that is unrelated to the levels of β-catenin in the cells. An increase in uPA was also seen with a knockdown of matriptase-2. This could indicate that matriptase-2 directly cleave uPA which would contribute to the anti-angiogenic nature of matriptase-2 in a β-catenin independent manner. To further support this theory is has been shown that matriptase-1 has the potential to cleave uPA (Takeuchi et al., 2000). As matriptase-1 and -2 have a high sequence homology, it is likely that they share potential substrates (Hooper et al., 2003). Although both proteases may claim uPA as a substrate, due to the tumour progressing nature of matriptase-1 and the tumour suppressing nature of matriptase-2, the cleavage of uPA may potentially have very different effects in the cancer.

This chapter has revealed some interesting possibilities that will contribute to understanding the mechanism of action of matriptase-2. It is evident that the effect of matriptase-2 on β-catenin may play some role in reducing the aggressiveness of prostate cancer and potentially reducing angiogenic ability through regulation of MMP-7. Although due to the differing results seen between the cell lines the ability of

Chapter 7

General discussion

matriptase-2 to alter the protein expression of β-catenin may not be the major player in the mechanism of matriptase-2. Also contributing to the anti-angiogenic nature of matriptase-2, uPA seems to play just as large a role as β-catenin. This reveals how complicated the mechanism of action of matriptase-2 actually is and it is possible that this project has only scratched the surface of the function of matritpase-2.

7.1 Prostate cancer metastasis

Prostate cancer is the most commonly diagnosed cancer in men in the UK. Approximately a quarter of new cancer cases diagnosed in men are prostate cancer. In 2007 around 36,000 men were diagnosed with prostate cancer in the UK. In 2008, there were 37,051 new cases of prostate cancer diagnosed in the UK, which is around 101 men every day or one man every 15 minutes. The lifetime risk of being diagnosed with prostate cancer is 1 in 9 for men in the UK. The strongest known risk factor for prostate cancer is age, with very low risk in men under 50 and rising risk with increasing age thereafter. Very few cases are registered in men under 50 and around three-quarters of cases occur in men over 65 years. The largest number of cases is diagnosed in those aged 70+. As prostate cancer is typically a slow growing cancer, most never grow to the point of causing symptoms. Because of this the majority of men die with prostate cancer rather than of it. Due to this lack of symptoms, prostate cancer is often diagnosed in an already advanced state. Around 75% of patients exhibit locally extensive or metastatic disease, resulting in a poor prognosis of less than 15% surviving over 5 years (Foster, 1990).

The metastasis of cancer to secondary sites in the body is responsible for the majority of cancer related deaths. There is however, no curative treatment for cancer metastasis. Due to this fact metastasis is the subject of intense research in the hope of producing treatments to delay or even prevent the process of metastasis. Prostate cancer metastasis is a complex multi-stage process that involves several crucial steps that facilitates the spread of the cancer cells to secondary sites. The steps involve

mutation of cells, epithelial to mesenchymal transition (EMT), degradation of the extracellular matrix (ECM), invasion, angiogenesis, intravasation, extravasation and colonisation of secondary sites. Angiogenesis is particularly important as it not only provides the tumour with the nutrients needs to grow larger; it also provides a means of escape for metastasising tumour cells. There is intense research into developing therapeutics targeting angiogenesis as a means to treat prostate cancer. .As most cells are not actively relying on angiogenesis, treatment with angiogenesis inhibitors will be more accurately targeted to cancer cells than a cytotoxic compound and will have a lower level of toxicity to normal non-cancerous cells.

7.2 Matriptase-2 and cancer

Cell surface proteolysis has become known as an important mechanism for the activation of proteins involved in managing a wide range of cellular functions. Matriptase-2 is a relatively newly discovered member of the Type II transmembrane serine protease (TTSP) family. The TTSP family is of great scientific interest due to the differing expression of TTSPs in normal and cancerous tissues and cells (Wallrapp *et al.*, 2000; Lang and Schuller, 2001; Magee *et al.*, 2001; Netzel-Arnett *et al.*, 2003; Lee *et al.*, 2005). Matriptase-2 was identified in 2002 when screening for sequences common to the TTSP family. Matriptase-2 shares a high homology with matriptase-1, which is also over-expressed in different human cancers (Shi *et al.*, 1993). However, where the over-expression of matriptase leads to cancer progression (Uhland, 2006; Tsai *et al.*, 2008) matriptase-2 over-expression significantly reduces breast and prostate cancer growth and reduced levels correlate

with poor patient outcome (Parr *et al.*, 2007; Sanders *et al.*, 2008). Altered expression of matriptase-2 in cancer has been reported in several studies. Matriptase-2 transcript was detected in mouse Leydig tumour cells (Odet *et al.*, 2006) and elevated levels of matriptase-2 have been reported in invasive ductal cell carcinoma (Overall *et al.*, 2004). Studies from within our laboratories showed that there were reduced levels of matriptase-2 immunostaining in cancerous breast tissue sections compared to normal tissue sections with the majority of matriptase-2 staining being confined to the epithelial sections (Parr *et al.*, 2007). In contrast to this quantitative PCR showed that matriptase-2 levels were up-regulated in tumour compared to normal tissues, however matriptase-2 levels were significantly higher in lower NPI and TNM stages and correlated with positive patient outcome and the over-expression of matriptase-2 reduced aggressive *in vitro* and *in vivo* traits of MDA-MB-231 breast cancer cells (Parr *et al.*, 2007). An additional study using the invasive prostate cancer cell lines PC-3 and DU-145 showed that increased expression of matriptase-2 reduced the invasiveness and motility of the cells (Sanders *et al.*, 2008). When the same cells were implanted into CD-1 athymic nude mice, the resulting tumours developed very poorly *in vivo* compared to control cells and significant reductions in tumour volume were observed between matriptase-2 over-expressing and control groups (Sanders *et al.*, 2008).

The molecular mechanisms involved in the activation of matriptase-2 remain largely unknown. There is very little information concerning the specific involvement of matriptase-2 in cancer currently in the literature.

7.3 Aims of thesis

As there is such a small amount of knowledgein the literature about matriptase-2 this project aimed to provide more information about the function of matriptase-2 and the mechanism by which it exerts its effects. This would provide much needed information about matriptase-2. Using methods well established within the laboratory matriptase-2 was over-expressed and knockdown in several cell lines. These altered cell lines were then used to conduct functional assays, *in vivo* mouse model trials and used in assays to examine the mechanistic action of matriptase-2.

7.4 The role of matriptase-2 in prostate cells

Using the ribozyme transgene technology to knockdown matriptase-2 in the normal prostate cell lines PZHPV7 and PNT2C2 allowed the effect of a removal of matriptase-2 to be examined. This revealed that matriptase appears to have no effect on the growth or adhesion of these two prostate cell lines. It also showed a significant increase in the motility and invasiveness of these cells. The ability of a cell to become motile and invasive is a mark of a developing cancer cell that will gain the ability to metastasise. The fact that a loss of matriptase-2 increases these cancerous characteristics in these cells suggests that matriptase-2 may prevent the development and/or progression of prostate cancer. These findings correlate with those found by Sanders *et al* 2006 and Parr *et al* 2007. In these studies it found that an over-expression of matriptase-2 in the aggressive cell lines PC3, DU145 and MDA-MB-231 significantly reduced the motility and invasiveness of all three of these cell lines. Due to the scarcity of research involving the possible cellular

functions matriptase-2 it is very difficult to hypothesize how the protease may be regulating the motility and invasiveness of prostate and breast cells. It is clear however, that matriptase-2 exerts its effects on key regulators of motility and invasion to prevent the cells from progressing to a more cancerous phenotype.

Due to the potential tumour suppressive role that these results suggest for matriptase-2 there is some discrepancy with the findings of Velasco *et al* 2002 who demonstrated the capacity of the matriptase-2 catalytic domain to degrade ECM components such as fibronectin, fibrinogen and type I collagen (Velasco *et al.*, 2002). This would suggest that matriptase-2 should promote the degradation of the artificial matrigel basement membrane as it contains a large portion of collagen, laminin, and fibronectin. A possible explanation for the opposite trends demonstrated in this chapter may be that Velasco *et al* only examined the catalytic domain of matriptase-2. This domain shows a large degree of homology to the catalytic domain of matriptase-1 (approximately 50%) and contains motifs and sequences which are characteristic of all members of the serine protease family. This would indicate that the catalytic domain of matriptase-2 would demonstrate the potential to degrade similar substrates to matriptase-1. However, the full length protein must be taken into account, not just the catalytic domain, as the large number of non-catalytic domains will undoubtedly contribute to protein folding and also interaction of the protease with substrates. Indeed the modular domains of the stem region of the TTSPs have been proposed to be involved in protease-substrate interaction (Netzel-Arnett *et al.*, 2003). Determining how matriptase-2 reduces the aggressive nature of prostate and breast cancer will be an important step in future research given the obvious importance of the protective capability of matriptase-2.

7.5 The role of matriptase-2 in tumour angiogenesis

It was decided to investigate any impact of matriptase-2 on HECV endothelial cells due to the fact that the mRNA screen showed no expression of matriptase-2 in the HECV cells. This allowed the investigation as to whether matriptase-2 had any effect on angiogenesis. An over-expression of matriptase-2 in these cells revealed results similar to those seen in the PC3 and DU145 cells over-expressing matriptase-2. As seen with the normal prostate cell lines, there was no change in the growth or adhesion of the HECV $^{mat2\ exp}$ cells. There was however, a significant decrease in the motility of the cells. This correlates perfectly with the results obtained from the other four cell lines examined. As the HECV cells are endothelial cells a tubule formation assay could be performed. An over-expression of matriptase-2 significantly reduced the HECV cells ability to form tubules in an artificial basement membrane. This revealed that matriptase-2 significantly reduced the angiogenic ability of the HECV cells.

These results show that matriptase-2 is likely to have a role in tumour angiogenesis. The results from this study clearly show a reduction in angiogenic potential in the presence of matriptase-2 over-expression. How matriptase-2 exerts its effect on the angiogenic process remains unknown. Several studies have suggested that fibrinogen and components of the uPA system can facillitate tumour angiogenesis and are possibly up-regulated in cancer (Bajou *et al.*, 2001; Noel *et al.*, 2004; Morrissey *et al.*, 2008). As matriptase-2 has been shown to proteolytically

process these proteins this may have some impact of the angiogenic ability of these cells.

These findings have shown that matriptase-2 is proving to be an incredibly important molecule in the area of preventing tumour metastasis. As matriptase-2 has been shown to reduce the aggressive nature of well known prostate and breast cancer cell lines and to reduce tumour volume *in vivo* it could have a significant impact on metastasis. As the cells over-expressing matriptase-2 are significantly less motile and invasive they are far less likely to become actively metastasising cells. Combined with matriptase-2 being capable of reducing the angiogenic ability of endothelial cells, it appears that matriptase-2 has significantly reduced the likelyhood that cells expressing matriptase-2 will be able to metastasise. This is an incredibly important fact as most prostate tumours are already found to be metastasising and matriptase-2 could potentially be utilised to reduce the chance of further metastases and to reduce the possibly aggressive nature of the cancer.

7.6 The importance of β-catenin in the mechanistic action of matriptase-2

The β-catenin nuclear signalling molecule, a key component of the Wnt signalling pathway, has been widely implicated as an oncogene in human cancer and current research is greatly interested in deepening the understanding of the role of β-catenin in the development of cancer in the hope of providing possible therapeutic stratagies for the treatment of cancer. The reduction of β-catenin degredation upon wnt

stimulation leads to greater β-catenin participation in two major cellular processes, nuclear signaling and cell–cell adhesion. β-catenin accumulation results in its translocation into the nucleus and interaction with DNA-binding transcription factors, the most prominent of which are those of the TCF/lymphoid enhancer factor (LEF) family. Once localized to the nucleus, β-catenin complexed with its DNA-binding transcription factors, initiates the transcription of its target genes. These target genes are highly involved in the regulation of many proteins that are involved in maintaining the proper functions of the cell. These target genes include c-MYC (He *et al.*, 1998), MMP-7 (Brabletz *et al.*, 1999; Crawford *et al.*, 1999), VEGF (Zhang *et al.*, 2001), MET (Boon *et al.*, 2002). Because of the importance of these target genes in maintaining the correct function of the cell the balance between the degredation and activation of β-catenin must remain tightly controlled. Deregulation of this pathway plays a huge role in the progression and possibly the development of cancer.

β-catenin was chosen to investigate in this study due to data (unpublished) gained during a previous study involving matriptase-2. This study was trying to determine how matriptase-2 mediated the reduction in migration seen in PC3 and DU145 cells over-expressing matriptase-2 and the reduction in adhesion seen in PC3 cells {Sanders, 2008 #225}. A screen of molecules involved with cell:cell and cell:matrix adhesion was performed using cells over-expressing matriptase-2. During this screen β-catenin was seen to be altered in response to matriptase-2 expression status. It was decieded that this result needed a further investigation. In this chapter PC3 [mat2 exp] and DU145 [mat2 exp] cells were used to provide a comprehensive examination of the

effect of matriptase-2 on β-catenin. The investigation started with examining the mRNA levels of β-catenin in each of the five cell lines. The PCR results revealed that matriptase-2 expression status had no effect at all on the mRNA levels of β-catenin in any of the cell lines. In light of this the protein levels of β-catenin were then examined using Western blotting. The Western blots revealed that an over-expression of matriptase-2 greatly decreased the protein levels of β-catenin in the PC3 $^{mat2\ exp}$ cell line. Conversely in the matriptase-2 knockdown cells PZHPV7 ^{mat2} ^{rib1} and PNT2C2 $^{mat2\ rib1}$ there was a large increase in β-catenin protein. The only exception was HECV $^{mat2\ exp}$ cells which showed no change in β-catenin protein levels. These results could indicate that in the normal prosate and prostate cancer cells matriptase-2 is potentially cleaving β-catenin. In the case of DU145 $^{mat2\ exp}$ there was an increase in β-catenin levels. This could be due to the differing expression of E-cadherin in the DU145 cell lines. The odd result with HECV $^{mat2\ exp}$ cells may indicate that β-catenin is not involved in the mechanism of action in endothelial cells.

IFC conducted on the cells also revealed a reduction in β-catenin staining at the cell membrane in the PC3 $^{mat2\ exp}$ cells, an increase in DU145 $^{mat2\ exp}$ and the HECV $^{mat2\ exp}$ cells also showed no increase in β-catenin but may indicate a shift in location which would need to be further investigated. As with the Westerns the PZHPV7 ^{mat2} ^{rib1} and PNT2C2 $^{mat2\ rib1}$ also showed an increase in β-catenin protein staining at the cell membrane.

This change in β-catenin levels in the cells may account for the changes in motility and invasion seen in the cells as the β-catenin target genes are often involved in regulating such cellular processes. It has also been shown that LNCaP cells stably transfected with a stabilised β -catenin mutant showed no significant advantage in cell growth either in the presence or absence of androgens in comparison to the parent line (Verras and Sun, 2006). Because of the importance of these target genes in maintaining the correct function of the cell the balance between the degradation and activation of β-catenin must remain tightly controlled. Deregulation of this pathway plays a huge role in the progression and possibly the development of cancer. If matriptase-2 does have a potential regulatory role for β-catenin at the cell membrane this could a huge impact on reducing the aggressiveness of prostate cancer. If the transcription of genes promoting a more aggressive phenotype are prevented this would cause the cells to shift toward a less cancerous nature.

In an attempt to investigate the anti-angiogenic nature of matriptase-2 the metalloproteinase MMP-7, which has previously been shown to be a β-catenin target gene in colorectal cancer (Brabletz et al., 1999; Crawford et al., 1999), was investigated in the cells. The expression of MMP-7 is correlated with tumour progression, metastasis, and unfavourable prognosis in the human oesophageal carcinoma, colon, and gastric carcinoma (Mori et al., 1995; Honda et al., 1996; Szarvas et al., 2010). MMPs have widely reported as being one of several angiogenic factors secreted by prostate cancer (van Moorselaar and Voest, 2002), if the accumulation of β-catenin also causes an increase in MMP-7 this could be one explanation to the anti-angiogenic nature of matriptase-2. It was shown that the

mRNA and protein levels of MMP-7 increased or decreased according to the changes seen in β-catenin protein levels in each of the cell lines. This data indicates that MMP-7 may play some role in the anti-angiogenic role of matriptase-2 but obviously cannot be the only player due to the results from DU145 $^{mat2\ exp}$ and HECV $^{mat2\ exp}$.

To further investigate the anti-angiogenic role of matriptase-2 a molecule unrelated to β-catenin was investigated. uPA is an extracellular matrix modulator that has been implicated in angiogenesis (Bajou *et al.*, 2001; Noel *et al.*, 2004; Morrissey *et al.*, 2008). This investigation revealed that there was no change in uPA mRNA levels in any of the cell lines. However, when the protein levels were examined it was seen that matriptase-2 over-expression reduced the levels of uPA protein in all three over-expression cell lines irrespective of the change in β-catenin levels. The trend continued with an increase in uPA protein in the matriptase-2 knockdown cell lines, again irrespective of β-catenin levels. This could indicate that matriptase-2 directly cleave uPA which would contribute to the anti-angiogenic nature of matriptase-2 in a β-catenin independent manner.

To further support this theory is has been shown that matriptase-1 has the potential to cleave uPA (Takeuchi *et al.*, 2000). As matriptase-1 and -2 have a high sequence homology, it is likely that they share potential substrates (Hooper *et al.*, 2003). Although both proteases may claim uPA as a substrate, due to the tumour progressing nature of matriptase-1 and the tumour suppressing nature of matriptase-2, the cleavage of uPA may potentially have very different effects in the cancer.

7.7 Future work

Further investigation into the relationship between matriptase-2 and β-catenin is essential. The findings from this study have added further weight to the theory that matriptase-2 is a potential tumour suppressor and its mechanism of action must be fully investigated. It would be ideal to break down matriptase-2 and examine the components of the protein to determine which areas are needed to produce these results. If only a small section is actually needed to produce the described effects recombinant protein could be generated and the effects of exogenous matriptase-2 can be investigated. This would be beneficial to the possible therapeutic application of matriptase-2. From the results of this study and previous studies any therapeutic treatment of matriptase-2 would involve increasing its expression. If only a small section of matriptase-2 is needed to produce the results seen in this study it would be far easier to administer. Although the involvement of matriptase-2 in iron metabolism would have to be taken into account if matriptase-2 was to be used as a therapeutic treatment. The association of matriptase-2 and β-catenin could be further investigated by examining β-catenin phosphorylation status, using TCF reporter assays to determine β-catenin activity. Potentially β-catenin could be knocked down in the cells or even use a Wnt inhibitor to further investigate the effect of matriptase-2 on Wnt/β-catenin signalling. Another aspect that must be considered is the potential involvement of the BMP pathway. As matriptase-2 has been irrefutably shown to cleave RGMc, a BMP co-receptor, there is scope for matriptase-2 to have an influence over the BMP signalling pathway. As the BMP pathway is highly important in driving prostate cancer progression this would be a highly relevant area to research.

There is also the potential to further investigate the involvement of matriptase-2 in prostate cancer. As DU145 cells appear to have a small amount of endogenous matriptase-2 there is the potential to knockdown this endogenous matriptase-2 and perform the functional assays again to asses the functional effect of knowcking down matriptase-2 in this cell line. To also further investigate the involvement of matriptase-2 in prostate cancer is to use databases containing clinical data. These data bases include microarray data derived from clinical samples of patients with prostate cancer. This could provide some insight into the expression of matriptase-2 throughout the different grades of prostate cancer and how that has affected patient outcome. Matriptase-2 is continuing to show itself as an important player in prostate cancer progression and fully determining its mechanistic actions will only increase the possibility of producing potential therapeutics that would be used to treat prostate cancer.

Chapter 8

References

(1995). Maximum androgen blockade in advanced prostate cancer: an overview of 22 randomised trials with 3283 deaths in 5710 patients. Prostate Cancer Trialists' Collaborative Group. *Lancet* **346**(8970): 265-269.

Abate-Shen, C. and M. M. Shen (2000). Molecular genetics of prostate cancer. *Genes Dev* **14**(19): 2410-2434.

Adib, T. R., S. Henderson, C. Perrett, D. Hewitt, D. Bourmpoulia, J. Ledermann and C. Boshoff (2004). Predicting biomarkers for ovarian cancer using gene-expression microarrays. *Br J Cancer* **90**(3): 686-692.

Afar, D. E., I. Vivanco, R. S. Hubert, J. Kuo, E. Chen, D. C. Saffran, A. B. Raitano and A. Jakobovits (2001). Catalytic cleavage of the androgen-regulated TMPRSS2 protease results in its secretion by prostate and prostate cancer epithelia. *Cancer Res* **61**(4): 1686-1692.

Aimes, R. T., A. Zijlstra, J. D. Hooper, S. M. Ogbourne, M. L. Sit, S. Fuchs, D. C. Gotley, J. P. Quigley and T. M. Antalis (2003). Endothelial cell serine proteases expressed during vascular morphogenesis and angiogenesis. *Thromb Haemost* **89**(3): 561-572.

Allione, F., F. Eisinger, P. Parc, T. Noguchi, H. Sobol and D. Birnbaum (1998). Loss of heterozygosity at loci from chromosome arm 22Q in human sporadic breast carcinomas. *Int J Cancer* **75**(2): 181-186.

Autzen, P., C. N. Robson, A. Bjartell, A. J. Malcolm, M. I. Johnson, D. E. Neal and F. C. Hamdy (1998). Bone morphogenetic protein 6 in skeletal metastases from prostate cancer and other common human malignancies. *Br J Cancer* **78**(9): 1219-1223.

Babitt, J. L., F. W. Huang, D. M. Wrighting, Y. Xia, Y. Sidis, T. A. Samad, J. A. Campagna, R. T. Chung, A. L. Schneyer, C. J. Woolf, N. C. Andrews and H. Y. Lin (2006). Bone morphogenetic protein signaling by hemojuvelin regulates hepcidin expression. *Nat Genet* **38**(5): 531-539.

Bajou, K., L. Devy, V. Masson, V. Albert, F. Frankenne, A. Noel and J. M. Foidart (2001). [Role of plasminogen activator inhibitor type 1 in tumor angiogenesis]. *Therapie* **56**(5): 465-472.

Bandyopadhyay, S., R. Zhan, A. Chaudhuri, M. Watabe, S. K. Pai, S. Hirota, S. Hosobe, T. Tsukada, K. Miura, Y. Takano, K. Saito, M. E. Pauza, S. Hayashi, Y. Wang, S. Mohinta, T. Mashimo, M. Iiizumi, E. Furuta and K. Watabe (2006). Interaction of KAI1 on tumor cells with DARC on vascular endothelium leads to metastasis suppression. *Nat Med* **12**(8): 933-938.

Batson, O. V. (1995). The function of the vertebral veins and their role in the spread of metastases. 1940. *Clin Orthop Relat Res*(312): 4-9.

Beaufort, N., D. Leduc, H. Eguchi, K. Mengele, D. Hellmann, T. Masegi, T. Kamimura, S. Yasuoka, F. Fend, M. Chignard and D. Pidard (2007). The human airway trypsin-like protease modulates the urokinase receptor (uPAR, CD87) structure and functions. *Am J Physiol Lung Cell Mol Physiol* **292**(5): L1263-1272.

Beliveau, F., A. Desilets and R. Leduc (2009). Probing the substrate specificities of matriptase, matriptase-2, hepsin and DESC1 with internally quenched fluorescent peptides. *FEBS J* **276**(8): 2213-2226.

Bellone, S., S. Anfossi, T. J. O'Brien, M. J. Cannon, D. A. Silasi, M. Azodi, P. E. Schwartz, T. J. Rutherford, S. Pecorelli and A. D. Santin (2009). Induction of human tumor-associated differentially expressed gene-12 (TADG-12/TMPRSS3)-specific cytotoxic T lymphocytes in human lymphocyte antigen-

A2.1-positive healthy donors and patients with advanced ovarian cancer. *Cancer* **115**(4): 800-811.

Betsunoh, H., S. Mukai, Y. Akiyama, T. Fukushima, N. Minamiguchi, Y. Hasui, Y. Osada and H. Kataoka (2007). Clinical relevance of hepsin and hepatocyte growth factor activator inhibitor type 2 expression in renal cell carcinoma. *Cancer Sci* **98**(4): 491-498.

Bierie, B., M. Nozawa, J. P. Renou, J. M. Shillingford, F. Morgan, T. Oka, M. M. Taketo, R. D. Cardiff, K. Miyoshi, K. U. Wagner, G. W. Robinson and L. Hennighausen (2003). Activation of beta-catenin in prostate epithelium induces hyperplasias and squamous transdifferentiation. *Oncogene* **22**(25): 3875-3887.

Blackard, C. E., R. P. Doe, G. T. Mellinger and D. P. Byar (1970). Incidence of cardiovascular disease and death in patients receiving diethylstilbestrol for carcinoma of the prostate. *Cancer* **26**(2): 249-256.

Bocheva, G., A. Rattenholl, C. Kempkes, T. Goerge, C. Y. Lin, M. R. D'Andrea, S. Stander and M. Steinhoff (2009). Role of matriptase and proteinase-activated receptor-2 in nonmelanoma skin cancer. *J Invest Dermatol* **129**(7): 1816-1823.

Boon, E. M., R. van der Neut, M. van de Wetering, H. Clevers and S. T. Pals (2002). Wnt signaling regulates expression of the receptor tyrosine kinase met in colorectal cancer. *Cancer Res* **62**(18): 5126-5128.

Borley, N. and M. R. Feneley (2009). Prostate cancer: diagnosis and staging. *Asian J Androl* **11**(1): 74-80.

Bostwick, D. G. and C. S. Foster (1999). Predictive factors in prostate cancer: current concepts from the 1999 College of American Pathologists Conference on Solid Tumor Prognostic Factors and the 1999 World Health Organization Second International Consultation on Prostate Cancer. *Semin Urol Oncol* **17**(4): 222-272.

Bottcher, E., T. Matrosovich, M. Beyerle, H. D. Klenk, W. Garten and M. Matrosovich (2006). Proteolytic activation of influenza viruses by serine proteases TMPRSS2 and HAT from human airway epithelium. *J Virol* **80**(19): 9896-9898.

Brabletz, T., A. Jung, S. Dag, F. Hlubek and T. Kirchner (1999). beta-catenin regulates the expression of the matrix metalloproteinase-7 in human colorectal cancer. *Am J Pathol* **155**(4): 1033-1038.

Bracarda, S., O. de Cobelli, C. Greco, T. Prayer-Galetti, R. Valdagni, G. Gatta, F. de Braud and G. Bartsch (2005). Cancer of the prostate. *Crit Rev Oncol Hematol* **56**(3): 379-396.

Bratt, O. (2002). Hereditary prostate cancer: clinical aspects. *J Urol* **168**(3): 906-913.

Bu, Q., H. M. Tang, J. Tan, X. Hu and D. W. Wang (2011). [Expression of RhoC and ROCK-1 and their effects on MAPK and Akt proteins in prostate carcinoma.]. *Zhonghua Zhong Liu Za Zhi* **33**(3): 202-206.

Bubendorf, L., A. Schopfer, U. Wagner, G. Sauter, H. Moch, N. Willi, T. C. Gasser and M. J. Mihatsch (2000). Metastatic patterns of prostate cancer: An autopsy study of 1,589 patients. *Human Pathology* **31**(5): 578-583.

Campbell, S. C. (1997). Advances in angiogenesis research: relevance to urological oncology. *J Urol* **158**(5): 1663-1674.

Canalis, E. (1980). Effect of insulinlike growth factor I on DNA and protein synthesis in cultured rat calvaria. *J Clin Invest* **66**(4): 709-719.

Cao, D. L. and X. D. Yao (2010). Advances in biomarkers for the early diagnosis of prostate cancer. *Chin J Cancer* **29**(2): 229-233.

Carmeliet, P. and R. K. Jain (2000). Angiogenesis in cancer and other diseases. *Nature* **407**(6801): 249-257.

Carter, H. B., J. D. Pearson, E. J. Metter, L. J. Brant, D. W. Chan, R. Andres, J. L. Fozard and P. C. Walsh (1992). Longitudinal evaluation of prostate-specific antigen levels in men with and without prostate disease. *JAMA* **267**(16): 2215-2220.

Carver, B. S., J. Tran, Z. Chen, A. Carracedo-Perez, A. Alimonti, C. Nardella, A. Gopalan, P. T. Scardino, C. Cordon-Cardo, W. Gerald and P. P. Pandolfi (2009). ETS rearrangements and prostate cancer initiation. *Nature* **457**(7231): E1; discussion E2-3.

Catalona, W. J., A. W. Partin, K. M. Slawin, M. K. Brawer, R. C. Flanigan, A. Patel, J. P. Richie, J. B. deKernion, P. C. Walsh, P. T. Scardino, P. H. Lange, E. N. Subong, R. E. Parson, G. H. Gasior, K. G. Loveland and P. C. Southwick (1998). Use of the percentage of free prostate-specific antigen to enhance differentiation of prostate cancer from benign prostatic disease: a prospective multicenter clinical trial. *JAMA* **279**(19): 1542-1547.

Catalona, W. J., J. P. Richie, F. R. Ahmann, M. A. Hudson, P. T. Scardino, R. C. Flanigan, J. B. deKernion, T. L. Ratliff, L. R. Kavoussi, B. L. Dalkin and et al. (1994). Comparison of digital rectal examination and serum prostate specific antigen in the early detection of prostate cancer: results of a multicenter clinical trial of 6,630 men. *J Urol* **151**(5): 1283-1290.

Chang, C. and Z. Werb (2001). The many faces of metalloproteases: cell growth, invasion, angiogenesis and metastasis. *Trends Cell Biol* **11**(11): S37-43.

Chen, J., S. De, J. Brainard and T. V. Byzova (2004). Metastatic properties of prostate cancer cells are controlled by VEGF. *Cell Commun Adhes* **11**(1): 1-11.

Chen, Z., Z. Fan, J. E. McNeal, R. Nolley, M. C. Caldwell, M. Mahadevappa, Z. Zhang, J. A. Warrington and T. A. Stamey (2003). Hepsin and maspin are inversely expressed in laser capture microdissectioned prostate cancer. *J Urol* **169**(4): 1316-1319.

Cheng, H., T. Fukushima, N. Takahashi, H. Tanaka and H. Kataoka (2009). Hepatocyte growth factor activator inhibitor type 1 regulates epithelial to mesenchymal transition through membrane-bound serine proteinases. *Cancer Res* **69**(5): 1828-1835.

Chesire, D. R., C. M. Ewing, W. R. Gage and W. B. Isaacs (2002). In vitro evidence for complex modes of nuclear beta-catenin signaling during prostate growth and tumorigenesis. *Oncogene* **21**(17): 2679-2694.

Chesire, D. R., C. M. Ewing, J. Sauvageot, G. S. Bova and W. B. Isaacs (2000). Detection and analysis of beta-catenin mutations in prostate cancer. *Prostate* **45**(4): 323-334.

Choi, S. Y., S. Bertram, I. Glowacka, Y. W. Park and S. Pohlmann (2009). Type II transmembrane serine proteases in cancer and viral infections. *Trends Mol Med* **15**(7): 303-312.

Chokki, M., S. Yamamura, H. Eguchi, T. Masegi, H. Horiuchi, H. Tanabe, T. Kamimura and S. Yasuoka (2004). Human airway trypsin-like protease increases mucin gene expression in airway epithelial cells. *Am J Respir Cell Mol Biol* **30**(4): 470-478.

Chung, D. C., S. B. Brown, F. Graeme-Cook, L. G. Tillotson, A. L. Warshaw, R. T. Jensen and A. Arnold (1998). Localization of putative tumor suppressor loci by

genome-wide allelotyping in human pancreatic endocrine tumors. *Cancer Res* **58**(16): 3706-3711.

Coluccia, A. M., D. Benati, H. Dekhil, A. De Filippo, C. Lan and C. Gambacorti-Passerini (2006). SKI-606 decreases growth and motility of colorectal cancer cells by preventing pp60(c-Src)-dependent tyrosine phosphorylation of beta-catenin and its nuclear signaling. *Cancer Res* **66**(4): 2279-2286.

Crawford, H. C., B. M. Fingleton, L. A. Rudolph-Owen, K. J. Goss, B. Rubinfeld, P. Polakis and L. M. Matrisian (1999). The metalloproteinase matrilysin is a target of beta-catenin transactivation in intestinal tumors. *Oncogene* **18**(18): 2883-2891.

Dai, J., Y. Kitagawa, J. Zhang, Z. Yao, A. Mizokami, S. Cheng, J. Nor, L. K. McCauley, R. S. Taichman and E. T. Keller (2004). Vascular endothelial growth factor contributes to the prostate cancer-induced osteoblast differentiation mediated by bone morphogenetic protein. *Cancer Res* **64**(3): 994-999.

Darragh, M. R., E. L. Schneider, J. Lou, P. J. Phojanakong, C. J. Farady, J. D. Marks, B. C. Hann and C. S. Craik (2010). Tumor detection by imaging proteolytic activity. *Cancer Res* **70**(4): 1505-1512.

David, L., J. J. Feige and S. Bailly (2009). Emerging role of bone morphogenetic proteins in angiogenesis. *Cytokine Growth Factor Rev* **20**(3): 203-212.

Dawelbait, G., C. Winter, Y. Zhang, C. Pilarsky, R. Grutzmann, J. C. Heinrich and M. Schroeder (2007). Structural templates predict novel protein interactions and targets from pancreas tumour gene expression data. *Bioinformatics* **23**(13): i115-124.

De Angelis, G., H. G. Rittenhouse, S. D. Mikolajczyk, L. Blair Shamel and A. Semjonow (2007). Twenty Years of PSA: From Prostate Antigen to Tumor Marker. *Rev Urol* **9**(3): 113-123.

de Klein, A., A. G. van Kessel, G. Grosveld, C. R. Bartram, A. Hagemeijer, D. Bootsma, N. K. Spurr, N. Heisterkamp, J. Groffen and J. R. Stephenson (1982). A cellular oncogene is translocated to the Philadelphia chromosome in chronic myelocytic leukaemia. *Nature* **300**(5894): 765-767.

de la Taille, A., M. A. Rubin, M. W. Chen, F. Vacherot, S. G. de Medina, M. Burchardt, R. Buttyan and D. Chopin (2003). Beta-catenin-related anomalies in apoptosis-resistant and hormone-refractory prostate cancer cells. *Clin Cancer Res* **9**(5): 1801-1807.

Del Rosso, M., G. Fibbi, M. Pucci, S. D'Alessio, A. Del Rosso, L. Magnelli and V. Chiarugi (2002). Multiple pathways of cell invasion are regulated by multiple families of serine proteases. *Clin Exp Metastasis* **19**(3): 193-207.

Denmeade, S. R. and J. T. Isaacs (2002). A history of prostate cancer treatment. *Nat Rev Cancer* **2**(5): 389-396.

Dhanasekaran, S. M., T. R. Barrette, D. Ghosh, R. Shah, S. Varambally, K. Kurachi, K. J. Pienta, M. A. Rubin and A. M. Chinnaiyan (2001). Delineation of prognostic biomarkers in prostate cancer. *Nature* **412**(6849): 822-826.

Du, X., E. She, T. Gelbart, J. Truksa, P. Lee, Y. Xia, K. Khovananth, S. Mudd, N. Mann, E. M. Moresco, E. Beutler and B. Beutler (2008). The serine protease TMPRSS6 is required to sense iron deficiency. *Science* **320**(5879): 1088-1092.

Ducy, P., M. Starbuck, M. Priemel, J. Shen, G. Pinero, V. Geoffroy, M. Amling and G. Karsenty (1999). A Cbfa1-dependent genetic pathway controls bone formation beyond embryonic development. *Genes Dev* **13**(8): 1025-1036.

Duque, J. L., K. R. Loughlin, R. M. Adam, P. W. Kantoff, D. Zurakowski and M. R. Freeman (1999). Plasma levels of vascular endothelial growth factor are increased in patients with metastatic prostate cancer. *Urology* **54**(3): 523-527.

Edwards, J., N. S. Krishna, K. M. Grigor and J. M. Bartlett (2003). Androgen receptor gene amplification and protein expression in hormone refractory prostate cancer. *Br J Cancer* **89**(3): 552-556.

Egeblad, M. and Z. Werb (2002). New functions for the matrix metalloproteinases in cancer progression. *Nat Rev Cancer* **2**(3): 161-174.

Elgamal, A. A., W. Van de Voorde, H. Van Poppel, J. Lauweryns and L. Baert (1994). Immunohistochemical localization of prostate-specific markers within the accessory male sex glands of Cowper, Littre, and Morgagni. *Urology* **44**(1): 84-90.

Engelhard, H. H., R. J. Homer, H. A. Duncan and J. Rozental (1998). Inhibitory effects of phenylbutyrate on the proliferation, morphology, migration and invasiveness of malignant glioma cells. *J Neurooncol* **37**(2): 97-108.

Erlebacher, A., E. H. Filvaroff, S. E. Gitelman and R. Derynck (1995). Toward a molecular understanding of skeletal development. *Cell* **80**(3): 371-378.

Esser, V., L. E. Limbird, M. S. Brown, J. L. Goldstein and D. W. Russell (1988). Mutational analysis of the ligand binding domain of the low density lipoprotein receptor. *J Biol Chem* **263**(26): 13282-13290.

Fan, A. (2002). Psychological and psychosocial effects of prostate cancer. *Nurs Stand* **17**(13): 33-37.

Ferrer, F. A., L. J. Miller, R. I. Andrawis, S. H. Kurtzman, P. C. Albertsen, V. P. Laudone and D. L. Kreutzer (1997). Vascular endothelial growth factor (VEGF) expression in human prostate cancer: in situ and in vitro expression of VEGF by human prostate cancer cells. *J Urol* **157**(6): 2329-2333.

Fizazi, K., J. Yang, S. Peleg, C. R. Sikes, E. L. Kreimann, D. Daliani, M. Olive, K. A. Raymond, T. J. Janus, C. J. Logothetis, G. Karsenty and N. M. Navone (2003). Prostate cancer cells-osteoblast interaction shifts expression of growth/survival-related genes in prostate cancer and reduces expression of osteoprotegerin in osteoblasts. *Clin Cancer Res* **9**(7): 2587-2597.

Folgueras, A. R., F. M. de Lara, A. M. Pendas, C. Garabaya, F. Rodriguez, A. Astudillo, T. Bernal, R. Cabanillas, C. Lopez-Otin and G. Velasco (2008). Membrane-bound serine protease matriptase-2 (Tmprss6) is an essential regulator of iron homeostasis. *Blood* **112**(6): 2539-2545.

Folkman, J. (1971). Tumor angiogenesis: therapeutic implications. *N Engl J Med* **285**(21): 1182-1186.

Foster, B. A., A. Evangelou, J. R. Gingrich, P. J. Kaplan, F. DeMayo and N. M. Greenberg (2002). Enforced expression of FGF-7 promotes epithelial hyperplasia whereas a dominant negative FGFR2iiib promotes the emergence of neuroendocrine phenotype in prostate glands of transgenic mice. *Differentiation* **70**(9-10): 624-632.

Foster, C. S. (1990). Predictive factors in prostatic hyperplasia and neoplasia. *Hum Pathol* **21**(6): 575-577.

Foster, C. S. and P. D. Abel (1992). Clinical and molecular techniques for diagnosis and monitoring of prostatic cancer. *Hum Pathol* **23**(4): 395-401.

Frixen, U. H., J. Behrens, M. Sachs, G. Eberle, B. Voss, A. Warda, D. Lochner and W. Birchmeier (1991). E-cadherin-mediated cell-cell adhesion prevents invasiveness of human carcinoma cells. *J Cell Biol* **113**(1): 173-185.

Galasko, C. S. (1986). Skeletal metastases. *Clin Orthop Relat Res*(210): 18-30.

Garnick, M. B. (1993). Prostate cancer: screening, diagnosis, and management. *Ann Intern Med* **118**(10): 804-818.

George, D. J., S. Halabi, T. F. Shepard, N. J. Vogelzang, D. F. Hayes, E. J. Small and P. W. Kantoff (2001). Prognostic significance of plasma vascular endothelial growth factor levels in patients with hormone-refractory prostate cancer treated on Cancer and Leukemia Group B 9480. *Clin Cancer Res* **7**(7): 1932-1936.

Gerstein, A. V., T. A. Almeida, G. Zhao, E. Chess, M. Shih Ie, K. Buhler, K. Pienta, M. A. Rubin, R. Vessella and N. Papadopoulos (2002). APC/CTNNB1 (beta-catenin) pathway alterations in human prostate cancers. *Genes Chromosomes Cancer* **34**(1): 9-16.

Gleason, D. F. and G. T. Mellinger (1974). Prediction of prognosis for prostatic adenocarcinoma by combined histological grading and clinical staging. *J Urol* **111**(1): 58-64.

Gleave, M., J. T. Hsieh, C. A. Gao, A. C. von Eschenbach and L. W. Chung (1991). Acceleration of human prostate cancer growth in vivo by factors produced by prostate and bone fibroblasts. *Cancer Res* **51**(14): 3753-3761.

Globus, R. K., P. Patterson-Buckendahl and D. Gospodarowicz (1988). Regulation of bovine bone cell proliferation by fibroblast growth factor and transforming growth factor beta. *Endocrinology* **123**(1): 98-105.

Gounari, F., S. Signoretti, R. Bronson, L. Klein, W. R. Sellers, J. Kum, A. Siermann, M. M. Taketo, H. von Boehmer and K. Khazaie (2002). Stabilization of beta-catenin induces lesions reminiscent of prostatic intraepithelial neoplasia, but terminal squamous transdifferentiation of other secretory epithelia. *Oncogene* **21**(26): 4099-4107.

Greene, F. L. and L. H. Sobin (2002). The TNM system: our language for cancer care. *J Surg Oncol* **80**(3): 119-120.

Grignon, D. J. (2004). Unusual subtypes of prostate cancer. *Mod Pathol* **17**(3): 316-327.

Hahner, S., M. Fassnacht, F. Hammer, M. Schammann, D. Weismann, I. A. Hansen and B. Allolio (2005). Evidence against a role of human airway trypsin-like protease--the human analogue of the growth-promoting rat adrenal secretory protease--in adrenal tumourigenesis. *Eur J Endocrinol* **152**(1): 143-153.

Han, B., R. Mehra, S. M. Dhanasekaran, J. Yu, A. Menon, R. J. Lonigro, X. Wang, Y. Gong, L. Wang, S. Shankar, B. Laxman, R. B. Shah, S. Varambally, N. Palanisamy, S. A. Tomlins, C. Kumar-Sinha and A. M. Chinnaiyan (2008). A fluorescence in situ hybridization screen for E26 transformation-specific aberrations: identification of DDX5-ETV4 fusion protein in prostate cancer. *Cancer Res* **68**(18): 7629-7637.

Hanahan, D. and J. Folkman (1996). Patterns and emerging mechanisms of the angiogenic switch during tumorigenesis. *Cell* **86**(3): 353-364.

Hansen, I. A., M. Fassnacht, S. Hahner, F. Hammer, M. Schammann, S. R. Meyer, A. B. Bicknell and B. Allolio (2004). The adrenal secretory serine protease AsP is a short secretory isoform of the transmembrane airway trypsin-like protease. *Endocrinology* **145**(4): 1898-1905.

Harper, M. E., E. Glynne-Jones, L. Goddard, V. J. Thurston and K. Griffiths (1996). Vascular endothelial growth factor (VEGF) expression in prostatic tumours and its relationship to neuroendocrine cells. *Br J Cancer* **74**(6): 910-916.

Hart, M., J. P. Concordet, I. Lassot, I. Albert, R. del los Santos, H. Durand, C. Perret, B. Rubinfeld, F. Margottin, R. Benarous and P. Polakis (1999). The F-box protein beta-TrCP associates with phosphorylated beta-catenin and regulates its activity in the cell. *Curr Biol* **9**(4): 207-210.

Hartikainen, J. M., H. Tuhkanen, V. Kataja, M. Eskelinen, M. Uusitupa, V. M. Kosma and A. Mannermaa (2006). Refinement of the 22q12-q13 breast cancer-- associated region: evidence of TMPRSS6 as a candidate gene in an eastern Finnish population. *Clin Cancer Res* **12**(5): 1454-1462.

Haseloff, J. and W. L. Gerlach (1988). Simple RNA enzymes with new and highly specific endoribonuclease activities. *Nature* **334**(6183): 585-591.

Hauschka, P. V., A. E. Mavrakos, M. D. Iafrati, S. E. Doleman and M. Klagsbrun (1986). Growth factors in bone matrix. Isolation of multiple types by affinity chromatography on heparin-Sepharose. *J Biol Chem* **261**(27): 12665-12674.

Hayama, M., Y. Okumura, E. Takahashi, A. Shimabukuro, M. Tamura, N. Takeda, T. Kubo and H. Kido (2007). Identification and analysis of the promoter region of the type II transmembrane serine protease polyserase-1 and its transcript variants. *Biol Chem* **388**(8): 853-858.

He, T. C., A. B. Sparks, C. Rago, H. Hermeking, L. Zawel, L. T. da Costa, P. J. Morin, B. Vogelstein and K. W. Kinzler (1998). Identification of c-MYC as a target of the APC pathway. *Science* **281**(5382): 1509-1512.

Heidenreich, A., G. Aus, M. Bolla, S. Joniau, V. B. Matveev, H. P. Schmid and F. Zattoni (2008). EAU guidelines on prostate cancer. *Eur Urol* **53**(1): 68-80.

Herter, S., D. E. Piper, W. Aaron, T. Gabriele, G. Cutler, P. Cao, A. S. Bhatt, Y. Choe, C. S. Craik, N. Walker, D. Meininger, T. Hoey and R. J. Austin (2005). Hepatocyte growth factor is a preferred in vitro substrate for human hepsin, a membrane-anchored serine protease implicated in prostate and ovarian cancers. *Biochem J* **390**(Pt 1): 125-136.

Hessels, D., F. P. Smit, G. W. Verhaegh, J. A. Witjes, E. B. Cornel and J. A. Schalken (2007). Detection of TMPRSS2-ERG fusion transcripts and prostate cancer antigen 3 in urinary sediments may improve diagnosis of prostate cancer. *Clin Cancer Res* **13**(17): 5103-5108.

Hirano, A., M. Emi, M. Tsuneizumi, Y. Utada, M. Yoshimoto, F. Kasumi, F. Akiyama, G. Sakamoto, S. Haga, T. Kajiwara and Y. Nakamura (2001). Allelic losses of loci at 3p25.1, 8p22, 13q12, 17p13.3, and 22q13 correlate with postoperative recurrence in breast cancer. *Clin Cancer Res* **7**(4): 876-882.

Holt, S. K., E. M. Kwon, D. W. Lin, E. A. Ostrander and J. L. Stanford (2010). Association of hepsin gene variants with prostate cancer risk and prognosis. *Prostate.*

Honda, M., M. Mori, H. Ueo, K. Sugimachi and T. Akiyoshi (1996). Matrix metalloproteinase-7 expression in gastric carcinoma. *Gut* **39**(3): 444-448.

Hong, S. M., A. Li, K. Olino, C. L. Wolfgang, J. M. Herman, R. D. Schulick, C. Iacobuzio-Donahue, R. H. Hruban and M. Goggins (2011). Loss of E-cadherin expression and outcome among patients with resectable pancreatic adenocarcinomas. *Mod Pathol.*

Hooper, J. D., L. Campagnolo, G. Goodarzi, T. N. Truong, H. Stuhlmann and J. P. Quigley (2003). Mouse matriptase-2: identification, characterization and comparative mRNA expression analysis with mouse hepsin in adult and embryonic tissues. *Biochem J* **373**(Pt 3): 689-702.

Hooper, J. D., J. A. Clements, J. P. Quigley and T. M. Antalis (2001). Type II transmembrane serine proteases. Insights into an emerging class of cell surface proteolytic enzymes. *J Biol Chem* **276**(2): 857-860.

Hooper, J. D., A. L. Scarman, B. E. Clarke, J. F. Normyle and T. M. Antalis (2000). Localization of the mosaic transmembrane serine protease corin to heart myocytes. *Eur J Biochem* **267**(23): 6931-6937.

Huang, H. C., S. Zheng, V. VanBuren and Z. Zhao (2010). Discovering disease-specific biomarker genes for cancer diagnosis and prognosis. *Technol Cancer Res Treat* **9**(3): 219-230.

Huang, W. and M. Waknitz (2009). ETS gene fusions and prostate cancer. *Am J Transl Res* **1**(4): 341-351.

Huang, Y., W. Li, D. Chu, J. Zheng, G. Ji, M. Li, H. Zhang, W. Wang, J. Du and J. Li (2011). Overexpression of Matrix Metalloproteinase-21 is Associated with Poor Overall Survival of Patients with Colorectal Cancer. *J Gastrointest Surg*.

Hudes, G. R., F. Nathan, C. Khater, N. Haas, M. Cornfield, B. Giantonio, R. Greenberg, L. Gomella, S. Litwin, E. Ross, S. Roethke and C. McAleer (1997). Phase II trial of 96-hour paclitaxel plus oral estramustine phosphate in metastatic hormone-refractory prostate cancer. *J Clin Oncol* **15**(9): 3156-3163.

Hudson, D. L. (2004). Epithelial stem cells in human prostate growth and disease. *Prostate Cancer Prostatic Dis* **7**(3): 188-194.

Humphrey, P. A. (2004). Gleason grading and prognostic factors in carcinoma of the prostate. *Mod Pathol* **17**(3): 292-306.

Huppi, K. and G. V. Chandramouli (2004). Molecular profiling of prostate cancer. *Curr Urol Rep* **5**(1): 45-51.

Hwang, C. and E. I. Heath (2010). Angiogenesis inhibitors in the treatment of prostate cancer. *J Hematol Oncol* **3**: 26.

Ibrahim, T., E. Flamini, L. Mercatali, E. Sacanna, P. Serra and D. Amadori (2010). Pathogenesis of osteoblastic bone metastases from prostate cancer. *Cancer* **116**(6): 1406-1418.

Iiizumi, M., S. Bandyopadhyay, S. K. Pai, M. Watabe, S. Hirota, S. Hosobe, T. Tsukada, K. Miura, K. Saito, E. Furuta, W. Liu, F. Xing, H. Okuda, A. Kobayashi and K. Watabe (2008). RhoC promotes metastasis via activation of the Pyk2 pathway in prostate cancer. *Cancer Res* **68**(18): 7613-7620.

Iwakiri, K., M. Ghazizadeh, E. Jin, M. Fujiwara, T. Takemura, S. Takezaki, S. Kawana, S. Yasuoka and O. Kawanami (2004). Human airway trypsin-like protease induces PAR-2-mediated IL-8 release in psoriasis vulgaris. *J Invest Dermatol* **122**(4): 937-944.

Jarzab, B., M. Wiench, K. Fujarewicz, K. Simek, M. Jarzab, M. Oczko-Wojciechowska, J. Wloch, A. Czarniecka, E. Chmielik, D. Lange, A. Pawlaczek, S. Szpak, E. Gubala and A. Swierniak (2005). Gene expression profile of papillary thyroid cancer: sources of variability and diagnostic implications. *Cancer Res* **65**(4): 1587-1597.

Jiang, W. G., T. A. Martin, K. Matsumoto, T. Nakamura and R. E. Mansel (1999). Hepatocyte growth factor/scatter factor decreases the expression of occludin and

transendothelial resistance (TER) and increases paracellular permeability in human vascular endothelial cells. *J Cell Physiol* **181**(2): 319-329.

Jin, J. S., D. S. Hsieh, S. H. Loh, A. Chen, C. W. Yao and C. Y. Yen (2006). Increasing expression of serine protease matriptase in ovarian tumors: tissue microarray analysis of immunostaining score with clinicopathological parameters. *Mod Pathol* **19**(3): 447-452.

Jin, X., M. Yagi, N. Akiyama, T. Hirosaki, S. Higashi, C. Y. Lin, R. B. Dickson, H. Kitamura and K. Miyazaki (2006). Matriptase activates stromelysin (MMP-3) and promotes tumor growth and angiogenesis. *Cancer Sci* **97**(12): 1327-1334.

Jung, H., K. P. Lee, S. J. Park, J. H. Park, Y. S. Jang, S. Y. Choi, J. G. Jung, K. Jo, D. Y. Park, J. H. Yoon, D. S. Lim, G. R. Hong, C. Choi, Y. K. Park, J. W. Lee, H. J. Hong, S. Kim and Y. W. Park (2008). TMPRSS4 promotes invasion, migration and metastasis of human tumor cells by facilitating an epithelial-mesenchymal transition. *Oncogene* **27**(18): 2635-2647.

Jung, K., M. Lein, C. Stephan, K. Von Hosslin, A. Semjonow, P. Sinha, S. A. Loening and D. Schnorr (2004). Comparison of 10 serum bone turnover markers in prostate carcinoma patients with bone metastatic spread: diagnostic and prognostic implications. *Int J Cancer* **111**(5): 783-791.

Kebebew, E., M. Peng, E. Reiff, Q. Y. Duh, O. H. Clark and A. McMillan (2005). ECM1 and TMPRSS4 are diagnostic markers of malignant thyroid neoplasms and improve the accuracy of fine needle aspiration biopsy. *Ann Surg* **242**(3): 353-361; discussion 361-353.

Kebebew, E., M. Peng, E. Reiff and A. McMillan (2006). Diagnostic and extent of disease multigene assay for malignant thyroid neoplasms. *Cancer* **106**(12): 2592-2597.

Kim, S., H. Y. Kang, E. H. Nam, M. S. Choi, X. F. Zhao, C. S. Hong, J. W. Lee, J. H. Lee and Y. K. Park (2010). TMPRSS4 induces invasion and epithelial-mesenchymal transition through upregulation of integrin alpha5 and its signaling pathways. *Carcinogenesis* **31**(4): 597-606.

Kim, T. S., C. Heinlein, R. C. Hackman and P. S. Nelson (2006). Phenotypic analysis of mice lacking the Tmprss2-encoded protease. *Mol Cell Biol* **26**(3): 965-975.

Kirby, R. S., J. M. Fitzpatrick and N. Clarke (2009). Abarelix and other gonadotrophin-releasing hormone antagonists in prostate cancer. *BJU Int* **104**(11): 1580-1584.

Klezovitch, O., J. Chevillet, J. Mirosevich, R. L. Roberts, R. J. Matusik and V. Vasioukhin (2004). Hepsin promotes prostate cancer progression and metastasis. *Cancer Cell* **6**(2): 185-195.

Kobel, M., S. E. Kalloger, N. Boyd, S. McKinney, E. Mehl, C. Palmer, S. Leung, N. J. Bowen, D. N. Ionescu, A. Rajput, L. M. Prentice, D. Miller, J. Santos, K. Swenerton, C. B. Gilks and D. Huntsman (2008). Ovarian carcinoma subtypes are different diseases: implications for biomarker studies. *PLoS Med* **5**(12): e232.

Krishnan, V., H. U. Bryant and O. A. Macdougald (2006). Regulation of bone mass by Wnt signaling. *J Clin Invest* **116**(5): 1202-1209.

Lai, Y., B. Wu, L. Chen and H. Zhao (2004). A statistical method for identifying differential gene-gene co-expression patterns. *Bioinformatics* **20**(17): 3146-3155.

Lang, J. C. and D. E. Schuller (2001). Differential expression of a novel serine protease homologue in squamous cell carcinoma of the head and neck. *Br J Cancer* **84**(2): 237-243.

Laxman, B., S. A. Tomlins, R. Mehra, D. S. Morris, L. Wang, B. E. Helgeson, R. B. Shah, M. A. Rubin, J. T. Wei and A. M. Chinnaiyan (2006). Noninvasive detection of TMPRSS2:ERG fusion transcripts in the urine of men with prostate cancer. *Neoplasia* **8**(10): 885-888.

Lee, J. W., S. Yong Song, J. J. Choi, S. J. Lee, B. G. Kim, C. S. Park, J. H. Lee, C. Y. Lin, R. B. Dickson and D. S. Bae (2005). Increased expression of matriptase is associated with histopathologic grades of cervical neoplasia. *Hum Pathol* **36**(6): 626-633.

Lee, S. L., R. B. Dickson and C. Y. Lin (2000). Activation of hepatocyte growth factor and urokinase/plasminogen activator by matriptase, an epithelial membrane serine protease. *J Biol Chem* **275**(47): 36720-36725.

Leman, E. S., A. Magheli, K. M. Yong, G. Netto, S. Hinz and R. H. Getzenberg (2009). Identification of nuclear structural protein alterations associated with seminomas. *J Cell Biochem* **108**(6): 1274-1279.

Lenoir, A., J. C. Deschemin, L. Kautz, A. J. Ramsay, M. P. Roth, C. Lopez-Otin, S. Vaulont and G. Nicolas (2010). Iron deficiency anemia due to matriptase-2 inactivation is dependent upon the presence of functional Bmp6. *Blood*.

Leytus, S. P., K. R. Loeb, F. S. Hagen, K. Kurachi and E. W. Davie (1988). A novel trypsin-like serine protease (hepsin) with a putative transmembrane domain expressed by human liver and hepatoma cells. *Biochemistry* **27**(3): 1067-1074.

Li, W., B. E. Wang, P. Moran, T. Lipari, R. Ganesan, R. Corpuz, M. J. Ludlam, A. Gogineni, H. Koeppen, S. Bunting, W. Q. Gao and D. Kirchhofer (2009). Pegylated kunitz domain inhibitor suppresses hepsin-mediated invasive tumor growth and metastasis. *Cancer Res* **69**(21): 8395-8402.

Lin, C. Y., J. Anders, M. Johnson and R. B. Dickson (1999). Purification and characterization of a complex containing matriptase and a Kunitz-type serine protease inhibitor from human milk. *J Biol Chem* **274**(26): 18237-18242.

Lin, C. Y., J. Anders, M. Johnson, Q. A. Sang and R. B. Dickson (1999). Molecular cloning of cDNA for matriptase, a matrix-degrading serine protease with trypsin-like activity. *J Biol Chem* **274**(26): 18231-18236.

Lin, C. Y., J. K. Wang, J. Torri, L. Dou, Q. A. Sang and R. B. Dickson (1997). Characterization of a novel, membrane-bound, 80-kDa matrix-degrading protease from human breast cancer cells. Monoclonal antibody production, isolation, and localization. *J Biol Chem* **272**(14): 9147-9152.

List, K., R. Szabo, A. Molinolo, V. Sriuranpong, V. Redeye, T. Murdock, B. Burke, B. S. Nielsen, J. S. Gutkind and T. H. Bugge (2005). Deregulated matriptase causes ras-independent multistage carcinogenesis and promotes ras-mediated malignant transformation. *Genes Dev* **19**(16): 1934-1950.

Littrup, P. J. and A. C. Goodman (1994). Costs and benefits of prostate cancer screening. Investigators of the American Cancer Society--National Prostate Cancer Detection Project. *In Vivo* **8**(3): 423-427.

Liu, T., A. J. DeCostanzo, X. Liu, H. Wang, S. Hallagan, R. T. Moon and C. C. Malbon (2001). G protein signaling from activated rat frizzled-1 to the beta-catenin-Lef-Tcf pathway. *Science* **292**(5522): 1718-1722.

Logothetis, C. J. and S. H. Lin (2005). Osteoblasts in prostate cancer metastasis to bone. *Nat Rev Cancer* **5**(1): 21-28.

Lopez-Otin, C. and L. M. Matrisian (2007). Emerging roles of proteases in tumour suppression. *Nat Rev Cancer* **7**(10): 800-808.

Los, M. and E. E. Voest (2001). The potential role of antivascular therapy in the adjuvant and neoadjuvant treatment of cancer. *Semin Oncol* **28**(1): 93-105.

Louvard, D., S. Maroux, J. Baratti and P. Desnuelle (1973). On the distribution of enterokinase in porcine intestine and on its subcellular localization. *Biochim Biophys Acta* **309**(1): 127-137.

Luo, J., D. J. Duggan, Y. Chen, J. Sauvageot, C. M. Ewing, M. L. Bittner, J. M. Trent and W. B. Isaacs (2001). Human prostate cancer and benign prostatic hyperplasia: molecular dissection by gene expression profiling. *Cancer Res* **61**(12): 4683-4688.

Lytton, B. (2001). Prostate cancer: a brief history and the discovery of hormonal ablation treatment. *J Urol* **165**(6 Pt 1): 1859-1862.

Maestracci, D., H. Preiser, T. Hedges, J. Schmitz and R. K. Crane (1975). Enzymes of the human intestinal brush border membrane. Identification after gel electrophoretic separation. *Biochim Biophys Acta* **382**(2): 147-156.

Magee, J. A., T. Araki, S. Patil, T. Ehrig, L. True, P. A. Humphrey, W. J. Catalona, M. A. Watson and J. Milbrandt (2001). Expression profiling reveals hepsin overexpression in prostate cancer. *Cancer Res* **61**(15): 5692-5696.

Matsuo, T., K. Nakamura, N. Takamoto, J. Kodama, A. Hongo, F. Abrzua, Y. Nasu, H. Kumon and Y. Hiramatsu (2008). Expression of the serine protease hepsin and clinical outcome of human endometrial cancer. *Anticancer Res* **28**(1A): 159-164.

Matsushima, R., A. Takahashi, Y. Nakaya, H. Maezawa, M. Miki, Y. Nakamura, F. Ohgushi and S. Yasuoka (2006). Human airway trypsin-like protease stimulates human bronchial fibroblast proliferation in a protease-activated receptor-2-dependent pathway. *Am J Physiol Lung Cell Mol Physiol* **290**(2): L385-395.

Maurer, E., M. T. Sisay, M. Stirnberg, T. Steinmetzer, J. Bajorath and M. Gutschow (2011). Insights into Matriptase-2 Substrate Binding and Inhibition Mechanisms by Analyzing Active-Site-Mutated Variants. *ChemMedChem*.

McNeal, J. E. (1969). Origin and development of carcinoma in the prostate. *Cancer* **23**(1): 24-34.

McNeal, J. E. (1981). Normal and pathologic anatomy of prostate. *Urology* **17**(Suppl 3): 11-16.

McNeal, J. E. (1981). The zonal anatomy of the prostate. *Prostate* **2**(1): 35-49.

McNeal, J. E., D. G. Bostwick, R. A. Kindrachuk, E. A. Redwine, F. S. Freiha and T. A. Stamey (1986). Patterns of progression in prostate cancer. *Lancet* **1**(8472): 60-63.

McQuibban, G. A., J. H. Gong, J. P. Wong, J. L. Wallace, I. Clark-Lewis and C. M. Overall (2002). Matrix metalloproteinase processing of monocyte chemoattractant proteins generates CC chemokine receptor antagonists with anti-inflammatory properties in vivo. *Blood* **100**(4): 1160-1167.

Meynard, D., V. Vaja, C. C. Sun, E. Corradini, S. Chen, C. Lopez-Otin, L. Grgurevic, C. C. Hong, M. Stirnberg, M. Gutschow, S. Vukicevic, J. L. Babitt and H. Y. Lin (2011). Regulation of TMPRSS6 by BMP6 and iron in human cells and mice. *Blood*.

Miki, M., Y. Nakamura, A. Takahashi, Y. Nakaya, H. Eguchi, T. Masegi, K. Yoneda, S. Yasuoka and S. Sone (2003). Effect of human airway trypsin-like protease on intracellular free Ca2+ concentration in human bronchial epithelial cells. *J Med Invest* **50**(1-2): 95-107.

Miyakawa, A., X. L. Wang, H. Nakanishi, F. L. Imai, M. Shiiba, T. Miya, Y. Imai and H. Tanzawa (1998). Allelic loss on chromosome 22 in oral cancer: possibility of the existence of a tumor suppressor gene on 22q13. *Int J Oncol* **13**(4): 705-709.

Miyake, Y., S. Tsuzuki, T. Fushiki and K. Inouye (2010). Matriptase does not require hepatocyte growth factor activator inhibitor type-1 for activation in an epithelial cell expression model. *Biosci Biotechnol Biochem* **74**(4): 848-850.

Moran, P., W. Li, B. Fan, R. Vij, C. Eigenbrot and D. Kirchhofer (2006). Pro-urokinase-type plasminogen activator is a substrate for hepsin. *J Biol Chem* **281**(41): 30439-30446.

Mori, M., G. F. Barnard, K. Mimori, H. Ueo, T. Akiyoshi and K. Sugimachi (1995). Overexpression of matrix metalloproteinase-7 mRNA in human colon carcinomas. *Cancer* **75**(6 Suppl): 1516-1519.

Morin, P. J. (1999). beta-catenin signaling and cancer. *Bioessays* **21**(12): 1021-1030.

Morrissey, C., L. D. True, M. P. Roudier, I. M. Coleman, S. Hawley, P. S. Nelson, R. Coleman, Y. C. Wang, E. Corey, P. H. Lange, C. S. Higano and R. L. Vessella (2008). Differential expression of angiogenesis associated genes in prostate cancer bone, liver and lymph node metastases. *Clin Exp Metastasis* **25**(4): 377-388.

Mulholland, D. J., H. Cheng, K. Reid, P. S. Rennie and C. C. Nelson (2002). The androgen receptor can promote beta-catenin nuclear translocation independently of adenomatous polyposis coli. *J Biol Chem* **277**(20): 17933-17943.

Netzel-Arnett, S., J. D. Hooper, R. Szabo, E. L. Madison, J. P. Quigley, T. H. Bugge and T. M. Antalis (2003). Membrane anchored serine proteases: a rapidly expanding group of cell surface proteolytic enzymes with potential roles in cancer. *Cancer Metastasis Rev* **22**(2-3): 237-258.

Noel, A., C. Maillard, N. Rocks, M. Jost, V. Chabottaux, N. E. Sounni, E. Maquoi, D. Cataldo and J. M. Foidart (2004). Membrane associated proteases and their inhibitors in tumour angiogenesis. *J Clin Pathol* **57**(6): 577-584.

Oberst, M., J. Anders, B. Xie, B. Singh, M. Ossandon, M. Johnson, R. B. Dickson and C. Y. Lin (2001). Matriptase and HAI-1 are expressed by normal and malignant epithelial cells in vitro and in vivo. *Am J Pathol* **158**(4): 1301-1311.

Oberst, M. D., M. D. Johnson, R. B. Dickson, C. Y. Lin, B. Singh, M. Stewart, A. Williams, A. al-Nafussi, J. F. Smyth, H. Gabra and G. C. Sellar (2002). Expression of the serine protease matriptase and its inhibitor HAI-1 in epithelial ovarian cancer: correlation with clinical outcome and tumor clinicopathological parameters. *Clin Cancer Res* **8**(4): 1101-1107.

Oberst, M. D., B. Singh, M. Ozdemirli, R. B. Dickson, M. D. Johnson and C. Y. Lin (2003). Characterization of matriptase expression in normal human tissues. *J Histochem Cytochem* **51**(8): 1017-1025.

Oberst, M. D., C. A. Williams, R. B. Dickson, M. D. Johnson and C. Y. Lin (2003). The activation of matriptase requires its noncatalytic domains, serine protease domain, and its cognate inhibitor. *J Biol Chem* **278**(29): 26773-26779.

Odet, F., A. Verot and B. Le Magueresse-Battistoni (2006). The mouse testis is the source of various serine proteases and serine proteinase inhibitors (SERPINs):

Serine proteases and SERPINs identified in Leydig cells are under gonadotropin regulation. *Endocrinology* **147**(9): 4374-4383.

Oesterling, J. E., S. J. Jacobsen, C. G. Chute, H. A. Guess, C. J. Girman, L. A. Panser and M. M. Lieber (1993). Serum prostate-specific antigen in a community-based population of healthy men. Establishment of age-specific reference ranges. *JAMA* **270**(7): 860-864.

Ohori, M., J. K. Dunn and P. T. Scardino (1995). Is prostate-specific antigen density more useful than prostate-specific antigen levels in the diagnosis of prostate cancer? *Urology* **46**(5): 666-671.

Overall, C. M. and C. Lopez-Otin (2002). Strategies for MMP inhibition in cancer: innovations for the post-trial era. *Nat Rev Cancer* **2**(9): 657-672.

Overall, C. M., E. M. Tam, R. Kappelhoff, A. Connor, T. Ewart, C. J. Morrison, X. Puente, C. Lopez-Otin and A. Seth (2004). Protease degradomics: mass spectrometry discovery of protease substrates and the CLIP-CHIP, a dedicated DNA microarray of all human proteases and inhibitors. *Biol Chem* **385**(6): 493-504.

Owen, K. A., D. Qiu, J. Alves, A. M. Schumacher, L. M. Kilpatrick, J. Li, J. L. Harris and V. Ellis (2010). Pericellular activation of hepatocyte growth factor by the transmembrane serine proteases matriptase and hepsin, but not by the membrane-associated protease uPA. *Biochem J* **426**(2): 219-228.

Oxford, G. and D. Theodorescu (2003). Ras superfamily monomeric G proteins in carcinoma cell motility. *Cancer Lett* **189**(2): 117-128.

Paget, S. (1889). The distribution of secondary growths of cancer of the breast. *The Lancet* **133**(3421): 571-573.

Paget, S. (1989). The distribution of secondary growths in cancer of the breast. 1889. *Cancer Metastasis Rev* **8**(2): 98-101.

Paoloni-Giacobino, A., H. Chen, M. C. Peitsch, C. Rossier and S. E. Antonarakis (1997). Cloning of the TMPRSS2 gene, which encodes a novel serine protease with transmembrane, LDLRA, and SRCR domains and maps to 21q22.3. *Genomics* **44**(3): 309-320.

Parekh, D. J., D. P. Ankerst, D. Troyer, S. Srivastava and I. M. Thompson (2007). Biomarkers for prostate cancer detection. *J Urol* **178**(6): 2252-2259.

Parr, C., A. J. Sanders, G. Davies, T. Martin, J. Lane, M. D. Mason, R. E. Mansel and W. G. Jiang (2007). Matriptase-2 inhibits breast tumor growth and invasion and correlates with favorable prognosis for breast cancer patients. *Clin Cancer Res* **13**(12): 3568-3576.

Peehl, D. M. (2005). Primary cell cultures as models of prostate cancer development. *Endocr Relat Cancer* **12**(1): 19-47.

Pepper, M. S. (2001). Role of the matrix metalloproteinase and plasminogen activator-plasmin systems in angiogenesis. *Arterioscler Thromb Vasc Biol* **21**(7): 1104-1117.

Petrovics, G., A. Liu, S. Shaheduzzaman, B. Furusato, C. Sun, Y. Chen, M. Nau, L. Ravindranath, A. Dobi, V. Srikantan, I. A. Sesterhenn, D. G. McLeod, M. Vahey, J. W. Moul and S. Srivastava (2005). Frequent overexpression of ETS-related gene-1 (ERG1) in prostate cancer transcriptome. *Oncogene* **24**(23): 3847-3852.

Pienta, K. J., B. Redman, M. Hussain, G. Cummings, P. S. Esper, C. Appel and L. E. Flaherty (1994). Phase II evaluation of oral estramustine and oral etoposide in

hormone-refractory adenocarcinoma of the prostate. *J Clin Oncol* 12(10): 2005-2012.

Qiu, D., K. Owen, K. Gray, R. Bass and V. Ellis (2007). Roles and regulation of membrane-associated serine proteases. *Biochem Soc Trans* 35(Pt 3): 583-587.

Rabbitts, T. H. (1994). Chromosomal translocations in human cancer. *Nature* 372(6502): 143-149.

Ramsay, A. J., V. Quesada, M. Sanchez, C. Garabaya, M. P. Sarda, M. Baiget, A. Remacha, G. Velasco and C. Lopez-Otin (2009). Matriptase-2 mutations in iron-refractory iron deficiency anemia patients provide new insights into protease activation mechanisms. *Hum Mol Genet* 18(19): 3673-3683.

Rawlings, N. D. and A. J. Barrett (1994). Families of serine peptidases. *Methods Enzymol* 244: 19-61.

Rhodes, D. R., T. R. Barrette, M. A. Rubin, D. Ghosh and A. M. Chinnaiyan (2002). Meta-analysis of microarrays: interstudy validation of gene expression profiles reveals pathway dysregulation in prostate cancer. *Cancer Res* 62(15): 4427-4433.

Rice, K. R., Y. Chen, A. Ali, E. J. Whitman, A. Blase, M. Ibrahim, S. Elsamanoudi, S. Brassell, B. Furusato, N. Stingle, I. A. Sesterhenn, G. Petrovics, S. Miick, H. Rittenhouse, J. Groskopf, D. G. McLeod and S. Srivastava (2010). Evaluation of the ETS-related gene mRNA in urine for the detection of prostate cancer. *Clin Cancer Res* 16(5): 1572-1576.

Rifkin, D. B., R. Mazzieri, J. S. Munger, I. Noguera and J. Sung (1999). Proteolytic control of growth factor availability. *APMIS* 107(1): 80-85.

Riker, A. I., S. A. Enkemann, O. Fodstad, S. Liu, S. Ren, C. Morris, Y. Xi, P. Howell, B. Metge, R. S. Samant, L. A. Shevde, W. Li, S. Eschrich, A. Daud, J. Ju and J. Matta (2008). The gene expression profiles of primary and metastatic melanoma yields a transition point of tumor progression and metastasis. *BMC Med Genomics* 1: 13.

Robey, P. G., N. S. Fedarko, T. E. Hefferan, P. Bianco, U. K. Vetter, W. Grzesik, A. Friedenstein, G. Van der Pluijm, K. P. Mintz, M. F. Young and et al. (1993). Structure and molecular regulation of bone matrix proteins. *J Bone Miner Res* 8 Suppl 2: S483-487.

Robinson, V. L., E. C. Kauffman, M. H. Sokoloff and C. W. Rinker-Schaeffer (2004). The basic biology of metastasis. *Cancer Treat Res* 118: 1-21.

Rosen, E. M., W. Carley and I. D. Goldberg (1990). Scatter factor regulates vascular endothelial cell motility. *Cancer Invest* 8(6): 647-650.

Rowley, J. D. (1973). Letter: A new consistent chromosomal abnormality in chronic myelogenous leukaemia identified by quinacrine fluorescence and Giemsa staining. *Nature* 243(5405): 290-293.

Saharinen, P., L. Eklund, K. Pulkki, P. Bono and K. Alitalo (2011). VEGF and angiopoietin signaling in tumor angiogenesis and metastasis. *Trends Mol Med.*

Sakr, W. A., D. J. Grignon, G. P. Haas, L. K. Heilbrun, J. E. Pontes and J. D. Crissman (1996). Age and racial distribution of prostatic intraepithelial neoplasia. *Eur Urol* 30(2): 138-144.

Samson, D. J., J. Seidenfeld, B. Schmitt, V. Hasselblad, P. C. Albertsen, C. L. Bennett, T. J. Wilt and N. Aronson (2002). Systematic review and meta-analysis of monotherapy compared with combined androgen blockade for patients with advanced prostate carcinoma. *Cancer* 95(2): 361-376.

Sanders, A. J., C. Parr, G. Davies, T. A. Martin, J. Lane, M. D. Mason and W. G. Jiang (2006). Genetic reduction of matriptase-1 expression is associated with a reduction in the aggressive phenotype of prostate cancer cells in vitro and in vivo. *J Exp Ther Oncol* **6**(1): 39-48.

Sanders, A. J., C. Parr, T. A. Martin, J. Lane, M. D. Mason and W. G. Jiang (2008). Genetic upregulation of matriptase-2 reduces the aggressiveness of prostate cancer cells in vitro and in vivo and affects FAK and paxillin localisation. *J Cell Physiol* **216**(3): 780-789.

Sardana, G., B. Dowell and E. P. Diamandis (2008). Emerging biomarkers for the diagnosis and prognosis of prostate cancer. *Clin Chem* **54**(12): 1951-1960.

Savarese, D. M., S. Halabi, V. Hars, W. L. Akerley, M. E. Taplin, P. A. Godley, A. Hussain, E. J. Small and N. J. Vogelzang (2001). Phase II study of docetaxel, estramustine, and low-dose hydrocortisone in men with hormone-refractory prostate cancer: a final report of CALGB 9780. Cancer and Leukemia Group B. *J Clin Oncol* **19**(9): 2509-2516.

Sawasaki, T., K. Shigemasa, L. Gu, J. B. Beard and T. J. O'Brien (2004). The transmembrane protease serine (TMPRSS3/TADG-12) D variant: a potential candidate for diagnosis and therapeutic intervention in ovarian cancer. *Tumour Biol* **25**(3): 141-148.

Scharpfenecker, M., M. van Dinther, Z. Liu, R. L. van Bezooijen, Q. Zhao, L. Pukac, C. W. Lowik and P. ten Dijke (2007). BMP-9 signals via ALK1 and inhibits bFGF-induced endothelial cell proliferation and VEGF-stimulated angiogenesis. *J Cell Sci* **120**(Pt 6): 964-972.

Scheble, V. J., M. Braun, R. Beroukhim, C. H. Mermel, C. Ruiz, T. Wilbertz, A. C. Stiedl, K. Petersen, M. Reischl, R. Kuefer, D. Schilling, F. Fend, G. Kristiansen, M. Meyerson, M. A. Rubin, L. Bubendorf and S. Perner (2010). ERG rearrangement is specific to prostate cancer and does not occur in any other common tumor. *Mod Pathol*.

Scott, H. S., J. Kudoh, M. Wattenhofer, K. Shibuya, A. Berry, R. Chrast, M. Guipponi, J. Wang, K. Kawasaki, S. Asakawa, S. Minoshima, F. Younus, S. Q. Mehdi, U. Radhakrishna, M. P. Papasavvas, C. Gehrig, C. Rossier, M. Korostishevsky, A. Gal, N. Shimizu, B. Bonne-Tamir and S. E. Antonarakis (2001). Insertion of beta-satellite repeats identifies a transmembrane protease causing both congenital and childhood onset autosomal recessive deafness. *Nat Genet* **27**(1): 59-63.

Sedghizadeh, P. P., S. R. Mallery, S. J. Thompson, L. Kresty, F. M. Beck, E. K. Parkinson, J. Biancamano and J. C. Lang (2006). Expression of the serine protease DESC1 correlates directly with normal keratinocyte differentiation and inversely with head and neck squamous cell carcinoma progression. *Head Neck* **28**(5): 432-440.

Sella, A., R. Kilbourn, R. Amato, C. Bui, A. A. Zukiwski, J. Ellerhorst and C. J. Logothetis (1994). Phase II study of ketoconazole combined with weekly doxorubicin in patients with androgen-independent prostate cancer. *J Clin Oncol* **12**(4): 683-688.

Sequeira, L., C. W. Dubyk, T. A. Riesenberger, C. R. Cooper and K. L. van Golen (2008). Rho GTPases in PC-3 prostate cancer cell morphology, invasion and tumor cell diapedesis. *Clin Exp Metastasis* **25**(5): 569-579.

Seth, A. and D. K. Watson (2005). ETS transcription factors and their emerging roles in human cancer. *Eur J Cancer* **41**(16): 2462-2478.

Shariat, S. F., M. Shalev, A. Menesses-Diaz, I. Y. Kim, M. W. Kattan, T. M. Wheeler and K. M. Slawin (2001). Preoperative plasma levels of transforming growth factor beta(1) (TGF-beta(1)) strongly predict progression in patients undergoing radical prostatectomy. *J Clin Oncol* **19**(11): 2856-2864.

Shi, Y. E., J. Torri, L. Yieh, A. Wellstein, M. E. Lippman and R. B. Dickson (1993). Identification and characterization of a novel matrix-degrading protease from hormone-dependent human breast cancer cells. *Cancer Res* **53**(6): 1409-1415.

Silvestri, L., A. Pagani, A. Nai, I. De Domenico, J. Kaplan and C. Camaschella (2008). The serine protease matriptase-2 (TMPRSS6) inhibits hepcidin activation by cleaving membrane hemojuvelin. *Cell Metab* **8**(6): 502-511.

Smith, D. S. and W. J. Catalona (1995). Interexaminer variability of digital rectal examination in detecting prostate cancer. *Urology* **45**(1): 70-74.

Smith, L. L., H. A. Coller and J. M. Roberts (2003). Telomerase modulates expression of growth-controlling genes and enhances cell proliferation. *Nat Cell Biol* **5**(5): 474-479.

Stamey, T. A., J. A. Warrington, M. C. Caldwell, Z. Chen, Z. Fan, M. Mahadevappa, J. E. McNeal, R. Nolley and Z. Zhang (2001). Molecular genetic profiling of Gleason grade 4/5 prostate cancers compared to benign prostatic hyperplasia. *J Urol* **166**(6): 2171-2177.

Stirnberg, M., E. Maurer, A. Horstmeyer, S. Kolp, S. Frank, T. Bald, K. Arenz, A. Janzer, K. Prager, P. Wunderlich, J. Walter and M. Gutschow (2010). Proteolytic processing of the serine protease matriptase-2: identification of the cleavage sites required for its autocatalytic release from the cell surface. *Biochem J* **430**(1): 87-95.

Szabo, R. and T. H. Bugge (2008). Type II transmembrane serine proteases in development and disease. *Int J Biochem Cell Biol* **40**(6-7): 1297-1316.

Szabo, R., S. Netzel-Arnett, J. P. Hobson, T. M. Antalis and T. H. Bugge (2005). Matriptase-3 is a novel phylogenetically preserved membrane-anchored serine protease with broad serpin reactivity. *Biochem J* **390**(Pt 1): 231-242.

Szabo, R., Q. Wu, R. B. Dickson, S. Netzel-Arnett, T. M. Antalis and T. H. Bugge (2003). Type II transmembrane serine proteases. *Thromb Haemost* **90**(2): 185-193.

Szarvas, T., M. Becker, F. vom Dorp, C. Gethmann, M. Totsch, A. Bankfalvi, K. W. Schmid, I. Romics, H. Rubben and S. Ergun (2010). Matrix metalloproteinase-7 as a marker of metastasis and predictor of poor survival in bladder cancer. *Cancer Sci* **101**(5): 1300-1308.

Takeuchi, T., J. L. Harris, W. Huang, K. W. Yan, S. R. Coughlin and C. S. Craik (2000). Cellular localization of membrane-type serine protease 1 and identification of protease-activated receptor-2 and single-chain urokinase-type plasminogen activator as substrates. *J Biol Chem* **275**(34): 26333-26342.

Talesa, V. N., C. Antognelli, C. Del Buono, F. Stracci, M. R. Serva, E. Cottini and E. Mearini (2009). Diagnostic potential in prostate cancer of a panel of urinary molecular tumor markers. *Cancer Biomark* **5**(6): 241-251.

Tammela, T. (2004). Endocrine treatment of prostate cancer. *J Steroid Biochem Mol Biol* **92**(4): 287-295.

Tanimoto, H., Y. Yan, J. Clarke, S. Korourian, K. Shigemasa, T. H. Parmley, G. P. Parham and T. J. O'Brien (1997). Hepsin, a cell surface serine protease identified in hepatoma cells, is overexpressed in ovarian cancer. *Cancer Res* **57**(14): 2884-2887.

Taplin, M. E., B. Rajeshkumar, S. Halabi, C. P. Werner, B. A. Woda, J. Picus, W. Stadler, D. F. Hayes, P. W. Kantoff, N. J. Vogelzang and E. J. Small (2003). Androgen receptor mutations in androgen-independent prostate cancer: Cancer and Leukemia Group B Study 9663. *J Clin Oncol* **21**(14): 2673-2678.

Thompson, I. M., D. P. Ankerst, C. Chi, M. S. Lucia, P. J. Goodman, J. J. Crowley, H. L. Parnes and C. A. Coltman, Jr. (2005). Operating characteristics of prostate-specific antigen in men with an initial PSA level of 3.0 ng/ml or lower. *JAMA* **294**(1): 66-70.

Tolis, G., D. Ackman, A. Stellos, A. Mehta, F. Labrie, A. T. Fazekas, A. M. Comaru-Schally and A. V. Schally (1982). Tumor growth inhibition in patients with prostatic carcinoma treated with luteinizing hormone-releasing hormone agonists. *Proc Natl Acad Sci U S A* **79**(5): 1658-1662.

Tomlins, S. A., A. Bjartell, A. M. Chinnaiyan, G. Jenster, R. K. Nam, M. A. Rubin and J. A. Schalken (2009). ETS gene fusions in prostate cancer: from discovery to daily clinical practice. *Eur Urol* **56**(2): 275-286.

Tomlins, S. A., D. R. Rhodes, S. Perner, S. M. Dhanasekaran, R. Mehra, X. W. Sun, S. Varambally, X. Cao, J. Tchinda, R. Kuefer, C. Lee, J. E. Montie, R. B. Shah, K. J. Pienta, M. A. Rubin and A. M. Chinnaiyan (2005). Recurrent fusion of TMPRSS2 and ETS transcription factor genes in prostate cancer. *Science* **310**(5748): 644-648.

Tripathi, M., S. Nandana, H. Yamashita, R. Ganesan, D. Kirchhofer and V. Quaranta (2008). Laminin-332 is a substrate for hepsin, a protease associated with prostate cancer progression. *J Biol Chem* **283**(45): 30576-30584.

Tsai, W. C., C. H. Chu, C. P. Yu, L. F. Sheu, A. Chen, H. Chiang and J. S. Jin (2008). Matriptase and survivin expression associated with tumor progression and malignant potential in breast cancer of Chinese women: tissue microarray analysis of immunostaining scores with clinicopathological parameters. *Dis Markers* **24**(2): 89-99.

Tuxhorn, J. A., G. E. Ayala and D. R. Rowley (2001). Reactive stroma in prostate cancer progression. *J Urol* **166**(6): 2472-2483.

Uhland, K. (2006). Matriptase and its putative role in cancer. *Cell Mol Life Sci* **63**(24): 2968-2978.

Uhlenbeck, O. C. (1987). A small catalytic oligoribonucleotide. *Nature* **328**(6131): 596-600.

Underwood, L. J., K. Shigemasa, H. Tanimoto, J. B. Beard, E. N. Schneider, Y. Wang, T. H. Parmley and T. J. O'Brien (2000). Ovarian tumor cells express a novel multi-domain cell surface serine protease. *Biochim Biophys Acta* **1502**(3): 337-350.

van Driel, I. R., J. L. Goldstein, T. C. Sudhof and M. S. Brown (1987). First cysteine-rich repeat in ligand-binding domain of low density lipoprotein receptor binds Ca2+ and monoclonal antibodies, but not lipoproteins. *J Biol Chem* **262**(36): 17443-17449.

van Moorselaar, R. J. and E. E. Voest (2002). Angiogenesis in prostate cancer: its role in disease progression and possible therapeutic approaches. *Mol Cell Endocrinol* **197**(1-2): 239-250.

Velasco, G., S. Cal, V. Quesada, L. M. Sanchez and C. Lopez-Otin (2002). Matriptase-2, a membrane-bound mosaic serine proteinase predominantly expressed in human liver and showing degrading activity against extracellular matrix proteins. *J Biol Chem* **277**(40): 37637-37646.

Verras, M. and Z. Sun (2006). Roles and regulation of Wnt signaling and beta-catenin in prostate cancer. *Cancer Lett* **237**(1): 22-32.

Vilchez-Martinez, J. A., E. Pedroza, A. Arimura and A. V. Schally (1979). Paradoxical effects of D-Trp6-luteinizing hormone-releasing hormone on the hypothalamic-pituitary-gonadal axis in immature female rats. *Fertil Steril* **31**(6): 677-682.

Viloria, C. G., J. R. Peinado, A. Astudillo, O. Garcia-Suarez, M. V. Gonzalez, C. Suarez and S. Cal (2007). Human DESC1 serine protease confers tumorigenic properties to MDCK cells and it is upregulated in tumours of different origin. *Br J Cancer* **97**(2): 201-209.

Vis, A. N. and F. H. Schroder (2009). Key targets of hormonal treatment of prostate cancer. Part 2: the androgen receptor and 5alpha-reductase. *BJU Int* **104**(9): 1191-1197.

Voeller, H. J., C. I. Truica and E. P. Gelmann (1998). Beta-catenin mutations in human prostate cancer. *Cancer Res* **58**(12): 2520-2523.

Vogel, L. K., M. Saebo, C. F. Skjelbred, K. Abell, E. D. Pedersen, U. Vogel and E. H. Kure (2006). The ratio of Matriptase/HAI-1 mRNA is higher in colorectal cancer adenomas and carcinomas than corresponding tissue from control individuals. *BMC Cancer* **6**: 176.

Wallrapp, C., S. Hahnel, F. Muller-Pillasch, B. Burghardt, T. Iwamura, M. Ruthenburger, M. M. Lerch, G. Adler and T. M. Gress (2000). A novel transmembrane serine protease (TMPRSS3) overexpressed in pancreatic cancer. *Cancer Res* **60**(10): 2602-2606.

Wang, E. A., V. Rosen, J. S. D'Alessandro, M. Bauduy, P. Cordes, T. Harada, D. I. Israel, R. M. Hewick, K. M. Kerns, P. LaPan and et al. (1990). Recombinant human bone morphogenetic protein induces bone formation. *Proc Natl Acad Sci U S A* **87**(6): 2220-2224.

Wang, J., Y. Cai, W. Yu, C. Ren, D. M. Spencer and M. Ittmann (2008). Pleiotropic biological activities of alternatively spliced TMPRSS2/ERG fusion gene transcripts. *Cancer Res* **68**(20): 8516-8524.

Welsh, J. B., L. M. Sapinoso, A. I. Su, S. G. Kern, J. Wang-Rodriguez, C. A. Moskaluk, H. F. Frierson, Jr. and G. M. Hampton (2001). Analysis of gene expression identifies candidate markers and pharmacological targets in prostate cancer. *Cancer Res* **61**(16): 5974-5978.

Wild, S. H., C. M. Fischbacher, A. Brock, C. Griffiths and R. Bhopal (2006). Mortality from all cancers and lung, colorectal, breast and prostate cancer by country of birth in England and Wales, 2001-2003. *Br J Cancer* **94**(7): 1079-1085.

Wilson, S., B. Greer, J. Hooper, A. Zijlstra, B. Walker, J. Quigley and S. Hawthorne (2005). The membrane-anchored serine protease, TMPRSS2, activates PAR-2 in prostate cancer cells. *Biochem J* **388**(Pt 3): 967-972.

Wong, G. W., Y. Tang, E. Feyfant, A. Sali, L. Li, Y. Li, C. Huang, D. S. Friend, S. A. Krilis and R. L. Stevens (1999). Identification of a new member of the tryptase

family of mouse and human mast cell proteases which possesses a novel COOH-terminal hydrophobic extension. *J Biol Chem* **274**(43): 30784-30793.

Wu, F. and Q. Wu (2003). Corin-mediated processing of pro-atrial natriuretic peptide in human small cell lung cancer cells. *Cancer Res* **63**(23): 8318-8322.

Wu, H., L. Sun, J. W. Moul, H. Y. Wu, D. G. McLeod, C. Amling, R. Lance, L. Kusuda, T. Donahue, J. Foley, A. Chung, W. Sexton and D. Soderdahl (2004). Watchful waiting and factors predictive of secondary treatment of localized prostate cancer. *J Urol* **171**(3): 1111-1116.

Wu, Q., H. C. Kuo and G. G. Deng (2005). Serine proteases and cardiac function. *Biochim Biophys Acta* **1751**(1): 82-94.

Wu, Q. and G. Parry (2007). Hepsin and prostate cancer. *Front Biosci* **12**: 5052-5059.

Xia, Y., J. L. Babitt, Y. Sidis, R. T. Chung and H. Y. Lin (2008). Hemojuvelin regulates hepcidin expression via a selective subset of BMP ligands and receptors independently of neogenin. *Blood* **111**(10): 5195-5204.

Yamaguchi, N., A. Okui, T. Yamada, H. Nakazato and S. Mitsui (2002). Spinesin/TMPRSS5, a novel transmembrane serine protease, cloned from human spinal cord. *J Biol Chem* **277**(9): 6806-6812.

Yamaoka, K., K. Masuda, H. Ogawa, K. Takagi, N. Umemoto and S. Yasuoka (1998). Cloning and characterization of the cDNA for human airway trypsin-like protease. *J Biol Chem* **273**(19): 11895-11901.

Yan, W., N. Sheng, M. Seto, J. Morser and Q. Wu (1999). Corin, a mosaic transmembrane serine protease encoded by a novel cDNA from human heart. *J Biol Chem* **274**(21): 14926-14935.

Yasuoka, S., T. Ohnishi, S. Kawano, S. Tsuchihashi, M. Ogawara, K. Masuda, K. Yamaoka, M. Takahashi and T. Sano (1997). Purification, characterization, and localization of a novel trypsin-like protease found in the human airway. *Am J Respir Cell Mol Biol* **16**(3): 300-308.

Yoshinaga, S., Y. Nakahori and S. Yasuoka (1998). Fibrinogenolytic activity of a novel trypsin-like enzyme found in human airway. *J Med Invest* **45**(1-4): 77-86.

Zacharski, L. R., D. L. Ornstein, V. A. Memoli, S. M. Rousseau and W. Kisiel (1998). Expression of the factor VII activating protease, hepsin, in situ in renal cell carcinoma. *Thromb Haemost* **79**(4): 876-877.

Zhang, A. S., S. A. Anderson, J. Wang, F. Yang, K. DeMaster, R. Ahmed, C. P. Nizzi, R. S. Eisenstein, H. Tsukamoto and C. A. Enns (2011). Suppression of hepatic hepcidin expression in response to acute iron deprivation is associated with an increase of matriptase-2 protein. *Blood* **117**(5): 1687-1699.

Zhang, X., J. P. Gaspard and D. C. Chung (2001). Regulation of vascular endothelial growth factor by the Wnt and K-ras pathways in colonic neoplasia. *Cancer Res* **61**(16): 6050-6054.

Zuker, M. (2003). Mfold web server for nucleic acid folding and hybridization prediction. *Nucleic Acids Res* **31**(13): 3406-3415.

Electronic references

Cancer Update Vol. 2, 2005: Prostate Cancer: An Overview

(URL: http://www.nccs.com.sg/pbcation/CU/vol2_05/weblink1.htm)

Prostate Cancer Incidence and Mortality Worldwide in 2008

(URL: http://globocan.iarc.fr/factsheets/cancers/prostate.asp)

Vala Sciences: Monitoring expression and distribution of β-catenin.

(URL: http://www.valasciences.com/articles/applications/monitoring-expression-and-distribution-of-catenin-z-05/)